Discrete Dynamics in Nature and Society

Stochastic Modeling and Financial Applications

Guest Editors: Ivan Ganchev Ivanov, Vasile Dragan, and Oswaldo Luiz do Valle Costa

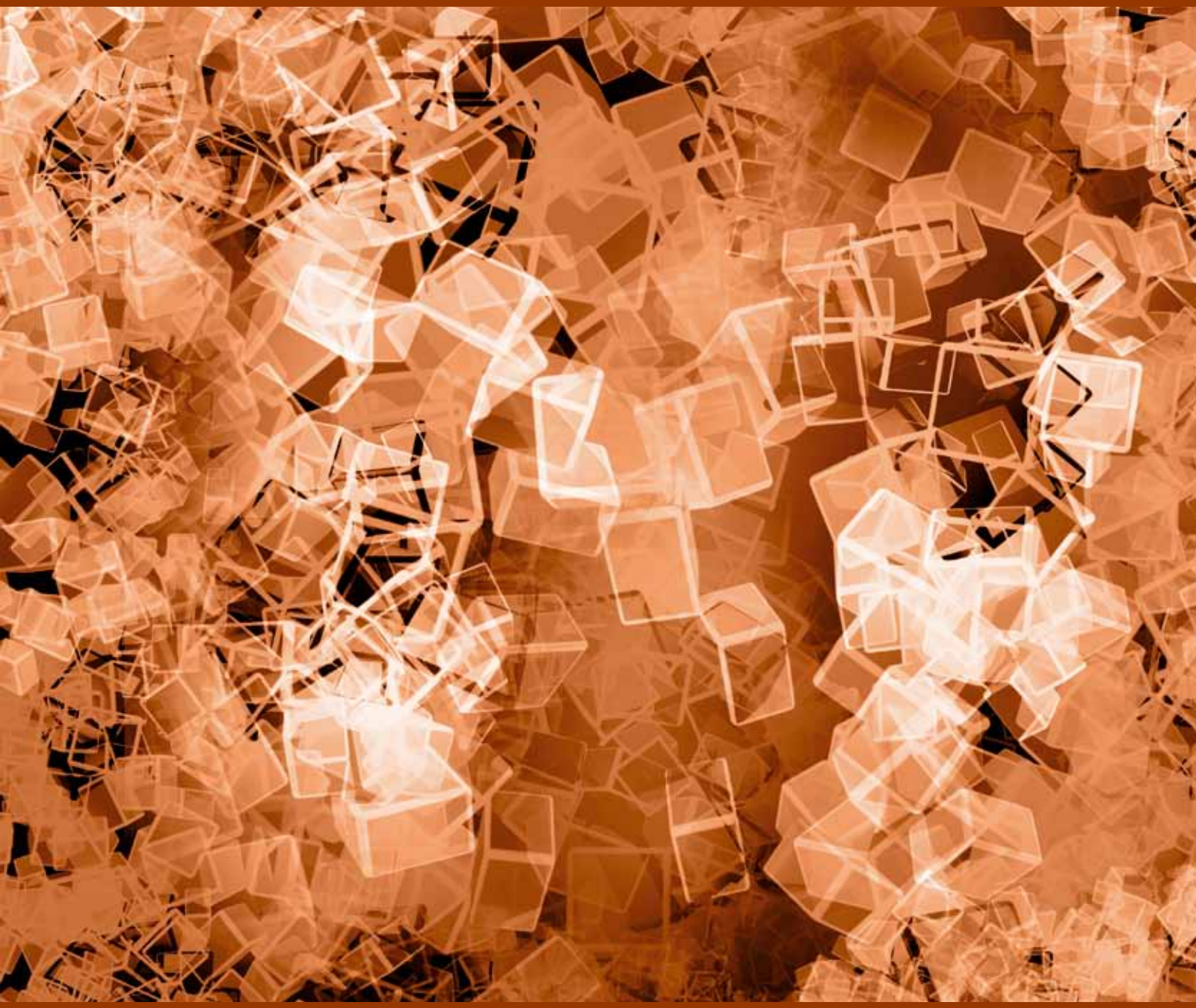

Stochastic Modeling and Financial Applications

Discrete Dynamics in Nature and Society

Stochastic Modeling and Financial Applications

Guest Editors: Ivan Ganchev Ivanov, Vasile Dragan,
and Oswaldo Luiz do Valle Costa

Copyright © 2013 Hindawi Publishing Corporation. All rights reserved.

This is a special issue published in "Discrete Dynamics in Nature and Society." All articles are open access articles distributed under the Creative Commons Attribution License, which permits unrestricted use, distribution, and reproduction in any medium, provided the original work is properly cited.

Editorial Board

M. A. Rami, Spain
D. R. Anderson, USA
V. Avrutin, Germany
S. Balint, Romania
K. S. Berenhaut, USA
G. Bonanno, Italy
E. Braverman, Canada
P. Candito, Italy
Jinde Cao, China
W.-D. Chang, Taiwan
C. Çinar, Turkey
D. Czamanski, Israel
R. H. Day, USA
M. De la Sen, Spain
J. Diblik, Czech Republic
Xiaohua Ding, China
Adam Doliwa, Poland
Zengji Du, China
E. Elabbasy, Egypt
H. A. El-Morshedy, Egypt
D. Fournier-Prunaret, France
V. Gontar, Israel
Taher S. Hassan, Egypt
Xue Z. He, Australia
W. Huang, Singapore
G. Izzo, Italy
S. Jagannathan, USA
Lee C. Jang, Korea
Jun Ji, USA
Zhen Jin, China
N. I. Karachalios, Greece
E. R. Kaufmann, USA
Recai Kilic, Turkey
Ryusuke Kon, Japan
V. S. Kozyakin, Russia
M. Kulenovic, USA
J. Kurths, Germany
Wei Nian Li, China
Xiaojie Lin, China
Xiaohui Liu, UK
R. López-Ruiz, Spain
Qing-hua Ma, China
A. Matsumoto, Japan
R. Medina, Chile
E. Messina, Italy
U. Mugan, Turkey
P. Huu Anh Ngoc, Vietnam
P. Niamsup, Thailand
Juan J. Nieto, Spain
P. K. Panigrahi, India
G. Papaschinopoulos, Greece
B. Paternoster, Italy
Mingshu Peng, China
Carlo Piccardi, Italy
Peter Plath, Germany
C. Qian, USA
V. S. Rabinovich, Mexico
I. Rachůnková, Czech Republic
M. Rafei, The Netherlands
Aura Reggiani, Italy
P. Rehak, Czech Republic
Marko Robnik, Slovenia
Y. Rogovchenko, Norway
V. G. Rumchev, Australia
B. S. Daya Sagar, India
R. Sahadevan, India
Leonid Shaikhet, Ukraine
Vimal Singh, Turkey
S. Sivasundaram, USA
F. J. Solís Lozano, Mexico
G. Solís-Perales, Mexico
Yihong Song, China
M. Sonis, Israel
Jian-Ping Sun, China
Stepan A. Tersian, Bulgaria
Gerald Teschl, Austria
Tetsuji Tokihiro, Japan
D. F. M. Torres, Portugal
Firdaus Udwadia, USA
Antonia Vecchio, Italy
Qi-Ru Wang, China
I. Yalcinkaya, Turkey
Xiang Ping Yan, China
Xiaofan Yang, China
Bo Yang, USA
Her-Terng Yau, Taiwan
Jianshe Yu, China
Agacik Zafer, Turkey
Guang Zhang, China
Binggen Zhang, China
Zhengqiu Zhang, China
Lu Zhen, China
Baodong Zheng, China
Yong Zhou, China
Zhan Zhou, China
Zuo-nong Zhu, China

Contents

Stochastic Modeling and Financial Applications, Ivan Ganchev Ivanov, Vasile Dragan, and Oswaldo Luiz do Valle Costa
Volume 2013, Article ID 405658, 2 pages

Empirical Evidence on Time-Varying Hedging Effectiveness of Emissions Allowances under Departures from the Cost-of-Carry Theory, Kai Chang
Volume 2013, Article ID 905329, 8 pages

Basel III and Asset Securitization, M. Mpundu, M. A. Petersen, J. Mukuddem-Petersen, and F. Gideon
Volume 2013, Article ID 439305, 19 pages

Terminal-Dependent Statistical Inference for the Integral Form of FBSDE, Qi Zhang
Volume 2013, Article ID 753025, 13 pages

Hyperchaos Numerical Simulation and Control in a 4D Hyperchaotic System, Junhai Ma and Yujing Yang
Volume 2013, Article ID 980578, 16 pages

Heuristic for Stochastic Online Flowshop Problem with Preemption Penalties, Mohammad Bayat, Mehdi Heydari, and Mohammad Mahdavi Mazdeh
Volume 2013, Article ID 916978, 10 pages

Basel III Liquidity Risk Measures and Bank Failure, L. N. P. Hlatshwayo, M. A. Petersen, J. Mukuddem-Petersen, and C. Meniago
Volume 2013, Article ID 172648, 19 pages

Sublinear Expectation Nonlinear Regression for the Financial Risk Measurement and Management, Yunquan Song and Lu Lin
Volume 2013, Article ID 398750, 10 pages

Hindawi Publishing Corporation
Discrete Dynamics in Nature and Society
Volume 2013, Article ID 405658, 2 pages
http://dx.doi.org/10.1155/2013/405658

Editorial
Stochastic Modeling and Financial Applications

Ivan Ganchev Ivanov,[1] Vasile Dragan,[2] and Oswaldo Luiz do Valle Costa[3]

[1] *Faculty of Economics and Business Administration, Sofia University "St. Kl. Ohridski," 125 Tsarigradsko Shosse Boulevard, bl.3, 1113 Sofia, Bulgaria*
[2] *Institute of Mathematics "Simion Stoilow" of the Romanian Academy, Calea Grivitei No. 21, P.O. Box 1-764, 014700 Bucharest, Romania*
[3] *Departamento de Engenharia de Telecomunicações de Controle, Institute Escola Politécnica da Universidade de São Paulo (EPUSP), 05508-900 São Paulo, SP, Brazil*

Correspondence should be addressed to Ivan Ganchev Ivanov; i_ivanov@feb.uni-sofia.bg

Received 3 December 2013; Accepted 3 December 2013

Copyright © 2013 Ivan Ganchev Ivanov et al. This is an open access article distributed under the Creative Commons Attribution License, which permits unrestricted use, distribution, and reproduction in any medium, provided the original work is properly cited.

This special issue brings together several works in the area of advanced modern theory of stochastic modeling and applications in financial and economic fields.

The Basel III banking regulation is a topic addressed in two paper. The paper by M. Mpundu et al. focuses on Basel III and asset securitization. It deals with aspects of the mechanism by which low- and high-quality entities securitize low and high quality assets, respectively, into collateralized debt obligations, under the new Basel III capital and liquidity regulations. The authors develop an illustrative example of low-quality asset securitization for subprime mortgages and present numerical examples to illustrate their key results. The paper by L. N. P. Hlatshwayo et al. focuses on Basel III liquidity risk measures and bank failure. The authors point out that Basel III banking regulation emphasizes the use of liquidity coverage and net stable funding ratios as measures of liquidity risk. The goal of this paper is to approximate these measures by using global liquidity data. In addition the authors compare the risk sensitivity of the aforementioned Basel III liquidity risk measures to those of traditional measures. The authors also use a discrete-time hazard model to study bank failure. One of their conclusions is that Basel III risk measures have limited ability to predict bank failure when compared with their traditional counterparts.

The paper by Kai Chang shows, from empirical evidences, that conditional variance, conditional covariance and their correlation between spot and futures exhibit time-varying trends. Moreover it is claimed that conditional volatility of spot prices, conditional volatility disturbed from futures market, and conditional correlation of market noises implied from spot and futures market have significant effects on dynamic hedge ratios and hedging effectiveness. From this a better hedging efficiency through dynamic hedge ratios with the departures from cost-of-carry theory is obtained.

The paper by Y. Song and L. Lin defines a sub-linear expectation nonlinear regression, having in mind its application on the management and measurement of financial risks. The paper presents a simulation study and a real data analysis to illustrate the new model and methods. The paper by Q. Zhang deals with the terminal-dependent statistical inference for backward stochastic differential equations (BSDE), which arises in financial and ecological modeling.

The paper focuses on the statistical inference for the integral form of forward-backward stochastic differential equations (FBSDE). Simulations are conducted to demonstrate finite sample behaviors of the proposed estimators.

Two papers are not related to financial systems but, instead, are concerned with stochastic modeling and numerical methods. The paper by M. Heydari et al. examines the preemptive stochastic online flowshop with the objective of minimizing the expected makespan. The model assumes that all the jobs arrive overtime, which means that the existence and the parameters of each job are unknown until its release date, the processing time of the jobs is stochastic, and actual processing time is unknown until completion of the job.

The authors propose a heuristic procedure for this problem, which is applicable whenever the job processing times are characterized by their means and standard deviation. The performance of the proposed heuristic method is explored using some numerical examples.

The paper by J. Ma and Y. Yang deals with hyperchaos numerical simulation and control in a 4D hyperchaotic system.

The bifurcation diagrams, Lyapunov exponents, hyperchaotic attractors, the power spectrums, and time charts are mapped out through the theory analysis and dynamic simulations. Linear feedback controllers are designed for stabilizing the hyperchaos to the unstable equilibrium points, achieving the goal of a second control which can be more useful in application.

By compiling these papers, we hope to enrich our readers and researchers with respect to these topics related to stochastic modeling and financial applications.

Ivan Ganchev Ivanov
Vasile Dragan
Oswaldo Luiz do Valle Costa

Hindawi Publishing Corporation
Discrete Dynamics in Nature and Society
Volume 2013, Article ID 905329, 8 pages
http://dx.doi.org/10.1155/2013/905329

Research Article

Empirical Evidence on Time-Varying Hedging Effectiveness of Emissions Allowances under Departures from the Cost-of-Carry Theory

Kai Chang

School of Finance, Zhejiang University of Finance & Economics, High Education Park in Xiasha District, Hangzhou, Zhejiang 310038, China

Correspondence should be addressed to Kai Chang; kchang16@163.com

Received 6 June 2013; Accepted 5 November 2013

Academic Editor: Ivan Ivanov

Copyright © 2013 Kai Chang. This is an open access article distributed under the Creative Commons Attribution License, which permits unrestricted use, distribution, and reproduction in any medium, provided the original work is properly cited.

Under departures from the cost-of-carry theory, traded spot prices and conditional volatility disturbed from futures market have significant impacts on futures price of emissions allowances, and then we propose time-varying hedge ratios and hedging effectiveness estimation using ECM-GARCH model. Our empirical results show that conditional variance, conditional covariance, and their correlation between between spot and futures prices exhibit time-varying trends. Conditional volatility of spot prices, conditional volatility disturbed from futures market, and conditional correlation of market noises implied from spot and futures markets have significant effects on time-varying hedge ratios and hedging effectiveness. In the immature emissions allowances market, market participants optimize portfolio sizes between spot and futures assets using historical market information and then achieve higher risk reduction of assets portfolio revenues; accordingly, we can obtain better hedging effectiveness through time-varying hedge ratios with departures from the cost-of-carry theory.

1. Introduction

Greenhouse gas (GHG) emission is an ever-increasingly hot topic in the 21st century for alarming phenomena of global warming and extreme climate deterioration. Most of the scientists and politicians believe that emissions trading scheme is a cost-effective market scheme in order to control GHG emissions. Since the launch of the European Union emissions trading scheme (EU ETS) in 2005, CO_2 emissions allowances have become valuable commodities which can be traded in CO_2 emissions allowances markets. Spot, futures, options, and other financial products of emissions allowances are important financial tools for market participants to increase assets portfolio revenues and achieve higher risk reduction. In recent years emissions allowances markets have become the most promising and are quickly growing markets in global commodities markets.

Spot and futures prices of emissions allowances depend on expected market scarcity induced by demand and supply quantity in the emissions allowances market. An early study of emissions allowances by Benz and Truck [1, 2] found that a good many complex factors such as GHS emissions reduction plan and regulation policy, low-technology promotion and application, energy prices volatility, and energy efficiency and extreme temperature changes have significant impacts on market scarcity. Seifert et al. [3], Daskalakis et al. [4], and Conrad et al. [5] asserted that spot and futures prices of emissions allowances have higher time-varying trends, spot prices follow asymmetric GARCH process, and accordingly spot assets exhibit higher market risks. Montagnoli and de Vries [6] endorsed that, in the Pilot phase, immature emissions allowances markets induce lower market efficiency, while market efficiency has better recovery signs in the Kyoto phase. Zhang and Wei [7] examined that favorable and unfavorable market information exhibits greater market overreaction induced by lower market efficiency in the Pilot phase, and emissions allowances prices have obvious divergent and unpredictable trends. Arouri et al. [8] presented that spot and futures prices have nonlinear dynamics correlations between spot and futures returns, and their volatilities exhibit asymmetric and nonlinear trends. Immature emissions markets push up higher trading risks of spot prices, and market

participants can gain instable investment revenues through optimizing assets portfolio policies. Based on cost-of-carry theory, Chang et al. [9] found that market participants adjust assets portfolio policies of futures contracts with different maturities and then they can attain excess exchange options value.

A good many complex factors bring about low efficiency and overreaction of price in the emissions allowances market. These complex market factors exert greater market price shock; however, price shock effectiveness exhibits a tremendous difference in time and channels of spot and futures prices in the immature emissions allowances markets. Current emissions allowances markets are weakly effective markets; they exhibit market bias, transaction cost, and market overreaction. In the immature emissions allowances markets, unexpected market information has a different change speed of spot and futures prices in the short term, emissions allowances markets exhibit a significant lead-lag relationship between between spot and futures prices, and the theoretical and traded futures prices exhibit time-varying deviation trends.

Futures mispricing errors are greater than market transaction cost, and then market paritcipants can achieve extra arbitrage revenues through adjusting portfolio sizes between spot and futures assets. Under departures from the cost-of-carry theory, historical market information, conditional variance, and conditional correlation implied from emissions allowances futures markets have significant impacts on time-varying hedge ratios and hedging effectiveness. It is urgent for market participants to know how to increase portfolio revenues and decrease returns risk reduction of emissions allowances assets between spot and futures under departures from the cost-of-carry theory.

The main innovation of this paper is that, under departures from the cost-of-carry theory, conditional volatility of spot prices, conditional volatility disturbed from futures market, and conditional correlation of market noises implied from spot and futures markets have significant effects on time-varying hedge ratios and hedging effectiveness. These empirical results are helpful for market participants to effectively optimize portfolio sizes between spot and futures assets using historical market information and achieve higher risk reduction of assets portfolio revenues. The remainder of our paper is organized as follows. Section 2 explains cost-of-carry theory. Section 3 proposes time-varying hedge ratios model under departures from the cost-of-carry theory. Section 4 presents conditional volatility disturbed from futures market and conditional correlation of market noises between spot and futures. Section 5 descripts data samples source. Section 6 discusses empirical results of conditional volatility and conditional correlation. Section 7 estimates and discusses empirical results of time-varying hedge ratios and hedging effectiveness. Section 8 provides a brief conclusion.

2. Cost-of-Carry Theory

Based on a pioneering study of cost-of-carry theory by Working [10] and Brennan [11], in the complete emissions allowances market, assumed emissions allowances markets have no transaction costs, no arbitrage behavior, and no storage costs; S_t denotes spot price of emissions allowances, $F^*_{t,T}$ denotes theoretical price of futures contracts for maturity T at time t, and r is the continuously compounded risk-free interest rate. Based on the cost-of-carry theory, the theoretical futures price is equal to

$$F^*_{t,T} = e^{(r-\delta)(T-t)} S_t, \tag{1}$$

where δ denotes convenience yield of emissions allowances and $r - \delta$ denotes cost-of-carry of emissions allowances; the logarithmic equation (1) can be expressed as follows:

$$f^*_t = s_t + (r - \delta)(T - t), \tag{2}$$

where $s_t = \ln S_t$, $f^*_t = \ln F^*_{t,T}$ denote the logarithm of spot price and theoretical futures price. Based on cost-of-carry theory, emissions allowances market is effective, spot and futures prices should keep synchronous correlation, and spot price volatility is similar to futures price volatility. Spot and futures prices keep similar change speeds, and they exhibit no lead-lag relationship. In the immature emissions allowances markets, emissions allowances markets exhibit transaction costs, asymmetric market information, excess capital demand, and unexpected market scarcity, and the theoretical and traded futures prices exhibit greater deviation errors according to the cost-of-carry model. Immature emissions allowances market produces a lead-lag relationship between spot and futures market returns, as well as between their volatilities. It may be possible to anticipate price motion trend and reduce revenues risk reduction in one market from historical market information in other markets and present a relevant question using historical information in futures market as a hedging instrument for risky assets portfolios.

3. Time-Varying Hedge Ratios

In order to achieve market arbitrage, market participants optimize their assets portfolio policies between spot and futures using the price-clustering effects. Rich quota distribution of emissions allowances and lower trading volume in futures market induced the overraction of emissions allowances market, then push greater difference in time and pannels induced by market shocks. These market shocks induce that short-run equilibrium price in futures market is deviated from long-run equilibrium prices, price distortions in futures market made market participants attain many arbitrage opportunities, so short-term market speculations are active. Based on hedging theory, minimum variance of hedge ratios is equal that conditional covariance between spot and futures is divided by conditional variance of futures prices. Wilson [12] and Lien and Tse [13] have examined that, if spot prices are similar to futures prices, optimal hedge ratios are equal to regression coefficients between spot and futures using linear regression equation, and hedge ratios are constant. If spot and futures prices exhibit different changing speed, market investors adjust assets portfolio sizes between spot and futures according to previous market information

set, and as a result optimal hedge ratios exhibit time-varying trends.

Assuming spot price and theoretical futures price of emissions allowances follow geometric Brownian process, accordingly

$$\begin{aligned} dS_t &= \mu_{s,t} S_t dt + \sigma_{s,t} S_t dz_{1,t}, \\ dF^*_{t,T} &= \mu_{f,t} F^*_{t,T} dt + \sigma_{s,t} F^*_{t,T} dz_{1,t}, \end{aligned} \tag{3}$$

where $\mu_{s,t}$, $\sigma_{s,t}$ denote instantaneous returns and volatility of spot prices, and the theoretical futures prices returns are equal to $\mu_{f^*,t} = \mu_{s,t} + (r - \delta)$. dz_1 denotes a standard Wiener process, $dz_{1,t} = \varepsilon_{1t}\sqrt{dt}$, spot market noise of emissions allowances follows standard normal distribution, and $\varepsilon_{1,t} \sim N(0,1)$. In the immature emissions allowances markets, the theoretical futures prices of emissions allowances are deviated from the traded futures prices under departures from the cost-of-carry theory. Based on the conclusion endorsed by Lafuente and Novales [14], we introduce the second market noise in order to correct market prices difference as follows:

$$dF_{t,T} = \mu_{f,t} F_{t,T} dt + \sigma_{s,t} F_{t,T} dz_{1,t} + \sigma_{c,t} F_{t,T} dz_{2,t}, \tag{4}$$

where $F_{t,T}$ denotes the traded futures prices of emissions allowances, $\sigma_{c,t}$ denotes the conditional volatility disturbed from emissions allowances futures market, and $dz_{2,t} = \varepsilon_{2,t}\sqrt{dt}$; market noise implied from emissions allowances futures market follows standard normal distribution, $\varepsilon_{2,t} \sim N(0,1)$. Based on (3) and (4), conditional correlation coefficient between spot and futures returns is equal to

$$\begin{aligned} \rho_{sf,t} &= \frac{\mathrm{Cov}\left(\left(dS_t/S_t dt\right), \left(dF_{t,T}/F_{t,T} dt\right)\right)}{\sqrt{\left[\mathrm{Var}_t\left(dS_t/S_t dt\right)\right]}\sqrt{\mathrm{Var}\left(dF_{t,T}/F_{t,T} dt\right)}} \\ &= \frac{\sigma^2_{s,t} + \rho_{12,t}\sigma_{s,t}\sigma_{c,t}}{\sqrt{\sigma^2_{s,t}\left(\sigma^2_{s,t} + \sigma^2_{c,t} + 2\rho_{12,t}\sigma_{s,t}\sigma_{c,t}\right)}}. \end{aligned} \tag{5}$$

Here $\rho_{12,t}$ denotes instantaneous correlation coefficient between spot market noise ε_1 and futures market noise ε_2 and $\rho_{sf,t}$ denotes instantaneous conditional correlation coefficient between spot and futures returns. If $\sigma^2_{ct} = 0$, spot and futures prices of emissions allowances exhibit similar market volatility, and then spot and futures prices have completely positive correlation.

Where we assume that the evolution of futures market returns is driven by heteroscedastic, geometric Brownian motion process, we incorporated a market-specific noise into the dynamics of theoretical futures returns; this market noise motivation produces a spread between the theoretical and traded futures price. Hence, spot and futures markets cannot share an identical source of volatility against the cost-of-carry model. We can estimate the motivation of spot and futures market returns as well as their volatilities and correlation of market noises disturbed from spot and futures markets using historical prices data in spot and futures markets. Accordingly, market participants take good use of historical market information and market noise disturbance implied from the futures markets and then optimize assets portfolio policies between spot and futures; accordingly, market participants can achieve stable arbitrage market revenues.

Spot prices of emissions allowances exhibit greater returns risk; market investors optimize portfolio sizes between spot and futures in order to decline assets investment risks. Assuming ϕ_{t-1} denotes market information set at time $t-1$, the hedgers buy X spot quantity of emissions allowances at time $t-1$, while selling Y futures quantity, and then hedge ratio is equal to $h_{t-1} = Y/X$. Based on a pioneering study of hedging theory by Johnson [15], the portfolio return in the period $(t-1, t)$ is equal to

$$R_{ht} = \Delta s_t - h_{t-1}\Delta f_t. \tag{6}$$

Here h_{t-1} is hedge ratio for period $t-1$, s_t, f_t represent the logarithm of spot price, of futures price for period t, $\Delta s_t = s_t - s_{t-1}$, $\Delta f_t = f_t - f_{t-1}$ are respectively the spot and futures returns for period t. Wilson [12] and Lien and Tse [13] have concluded that conditional variances estimate assets portfolio risks by using market information set at time $t-1$ as follows:

$$\begin{aligned} \mathrm{Var}\left(R_{ht} \mid \phi_{t-1}\right) = {} & \mathrm{Var}\left(\Delta s_t \mid \phi_{t-1}\right) + h^2_{t-1}\mathrm{Var}\left(\Delta f_t \mid \phi_{t-1}\right) \\ & - 2h_{t-1}\,\mathrm{cov}\left(\Delta s_t, \Delta f_t \mid \phi_{t-1}\right). \end{aligned} \tag{7}$$

Lafuente and Novales [14] endorsed that minimum variance hedge ratio using minimum hedging risk is equal to

$$h^* = \frac{\mathrm{cov}\left(\Delta s_t, \Delta f_t \mid \phi_{t-1}\right)}{\mathrm{Var}\left(\Delta f_t \mid \phi_{t-1}\right)} = \frac{\sigma^2_{s,t} + 2\rho_{12,t}\sigma_{s,t}\sigma_{c,t}}{\sigma^2_{s,t} + \sigma^2_{c,t} + 2\rho_{12,t}\sigma_{s,t}\sigma_{c,t}}, \tag{8}$$

where $\mathrm{cov}(\Delta s_t, \Delta f_t \mid \phi_{t-1})$ denotes the covariance between spot and futures under market information set ϕ_{t-1} and h^* denotes optimal hedge ratio. From (8), when spot and futures markets engender new market information, information set ϕ_{t-1} exhibit time-varying trends, and then optimal hedge ratios exhibit time-varying trends.

4. Conditional Volatility and Correlation Estimation

Based on higher degree of liquidity in the spot market relative to the futures market, these market overreactions have more quick transition speed of spot prices relative to futures prices. In traded CO_2 emissions allowances markets, the conditional covariance matrix between spot prices and futures prices showed strongly time-varying trends. The OLS hedging cannot exhibit that time-varying price trends and lead-lag relationship have significant impacts on hedge ratio and hedging effectiveness and then decrease portfolio returns risk of emissions allowances assets. Accordingly optimally time-varying hedge ratios exhibit significantly time-varying trends. Error-correction model (ECM) is a dynamic model based on correlations in returns of two underlying assets; ECM reflects that short-term deviation is away from long-term equilibrium. Accordingly ECM considers nonstationary prices of both spot and futures, long-run equilibrium, and

short-run dynamics. A bivariate error-correction model with GARCH perturbations is used to estimate the conditional second moments of market returns.

Here we assume price-clustering effects of both spot and futures are symmetric process in order to estimate conditional volatility and correlated coefficients of market noises implied from futures market. In following section, the hedgers can attain optimally time-varying hedge ratios and hedging effectiveness using ECM-GARCH.

Lien et al. [16], Lien and Yang [17], and Peng and Ye [18] proposed that previously historical market information has a significant impact on prices of both spot and futures; here the basis $\varepsilon_{t-1} = s_{t-1} - f_{t-1}$ denotes the error-correction term, incorporated into the GARCH model, as follows:

$$\begin{aligned}
\Delta s_t &= \alpha_s \left(s_{t-1} - f_{t-1}\right) + \xi_{st},\\
\Delta f_t &= \alpha_f \left(s_{t-1} - f_{t-1}\right) + \xi_{ft},\\
\sigma_{st}^2 &= a_s + b_s \xi_{s(t-1)}^2 + c_s \sigma_{s(t-1)}^2,\\
\sigma_{ft}^2 &= a_f + b_f \xi_{s(t-1)} + c_f \sigma_{f(t-1)},\\
\sigma_{sft} &= a_s a_f + b_s b_f \xi_{s(t-1)} \xi_{f(t-1)}\\
&\quad + c_s c_f \sigma_{sf(t-1)}.
\end{aligned} \tag{9}$$

Based on (9), we can estimate conditional variance coefficients of spot price and of futures price, conditional covariance coefficient between spot and futures. Conditional variance of futures prices of emissions allowances can be expressed using (3) and (4) as follows:

$$\sigma_{ft}^2 = \sigma_{st}^2 + \sigma_{ct}^2 + 2\rho_{12t}\sigma_{st}\sigma_{ct}, \tag{10}$$

$$\sigma_{sft} = \sigma_{st}^2 + \rho_{12t}\sigma_{st}\sigma_{ct}. \tag{11}$$

We can propose a new equation (12) using (11) as follows:

$$\rho_{12t}\sigma_{st} = \frac{\sigma_{sft} - \sigma_{st}^2}{\sigma_{ct}}. \tag{12}$$

Substituting (12) into (10), conditional volatility disturbed from emissions allowances futures market can be expressed as follows:

$$\sigma_{ct}^2 = \sigma_{st}^2 + \sigma_{ft}^2 - 2\sigma_{sft}. \tag{13}$$

Substituting (12) into (10), conditional correlation coefficient of markets noises implied from spot and futures markets is

$$\rho_{12t} = \frac{\sigma_{sft} - \sigma_{st}^2}{\sigma_{st}\sqrt{\sigma_{st}^2 + \sigma_{ft}^2 - 2\sigma_{sft}}}. \tag{14}$$

Our model has four specific features as follows. Firstly, it incorporates long-term equilibrium relationship both spot and futures prices. Secondly, it takes into account cross-market interactions between market returns and volatilities. Thirdly, it does not impose constant conditional correlation coefficients. Fourthly, it captures seasonal pattern for both spot and futures market volatilities. Our model specification and technique estimation allow us to capture stochastically seasonal pattern for market volatilities of emissions allowances rather than through deterministic variables. Our estimations imply a less than perfect correlation between spot and futures returns and lead to an optimal hedge below one to hedge spot assets portfolio, without losing any hedging effectiveness in ex-ante simulations of hedging strategies using traded data.

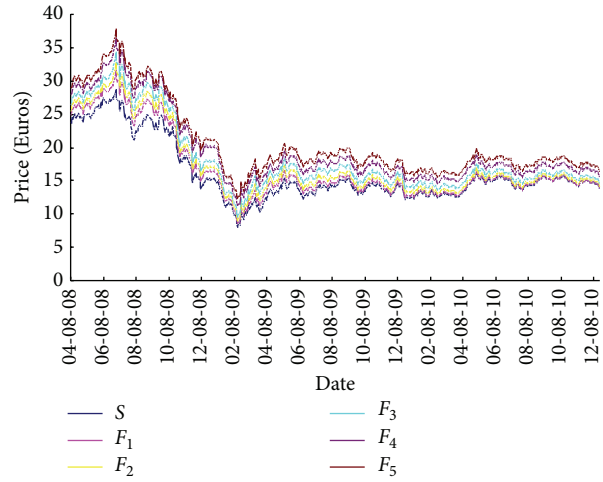

Figure 1: Spot and futures prices of emissions allowances.

5. Data Source

Since the introduction of emissions allowances markets in the European Union in 2005, there are two phases: the Pilot phase (2005–2007) and the Kyoto phase (2008–2012). There are three flexible schemes in the Kyoto protocol: emissions trading scheme (ETS), clean development scheme (CDM), and joint implementation (JI). One European Union allowance (EUA) has the right to emit one tone CO_2 into the atmosphere under the EU ETS. The minimum trading volumes for each futures contract are 1,000 tons of CO_2 equivalent. EUA spot samples are from Bluenext exchange which which has become the most liquid spot trading platform; EUA futures samples are from ICE exchange which has become the most liquid futures trading platform. We choose daily settlement prices for EUA futures contracts with different maturities from December 2010 to December 2014. The trading of futures contracts with vintages December 2013 and December 2014 were started on April 8, 2008. Considering the continuity and availability of numerical samples, we select that date samples cover the period from April 8, 2008 to December 20, 2010 in the Kyoto phrase.

In Figure 1, S denotes spot price of CO_2 emissions allowances, F_1 denotes EUA futures contracts that are the closest to maturity, F_2 denotes the second closest to maturity, and F_3, F_4, and F_5 are defined similarly. From Figure 1, we obviously observe that CO_2 price series both spot and futures with

Table 1: Statistical description of conditional volatility with different maturities disturbed from futures market ($\times 10^{-4}$).

Conditional volatility	Mean	Standard deviation	Maximum	Minimum
cvc_1	2.3389	2.5710	24.3276	0.4901
cvc_2	2.2851	2.5063	24.1736	0.4827
cvc_3	2.2067	2.4255	23.8514	0.4679
cvc_4	2.0228	2.1359	19.4869	0.4219
cvc_5	2.0486	2.1352	19.1370	0.4211

different maturities exhibit similarly time-varying trends throughout data sample period.

6. Empirical Discuss of Conditional Volatility and Correlation

6.1. Conditional Volatility σ_{ct}^2 Estimation Disturbed from Futures Markets. In Figure 2 and Table 1, we estimate conditional volatility σ_{ct}^2 with different maturities disturbed from futures markets using ECM-GARCH (1, 1) model. *cvc*1 denotes conditional volatility of futures prices that are closest to maturity, *cvc*2 denotes conditional volatility with the second closest to maturity, and *cvc*3, *cvc*4, and *cvc*5 are defined similarly. Seen from Figure 2, conditional volatility with different maturities disturbed from futures markets exhibits a time-varying trend. Assuming conditional volatility is constant, static hedge ratio is inappropriate to measure trading risk of emissions allowances. Based on previous historical market information set, we can estimate time-varying hedge ratios using ECM-GARCH (1, 1) model, and then market participants can effectively decrease market trading risks of assets portfolio. From Table 1, mean values of conditional volatility with different maturities disturbed from futures markets are all positive and standard deviations exhibit obvious decline trends with an increase of time-to-maturity. These results show that market noises implied from futures market have higher impacts on conditional volatility of futures contract with shorter time-to-maturity, while they have lower impacts on conditional volatility of futures contract with longer time-to-maturity.

6.2. Conditional Correlation Estimation of Market Noises. In Figure 3 and Table 2, we estimate conditional correlation of market noises between spot and futures, cr_{121} denotes conditional correlation of market noises between spot and futures markets that are the closest to maturity, cr_{122} denotes conditional correlation of market noises between spot and futures markets that are the second closest to maturity, and cr_{123}, cr_{124}, and cr_{125} are defined similarly. Seen from (14) and Figure 3, conditional variance of spot price and of futures price $\sigma_{s,t}^2$, $\sigma_{f,t}^2$ and conditional covariance of prices between spot and futures $\sigma_{sf,t}$ show higher time-varying trends; conditional correlation of market noises between spot and future markets exhibits a strongly time-varying trend. From Table 2, mean values of cr_{121}–cr_{125} are all negative, mean absolute values of cr_{121}–cr_{125} exhibit an increasing trend with

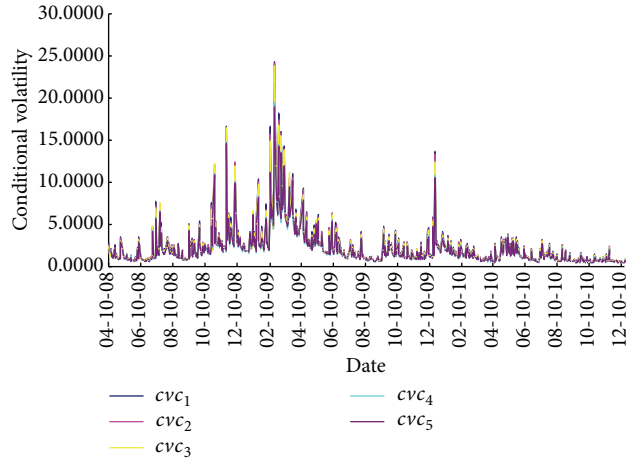

Figure 2: Conditional volatility with different maturities disturbed from futures market ($\times 10^{-4}$).

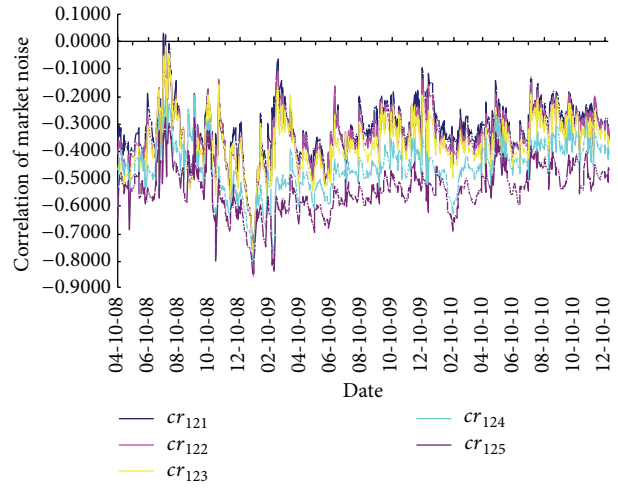

Figure 3: Conditional correlation of market noises between spot and futures.

Table 2: Statistical description of conditional correlation of market noises between spot and futures markets.

Correlation of market noises	Mean	Standard deviation	Maximum	Minimum
cr_{121}	−0.3222	0.0987	0.0321	−0.7470
cr_{122}	−0.3451	0.0960	−0.0291	−0.7596
cr_{123}	−0.3704	0.0958	−0.0131	−0.7662
cr_{124}	−0.4580	0.0937	−0.1914	−0.8179
cr_{125}	−0.5369	0.0865	−0.2759	−0.8539

an increase of time-to-maturity, and their standard deviations show a declining trend.

6.3. Conditional Correlation Estimation. In Figure 4, cr_1 denotes conditional correlation between spot and futures contracts that are the closest to maturity, cr_2 denotes conditional correlation between spot and futures contracts that

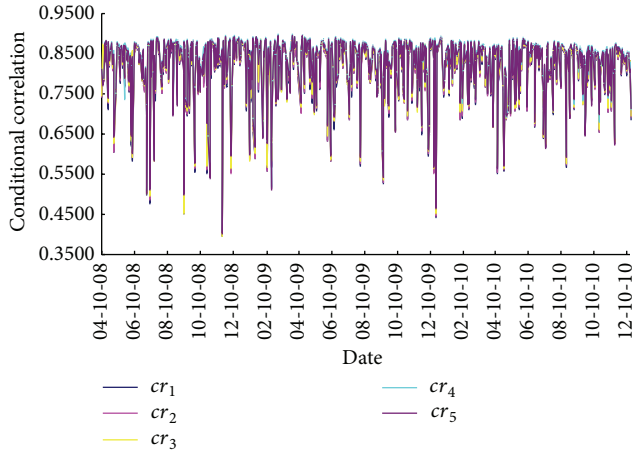

Figure 4: Conditional correlation coefficients between spot and futures with different maturities.

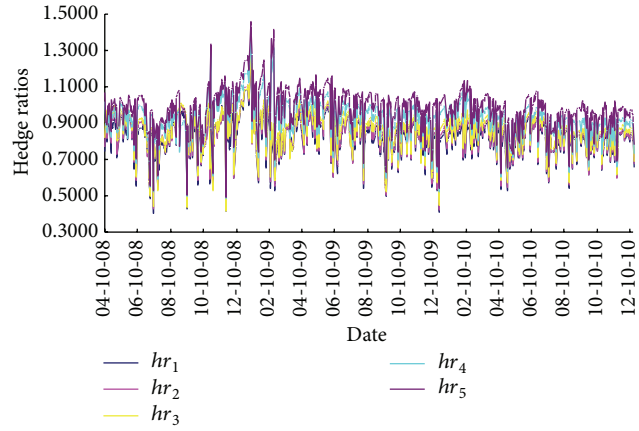

Figure 5: Time-varying hedge ratios of futures contracts with different maturities.

Table 3: Statistical description of conditional correlation coefficients between spot and futures with different maturities.

Conditional correlation	Mean	Standard deviation	Maximum	Minimum
cr_1	0.8142	0.0766	0.8916	0.3935
cr_2	0.8155	0.0764	0.8927	0.3997
cr_3	0.8193	0.0758	0.8951	0.3942
cr_4	0.8275	0.0738	0.8989	0.4062
cr_5	0.8235	0.0747	0.8962	0.4003

Table 4: Statistical description of time-varying hedge ratios of futures contracts with different maturities.

Hedge ratios	Mean	Standard deviation	Maximum	Minimum
hr_1	0.8279	0.1036	1.2421	0.4015
hr_2	0.8423	0.1045	1.2612	0.4168
hr_3	0.8619	0.1050	1.2716	0.4144
hr_4	0.9271	0.1097	1.3690	0.4792
hr_5	0.9776	0.1200	1.4596	0.4892

Table 5: Hedging effectiveness estimation of different-maturity futures contracts.

Futures	F_1	F_2	F_3	F_4	F_5
Hedging effectiveness	0.9080	0.9052	0.8992	0.8599	0.8549

are the second closest to maturity, and cr_3, cr_4, and cr_5 are defined similarly. From Figure 4, optimal hedge ratios with different maturities exhibit strongly time-varying trends using ECM-GARCH (1, 1) model. Seen from Table 3, conditional correlation coefficients between spot and futures with different maturities show greater ranges from 0.39 to 0.90. Mean values of cr_1–cr_4 indicate an increasing trend with an increase of time-to-maturity, and their standard deviations show a decreasing trend.

7. Time-Varying Hedge Ratios and Hedging Effectiveness

7.1. Time-Varying Hedge Ratios. In Figure 5 and Table 4, hr_1 denotes optimal hedge ratio of futures contracts that are the closest to maturity, hr_2 denotes optimal hedge ratio of futures contracts that are the second closest to maturity, and hr_3, hr_4, and hr_5 are defined similarly. Optimal hedge ratios of futures contracts with different maturities exhibit significantly time-varying trends using ECM-GARCH (1, 1) model; they show greater ranges from 0.40 to 1.5. From Table 4, mean values of optimal hedge ratios exhibit an increasing trend with an increase of time-to-maturity, and their standard deviations show an enlarging trend.

7.2. Hedging Effectiveness Estimation. Compared with the minimum variance of unhedged portfolio returns, Edderington [19] asserted that percentage reduction in the variance of hedged portfolio returns estimate hedging effectiveness (HE). Hedging portfolio returns are estimated using time-varying hedge ratios from ECM-GARCH model as follows (Table 5):

$$\mathrm{HE} = \frac{\mathrm{Var}\left(U_t\right) - \mathrm{Var}\left(H_t\right)}{\mathrm{Var}\left(U_t\right)}, \tag{15}$$

where $\mathrm{Var}(U_t)$ denotes the variance of unhedged assets portfolio returns and $\mathrm{Var}(H_t)$ denotes the variance of hedged assets portfolio returns. When futures prices for CO_2 emissions allowances completely decrease the risks of hedging portfolio returns, we can obtain HE = 1 which indicates

a 100% reduction in the variance of hedging portfolio returns, whereas we can obtain HE = 0 when hedging portfolio returns do not eliminate risk. Large number of HE shows better hedging performance between spot and futures with different maturities.

Compared with unhedged assets portfolio returns, market investors optimize hedge sizes between spot and futures with different maturities using previous optimal hedge ratios, and then the variance of hedging portfolio returns exhibits a significantly declining trend. The hedging risk of futures contracts that are the closest to maturity has an obvious 90.80% reduction, while the hedging risk of futures contracts that are the longest to maturity has an obvious 85.49% reduction. With an increase of time-to-maturity, hedging risks of futures contracts with different maturities exhibit a significantly declining trend.

8. Conclusion

Under departures from the cost-of-carry theory, conditional variance disturbed from futures market and conditional covariance between spot and futures of emissions allowances exhibit significantly time-varying trends, and market noises implied from futures market have significant impacts on conditional volatility. Conditional correlations of market noises between spot and futures markets are all negative, while conditional correlations between spot and futures are all positive; they exhibit obviously time-varying trends. Under departures from the cost-of-carry theory, optimal hedge ratios exhibit significantly time-varying trends using ECM-GARCH model, and time-varying hedge ratios show an enlarging trend with an increase of time-to-maturity. The conditional volatility of spot prices, conditional volatility disturbed from futures market, and conditional correlation coefficients of market noises implied from spot and futures markets have significant impacts on time-varying hedge ratios and hedging effectiveness. Market participants optimize assets portfolio sizes between spot and futures with different maturities using time-varying hedge ratios with departures from the cost-of-carry theory; the hedging risks of assets portfolio revenues have a significantly declining reduction, and they can achieve better hedging effectiveness.

Compared with financial markets and commodities markets such as gold, crude oil, and agriculture, current emissions allowances market has a more nascent and weaker market efficiency. Based on empirical results by Lafuente and Novales [14], Andani et al. [20] found that stock index futures markets in fully developed market exhibit a less liquid market, conditional volatility implied from futures market and conditional correlation of market noises exhibit lower fluctuated trends, and the discrepancy between theoretical and traded prices in fully mature financial markets does not represent a market noise factor that can be successfully exploited for hedging effectiveness. Some commodities markets have been significantly affected by specific market factors, such as agriculture market affected by extreme weather and specific geographic features and gold and crude oil commodities markets affected by production and transportation conditions. Emissions allowances market is quite different with general financial markets and commodities markets, emissions allowances prices are directly determined by the expected market scarcity induced by some specific market factors such as emissions reduction plan, government regulation policy, extreme weather deterioration, prices volatilities of different fossil energy, and emissions-reducing technology promotion and application. A good many complex markets factors exert greater market price shocks; however, price shock effectiveness has a tremendous difference in time and channel between emissions allowances spot and futures prices in the immature emissions allowances markets. Unexpected market information exhibits a different change speed for spot and futures prices; emissions allowances markets exhibit a greater lead-lag relationship between spot and futures. Based on the cost-of-carry theory, the theoretical and traded futures prices have a higher time-varying market deviation trends; their conditional volatility disturbed from futures market and conditional correlation coefficients of market noises implied from spot and futures markets are significantly greater than financial markets and commodities markets. An active hedging strategy involving spot and futures markets seems to be of interest in previous historical market information, conditional volatility disturbed from futures market, and conditional correlation of market noises between spot and futures when market participants attempt to achieve risk reduction. Market participants can flexibly adjust their assets portfolio policies between spot and futures and then achieve additional arbitrage returns under departures from cost-of-carry theory.

Effective macrocontrol and macroregulation are necessary to improve market efficiency in the emissions allowances markets. Macrocontrolling failure, uncertain decision, and inactive trading volumes have significant impacts on time-varying hedging effectiveness for emissions allowances. Government regulators should establish scientific emissions reduction plan and strict emissions quota allocation rules. Government should make consistent and systematic decision in the greenhouse emissions reduction, support regime-switching behaviors among different emissions markets, and strengthen international cooperation in the greenhouse emissions reduction. Government should present an international information network system of emissions trading markets, motor and check emissions reduction information. Market participants time capture demand and supply information, and then achieve fair, transparent, and symmetric emissions information. Emissions investors, hedgers, and arbitragers should be aware of risk reduction between spot and futures, regime switches, and threshold effects when attempting to forecast both spot and futures prices. An active hedging strategy involving spot and futures markets seems to be of interest in conditional volatility and correlation coefficients implied from futures markets. Our empirical pieces of evidence in this paper are helpful to more effectively reduce fluctuations risk of assets portfolio; market investors and hedgers should make optimally time-varying hedging policy to optimize hedging portfolio returns using time-varying hedge ratios under departures from cost-of-carry theory and then enhance the capabilities in risk reduction of assets portfolio for emissions allowances.

Acknowledgments

The authors are grateful for research support from the Center for Research of Regulation and Policy of Zhejiang Province (13JDGZ03YB), Research Planning of Statistical Science in China (2013LY125), and Research Planning Foundation on Humanities and Social Sciences of the Ministry of Education (11YJA790152).

References

[1] E. Benz and S. Truck, "CO_2 emission allowances trading in Europe—specifying a new class of assets," *Problems and Perspectives in Management*, vol. 4, pp. 30–40, 2006.

[2] E. Benz and S. Truck, "Modeling the price dynamics of CO_2 emission allowances," *Energy Economics*, vol. 31, no. 1, pp. 4–15, 2009.

[3] J. Seifert, M. Uhrig-Homburg, and M. Wagner, "Dynamic behavior of CO_2 spot prices," *Journal of Environmental Economics and Management*, vol. 56, no. 2, pp. 180–194, 2008.

[4] G. Daskalakis, D. Psychoyios, and R. N. Markellos, "Modeling CO_2 emission allowance prices and derivatives: evidence from the European trading scheme," *Journal of Banking and Finance*, vol. 33, no. 7, pp. 1230–1241, 2009.

[5] C. Conrad, D. Rittler, and W. Rotfuß, "Modeling and explaining the dynamics of European Union Allowance prices at high-frequency," *Energy Economics*, vol. 34, no. 1, pp. 316–326, 2012.

[6] A. Montagnoli and F. P. de Vries, "Carbon trading thickness and market efficiency," *Energy Economics*, vol. 32, no. 6, pp. 1331–1336, 2010.

[7] Y.-J. Zhang and Y.-M. Wei, "Interpreting the mean reversion of international carbon futures price: empirical evidence from the EU ETS," *System Engineering Theory and Practice*, vol. 31, no. 2, pp. 214–220, 2011.

[8] M. E. H. Arouri, F. Jawadi, and D. K. Nguyen, "Nonlinearities in carbon spot-futures price relationships during Phase II of the EU ETS," *Economic Modelling*, vol. 29, no. 3, pp. 884–892, 2012.

[9] K. Chang, S. Wang, and H. Chang, "Convenience yields and options value on futures spread for carbon emission," in *Proceedings of the IEEE 2nd International Conference on Computing, Control and Industrial Engineering (CCIE '11)*, pp. 182–185, August 2011.

[10] H. Working, "The theory of the price of storage," *American Economic Review*, vol. 39, pp. 1254–1262, 1949.

[11] M. Brennan, "The supply of storage," *American Economic Review*, vol. 48, pp. 50–72, 1958.

[12] W. Wilson, "Price discovery and hedging in the sunflower market," *The Journal of Futures Markets*, vol. 9, pp. 377–391, 1989.

[13] D. Lien and Y. K. Tse, "Fractional cointegration and futures hedging," *Journal of Futures Markets*, vol. 19, no. 4, pp. 457–474, 1999.

[14] J. A. Lafuente and A. Novales, "Optimal hedging under departures from the cost-of-carry valuation: evidence from the Spanish stock index futures market," *Journal of Banking and Finance*, vol. 27, no. 6, pp. 1053–1078, 2003.

[15] L. L. Johnson, "The theory of hedging and speculation in commodity futures," *Review of Financial Studies*, vol. 27, pp. 139–151, 1960.

[16] D. Lien, Y. K. Tse, and A. K. C. Tsui, "Evaluating the hedging performance of the constant-correlation GARCH model," *Applied Financial Economics*, vol. 12, no. 11, pp. 791–798, 2002.

[17] D. Lien and L. Yang, "Asymmetric effect of basis on dynamic futures hedging: empirical evidence from commodity markets," *Journal of Banking and Finance*, vol. 32, no. 2, pp. 187–198, 2008.

[18] H. F. Peng and Y. G. Ye, "The evaluation and comparison research of dynamic optimal hedging ratios based on modified ECM-GARCH," *Chinese Journal of Management Science*, vol. 15, pp. 29–35, 2007.

[19] L. H. Ederington, "The hedging performance of the new futures markets," *Journal of Finance*, vol. 34, pp. 157–170, 1960.

[20] A. Andani, J. A. Lafuente, and A. Novales, "Liquidity and hedging effectiveness under futures mispricing: International evidence," *Journal of Futures Markets*, vol. 29, no. 11, pp. 1050–1066, 2009.

Hindawi Publishing Corporation
Discrete Dynamics in Nature and Society
Volume 2013, Article ID 439305, 19 pages
http://dx.doi.org/10.1155/2013/439305

Research Article

Basel III and Asset Securitization

M. Mpundu, M. A. Petersen, J. Mukuddem-Petersen, and F. Gideon

Faculty of Commerce & Administration, North-West University (Mafikeng Campus), Private Bag x2046, Mmabatho 2735, South Africa

Correspondence should be addressed to M. A. Petersen; mark.petersen@nwu.ac.za

Received 14 June 2013; Revised 28 September 2013; Accepted 30 September 2013

Academic Editor: Oswaldo Luiz do Valle Costa

Copyright © 2013 M. Mpundu et al. This is an open access article distributed under the Creative Commons Attribution License, which permits unrestricted use, distribution, and reproduction in any medium, provided the original work is properly cited.

Asset securitization via special purpose entities involves the process of transforming assets into securities that are issued to investors. These investors hold the rights to payments supported by the cash flows from an asset pool held by the said entity. In this paper, we discuss the mechanism by which low- and high-quality entities securitize low- and high-quality assets, respectively, into collateralized debt obligations. During the 2007–2009 financial crisis, asset securitization was seriously inhibited. In response to this, for instance, new Basel III capital and liquidity regulations were introduced. Here, we find that we can explicitly determine the transaction costs related to low-quality asset securitization. Also, in the case of dynamic and static multipliers, the effects of unexpected negative shocks such as rating downgrades on asset price and input, debt obligation price and output, and profit will be quantified. In this case, we note that Basel III has been designed to provide countercyclical capital buffers to negate procyclicality. Moreover, we will develop an illustrative example of low-quality asset securitization for subprime mortgages. Furthermore, numerical examples to illustrate the key results will be provided. In addition, connections between Basel III and asset securitization will be highlighted.

1. Introduction

Asset securitization involves the process by which securities are created by a special purpose entity (SPE)—hereafter, simply known as an entity—and then issued to investors with a right to payments supported by the cash flows from a pool of financial assets held by the entity. There is broad-based usage of entities by financial institutions of many types, in various jurisdictions, and for many purposes (see, e.g., [1]). Securitization has been popular as an alternative funding source for consumer and asset lending in market economies. Its main objective is to improve credit availability by converting hard-to-trade and nontradable assets into securities that can be traded on capital markets. The categorization of the payment rights into "tranches" paid in a specific order and supported by credit enhancement mechanisms provides investors with diversified credit risk exposure to particular investor risk appetites (see, e.g., [2, 3]). Immediately prior to the securitization market collapse in 2007-2008, structured asset products (SAPs) such as asset-backed securities (ABSs) and collateralized debt obligations (CDOs) as well as covered bonds provided between 25 and 65% of the funding for new residential assets originated in the US and Western Europe (see, e.g., [4]). In most developed economies, SAP growth peaked by 2007 before declining rapidly due to a lack of liquidity in secondary markets and decreases in primary issuance (see [5] for more details). For example, SAP issuance in the US decreased from about US $2 trillion in 2007 to around US $400 billion in 2008. The impact of the financial crisis on securitization in emerging markets was more modest as initial growth had been more subdued.

The contribution of securitization to the financial crisis necessitated changes to banking regulation. In this regard, the introduction of Basel III capital and liquidity regulation includes elements that will potentially affect the incentives for banks to securitize assets (see, e.g., the Basel documents [2, 5–7]). There are several Basel III provisions that address areas of concern that were highlighted during the financial crisis and which supervisors determined as not adequately addressed under the previous framework (see, e.g., [6]). More specifically, in July 2009, the Basel Committee for Banking Supervision (BCBS) published enhancements to the Basel II framework that were intended to strengthen the framework and respond to lessons learned from the financial crisis (see [8] for more details). For instance, because of the higher degree of inherent risk in resecuritization exposures,

the BCBS significantly increased the risk weights applicable to such exposures under both the standardized (SA) and internal ratings based (IRB) approaches relative to the risk weights for other securitization exposures (see, e.g., [3, 9, 10]). As a result, the capital requirements for resecuritization have risen dramatically. In addition, to address the lack of appropriate due diligence on the part of investing institutions and deter them from relying solely on external credit ratings, the Basel framework now requires banks to meet specific operational criteria in order to use the risk weights specified in the Basel II securitization framework. During the financial crisis, credit rating agencies (CRAs) downgraded the ratings of many securitization tranches, including senior trances, highlighting deficiencies in credit rating agency models originally used to determine the ratings. Capital requirements assigned to highly rated (e.g., AAA) senior and mezzanine securitization exposures were too low and this was illustrated by the poor performance of these securities (see, e.g., [9, 10]). As CRAs downgraded highly rated securitization exposures below investment grade, regulatory capital requirements increased rapidly and significantly due to the presence of cliff effects within the securitization framework (in this context, cliff effects refer to significant increases in capital requirements resulting from a change to a factor used to assign regulatory capital) (see, e.g., [9, 10]). The BCBS also revised the market risk rules to increase the level of capital that must be maintained against securitization exposures held in the trading book. In addition, the BCBS is reviewing whether the risk weights for all securitization exposures should be recalibrated, which could lead to higher capital requirements (see, for instance, the Basel papers [9, 10]).

The main motivation for this paper is that securitization has to be reestablished on a sound basis in order to support credit provision to the real economy and enhance banks' access to funding globally (see, e.g., [4]). Basel III would like to ensure an appropriate risk-sensitive and prudent capitalization of risks arising from securitization exposures while reducing cliff effects and mitigating mechanistic reliance on external credit ratings (see [3, 9]). The interplay between Basel III and asset securitization will be the central theme of this paper. As far as the contribution of this paper is concerned, we investigate the securitization of low- and high-quality assets (denoted by LQAs and HQAs, resp.) into CDOs via low-quality entities (LQEs) and high-quality entities (HQEs), respectively, (see, e.g., the BCBS publications [9, 10]).

1.1. Literature Review about Asset Securitization and Basel III. In this subsection, we provide literature reviews about asset securitization and Basel III capital and liquidity regulation (see [5] for more details).

1.1.1. Literature Review about Asset Securitization. Motivated by the 2007–2009 financial crisis, there is an ever-growing body of literature on LQA-related issues such as shocks to LQEs, investors, and CDOs via, for instance, rating changes. The contribution [11] studies the pricing of LQAs and related SAPs on the basis of data for the ABX.HE family of indices (see [12] for further details). This, of course, is a recurring theme in our contribution where we consider asset and CDO pricing during the financial crisis. Moreover, [4] addresses the impact of speculative asset funding on the pricing of LQAs (measured by risk premia) and securities backed by these assets (measured by ABX.HE indices). In addition, the paper [13] extends a Kiyotaki-Moore-type model that shows how relatively small shocks might suffice to explain business cycle fluctuations, if credit markets are imperfect (see [14] for more details). Our work has a connection with this paper via the consideration of the effect of shocks on asset parameters although we do not emphasize the imperfection of credit markets (see [15] for additional analysis). The paper [16] studies the impact of penalties on LQ-loans (see, also, [17]). Here, asset prices and penalties are chosen simultaneously with the latter being associated with lower asset prices (see [15] for more details). The paper also contains discussions on prices and penalties and their relationship with loan-to-value ratios (see, also, [18] for more on house equity). In our contribution, we will use the framework introduced in [16] to show how a change in profit subsequent to a negative shock is influenced by subprime mortgage features (see, also, [19]).

1.1.2. Literature Review about Basel III. In July 2009, the BCBS introduced enhancements to the Basel II framework via [8]. This was done in order to address deficiencies identified during the 2007–2009 financial crisis. These measures primarily addressed immediate concerns over resecuritization and was part of reforms known as "Basel 2.5" (see the Basel documents [8, 9] for more details about securitization). The BCBS subsequently agreed to conduct a more fundamental review of the securitization framework, including its reliance on external ratings (see, e.g., [20]). The performance of and role played by securitization exposures during the financial crisis were a key motivation for studying this category of the capital framework. Subsequently, in [2], the BCBS noted that it was "conducting a more fundamental review of the securitization framework, including its reliance on external ratings." The BCBS has now performed a broader review of the securitization framework for regulatory capital requirements with objectives motivated by events during the financial crisis (see, also, [7]). Furthermore, the consultative document [6] reflects the BCBS's proposal to revise the Basel framework's treatment of securitization exposures. In developing this proposal, the BCBS seeks to make capital requirements more prudent and risk sensitive, mitigate reliance on external credit ratings, and reduce cliff effects (see, e.g., [3, 6]). In particular, our paper adds to the debate about rating downgrades and shocks associated with them. The policy directions set out in [6] form part of the BCBS's broader agenda of reforming bank regulatory capital standards to address the lessons of the crisis. These proposals build on a series of reforms that the BCBS has delivered through Basel III and explain the approaches under consideration by the BCBS to revise the securitization framework (see [6, 21] for further discussion). As in our paper, the features of SPEs are discussed in some detail in [1].

1.2. Preliminaries about Asset Securitization. In this subsection, we provide preliminaries about low- and high-quality

Table 1: Defining features of LQAs and HQAs; source: [5].

Feature	LQAs	HQAs
External information		
External ratings	Low	High
Market data	Poor	Rich
Analysts' reports	Negative	Positive
Internal information		
Credit risk	High	Low
Liquidity risk	High	Low
Securitization exposure	Not understood	Understood
Financial obligations	Not easily met	Easily met

classification as well as LQA and HQA securitization (see Table 1 for more information).

1.2.1. Preliminaries about Low- and High-Quality Classification. As indicated in the BCBS documents [2, 7], the characterization of "high quality" is based both, on available external information, such as external ratings, market data, and analyst's reports, and the entity's own assessment of credit and liquidity risk, whereby the entity should demonstrate its understanding of the terms of the securitization exposure and the risks of the underlying collateral (see, e.g., [1, 5]). The entity would be required to demonstrate that the credit quality of the position is strong, with very low default risk, and is invulnerable to foreseeable events, implying that financial commitments would be met in a timely manner with a very high probability (see [6, 21] for further discussion). Where this determination could not be made, the position would be assumed to be "low quality." In particular, in the Basel III document [1], the Joint Forum Working Group on Risk Assessment and Capital (JFWGRAC) consisting of the BCBS, International Organization of Securities Commissions (IOSC), and the International Association of Insurance Supervisors (IAIS) under the support of the Bank for International Settlements (BIS), make recommendations about such entities.

1.2.2. Preliminaries about LQA and HQA Securitization. In this paper, we have that the reference asset portfolios are both a means of generating CDOs and collateral for interentity sponsoring (see, e.g., [1]). Our paper quantifies the effects of unexpected negative shocks such as rating downgrades on asset price and input, CDO price and output, and profit in a Basel III context (see, also, [19]). For instance, the aforementioned result demonstrates how the proportional change in profit subsequent to a rating downgrade is influenced by LQA features such as asset rates. Finally, we present examples that illustrate that asset price is most significantly affected by unexpected negative shocks from asset rates, while, for CDO price, shocks to speculative asset funding, investor risk characteristics, and prepayment rate elicit statistically significant responses (compare with [3]).

LQAs were financed by securitizing these assets into SAPs such as ABSs and CDOs. The lower-rated tranches of low-quality ABSs formed 50 to 60% of the collateral for CDOs during 2007. These were extremely sensitive to a deterioration in asset credit quality. Housing went through a classic inventory cycle with a worsening of the inventory-to-sales cycle being evident in the midst of the 2007–2009 financial crisis. When this inventory situation worsened, the risk that price would fall more rapidly deepened. The more substantial fall in prices accelerated the delinquency and foreclosure rater and spelt doom for the CDO market which was further revised in Basel III (see, e.g., the BCBS paper [3, 9]). We briefly describe the aforementioned SAPs in turn.

LQ-ABSs are quite different from other securitizations because of the unique features that differentiate low-quality assets from other assets. Like other securitizations, LQ-ABSs of a given transaction differ by seniority. But unlike other securitizations, the amount of *credit enhancement* for and the size of each tranche depend on the *cash flow* coming into the deal in a very significant way. The cash flow comes largely from prepayment of the reference asset portfolios through refinancing. What happens to the cash coming into the deal depends on *triggers* which measure (prepayment and default) performance of the reference asset portfolios. The triggers can potentially divert cash flows within the structure. In some case, this can lead to a leakage of protection for higher-rated tranches. Time tranching in low-quality transactions is contingent on these triggers. The structure makes the degree of credit enhancement dynamic and dependent on the cash flows coming into the deal.

In our case, a CDO issues debt and equity and uses the income to invest in financial assets such as assets and ABSs. It distributes the cash flow from its asset portfolio to holders of various liabilities—usually a capital structure consisting of equity or preferred shares, subordinated debt, mezzanine debt and AAA-rated senior debt, and borrowings—in set ways taking into account the relative seniority of the aforementioned liabilities. A key feature of such CDOs is that they are mainly constituted by ABS portfolios that are rated according to their prevailing credit risk and put into tranches (compare with [3]). CDO tranches include LQ- and Alt-A deals and consist of three categories, namely, senior, mezzanine, and equity or low tranches according to increasing credit risk. This risk is spread to investors who invest in these risky CDO tranches. It is difficult for investors to locate the risk exposure of these CDOs because of their complex design structure. Despite this, CDOs have additional structural credit protection which can be characterized as either cash flow or market value protection. Finally, all CDOs are created to fulfill a given purpose that can be classified as arbitrage, balance sheet, or origination.

1.3. Main Contributions and Outline. The main contributions about Basel III regulation and asset securitization in this paper are constituted by the answers to the questions listed below.

Question 1 (LQA securitization). How can we characterize the securitization of LQAs into CDOs by the LQE? For instance, can we determine the LQE cash flow constraint? (see Lemma 3 in Section 2.1).

Question 2 (HQA securitization). How can we characterize the securitization of HQAs into CDOs by HQEs? For instance, can we determine the HQEs' cash flow constraint? (see Lemma 5 in Section 2.2).

Question 3 (LQE at steady state). How can we characterize the behavior of an LQE at steady state? (see Theorem 7 in Section 2.3).

Question 4 (dynamic multiplier: negative shocks to asset securitization). For a dynamic multiplier, how do negative shocks affect asset price and input, CDO price and output, and profit? (see Theorem 8 in Section 3.1).

Question 5 (static multiplier: temporary shocks to asset securitization). For a static multiplier, how do negative shocks affect asset price and input? (see Corollary 9 in Section 3.2).

Question 6 (example of subprime mortgage securitization). How can we provide an example to illustrate the main features of LQA securitization specifically for subprime mortgages? (see Corollary 10 in Section 4.1).

Question 7 (numerical examples of asset securitization). How can we provide numerical examples to illustrate the main results obtained in this paper? (see Section 4.2).

Question 8 (Basel III and asset securitization in general). In general, how does Basel III capital and liquidity regulation assist in eliminating flaws in existing asset securitization practice in banking? (see Sections 2, 3, and 4 for more details).

This paper is arranged as follows. Section 2 describes HQA and LQA securitization. Also, Section 3 sheds light on the effect of negative shocks like rating downgrades on the asset securitization process in a Basel III context while Section 4 provides numerical examples of the aforementioned. Finally, Section 5 provides some concluding remarks and possible topics for future research.

2. Low- and High-Quality Entities

In this section, we consider LQEs and HQEs and their equilibrium features. We study an economy consisting of LQAs with a fixed total supply of $\overline{A}$ and CDOs that cannot be retained by the entity. In the sequel, for the sake of argument, we assume that the CDOs correspond to senior CDO tranches. In this model, CDOs are taken as the numeraire. There is a continuum of infinitely lived LQEs and HQEs, with population sizes 1 and n, respectively. Both these entities take one period to securitize assets into CDOs—the LQEs and HQEs produce CDOs from HQAs and LQAs, respectively—but they differ in their securitization technologies (refer to Table 1). At each date, t, there is a competitive spot market in which assets for CDOs are purchased by entities at a price of p_t^A. The only other market is a one-period credit market in which one CDO unit at date t is exchanged for a claim to $1 + r_t^B$ units of CDOs at date $t + 1$. These markets are opaque and are dominated by a handful of interests. During the 2007–2009 financial crisis, because CDOs were lightly regulated their details often went undisclosed. This created major problems in the monitoring of these credit derivatives and the new regulatory framework in Basel III focuses on correcting such problems (see [9] for further explanation).

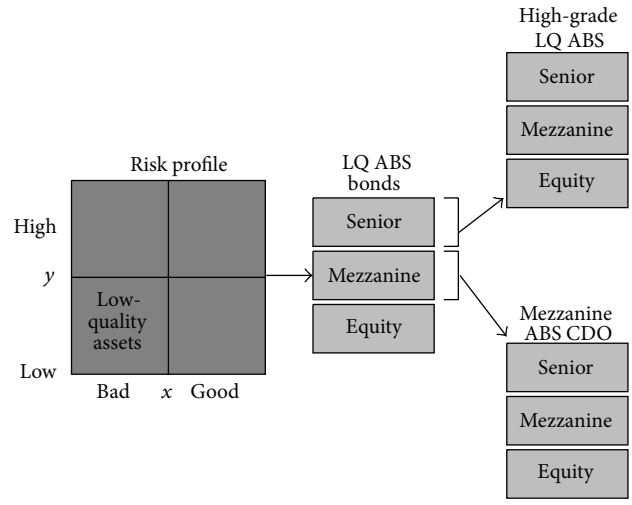

Figure 1: Chain of LQAs and their SAPs; source: [4].

2.1. The LQE. Figure 1 illustrates the securitization of assets into ABSs and ABS CDOs by the LQE.

We notice from Figure 1 that LQAs are securitized into ABSs that, in turn, get securitized into ABS CDOs. As far as the latter is concerned, it is clearly shown that senior ABS bonds rated AAA, AA, and A constitute the *high-grade* ABS CDO portfolio. On the other hand, the mezzanine-rated ABS bonds are securitized into *mezzanine ABS CDOs*, since its portfolio is based on BBB-rated ABSs and their tranches which expose the portfolio to an increase in credit risk (see, e.g., [3]). From Figure 1, it is clear that the LQEs (and any other entities), rather than banks, hold assets and ABSs. As a result, there are reductions in the incentives of banks to play their traditional monitoring function. The fundamental role of banks in financial intermediation according to Basel III in the document [22] (see, also, [21]) makes them inherently vulnerable to liquidity risk, of both an institution-specific and market nature (see [5] for more details). Financial market developments have increased the complexity of liquidity risk and its management. During the early "liquidity phase" of the financial crisis that began in 2007, many banks—despite adequate capital levels—still experienced difficulties because they did not manage their liquidity in a prudent manner (see [5] for further discussion). The difficulties experienced by some banks, which, in some cases, created significant contagion effects on the broader financial system, were due to lapses in basic principles of liquidity risk measurement and management (see, e.g., [5] for more details). During the 2007–2009 financial crisis, systemic risk from CDOs was problematic. In this case, the default of one or more collateral

assets or bond classes generated a ripple effect on CDO defaults. Figure 1 suggest how this may have happened. The LQE is risk neutral, with its expected utilities being

$$\mathbf{E}_t\left(\sum_{s=0}^{\infty}\beta^s x_{t+s}\right), \qquad \mathbf{E}_t\left(\sum_{t=0}^{\infty}\beta^t x_t\right), \tag{1}$$

where x_{t+s} and x_t are their respective LQE CDO consumption at dates $t+s$ and t, with $\mathbf{E}_t$ denoting the expectation formed at date t. These entities have constant returns on scale securitization function of

$$C_{t+1} = S\left(A_t\right) \equiv \left(\mu+\nu\right)A_t, \qquad \nu = c + r^f, \qquad \left(\frac{\mu}{\mu+\nu}\right) < \beta, \tag{2}$$

where A_t are the input assets securitized at date t and C_{t+1} is the CDO output at date $t+1$. Also, r^f is the fraction of assets that have refinanced and c the fraction of CDOs consumed. However, only μA_t of the CDO output is marketable. Here, νA_t is nonmarketable and can be consumed by the LQE. We introduce νA_t in order to avoid the situation in which the LQE continually postpones consumption. The ratio $\mu(\mu+\nu)^{-1}$ may be thought of as a technological upper bound on the LQE's retention rate. Since β is near 1, the inequality in (2) amounts to a weak assumption. We shall see later that this inequality ensures that in equilibrium the LQE will not want to consume more than illiquid CDOs as observed in Basel III (see, e.g., [21]). The overall return from investment, $\mu+\nu$, is high enough that all its marketable CDO outputs are used for investment. There is a further critical assumption we make about investing.

Assumption 1 (LQE CDO technology and labor). We assume that each LQE's CDO technology is distinct in the sense that, once securitization has started at date t with assets, A_t, only the LQE has the skill necessary for securitizing assets into CDOs at date $t+1$, subject to the availability of appropriate technology and labor. Secondly, we assume that an LQE always has the option to withdraw its labor.

In other words, if the LQE were to withdraw its labor between dates t and $t+1$, there would be no CDO output at $t+1$. Assumption 1 leads to the fact that if an LQE is highly leveraged, it may find it advantageous to threaten the HQEs by withdrawing its labor and repudiating its debt contract. HQEs as interentity lenders protect themselves from the threat of repudiation by collateralizing the LQAs. However, because assets yield no SAPs without the LQE's labor, the asset liquidation value (outside value) are less than what the assets would earn under its control (inside value). Thus, following a repudiation, it is efficient for the LQE to persuade the sponsoring HQE into letting it keep the assets. In effect, the LQE can renegotiate a smaller loan. HQEs know of this possibility in advance, and so take care never to allow the size of the debt (gross of interest) to exceed the value of the collateral as in the following assumption.

Assumption 2 (credit limit). If at date t, the LQE possesses the assets, A_t, then it can borrow $\mathtt{B}_t$ in total, as long as the repayment does not exceed the market value of assets at date $t+1$ given by

$$\left(1+r^{\mathtt{B}}\right)\mathtt{B}_t \le p_{t+1}^A A_t, \tag{3}$$

where p_{t+1}^A represents the asset price in period $t+1$ while A_t represents the LQE's asset holdings in period t. In this case, given rational expectations, agents have perfect foresight of future asset prices.

As noted in the Basel III document [21], the objective of the LCR is to promote the short-term resilience of the liquidity risk profile of banks (see [5] for additional). It does this by ensuring that banks have an adequate stock of unencumbered high-quality liquid assets (HQLA) that can be converted easily and immediately in private markets into cash to meet their liquidity needs for a 30-calendar-day liquidity stress scenario. Of course, during the 2007–2009 financial crisis, when monitoring incentives was reduced, it is unlikely that the HQE monitored the LQE closely. The LQE's balance sheet consists of assets and marketable securities (assets) as well as borrowings and capital (liabilities). Therefore, an LQE's balance sheet constraint can be represented at time t as

$$p_t^A A_{t-1} + B_t = \mathtt{B}_t + K_t, \tag{4}$$

where $p^A, A, B, \mathtt{B}$, and K represent the LQE's asset price, asset holdings, marketable securities, borrowings, and capital, respectively. As we have mentioned before, the entities' capital structure consisting of equity or preferred shares, subordinated debt, and mezzanine debt LQE enforces a price cap (PC), with the weighted average PC being denoted by $\overline{p}$ (see, e.g., [4] for more details). In this case, we have that the CDO price is given by

$$p_t^C = \min\left[p_t^A, \overline{p}_t\right], \tag{5}$$

where C_{t-1} denotes the quantity of CDOs in period $t-1$. Hedge funds and other sophisticated investors have incentives to manipulate the pricing and structuring of CDOs. Some studies suggest that CDO managers manipulate collateral in order to shift risks among various tranches. The potential for this can be clearly seen in (5) where the PC offers a means of changing collateral features that is important in determining the CDO price, p_t^C. During the 2007–2009 financial crisis, collateral according to Basel III was also manipulated via the violation of restrictions on asset portfolio composition, rating category, weighted average life, weighted average weighting factor, correlation factors, and the number of obligors (see [2]). Nevertheless, in our case, the value of assets in period t can be represented as

$$p_t^A A_{t-1} = \mathtt{B}_t + K_t - B_t. \tag{6}$$

In general, the asset rate, r^A, for profit maximizing entities (see, also, [19]), may be represented as

$$r_t^A = r_t^L + \varrho_t, \tag{7}$$

where r^L is, for instance, the 6-month LIBOR rate and ϱ is the risk premium, that is indicative of asset price (see, e.g., [3]). Next, the LQE's profit may be expressed as

$$\Pi_t = \left(r_t^A + c_t^p r_t^f - \left(1 - r_t^R\right) r_t^S\right) p_t^A A_{t-1} + r^B B_t - r^{\mathrm{B}} \mathrm{B}_t, \quad (8)$$

where r^A, c^p, r^f, r^R, r^S, r^B, and r^{B} represent the asset rate, prepayment costs, fraction of assets that refinance, recovery rate, default rate, returns on marketable securities, and borrowing rate in period t, respectively. In this case, asset value can be represented by

$$p_t^A A_{t-1} = \frac{\Pi_t - r^B B_t + r^{\mathrm{B}} \mathrm{B}_t}{r_t^A + c_t^p r_t^f - \left(1 - r_t^R\right) r_t^S}. \quad (9)$$

From (9), it is clear that, as recognized by Basel III regulation, even a relatively small default rate can trigger a crisis. The unwinding of contracts involving the securitization of such assets—such as CDO contracts—created serious liquidity problems during the 2007–2009 financial crisis as detailed in Basel III (see [5, 21, 22]). Since the CDO market was quite large, the crisis caused convulsions throughout global financial markets. By considering the above, we can deduce an appropriate LQE cash flow constraint in the following result.

Lemma 3 (LQE cash flow constraint). *Suppose that the credit constraint* (3) *as well as* (6) *to* (9) *holds. In this case, the LQE's cash flow is subject to the constraint*

$$\begin{aligned}\Pi_t \geq{}& \left(r_t^A + c_t^p r_t^f - \left(1 - r_t^R\right) r_t^S\right) p_t^A A_{t-1} + r^B B_t \\ &- p_{t+1}^A A_t + \mathrm{B}_t.\end{aligned} \quad (10)$$

Proof. The proof follows from taking constraint (3) from Assumption 2 and (10) into consideration. □

The LQE can expand its scale of securitization by investing in more assets. Consider an LQE that holds A_{t-1} assets at the end of date $t-1$ and incurs a total debt of B_{t-1}. At date t, the LQE harvests μA_{t-1} marketable CDOs, which, together with a new loan B_t, is available to cover the cost of purchasing new assets, to repay the accumulated debt $(1 + r^{\mathrm{B}})\mathrm{B}_{t-1}$ (which includes interest), and to meet any additional consumption $x_t - \nu A_{t-1}$ that exceeds the normal consumption of non-marketable output νA_{t-1}. The LQE's flow-of-funds constraint is thus

$$p_t^A \left(A_t - A_{t-1}\right) + \left(1 + r^{\mathrm{B}}\right) \mathrm{B}_{t-1} + x_t - \nu A_{t-1} = \mu A_{t-1} + \mathrm{B}_t. \quad (11)$$

2.2. HQEs. For HQEs, Figure 2 shows the chain formed by HQAs, ABSs, and ABS CDOs.

As we proceed from left to right in Figure 2, HQAs are securitized into ABSs that, in turn, get securitized into ABS CDOs. Only the higher-grade ABS bonds rated AAA, AA, and A are securitized that make out the high-grade ABS CDO portfolio. Figure 2 also suggests that HQE ABSs and CDOs are not as risky as those of the LQE since the reference asset

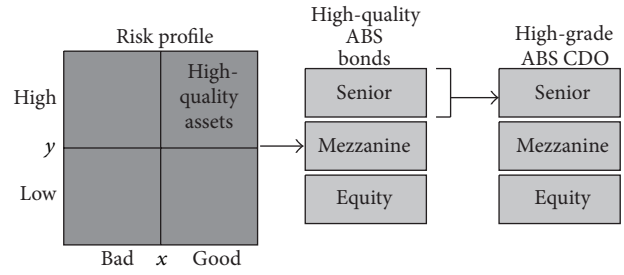

Figure 2: Chain of HQAs and their SAPs; source: [4].

portfolios have higher credit quality. HQE capital levels will also be greater than those of the LQE, in the sense that the LQE used its capital to provision for low-quality default. In this regard, we have the secondary effect of securitization where credit risk is transferred to investors. Basel III identifies a number of shortcomings within the current securitization framework some of which were categorised broadly as too low-risk weights for highly rated securitizations and too high-risk weights for low-rated senior securitization exposures (see [9] for detailed explanation). Furthermore, we assume that HQEs are risk neutral, with expected utilities:

$$\mathbf{E}_t\left(\sum_{s=0}^{\infty} \beta'^s x'_{t+s}\right), \qquad \mathbf{E}_t\left(\sum_{t=0}^{\infty} \beta'^t x'_t\right), \quad (12)$$

where x'_{t+s} and x'_t are their respective consumptions of CDOs at dates $t+s$ and t. For the discount factors β^s and β'^s, we have that $0 < \beta^s, \beta'^s < 1$ and suppose that $\beta < \beta'$. This inequality ensures that, in equilibrium, the LQEs will not want to postpone securitization because they are relatively impatient (compare with [13] and the references contained therein). The following assumption is made for ease of computation.

Assumption 4 (HQE price, asset, default and borrowing rate). For HQEs, suppose that $p^{A'}$, $r^{A'}$, and $r^{\mathrm{B}'}$ are the asset price, asset rate, and borrowing rate, respectively. For all t, we assume that

$$p_t^{A'} = p_t^A, \qquad r_t^{A'} = r_t^A, \qquad r_t^{\mathrm{B}'} = r_t^{\mathrm{B}}, \quad (13)$$

where p^A, r^A, and r^{B} are as before for HQEs. Also, we assume that the assets held by HQEs do not default or refinance.

In reality, this assumption may be violated since LQAs are more expensive than HQAs. However, this adjustment can be catered for in the sequel. We shall see that in equilibrium the LQE borrows from HQEs and that the rate of interest always equals the HQEs' constant rate of time preference so that

$$r^{\mathrm{B}} = r_t^{\mathrm{B}} \equiv \frac{1}{\beta'} - 1. \quad (14)$$

All HQEs have an identical securitization function that exhibits decreasing returns to scale. In a Basel III context, the

additional quantitative information that HQEs may consider disclosing could include customised measurement tools or metrics that assess the structure of HQEs' balance sheets, as well as metrics that project cash flows and future liquidity positions, taking into account off-balance sheet risks, which are specific to that HQE (see the BCBS publications [5, 21, 22]). In this case, per unit of population, an asset input of A'_t at date t yields an output of $\widetilde{C}_{t+1}$ marketable CDOs at date $t+1$, according to

$$\begin{aligned} &\widetilde{C}_{t+1} = P\left(A'_t\right), \quad \text{where } P' > 0, \\ &P'' < 0, \qquad P'\left(\frac{\overline{A}}{n}\right) < \mu\left(1 + r^{\mathrm{B}}\right) < P'(0). \end{aligned} \tag{15}$$

The last two inequalities in (15) are included to ensure that both the LQE and HQEs are producing in the neighborhood of the steady-state equilibrium. HQEs securitization does not require any specific skill nor do they produce any non-marketable CDOs. As a result, no HQE is credit constrained as noted in Basel III (see [9]). At date t, such entities' budget constraint can be expressed as

$$p_t^A\left(A'_t - A'_{t-1}\right) + \left(1 + r^{\mathrm{B}}\right)\mathrm{B}'_{t-1} + x'_t = P\left(A'_{t-1}\right)_{t-1} + \mathrm{B}'_t, \tag{16}$$

where x'_t is secondary securitization at date t, $(1 + r^{\mathrm{B}})\mathrm{B}'_{t-1}$ is debt repayment, and B'_t is new interbank sponsoring. The HQEs' balance sheet constraint

$$p_t^A A'_{t-1} + B'_t = \mathrm{B}'_t + K'_t, \tag{17}$$

is the same as in the case for an LQE, but the ratios of these variables will differ from those of the LQEs with much lower risk (compare with (4)). In this regard, assets held by HQEs are less risky, long-term loans with fixed rates (compare with [3]). Next, the HQEs' profit may be expressed as

$$\Pi'_t = r_t^A p_t^A A'_{t-1} + r^B B'_t - r^{\mathrm{B}}\mathrm{B}'_t, \tag{18}$$

where r^A, r^B, and r^{B} represent the asset rate, returns on marketable securities, and borrowing rate in period t, respectively. Notice that the prepayment cost is zero in the case for HQEs (see (10)). Thus, the value of HQAs is represented by

$$p_t^A A'_{t-1} = \frac{\Pi'_t - r^B B'_t + r^{\mathrm{B}}\mathrm{B}'_t}{r^A}. \tag{19}$$

We provide an appropriate HQE cash flow constraint in the following result.

Lemma 5 (HQE cash flow constraint). *Suppose that the credit constraint* (3) *as well as* (16) *to* (19) *holds. In this case, the HQEs' cash flow constraint is given by*

$$\Pi'_t \geq r^A p_t^A A'_{t-1} + r^B B'_t - p_{t+1}^A A'_t + \mathrm{B}'_t. \tag{20}$$

2.3. Market Equilibrium. In equilibrium, B'_{t-1} and B'_t are negative, reflecting the fact that HQEs lend the LQE. For our purposes, market equilibrium is defined as follows.

Definition 6 (market equilibrium). Market equilibrium is a sequence of asset prices and allocations, debt, and securitization by the LQE and HQEs, given by

$$\left\{p_t^A, A_t, A'_t, \mathrm{B}_t, \mathrm{B}'_t, x_t, x'_t\right\}, \tag{21}$$

such that each LQE chooses (A_t, B_t, x_t) to maximize the expected discounted utilities of the LQE and HQEs subject to the securitization function, sponsoring constraint and flow-of-funds constraint given by (2), (3), and (11), respectively. On the other hand, each HQE chooses $(A'_t, \mathrm{B}'_t, x'_t)$ to maximize the above expected discounted utilities subject to the securitization function (15) and budget constraint (16). Also, in the case of the HQE, we have that the markets for assets, CDOs, and debt clear.

2.3.1. LQE at Equilibrium. In the sequel, we assume that the asset price bubble does not burst during securitization. In this case, it turns out that there is a locally unique perfect-foresight equilibrium path starting from initial values A_{t-1} and B_{t-1} in the neighborhood of the steady state. In this state, the LQE's marketable output, μA^*, is just enough to cover the interest on their debt, $r^{\mathrm{B}}\mathrm{B}^*$. Equivalently, the required screening costs per asset unit, u^*, equal the LQE's securitization of marketable output, μ. As a result, entities neither expand nor shrink. To further characterize entity equilibrium, we provide the following Kiyotaki-Moore-type result (see [14] for further discussion).

Theorem 7 (LQE behavior at steady state). *Assume that the asset bubble does not burst during the securitization process. In the neighborhood of the steady state, the LQE prefers to borrow up to the maximum and invest in assets, consuming no more than its current output of non-marketable CDOs. In this case, there is a unique steady-state* $(p^{A^*}, A^*, \mathrm{B}^*)$*, with the associated transaction cost,* u^**, being given by*

$$u^* = \frac{r^{\mathrm{B}}}{1 + r^{\mathrm{B}}} p^{A^*} = \frac{1}{1 + r^{\mathrm{B}}} P'\left[\frac{1}{n}\left(\overline{A} - A^*\right)\right] = \mu, \tag{22}$$

$$\mathrm{B}^* = \frac{\mu}{r^{\mathrm{B}}} A^*. \tag{23}$$

Proof. The result follows by considering the LQE's marginal unit of marketable CDOs at date t. This entity can invest in $1/u_t$ assets, which yields c/u_t non-marketable CDOs and a/u_t marketable CDOs at date $t+1$. The former are consumed while the latter are reinvested. This, in turn, yields

$$\frac{a}{u_t}\frac{c}{u_{t+1}} \tag{24}$$

non-marketable CDOs and

$$\frac{a}{u_t}\frac{a}{u_{t+1}} \tag{25}$$

marketable CDOs at date $t+2$ and so on.

Next, we appeal to the principle of unimprovability, which states that we need to only consider single deviations at date t to show that this investment strategy is optimal. There are two alternatives open to the LQE at date t. Either it can save the marginal unit—equivalently, reduce its current borrowing by one—and use the return R to commence a strategy of maximum levered investment from date $t+1$ onward or the LQE can simply consume the marginal unit. Its choice is equivalent to choosing one of the following consumption paths:

$$\text{Invest}:\ 0, \frac{c}{u_t}, \frac{a}{u_t}\frac{c}{u_{t+1}}, \frac{a}{u_t}\frac{a}{u_{t+1}}\frac{c}{u_{t+2}}, \ldots \tag{26}$$

$$\text{Save}:\ 0, 0, r^{\mathrm{B}}\frac{c}{u_t}, r^{\mathrm{B}}\frac{a}{u_t}\frac{c}{u_{t+2}}, \ldots \tag{27}$$

$$\text{Consumption}:\ 1, 0, 0, 0, \ldots \tag{28}$$

at dates $t, t+1, t+2, t+3, \ldots$, respectively.

To complete the proof of the result, we need to confirm that, given the LQE's discount factor, β, consumption path (26) offers a strictly higher utility than (27) or (28), in the neighborhood of the steady-state. We shall be in a position to show this once we have found the steady-state value of u_t in (34) below.

Since the optimal a_t and b_t are linear in a_{t-1} and b_{t-1}, we can aggregate across entities to find the equations of motion of the aggregate asset holding and borrowing, A_t and B_t, respectively, of entities may be given by

$$A_t = \frac{1}{u_t}\left[\left(\mu + p_t^A\right)A_{t-1} - \left(1 + r^{\mathrm{B}}\right)\mathrm{B}_{t-1}\right], \tag{29}$$

$$\mathrm{B}_t = \frac{1}{1 + r^{\mathrm{B}}}p_{t+1}^A A_t. \tag{30}$$

Next, we consider market clearing. Since all HQEs have identical securitization functions, their aggregate asset demand equals A_t' times their population n. The sum of the aggregate demand for assets by the LQE and HQEs is equal to the total supply given by

$$\overline{A} = A_t + nA_t'. \tag{31}$$

In this case, from (35), we obtain the asset market (clearing) equilibrium condition

$$\begin{aligned} &u_t = p_t^A - \frac{p_{t+1}^A}{1 + r^{\mathrm{B}}} = u\left(A_t\right), \\ &\text{where } u(A) \equiv \frac{1}{1 + r^{\mathrm{B}}}P'\left[\frac{1}{n}\left(\overline{A} - A\right)\right]. \end{aligned} \tag{32}$$

Next, it is useful to look at the steady-state equilibrium. From (29), (30), and (32), it is easily shown that there is a unique steady-state (p^*, A^*, B^*), with associated steady-state transaction cost u^*, where (22) and (23) hold. □

Theorem 7 postulates that at each date t, the LQE's optimal choice of (A_t, B_t, x_t) satisfies $x_t = \nu A_{t-1}$ in (11), and the borrowing constraint (3) is binding so that

$$\begin{aligned} \mathrm{B}_t &= \frac{p_{t+1}^A}{1 + r^{\mathrm{B}}}A_t, \\ A_t &= \frac{1}{p_t^A - 1/\left(1 + r^{\mathrm{B}}\right)p_{t+1}^A}\left[\left(\mu + p_t^A\right)A_{t-1} - \left(1 + r^{\mathrm{B}}\right)\mathrm{B}_{t-1}\right]. \end{aligned} \tag{33}$$

Here, the term $(\mu + p_t^A)A_{t-1} - (1 + r^{\mathrm{B}})\mathrm{B}_{t-1}$ is the LQE's nett worth at the beginning of date t. This corresponds to the value of its marketable CDOs and assets held from the previous period nett of debt repayment. In effect, (33) says that the LQE uses all its nett worth to finance the difference between the asset price, p_t^A, and the amount the entity can borrow against each asset unit, $p_{t+1}^A/1 + r^{\mathrm{B}}$. This difference is given by

$$u_t = p_t^A - \frac{p_{t+1}^A}{1 + r^{\mathrm{B}}} \tag{34}$$

and can be thought of as the screening costs required to purchase an asset unit. The equations of motion of the aggregate asset holding and borrowing, A_t and B_t, respectively, of entities may be given by (29) and (30). Notice from (29) that if, for example, present and future asset prices, p_t^A and p_{t+1}^A, were to rise, then the LQE's asset demand at date t would also rise—provided that leverage is sufficient that debt repayments $(1 + r^{\mathrm{B}})\mathrm{B}_{t-1}$ exceed current output μA_{t-1}, which holds in equilibrium. The usual notion that a higher asset price p_t^A reduces the LQE's demand is more than offset by the facts that they can borrow more when p_{t+1}^A is higher and their nett worth increases as p_t^A rises. Even though the required screening costs, u_t, per asset unit rises proportionately with p_t^A and p_{t+1}^A, the LQE's nett worth is increasing more than proportionately with p_t^A because of the leverage effect of the outstanding debt.

2.3.2. HQEs at Equilibrium. Next, we examine the HQEs' behavior at equilibrium. Such entities are not credit constrained, and so their asset demand is determined at the point at which the present value of the marginal product of assets is equal to the transaction fee associated with assets (refer to Basel III in [1]). In this case, we have that

$$u_t = p_t^A - \frac{p_{t+1}^A}{1 + r^{\mathrm{B}}} = \frac{1}{1 + r^{\mathrm{B}}}P'\left(A_t'\right). \tag{35}$$

In the model, u_t is both the HQEs' opportunity cost of holding an asset unit and the required screening costs per unit of assets held by the LQE.

2.3.3. LQE and HQE Market Clearing. In this subsection, we consider market clearing that refers to either a simplifying assumption made that markets always go to where the assets supplied equal the assets demanded or the process of getting there via price adjustment. A market clearing price is the price

of goods or a service at which assets supplied are equal to assets demanded, also called the equilibrium price. Another market clearing price may be a price below equilibrium price to stimulate demand.

Since all HQEs have identical securitization functions (see Basel III and revision to securitization in [9]), their aggregate asset demand equals A_t' times their population n. The sum of the aggregate demand for assets by the LQE and HQEs is equal to the total supply given by (31). In this case, from (35), we obtain the asset market (clearing) equilibrium condition (32). The function $u(\cdot)$ is increasing. This arises from the fact that if the LQE's asset demand, A_t, goes up, then in order for the asset market to clear, the HQEs' demand has to be stymied by a rise in the transaction fee, u_t. Given that the HQEs have linear preferences and are not credit constrained, in equilibrium they must be indifferent about any path of consumption and debt (or credit). In this case, the interest rate equals their rate of time preference so that

$$r^{\mathrm{B}} = \frac{1}{\beta'} - 1. \tag{36}$$

Moreover, given (32), the CDO markets and credit are in equilibrium.

We restrict attention to perfect-foresight equilibria in which, without unanticipated shocks, the expectations of future variables realize themselves. For a given level of the LQE's asset holding and debt at the previous date, A_{t-1} and B_{t-1}, an equilibrium from date t onward is characterized by the path of asset price, LQE asset holding, and interbank borrowings given by

$$\left\{\left(p_{t+s}^{A}, A_{t+s}, \mathrm{B}_{t+s}\right) s \geq 0\right\}, \tag{37}$$

satisfying (29), (30), and (32) at dates $t, t+1, t+2, \ldots$.

2.4. LQE and HQE Equilibrium Summary. Figure 3 displays the main features of market equilibrium for the LQE and HQEs.

The horizontal axis represents LQA and HQA demand from the left-hand side and right-hand-side, respectively. We note that the total asset supply is denoted by $\overline{A}$. The vertical axis represents the marginal products of assets for LQE and HQEs given by $\mu + \nu$ and $P'(A'/n)$, respectively. The HQEs' marginal product decreases with asset use. If there are no credit limits, then E^0 would be the best allocation for where the LQE and HQE marginal products are in equilibrium. The asset price would then be $p^0 = (\mu + \nu)(r^{\mathrm{B}})^{-1}$. On the other hand, when credit limits exist, then the equilibrium is at point E^*, where the marginal product of the LQE is greater than that of the HQE. In this case, we have

$$\mu + \nu > P'\left[\frac{\left(\overline{A} - A^*\right)}{n}\right] = \mu\left(1 + r^{\mathrm{B}}\right). \tag{38}$$

This means that the LQE's asset use is not enough. The output of CDOs per period in equilibrium is represented by the light gray area under the thick line, whereas the gray triangle represents the CDO loss per period. In this case, CDO output increases relative to LQA holdings. If A_t increases, then the CDO output will also increase in period $t+1$.

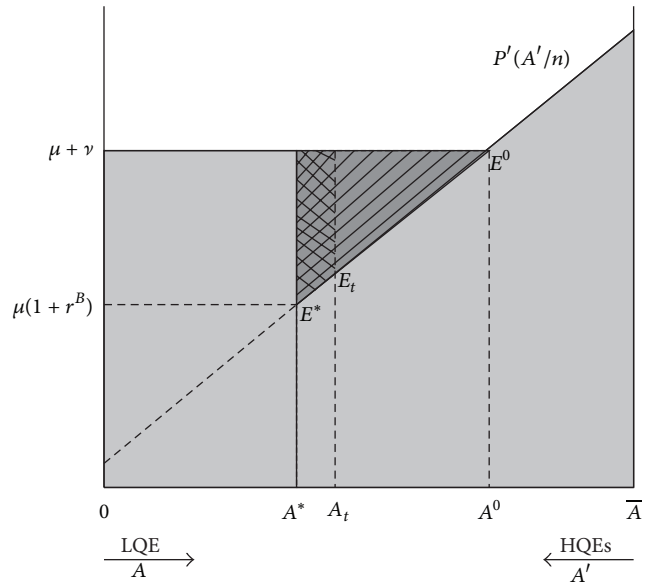

Figure 3: LQE and HQE market equilibrium.

3. Asset Securitization Shocks

In this section, we describe the effect of unexpected negative shocks on LQA price and input, CDO price in a Basel III context and output, and profit (see, e.g., [19]). In this regard, two kinds of multiplier processes are considered. The first is the within-period or static multiplier process. Here, the shock such as a ratings downgrade reduces the nett worth of the constrained LQE and compels it to reduce its asset demand. In this case, by keeping the future constant, the transaction fees decrease to clear the market and the asset price drops by the same amount. In turn, this lowers the value of the LQE's existing assets and reduces their nett worth even more. Since the future is not constant, this multiplier misses the intuition offered by the more realistic intertemporal or dynamic multiplier. In this case, the decrease in asset prices results from the cumulative decrease in present and future opportunity costs, stemming from the persistent reductions in the constrained LQE's nett worth and asset demand, which are in turn exacerbated by a decrease in asset price and nett worth in period t.

3.1. Dynamic Multiplier: Response to Temporary Shock. In order to understand the effect of unexpected inter-temporal shocks on the economy, suppose at date $t-1$ that it is in steady state with

$$A^* = A_{t-1}, \qquad \mathrm{B}^* = \mathrm{B}_{t-1}. \tag{39}$$

3.1.1. Dynamic Multiplier: Shock Equilibrium Path. We introduce an unexpected inter-temporal shock where the CDO output of the LQE and HQEs at date t are $1 - \Sigma$ times their expected levels. In order for our model to resonate with the 2007–2009 financial crisis, we take Σ to be positive. Eventually, the LQE and HQEs' securitization technologies between dates t and $t+1$ (and thereafter) return to (2) and (15),

respectively. Combining the market-clearing condition (32) with LQA demand under a temporary shock and borrowing constraint given by (29) and (30), respectively, we obtain

$$u\left(A_t\right)A_t = \left(\mu - \mu\Sigma + p_t^A - p^{A^*}\right)A^*, \quad (\text{date } t), \tag{40}$$

$$u\left(A_{t+s}\right)A_{t+s} = \mu A_{t+s-1}, \quad (\text{dates } t+1, t+2, \ldots). \tag{41}$$

The formulae (40) and (41) imply that at each date the LQE can hold assets up to the level A at which the required cost of funds, $u(A)A$, is covered by its nett worth. Notice that in (41), at each date $t+s, s \geq 1$, the LQE's nett worth is just its ambient output of marketable CDOs, μA_{t+s-1}. In this case, from the borrowing constraint at date $t+s-1$, the value of the LQE's assets at date $t+s$ is exactly offset by the amount of debt outstanding. From (40), subsequent to the shock, we see that the LQE's nett worth at date t is more than only their current output given by

$$(1-\Sigma)\mu A^* \tag{42}$$

because p_t^A changes in response to the shock and unexpected capital gains of

$$\left(p_t^A + p^{A^*}\right)A^* \tag{43}$$

result in their asset holdings. In this case, the asset value held from date $t-1$ is now $p_t^A A^*$, while the debt repayment is

$$\left(1+r^{\mathrm{B}}\right)\mathrm{B}^* = p^{A^*}A^*. \tag{44}$$

To find closed-form expressions for the new equilibrium path, we take Σ to be small and linearized around the steady state. In the sequel, we let the proportional changes in A_t, p_t^A, and Π_t relative to their steady-state values A^*, p^{A^*}, and Π^*, respectively, be given by

$$\widehat{A}_t = \frac{A_t - A^*}{A^*}, \qquad \widehat{p}_t^A = \frac{p_t^A - p^{A^*}}{p^{A^*}}, \qquad \widehat{\Pi}_t = \frac{\Pi_t - \Pi^*}{\Pi^*}, \tag{45}$$

respectively. For our purpose, assume that steady-state profit, Π_t^*, represents profit when the asset value and borrowings are in steady state (compare with [19]). Thus, steady-state profit for the LQE and HQEs are represented by

$$\begin{aligned}\Pi_t^* &= \left(r_t^A + c_t^p r_t^f - \left(1-r_t^R\right)r_t^S\right)p^{A^*}{}_t A_{t-1}^* + r^B B_t - r^{\mathrm{B}}\mathrm{B}_t^*,\\ \Pi'^*_t &= r^A p^{A^*}{}_t A'^*_{t-1} + r^B B'_t - r^{\mathrm{B}}\mathrm{B}'^*_t,\end{aligned} \tag{46}$$

respectively. Then, by using the steady state, transaction fee, and (22), we have from (40) and (41) that

$$\left(1+\frac{1}{\eta}\right)\widehat{A}_t = \frac{1+r^{\mathrm{B}}}{r^{\mathrm{B}}}\widehat{p}_t^A - \Sigma, \quad (\text{date } t), \tag{47}$$

$$\begin{aligned}&\left(1+\frac{1}{\eta}\right)\widehat{A}_{t+s} = \widehat{A}_{t+s-1},\\ &\text{for } s \geq 1, (\text{dates } t+1,\ t+2, \ldots),\end{aligned} \tag{48}$$

where $\eta > 0$ denotes the elasticity of the residual asset supply to the LQE with respect to the transaction fee at the steady state. Here, we have

$$\begin{aligned}\frac{1}{\eta} &= \left.\frac{d\log u(A)}{d\log A}\right|_{A=A^*}\\ &= -\left.\frac{d\log P'(A')}{d\log A'}\right|_{A'=1/n(\overline{A}-A^*)} \times \frac{A^*}{\overline{A}-A^*}.\end{aligned} \tag{49}$$

The right-hand side of (47) divides the change in the LQE's nett worth at date t into two components: the direct effect of the securitization shock, Σ, and the indirect effect of the capital gain arising from the unexpected rise in price, $\widehat{p}_t^A$. In order to compute (47), from (22), (40), and (45), we have that the RHS of (47) is given by

$$\frac{1+r^{\mathrm{B}}}{r^{\mathrm{B}}}\widehat{p}_t^A - \Sigma = \frac{u\left(A_t\right)A_t}{\mu A^*} - 1. \tag{50}$$

Also, from (22), (40), and (45), we have that the LHS of (47) is given by

$$\begin{aligned}&\left(1+\frac{1}{\eta}\right)\widehat{A}_t\\ &= \left(\frac{A_t - A^*}{A^*}\right) + \left(-\left.\frac{d\log P'\left(A'\right)}{d\log A'}\right|_{A'=1/n(\overline{A}-A^*)}\right.\\ &\qquad \left.\times \frac{A^*}{\overline{A}-A^*}\right)\left(\frac{A_t - A^*}{A^*}\right).\end{aligned} \tag{51}$$

Crucially, the impact of $\widehat{p}_t^A$ is scaled up by the factor $(1 + r^{\mathrm{B}})/(r^{\mathrm{B}})$ because of leverage. Furthermore, the factor $1 + 1/\eta$ on the left-hand sides of (47) and (48) reflects the fact that as LQA demand rises, the transaction fee must rise for the market to clear and, this in turn, partially chokes off the increase in the LQE's demand. The key point to note from (48) is that, except for the limit case of a perfectly inelastic supply $\eta = 0$, the effect of a shock persists into the future. The reason is that the LQE's ability to invest at each date $t+s$ is determined by how much screening costs they can afford from their nett worth at that date, which in turn is historically determined by their level of securitization at the previous date $t+s-1$.

3.1.2. Dynamic Multiplier: Asset Price and Input, CDO Price and Output, and Profit. We will determine the size of the initial change in the LQE's asset holdings, $\widehat{A}_t$, which, from (47), can be jointly determined with the change in asset price, $\widehat{p}_t^A$. Also, we would like to compute the proportional change in CDO output and profit denoted by $\widehat{C}_{t+1}$ and $\widehat{\Pi}_t$, respectively (see, e.g., [19]).

Theorem 8 (dynamic multiplier: shocks to asset price and input, CDO price and output, and profit). *Assume that the asset bubble does not burst during the securitization process and that* $p_t^A \leq \overline{p}_t$, *for all* t *in* (5). *In this case, one has that the*

proportional change in asset price and input, CDO price and output, and profit subject to a negative shock is given by

$$\widehat{p}_t^A = -\frac{1}{\eta}\Sigma, \tag{52}$$

$$\widehat{A}_t = -\frac{1}{1+1/\eta}\left(1+\frac{1+r^{\mathrm{B}}}{\eta r^{\mathrm{B}}}\right)\Sigma, \tag{53}$$

$$\widehat{p}_t^C = -\frac{1}{\eta}\Sigma \tag{54}$$

$$\widehat{C}_{t+1} = \frac{\mu+\nu-\left(1+r^{\mathrm{B}}\right)\mu}{\mu+\nu}\frac{(\mu+\nu)A^*}{C^*}\widehat{A}_t, \tag{55}$$

$$\widehat{\Pi}_t = \frac{\left(r_t^A + c_t^p r_t^f - \left(1-r_t^R\right)r_t^S\right)p_t^A A_{t-1} + r^B B_t - r^{\mathrm{B}}\mathrm{B}_t}{\left(r_t^A + c_t^p r_t^f - \left(1-r_t^R\right)r_t^S\right)p^{A^*}_t A^*_{t-1} + r^B B_t - r^{\mathrm{B}}\mathrm{B}_t^*} - 1, \tag{56}$$

respectively.

Proof. Since there are no bursting bubbles, (32) intimates that the asset price, p_t^A, is the discounted sum of future opportunity costs given by

$$u_{t+s} = u\left(A_{t+s}\right), \quad s \geq 0. \tag{57}$$

Linearizing around the steady state and then substituting from (48) given by

$$\left(1+\frac{1}{\eta}\right)\widehat{A}_{t+s} = \widehat{A}_{t+s-1}, \qquad \text{for } s \geq 1, \quad (\text{dates } t+1, t+2, \ldots), \tag{58}$$

we obtain

$$\begin{aligned}\widehat{p}_t^A &= \frac{1}{\eta}\frac{r^{\mathrm{B}}}{1+r^{\mathrm{B}}}\sum_{s=0}^{\infty}\left(1+r^{\mathrm{B}}\right)^{-s}\widehat{A}_{t+s} \\ &= \frac{1}{\eta}\frac{r^{\mathrm{B}}}{1+r^{\mathrm{B}}}\frac{1}{1-\eta/\left(1+r^{\mathrm{B}}\right)(1+\eta)}\widehat{A}_t.\end{aligned} \tag{59}$$

We have to verify that

$$\begin{aligned}\sum_{s=0}^{\infty}\left(1+r^{\mathrm{B}}\right)^{-s}\widehat{A}_{t+s} &= \frac{1}{1-\eta/\left(1+r^{\mathrm{B}}\right)(1+\eta)}\widehat{A}_t \\ &= \frac{\left(1+r^{\mathrm{B}}\right)(1+\eta)}{\left(1+r^{\mathrm{B}}\right)(1+\eta)-\eta}\widehat{A}_t\end{aligned} \tag{60}$$

is standard for infinite series. The dynamic multiplier

$$\left[1-\frac{\eta}{\left(1+r^{\mathrm{B}}\right)(1+\eta)}\right]^{-1} = \frac{\left(1+r^{\mathrm{B}}\right)(1+\eta)}{\left(1+r^{\mathrm{B}}\right)(1+\eta)-\eta} \tag{61}$$

in (59) captures the effects of persistence in entities' reference asset portfolio holdings and has a dramatic effect on the sizes of $\widehat{p}_t^A$ and $\widehat{A}_t$. In order to find $\widehat{p}_t^A$ and $\widehat{A}_t$ in terms of the size of the shock Σ, we utilize (47) and (59). The calculations above verify that (52) and (53) as well as (54) hold.

Next, we prove that (55) holds. As we saw in Figure 3, aggregate CDO output—the combined harvest of the LQE and HQEs—is positively correlated to the LQA holdings, since such entities' marginal product is higher than the HQEs'. Suppose that the proportional change in aggregate output, $\widehat{C}_{t+s}$, is given (compare with $\widehat{p}_t^A$ and $\widehat{A}_t$ above) by

$$\widehat{C}_t = \frac{C_t - C^*}{C^*}, \qquad C_t = \left(\widehat{C}_t + 1\right)C^*, \qquad C^* = \frac{C_t}{\widehat{C}_t + 1}. \tag{62}$$

In this case, we can verify that at each date $t+s$ the proportional change in aggregate output, $\widehat{C}_{t+s}$, is given by

$$\widehat{C}_{t+s} = \frac{\mu+\nu-\left(1+r^{\mathrm{B}}\right)\mu}{\mu+\nu}\frac{(\mu+\nu)A^*}{C^*}\widehat{A}_{t+s-1}, \quad \text{for } s \geq 1. \tag{63}$$

The RHS of (63) yields

$$\begin{aligned}&\frac{\mu+\nu-\left(1+r^{\mathrm{B}}\right)\mu}{\mu+\nu}\frac{(\mu+\nu)A^*}{C^*}\widehat{A}_{t+s-1} \\ &\quad = \frac{C_{t+s} - \left[\left(1+r^{\mathrm{B}}\right)\mu A_{t+s-1} + \left(\mu+\nu-\left(1+r^{\mathrm{B}}\right)\mu\right)A^*\right]}{C^*}.\end{aligned} \tag{64}$$

In order to verify (63), we have to show that

$$\begin{aligned}C^* &= \left(1+r^{\mathrm{B}}\right)\mu A_{t+s-1} + \left(\mu+\nu-\left(1+r^{\mathrm{B}}\right)\mu\right)A^* \\ &= \left[\left(1+r^{\mathrm{B}}\right)\mu\widehat{A}_{t+s-1} + \mu + \nu\right]A^*.\end{aligned} \tag{65}$$

This, of course, is true since

$$C^* = (\mu+\nu)A^*, \qquad \left(1+r^{\mathrm{B}}\right)\mu A_{t+s-1} = \left(1+r^{\mathrm{B}}\right)\mu A^* \quad \text{or } A_{t+s-1} = A^*. \tag{66}$$

The proportional change in profit, $\widehat{\Pi}_t$, given by (56), is a direct consequence of its definition. □

The proportional changes in CDO output, $\widehat{C}$, and profit, $\widehat{\Pi}$, given by (55) and (56), respectively, have important connections with the 2007–2009 financial crisis and Basel III. For mortgage loans, this relationship stems from the terms involving the asset and prepayment rates, refinancing, and house equity.

At date t, (52) tells us that, in percentage terms, the effect on the asset price is of the same order of magnitude as the temporary securitization shock. As a result, the effect of the shock on the LQA holdings at date t is large. In this case, the multiplier in (53) exceeds unity, and can do so by a sizeable margin, thanks to the factor $(1+r^{\mathrm{B}})(r^{\mathrm{B}})^{-1}$. In terms of (47), the indirect effect of $\widehat{p}_t^A$, scaled up by the leverage factor $(1+r^{\mathrm{B}})(r^{\mathrm{B}})^{-1}$, is easily enough to ensure that the overall effect on $\widehat{A}_t$, is more than one-for-one.

3.2. Static Multiplier: Response to Temporary Shocks. At the beginning of this section, we made a distinction between static and dynamic multipliers. Imagine, hypothetically, that there was no dynamic multiplier. In this case, suppose p_{t+1}^{A} were artificially pegged at the steady-state level p^{A^*}. Equation (47) would remain unchanged. However, the right-hand side of (59) would contain only the first term of the summation—the term relating to the change in transaction fee at date t—so that the multiplier (61) would disappear. Combining the modified equation, we have

$$\widehat{p}_t^{A} = \left[\frac{r^{\mathrm{B}}}{\eta\left(1+r^{\mathrm{B}}\right)}\right]\widehat{A}_t. \tag{67}$$

The following result follows from the above.

Corollary 9 (static multiplier: shocks to asset price and input). *For the static multiplier, suppose that the hypothesis of Theorem 8 holds. Then, one has that*

$$\widehat{p}_t^{A}\Big|_{p_{t+1}^{A}=p^{A^*}} = -\frac{r^{\mathrm{B}}}{\eta\left(1+r^{\mathrm{B}}\right)}\Sigma, \tag{68}$$

$$\widehat{A}_t\big|_{p_{t+1}^{A}=p^{A^*}} = -\Sigma. \tag{69}$$

Proof. We prove the result by considering (47) and (59) where the changes in the asset price and the LQA holdings can be solely traced to the static multiplier. □

Subtracting (68) from (52), we find that the additional movement in asset price attributable to the dynamic multiplier is $(1 + r^{\mathrm{B}})^{-1}$ times the movement due to the static multiplier. And a comparison of (53) with (69) shows that the dynamic multiplier has a similarly large proportional effect on LQA holdings. The term

$$\frac{\mu+\nu-\left(1+r^{\mathrm{B}}\right)\mu}{\mu+\nu} \tag{70}$$

reflects the difference between LQA (equal to $\mu + \nu$) and HQA securitization (equal to $(1 + r^{\mathrm{B}})\mu$ in the steady state). The ratio $(\mu + \nu)A^*C^{*-1}$ is the share of the LQE's output. If aggregate securitization was measured by $C_{t+s}\overline{A}^{-1}$, it would be persistently above its steady-state level, even though there are no positive securitization shocks after date t. The explanation lies in a composition effect. In this regard, there is a persistent change in asset usage between the LQE and HQEs, which is reflected in increased aggregate output.

4. Illustrative Examples of Asset Securitization

In this section, we present examples of asset securitization. Firstly, we consider a LQA securitization example involving subprime mortgages. Next, we illustrate LQE and HQE equilibrium from Section 2 as well as the effects of shocks to asset and CDO prices as discussed in Section 3.

4.1. Example of Subprime Mortgage Securitization. In this subsection, we provide a specific example of LQA securitization involving subprime mortgages (see, e.g., [4, 15]). For such securitization, we bring into play the main results contained in [16]. Subprime mortgages are usually adjustable rate mortgages (ARMs), where high step-up rates are charged in period $t+1$ after low teaser rates apply in period t. Secondly, this higher step-up rate causes an incentive to refinance in period $t + 1$. Refinancing is subject to the fluctuation in house prices. When house prices rise, the entity is more likely to refinance. This means that investors could receive further assets with lower interest rates as house prices increase. Thirdly, a high prepayment penalty is charged to dissuade investors from refinancing (see [4] for more details).

In subprime mortgage context, the paper [16] provides a relationship between the mortgage rate, r^{M}, loan-to-value ratio (LTVR), L, and prepayment cost, c^{p}, by means of the simultaneous equations model

$$\begin{aligned} r_t^{M} &= \alpha^0 L_t + \alpha^1 c_t^{p} + \alpha^2 X_t + \alpha^3 Z_t^{r^{M}} + u_t, \\ L_t &= \psi^1 r_t^{M} + \psi^2 X_t + \psi^3 Z_t^{L} + v_t, \\ c_t^{p} &= \gamma^1 r_t^{M} + \gamma^2 X_t + \gamma^3 Z_t^{c^{p}} + w_t. \end{aligned} \tag{71}$$

Investors typically have a choice of r^{M} and L, while the choice of c^{p} triggers an adjustment to the mortgage rate, r^{M}. Thus, L and c^{p} are endogenous variables in the r^{M}-equation. There is no reason to believe that L and c^{p} are simultaneously determined. Therefore, c^{p} does not appear in the L-equation and L does not make an appearance in the c^{p}-equation. From [16], X comprises explanatory variables such as asset characteristics (owner occupation, asset purpose, and documentation requirements); investor characteristics (income and Fair Isaac Corporation (FICO) score); and distribution channel (broker origination). The last term in each equation $Z^{r^{M}}$, Z^{L}, or $Z^{c^{p}}$ comprises the instruments excluded from either of the other equations. Reference [16] points out that the model is a simplification with other terms such as type of interest rate, the term to maturity, and distribution channel possibly also being endogenous.

Corollary 10 (dynamic multiplier: shocks to profit for subprime mortgages). *Suppose that the hypothesis of Theorem 8 holds. Then, the relative change in profit may be expressed in terms of r^{M}, c^{p}, and L as*

$$\widehat{\Pi}_t\left(r^{M}\right) = \frac{F_t p_t^{A} A_{t-1} + r^{B} B_t - r^{\mathrm{B}}\mathrm{B}_t}{F_t p^{A^*}{}_t A_{t-1}^{*} + r^{B} B_t - r^{\mathrm{B}}\mathrm{B}_t^{*}} - 1, \tag{72}$$

$$\widehat{\Pi}_t\left(c^{p}\right) = \frac{G_t p_t^{A} A_{t-1} + r^{B} B_t - r^{\mathrm{B}}\mathrm{B}_t}{G_t p^{A^*}{}_t A_{t-1}^{*} + r^{B} B_t - r^{\mathrm{B}}\mathrm{B}_t^{*}} - 1, \tag{73}$$

$$\widehat{\Pi}_t\left(L\right) = \frac{H_t p_t^{A} A_{t-1} + r^{B} B_t - r^{\mathrm{B}}\mathrm{B}_t}{H_t p^{A^*}{}_t A_{t-1}^{*} + r^{B} B_t - r^{\mathrm{B}}\mathrm{B}_t^{*}} - 1, \tag{74}$$

respectively. Here, one has in (72), (73), *and* (74) *that*

$$F_t = r_t^M \left(1 + \gamma^1 r_t^f\right) + \left(\gamma^2 X_t + \gamma^3 Z_t^{c^p} + w_t\right) r_t^f - \left(1 - r_t^R\right) r_t^S,$$

$$G_t = c_t^p \left(\frac{1}{\gamma^1} + r_t^f\right) - \frac{1}{\gamma^1}\left(\gamma^2 X_t + \gamma^3 Z_t^{c^p} + w_t\right) - \left(1 - r_t^R\right) r_t^S,$$

$$H_t = \left[\gamma^1 \left\{\frac{1}{\psi^1} L_t - \frac{\psi^2}{\psi^1} X_t - \frac{\psi^3}{\psi^1} Z_t^L - \frac{1}{\psi^1} v_t\right\} + \gamma^2 X_t + \gamma^3 Z_t^{c^p} + w_t\right]\left[\gamma^1 + r_t^f\right] + \alpha^0 L_t + \alpha^2 X_t + \alpha^3 Z_t^{r^M} + u_t - \left(1 - r_t^R\right) r_t^S, \tag{75}$$

respectively.

The most important contribution of the aforementioned result is that it demonstrates how the proportional change in profit subsequent to a negative shock is influenced by quintessential low-quality asset features such as asset and prepayment rates, refinancing, and house equity given by r^M, c^p, r^f, and L, respectively, The default rate is also implicitly embedded in formulas (72) to (74) in Corollary 10. In this regard, by consideration of simultaneity in the choice of r^M and c^p, it is possible to address the issue of possible bias in estimates of the effect of c^p on r^M.

4.2. Numerical Examples of Asset Securitization. In this subsection, we provide numerical examples to illustrate LQE and HQE equlibrium as described in Section 2 as well as the effects of shocks on asset and CDO prices as in Section 3. Initial asset securitization parameter choices are given in Table 2.

The financial crisis has exposed the limits of liability management and the proposed regulation will make the retreat from liability management permanent. To a much greater extent than at any time since the 1970s, banks will be forced back towards "asset management," in other words towards a business model in which balance sheet size is determined from the liabilities side of the balance sheet, by the amount of funding which the bank can raise, and in which asset totals have to be adjusted to meet the available liabilities. This amounts to a "macroprudential" policy—that is, a policy designed to prevent credit creation from spiralling out of control as it did in the run-up to the recent crisis as expressed in Basel III on the the macroprudential overlay (see, e.g., [21, 22]).

4.2.1. Numerical Example: LQE and HQE Equilibrium. Suppose that the LQE's and HQEs' deposits, borrowings, marketable securities and capital are equal. In this case, notice that the LQE's and HQEs' asset holdings, A and A', are a proportion, α and $1-\alpha$, of the aggregate assets, $\overline{A}$, respectively. Thus, we have that

Table 2: Asset securitization parameter choices.

Parameter	Value
μ	0.002
p_{t+1}	0.113
$\overline{A}_t$	720 000
r^R	0.5
B_{t-1}	\$2 600
r^B	0.205
Σ	0.002
ν	0.2
c^p	0.03
$\overline{A}_{t-1}$	460 000
r^S	0.15
r^{B}	0.2
K_t	\$3 000
C^*	240 000
α	0.3
r^f	0.2
r^A	0.061
B_t	\$4 800
B_t	\$5 000
n	1
$P(A'_{t-1})$	240 000

$$A = \alpha\overline{A} = 0.3 \times 720000 = 216000;$$
$$A' = (1-\alpha)\,\overline{A} = (1 - 0.3)\,720000 = 504000. \tag{76}$$

We compute the LQE's debt obligation output in period $t+1$ by considering the securitization function (2). Therefore, the CDO output can be computed by

$$C_{t+1} = (\mu + \nu)\,A_t = (\mu + \nu)\,\alpha\overline{A}_t = (0.002 + 0.2) \times 0.3 \times 720000 = 43632. \tag{77}$$

Next, the upper bound of the LQE's retention rate should be less that the discount factor β; thus,

$$\beta\left(\frac{0.002}{0.002 + 0.2}\right) = 0.0099099. \tag{78}$$

The value of LQAs in period t is computed by using (6). Thus, we have

$$p_t^A A_{t-1} = D_t + B_t + K_t - B_t = 1200 + 4800 + 3000 - 5000 = 4000. \tag{79}$$

The asset price in period t is therefore

$$p_t^A = \frac{4000}{A_{t-1}} = \frac{4000}{\alpha\overline{A}_{t-1}} = \frac{4000}{(0.3 \times 460000)} = 0.0289855072. \tag{80}$$

The LQE's profit is computed by considering the cash flow constraint (10):

$$\Pi_t = \left(r^A + c_t^p r_t^f\right) p_t^A A_{t-1} + r^B B_t - r^D D_t - r^B B_t$$
$$\Pi_t = (0.061 + 0.03 \times 0.2) \times 4000 + 0.205 \times 5000 - 0.205 \times 1200 - 0.2 \times 4800 = 87. \quad (81)$$

Furthermore, the LQE's profit is subject to the constraint (15); thus,

$$\Pi_t = (0.061 + 0.03 \times 0.2)\, 4000 + 0.205 \times 5000 - 0.205 \times 1200 - 0.113 \times 0.3 \times 720000 + 4800 = -18561. \quad (82)$$

We compute the LQE's additional consumption, $x_t - \nu A_{t-1}$ by considering the flow of funds constraint given by

$$0.002 \times 0.3 \times 460000 + 8000 - (1 + 0.2) \times 2600 - 0.011904761\,(0.3 \times 720000 - 0.3 \times 460000) = 4227.4286. \quad (83)$$

Next, we concentrate on HQE constraints. In this case, HQEs' secondary securitization at date t is computed by using the budget constraint (16); thus,

$$x_t' = 280000 + 4800 - 0.011904761\,(1 - 0.3)\,720000 - (1 - 0.3) \times 460000 - (1 + 0.2) \times 2600 = -46319.99954. \quad (84)$$

Thus, $x_t = 54103.64210$. Next, we consider the HQE's profit (18) at face value to compute profit at date t; thus,

$$\Pi_t' = 0.061 \times 4000 + 0.205 \times 5000 - 0.205 \times 1500 - 0.2 \times 4800 = 123.5. \quad (85)$$

In this regard, the value of assets can be computed as

$$p_t^A A_{t-1}' = \frac{123.5 - 0.205 \times 5000 + 0.205 \times 1200 + 0.2 \times 4800}{0.061} = 4991.8. \quad (86)$$

The HQEs' cash flow constraint (20) is given by

$$\Pi_t' \geq 0.061 \times 4000 + 0.205 \times 5000 - 0.205 \times 1200 - 0.113 \times (1 - 0.3) \times 720000 + 4800 = -51007. \quad (87)$$

The screening cost an LQE has to pay to purchase an asset unit is financed by the HQE's nett worth. This screening cost is represented by

$$u_t = p_t^A - \frac{p_{t+1}^A}{1 + r^B} = 0.011904761 - \frac{0.113}{1 + 0.2} = -0.082261905. \quad (88)$$

The motion of the aggregate asset holding and borrowing, A_t and B_t, of the entity may be computed as

$$A_t = \frac{1}{0.082261905}\left[(0.002 + 0.011904761) \times 0.3 \times 460000 - (1 + 0.2) \times 2600 = 14601.44865\right],$$
$$B_t = \frac{1}{1 + 0.2} 0.113 \times 0.3 \times 720000 = 20340. \quad (89)$$

The sum of the aggregate asset demand from asset originators by the LQE and HQEs' is computed by

$$\overline{A} = A_t + nA_t' = 0.3 \times 720000 + 1\,(1 - 0.3)\,720000 = 720000. \quad (90)$$

The steady-state asset price and borrowings for the LQE are

$$p^{A^*} = 0.002 \frac{1 + 0.2}{0.2} = 0.012, \qquad B^* = \frac{0.002}{0.2} 260000 = 2600. \quad (91)$$

Notice that the required screening costs per asset unit equals the LQE's securitization of marketable output, $u^* = \mu = 0.001$. Also, we have $A_{t-1} = A^*$ and $B_{t-1} = B^*$.

4.2.2. Numerical Example: Negative Shocks to LQAs and Their CDOs. LQA demand and borrowings under a temporary shock at date t are computed by

$$A_t = \frac{1}{-0.082261905}\left[(0.002 - 0.002 \times 0.002 + 0.011904761) \times 0.3 \times 460000 - (1 + 0.2) \times 2600\right] = 14608.15893,$$
$$B_t = \frac{1}{1 + 0.2} 0.113 \times 0.3 \times 720000 = 20340, \quad (92)$$

respectively. In this regard, we compute the cost of funds in period t as

$$u\left(A_t\right) A_t = (0.002 - 0.002 \times 0.002 + 0.011904761 - 0.022) \times 0.3 \times 460000 = -1117.69. \quad (93)$$

Also, we see that the LQE's nett worth at date t is more than their current output just after the shock; thus,

$$(1 - \Sigma)\, uA^* = (1 - 0.002)\, 0.002 \times 0.3 \times 460000 = 275.448. \quad (94)$$

With unexpected capital gains,

$$\left(p_t^A + p^{A*}\right) A^* = (0.011904761 + 0.022) \times 0.3 \times 460000 = 4679. \quad (95)$$

While the debt repayment is given by

$$\left(1 + r^{B}\right) B^{*} = p^{A*} A^{*} = (1 + 0.2)\, 2600 = 3120. \tag{96}$$

Proportional change in A_t and p_t^A can be computed as

$$\widehat{A}_t = \frac{0.3\,(720000 - 460000)}{0.3 \times 460000} = 0.565217391,$$
$$\widehat{p}_t^A = \frac{0.011904761 - 0.022}{0.022} = -0.4588745. \tag{97}$$

The steady-state profit for LQE is

$$\Pi_t^{*} = (0.061 + 0.03 \times 0.2)\, 0.022 \times 0.3 \times 460000 + 0.205 \times 5000 - 0.205 \times 1200 - 0.2 \times 2600 = 462.412. \tag{98}$$

and steady-state profit for HQEs is

$$\Pi_t^{\prime *} = 0.061 \times 0.022 \times (1 - 0.3) \times 460000 + 0.205 \times 5000 - 0.205 \times 1200 - 0.2 \times 2600 = 691.124. \tag{99}$$

Thus, the proportional changes in Π_t and Π_t' are

$$\widehat{\Pi}_t = \frac{87 - 462.412}{462.412} = -0.81186,$$
$$\widehat{\Pi}_t' = \frac{123.5 - 691.124}{691.124} = -0.82131. \tag{100}$$

Elasticity of the residual asset supply to the LQE with respect to the monitoring cost at the steady-state at date t is

$$\eta = \left[\frac{((2 + 0.2)/0.2)\, 0.4588745 - 0.002}{0.565217391} - 1\right]^{-1} = 0.126718931. \tag{101}$$

The proportional changes for $\widehat{p}_t^A$ and $\widehat{A}_t$ in terms of the size of the shock Σ are computed by

$$\widehat{p}_t^A = -\frac{1}{0.126718931} 0.002 = -0.015782961,$$
$$\widehat{A}_t = -\frac{1}{1 + 1/0.126718931}\left(1 + \frac{1 + 0.2}{0.126718931 \times 0.2}\right) 0.002 = -0.010875327, \tag{102}$$

respectively. By considering (47), we see from (63) and (71) that $\widehat{p}_t^A$ and $\widehat{A}_t$ become

$$\widehat{p}_t^A\Big|_{p_{t+1}^A = p^{A*}} = -\frac{0.2}{0.126718931\,(2 + 0.2)} 0.002 = -0.001434814,$$
$$\widehat{A}_t\Big|_{p_t^A + 1 = p^{A*}} = -0.002, \tag{103}$$

Table 3: Computed asset securitization parameters.

Parameter	Value
C_{t+1}	43 632
$p_t^A A_{t-1}$	\$4 000
$\Pi_t \geq$	\$−18 561
x_t'	\$−46 319.9995
$p_t^A A_{t-1}'$	\$4 991.8
u_t	−0.082261905
Aggregate B_t	\$20 340
p^{A^*}	0.012
A_t under shock	\$14 608.15893
$u(A_t)A_t$	−1 117.69
$(p_t^A + p^{A^*})A^*$	\$4 679
$\widehat{A}_t$	0.565217391
Π_t^*	\$462.412
$\widehat{\Pi}_t$	\$−2.1118
η	0.126718931
$\widehat{A}_t$ in terms of shock	0.01
$\widehat{A}_t$ where $p_{t+1}^A = p^{A^*}$	−0.002
$\beta >$	0.0099099
Π_t	\$87
x_t	\$54 103.6421
Π_t'	\$123.5
$\Pi_t' \geq$	\$−51 007
Aggregate A_t	14 601.44865
$\overline{A}$	720 000
B^*	\$2 600
B_t under shock	\$20 340
$(1 - \Sigma)\mu A^*$	275.448
$(1 + r^{\mathrm{B}})\mathrm{B}^*$	\$3 120
$\widehat{p}_t^A = \widehat{p}_t^C$	−0.4588745
$\Pi^{*\prime}$	\$275.31
$\widehat{\Pi}_t'$	\$691.124
$\widehat{p}_t^A$ in terms of shock	−0.015782961
$\widehat{p}_t^A$ where $p_{t+1}^A = p^{A^*}$	−0.001434814
$\widehat{C}_{t+1}$	0.064869

respectively. The proportional change in aggregate output, C_{t+1}, represented by (54) is given by

$$\widehat{C}_{t+1} = \frac{0.002 + 0.2 - (1 + 0.2)\, 0.002}{0.002 + 0.2} \times \frac{(0.002 + 0.2)\, 0.3 \times 460000}{240000} 0.565217391 = 0.064869. \tag{104}$$

We provide a summary of computed asset securitization parameters in Table 3.

An analysis of the computed shock parameters in Table 3 shows that the aggregate output, $\widehat{C}_{t+1}$, increases to \$43632. The value of LQAs, $p_t^A A_{t-1}$, increases to \$5 000. LQA demand, A_t, has declined to \$14 608.15893 while the borrowings B_t have increased to \$20 340. This implies that HQAs

were more sensitive to changes in market conditions and that asset transformation may have been a greater priority. The proportional negative change in profit for the LQE subsequent to a temporary shock is higher than that of the HQEs. In addition, the steady-state asset price p^{A^*} and the borrowings B^* for the LQE increased to \$0.012 and \$2 600, respectively. In summary, this example shows that when parameter choices are altered and the size of shock increased, the LQE suffers bigger losses on their asset holdings and the rate of borrowing to refinance increases. This explains why most people could not pay back their loans during the 2007–2009 financial crisis.

4.2.3. Numerical Example: Financial Intuition. A financial motivation for the numerical example discussed in Section 4.2.1 is outlined in the current paragraph. According to Basel III capital and liquidity regulation, LQEs and HQEs have a couple of obligations in terms of transaction costs (refer to (22)). The first is towards the originator for acquiring the assets while the second is for using the assets for securitization into CDOs, a type of user cost. In Section 4.2.1, we compute LQE and HQE equilibrium variables to add credence to the aforementioned statements.

The financial intuition behind the numerical example discussed in Section 4.2.2 is given below. Investors sought SAPs because they met certain prudential standards such as restrictions to purchase only investment grade debt (see the Basel documents [8, 9] for more details about securitization). Investors could meet relative "safety requirements" since securitization is essentially a form of bankruptcy-remote secured lending (as assets are legally isolated in a SPE) with credit enhancement (or government guarantees for RABS in some jurisdictions) that often resulted in the securities being highly rated (e.g., AAA, AA, or A). However, as noted before, the reliance on credit ratings sowed the seeds of later difficulties, as many investors relied too heavily on credit ratings and effectively "outsourced" their due diligence to the credit rating agencies (see the BCBS papers [8, 9] for further discussion). It is also worth noting that investor requirements for HQLAs created liquidity concerns during the crisis when policies or requirements forced investors to sell assets after ratings downgrades (see [5] for more details). This tested the liquidity assumptions about securitized products when many investors were simultaneously forced to sell, driving prices ever lower in a down market (see, e.g., [5, 21, 22]). Investors could avoid exceeding concentration limits, both regulatory restrictions and internal limits on exposures to a single name, by purchasing SAPs. Further, investors could manage risk in the entire portfolio by holding securitized assets that had a low correlation with other components of the investors' portfolios, such as equities and corporate bonds (see [3] for further discussion). Also, investors could meet their internal portfolio diversification requirements by increasing the types of assets as well as the geographical location of the assets' origination. Synthetic securitizations also allowed investors to increase the variety and volume of instruments they could acquire without funding the credit exposure (see [8, 9] for further discussion on asset securitization). However, as the crisis unfolded, investors learned that their expected diversification benefits were partially false and that in some cases the underlying assets were highly correlated. SAPs helped investors achieve higher yield thresholds since the risk-adjusted return on ABS was typically higher relative to a similarly rated nonsecuritization investment. In the period before the crisis, investors were seeking higher yields at the same time spreads in the broader fixed income markets were narrowing (see the Basel documents [8, 9]).

5. Conclusions about Basel III and Asset Securitization

The main conclusions about LQA and HQA securitization, an LQE at equilibrium, negative shocks to asset securitization for dynamic and static multipliers, and illustrative examples involving asset securitization are summarized in this section.

5.1. Conclusions about LQA Securitization. We answered Question 1 in Section 2.1 by characterizing the securitization of LQAs by an LQE. In this case, the cash flow constraint is given by (10). The discussion on LQE cash flow has connections with Basel III capital and liquidity regulation (see [5] for further discussion). In this regard, it is clear that investors may be motivated to purchase securities issued by LQEs to avert Basel III regulatory limits, such as those relating to LQAs. In the case of synthetic transactions, investors may find it beneficial that they would not have to fund credit exposures at the outset (see, e.g., the Joint Forum paper [1]). In cases where parties to entities possessed a comprehensive understanding of the associated risks and possible structural behaviors of these LQEs under various scenarios, they have effectively engaged in and reaped benefits from their LQE activities (see [1, 3, 6] for more details). However, it is unclear that LQAs sold into the LQE can be attributed to the existence of these structures, that were simply the legal form in which such assets were held to issue bonds backed by them. Nonetheless, it is important for Basel III to address why some of the recent failures of LQE usage occurred (see, e.g., the Basel publications [1, 6]).

5.2. Conclusions about HQA Securitization. Next, we answered Question 2 in Section 2.2 by describing the securitization of HQAs by HQEs. In this case, the HQE cash flow constraint is expressed as in (20). In Section 2.2, the discussion on HQEs has relationships with Basel III capital and liquidity regulation (see [5] for more details). For example, a bank might view the Basel III risk-based capital charge applied to HQAs as being excessive and therefore might engage in securitization activities of these receivables to benefit from a slightly lower capital charge resulting from other aspects of the risk-based capital rules (see, e.g., [1]). In the bank's view, this slightly lower Basel III charge might be more rational in terms of the true risks and capital needed for corporate lending activities (see, e.g., the Basel documents [1, 6]).

5.3. Conclusions about an LQE at Steady State. Theorem 7 in Section 2.3 provides the answer to Question 3. Here, a characterization of the behaviour of an LQE in equilibrium

is given. According to the Basel III securitization framework, LQEs and HQEs have at least two obligations in terms of transaction costs (refer to (22)). The first is towards the originator for acquiring the assets while the second is for using the assets for securitization into CDOs, a type of user cost. The latter fee involves, for instance, an external credit rating agency (see Section 2.4 for more details). Also, because of information asymmetry and regulatory dysfunction, CDOs open up opportunities for arbitrage, a point that has been considered in Basel III for balanced information distribution (see, e.g., [9]). In this regard, sophisticated CDO entities, often circumvent regulatory constraints. This type of arbitrage is accompanied by high costs with originators and other financial intermediaries earning huge transaction fees and eroding value for entities and investors (see, e.g., the Basel papers [9, 10]).

5.4. Conclusions about Negative Shocks to Asset Securitization (Dynamic Multiplier). In the presence of a dynamic multiplier, in Theorem 8 from Section 3.1, we quantify changes to asset price and holdings, CDO output, and profit subsequent to negative shocks. Also, we quantify changes to profit in terms of asset and prepayment rates as well as equity subsequent to negative shocks (refer to Question 4). We conclude that the proportional change in asset price, $\widehat{p}_t^A$, and input, $\widehat{A}_t$, as well as CDO price, $\widehat{p}_t^C$, is negative in response to a negative shock like a ratings downgrade. Basel III endeavours to make provision for these negative changes in a countercyclical way (see, e.g., [1, 6, 23]). The same observation can be made about CDO output, $\widehat{C}_{t+1}$, and profit, $\widehat{\Pi}_t$, where a ratings downgrade has a negative impact (see, e.g., Basel III's (see, e.g., the BCBS documents [1, 6]).

5.5. Conclusions about Temporary Shocks to Asset Securitization (Static Multiplier). When a static multiplier is present, in Corollary 9 in Section 3.2, we determine changes to asset price, $\widehat{p}_t^A|_{p_{t+1}^A}$, and input, $\widehat{A}_t|_{p_{t+1}^A}$, given by (68) and (69), respectively, subsequent to a negative shock such as a ratings downgrade (refer to Question 5). As before, Basel III capital regulation attempts to negate the deleterious effects of ratings downgrades on price and input in a countercyclical manner (see, e.g., [23]).

5.6. Conclusions about Example of Subprime Mortgage Securitization. Question 6 is answered in Corollary 10 from Section 4.1. Here, an example of LQA securitization for subprime mortgages is provided. Of course, the subprime mortgage crisis preceded the 2007–2009 financial crisis and as such its connection with Basel III is very important (see, e.g., [4, 15]). The BCBS reports in Basel III documents that risk weights for low-rated senior subprime securitization exposures were too high. Many senior securitization exposures were downgraded during the crisis (compare with [3]). While some of these exposures resulted in total loss to investors, most of these exposures have resulted in recovery of some principal (see the Basel documents [8, 9]).

5.7. Conclusions about Example of Numerical Examples of Asset Securitization. Section 4.2 produces a numerical example to illustrate the impact of negative shocks on asset securitization by the LQE and HQEs. In particular, the example illustrates the impact of negative shocks on assets and CDOs. It shows that when parameter choices are altered and the size of the shock increased, the LQE suffers significant losses to their asset holdings and the rate of borrowing increases (compare with Question 7). Also, we illustrated that asset price is most significantly affected by unexpected negative shocks from asset rates, while, for CDO price, shocks to speculative asset funding, investor risk characteristics, and prepayment rate elicit statistically significant responses (compare with [3]). Problems from the financial crisis relate to our models for assets and CDOs with respect to the reduction in incentives for banks to monitor entities, transaction costs, manipulation of CDO price and structure, CDO market opacity, self-regulation, systemic risks associated with CDOs, and the mispricing of debt (see the BCBS papers [3, 8, 9]).

According to [8, pages 9–11], the role of Basel III in the numerical example from Section 4.2 can be considered from two perspectives which are the

(i) quantitative perspective—the amount of HQLAs that the banks will have to amass in the next few years, both to meet the new requirements and to repay special facilities provided by governments and central banks, which is assumed to not be renewed. There is clearly a potential transition problem which needs to be considered in determining the timing of implementation of new regulations (see the BCBS publication [8] for more details);

(ii) structural perspective—this refers to the ways in which the funding and liquidity management, not only of banks but also of their customers, will be permanently affected by the proposed regulations (see [5] for further details). What may appear to be rather detailed aspects of the proposed regulations may in fact have very serious implications for financial stability in the future (see the Basel document [8] for further discussion).

5.8. General Conclusions about Basel III and Asset Securitization. In answering Question 8, we note that in the Basel III document [1], the JFWGRAC makes the following recommendations about the supervision of the LQE and HQEs discussed in previous subsections.

5.8.1. LQE and HQE Economic Risks and Purposes. Firstly, supervisors should make sure that market participants assess all economic risks and business purposes of LQEs and HQEs during the lifespan of a transaction distinguishing between risk transfer and transformation. We note that, over time, the nature of these risks can change. Supervisors should ensure that such assessment is ongoing and that management has sufficient understanding of the risks (see the Basel document [1, 3] for more details).

5.8.2. LQE and HQE Transaction Complexity. Secondly, market participants should be able to assess and risk manage factors that increase transaction complexity, such as structural features of the LQE and HQEs including triggers and the roles of parties involved (see, e.g., the Basel documents [1, 6]).

5.8.3. LQE and HQE Governance Processes. In the third place, banks and supervisors should ensure the governance process of LQEs and HQEs commensurate with the degree of active intervention and discretion of the parties participating in these entities (see [1] for more discussions).

5.8.4. LQE and HQE Portfolio Risk Profiles. The fourth recommendation is that banks should continually monitor the quality of transferred exposures in relation to the risk profile of LQEs' and HQEs' remaining portfolios and the impact on its balance sheet components, and supervisors should where appropriate assess systemic implications of risk dispersion to transferees (see the Basel documents [1, 3, 6] for more details).

5.8.5. LQE and HQE Risk Exposures. Fifthly, banks should have the capability of aggregating, assessing and reporting all their LQE and HQE risk exposures in conjunction with all other bank-wide risks (see, e.g., [1, 3]).

5.8.6. LQE and HQE Support. In the sixth place, if at inception or at any point during LQE and HQE existence there is a likelihood or evidence of support by the bank, including noncontractual support, then the activities and risks of those entities should be aggregated with those of the bank for both supervisory assessment and internal risk management purposes (see the Basel documents [1, 6] for more discussions).

5.8.7. LQE and HQE Transaction Standardization. The seventh recommendation is that supervisors should support market participants' efforts towards greater standardization of definitions, documentation, and disclosure requirements of LQE and HQE transactions and provide for the communication of any material divergence from these standards to investors in individual transactions (see [1, 3] for more details).

5.8.8. LQE and HQE Weakness, Contagion, or Procyclicality. Finally, supervisors should regularly oversee and monitor the use of all LQE and HQE activities and assess the implications for regulated banks of the activities of such entities, in order to identify developments that can lead to systemic weakness and contagion or that can exacerbate procyclicality (see, e.g., the Basel discussion documents [1, 6]).

5.9. Future Directions Related to Basel III and Asset Securitization. A topic of future research may be the effects of shocks on high-quality liquid assets (HQLA) as in [21]. In this regard, we recall that an asset is considered to be a HQLA if it can be easily and immediately converted into cash at little or no loss of value. Asset liquidity depends on the underlying stress scenario, the volume to be monetized, and the time-frame considered (see [5] for more details). Nevertheless, there are certain assets that are more likely to generate funds without incurring large discounts in sale or repurchase agreement (repo) markets due to fire-sales even in times of stress (see, e.g., [6, 21] for more details). While [6] lays out proposed revisions to the securitization framework, it does not include proposed rules text that would effectuate these changes. The BCBS is seeking industry feedback on some key elements of the proposed changes and will, in the coming months, conduct a quantitative impact study (QIS) of the proposals before deciding on a definitive way forward (see, e.g., [1]). The BCBS will consider all comments received along with the results of the QIS before determining the appropriate next steps in the process of moving forward with revisions to the securitization framework. This would mean that the contents of the current paper would have to be refined quite considerably.

Conflict of Interests

The authors of this paper, do not have a direct financial relationship with the commercial entities mentioned in this paper that might lead to a conflict of interests.

References

[1] Basel Committee on Banking Supervision, *The Joint Forum: Report on Special Purpose Entities*, Bank for International Settlements (BIS) Publications, 2009, http://www.bis.org/publ/joint23.pdf.

[2] Basel Committee on Banking Supervision, *Basel III: A Global Regulatory Framework for More Resilient Banks and Banking Systems*, Bank for International Settlements (BIS) Publications, 2010, http://www.bis.org/publ/bcbs189.htm.

[3] F. Gideon, J. Mukuddem-Petersen, and M. A. Petersen, "Minimizing banking risk in a Lévy process setting," *Journal of Applied Mathematics*, vol. 2007, Article ID 32824, 25 pages, 2007.

[4] M. A. Petersen, M. C. Senosi, and J. Mukuddem-Petersen, *Subprime Mortgage Models*, Nova Science, New York, NY, USA, 2012.

[5] M. A. Petersen and J. Mukuddem-Petersen, *Basel III Liquidity Regulation and Its Implications*, Business Expert Press, McGraw-Hill, New York, NY, USA, 2013.

[6] Basel Committee on Banking Supervision, *Consultative Document: Revisions to the Basel Securitisation Framework*, Bank for International Settlements (BIS) Publications, 2012, http://www.bis.org/publ/bcbs236.htm.

[7] Basel Committee on Banking Supervision, *Basel III: A Global Regulatory Framework for More Resilient Banks and Banking Systems*, Bank for International Settlements (BIS) Publications, 2011, http://www.bis.org/publ/bcbs189.htm.

[8] Basel Committee on Banking Supervision, *Enhancements to the Basel II Frame-Work*, Bank for International Settlements (BIS) Publications, 2009, http://www.bis.org/publ/bcbs157.htm.

[9] Basel Committee on Banking Supervision, *Revisions to the Basel Securitization Framework*, Bank for International Settlements (BIS) Publications, 2012, http://www.bis.org/publ/bcbs158.htm.

[10] Basel Committee on Banking Supervision, *Report on Asset Securitization Incentives*, Bank for International Settlements (BIS) Publications, 2011, http://www.bis.org/publ/bcbs174.htm.

[11] I. Fender and M. Scheicher, "The pricing of subprime mortgage risk in good times and bad: evidence from the ABX.HE indices," Working Paper Series No 1056, European Central Bank, 2009.

[12] Housing Derivatives, *ABX Subprime Mortgage Index Still Making New Lows*, Housing Derivatives Applications and Economics for the US Housing Market, 2008, http://housingderivatives.typepad.com/housing_derivatives/2008/02/abx-subprime-mo.html.

[13] M. Iacoviello, "House prices, borrowing constraints, and monetary policy in the business cycle," *American Economic Review*, vol. 95, no. 3, pp. 739–764, 2005.

[14] N. Kiyotaki and J. Moore, "Credit cycles," *Journal of Political Economy*, vol. 105, no. 2, pp. 211–248, 1997.

[15] J. Mukuddem-Petersen, M. A. Petersen, T. Bosch, and B. de Waal, "Speculative funding and its impact on subprime mortgage product pricing," *Applied Financial Economics*, vol. 21, no. 19, pp. 1397–1408, 2011.

[16] G. Elliehausen, M. E. Staten, and J. Steinbuks, "The effect of prepayment penalties on the pricing of subprime mortgages," *Journal of Economics and Business*, vol. 60, no. 1-2, pp. 33–46, 2008.

[17] R. S. J. Koijen, O. van Hemert, and S. van Nieuwerburgh, "Mortgage timing," *Journal of Financial Economics*, vol. 93, no. 2, pp. 292–324, 2009.

[18] G. Elliehausen and M. Hwang, *Mortgage Contract Choice in Subprime Mortgage Markets*, Finance and Economics Discussion Series, Working Paper No. 2010-53, Divisions of Research & Statistics and Monetary Affairs, Federal Reserve Board, Washington, DC, USA, 2010.

[19] J. Mukuddem-Petersen, M. A. Petersen, I. M. Schoeman, and B. A. Tau, "Maximizing banking profit on a random time interval," *Journal of Applied Mathematics*, vol. 2007, Article ID 29343, 22 pages, 2007.

[20] Basel Committee on Banking Supervision, *Revisions to the Basel II Market Risk Framework*, Bank for International Settlements (BIS) Publications, 2009, http://www.bis.org/publ/bcbs158.htm.

[21] Basel Committee on Banking Supervision, *Basel III: The Liquidity Coverage Ratio and Liquidity Risk Monitoring Tools*, Bank for International Settlements (BIS) Publications, 2013, http://www.bis.org/publ/bcbs238.htm.

[22] Basel Committee on Banking Supervision, *Liquidity Coverage Ratio Disclosure Standards*, Bank for International Settlements (BIS) Publications, 2013, http://www.bis.org/publ/bcbs144.htm.

[23] M. Drehmann, C. Borio, L. Gambacorta, G. Jiménez, and C. Trucharte, "Countercyclical capital buffers: exploring options," BIS Working Papers No 317, Monetary and Economic Department, Bank for International Settlements (BIS) Publications, 2010.

Hindawi Publishing Corporation
Discrete Dynamics in Nature and Society
Volume 2013, Article ID 753025, 13 pages
http://dx.doi.org/10.1155/2013/753025

Research Article

Terminal-Dependent Statistical Inference for the Integral Form of FBSDE

Qi Zhang[1,2]

[1] *School of Mathematics, Shandong University, Jinan 250100, China*
[2] *College of Mathematics, Qingdao University, Qingdao 266071, China*

Correspondence should be addressed to Qi Zhang; qizhang8409@gmail.com

Received 14 June 2013; Revised 4 September 2013; Accepted 22 September 2013

Academic Editor: Vasile Dragan

Copyright © 2013 Qi Zhang. This is an open access article distributed under the Creative Commons Attribution License, which permits unrestricted use, distribution, and reproduction in any medium, provided the original work is properly cited.

Backward Stochastic Differential Equation (BSDE) has been well studied and widely applied. The main difference from the Original Stochastic Differential Equation (OSDE) is that the BSDE is designed to depend on a terminal condition, which is a key factor in some financial and ecological circumstances. However, to the best of knowledge, the terminal-dependent statistical inference for such a model has not been explored in the existing literature. This paper is concerned with the statistical inference for the integral form of Forward-Backward Stochastic Differential Equation (FBSDE). The reason why I use its integral form rather than the differential form is that the newly proposed inference procedure inherits the terminal-dependent characteristic. In this paper the FBSDE is first rewritten as a regression version, and then a semiparametric estimation procedure is proposed. Because of the integral form, the newly proposed regression version is more complex than the classical one, and thus the inference methods are somewhat different from those designed for the OSDE. Even so, the statistical properties of the new method are similar to the classical ones. Simulations are conducted to demonstrate finite sample behaviors of the proposed estimators.

1. Introduction

The Backward Stochastic Differential Equation (BSDE) was first presented by Bismut [1] for the linear case and by Pardoux and Peng [2] for the general case. The solution of a BSDE consists of a pair of adapted processes (Y_t, Z_t) satisfying

$$-dY_t = g(t, Y_t, Z_t)\,dt - Z_t dB_t; \quad Y_T = \xi, \tag{1}$$

where g is the generator, B_t is the standard Brownian motion, and ξ is the terminal condition. Usually the terminal condition is designed as a random variable with given distribution. If g meets certain conditions, the BSDE has a unique solution. The integral form of the BSDE can be expressed as

$$Y_t = \xi + \int_t^T g(s, Y_s, Z_s)\,ds - \int_t^T Z_s dB_s. \tag{2}$$

The study history of the BSDE was relatively short but progressed rapidly. In addition to the interesting mathematical nature, its extensive applications gained more and more attentions; see for example Peng [3], Pardoux and Peng [4], Pardoux and Tang [5], Peng and Wu [6], Ma and Yong [7], and Nualart and Schoutens [8]. Duffie and Epstein [9] used the BSDE to describe the consumer preferences under uncertain economic environment (i.e., the stochastic differential utility). El Karoui and Quenez [10] stated that in financial markets, prices of many important derivative securities could be solved by a certain BSDE. Lin et al. [11] used an extended statistical model to describe an ecological problem. Furthermore, the BSDE is closely related to nonlinear partial differential equation, more generally, the inseparability of nonlinear semigroup or stochastic control problems. Meanwhile, this type of equation appears frequently in mathematical finance as pointed out by Quenez [12]. Recently, Delong [13] introduced the most recent advances in BSDE (including FBSDE) and applied BSDE with jumps to insurance and finance fields.

In terms of the backward equation, within a complete market it serves to characterize the dynamic value of replicating portfolio Y_t with a final wealth ξ and a special quantity Z_t that depends on the hedging portfolio. Especially when the randomness of (g, ξ) of BSDE comes from the state of

the forward equation, the corresponding equation is proved to be a Forward-Backward Stochastic Differential Equation (FBSDE), which can be expressed as

$$dY_t = -g(X_t, Y_t, Z_t, t)\,dt + Z_t dB_t; \quad Y_T = \xi, \tag{3}$$

with X_t satisfying

$$dX_s = \mu(s, X_s)\,ds + \sigma(s, X_s)\,dB_s. \tag{4}$$

Compared to the Ordinary Stochastic Differential Equation (OSDE) that contains an initial condition, the solution of the FBSDE is affected by the terminal condition $Y_T = \xi(X_T)$. As is well known, there exist a number of parametric and nonparametric methods to deal with estimation and test for the OSDE. However, these methods can not be directly employed to infer the BSDE and FBSDE because the two models are related to a terminal condition.

For the FBSDE defined above, the statistical inference was investigated initially by Su and Lin [14], Chen and Lin [15], and a relevant model which was proposed by Lin et al. [11]. However, they did not take the terminal condition into account in the inference procedure. In the framework of the FBSDE mentioned above, the terminal condition is additional, which is not nested into the equation. Thus, there is an essential difficulty to use the terminal condition to refine the inference procedure. As a result, their methods fail to cover the full problems given in the FBSDE.

As well the FBSDE could turn to the integral form:

$$\begin{aligned} Y_t &= \xi + \int_t^T g(s, X_s, Y_s, Z_s)\,ds - \int_t^T Z_s dB_s, \\ dX_t &= \mu(t, X_t)\,dt + \sigma(t, X_t)\,dB_t; \quad X_0 = x. \end{aligned} \tag{5}$$

In this paper I focus only on the integral form because it contains the terminal condition as an additive term of the equation. With such a construction, a terminal-dependent inference could be built. I am concerned with the semiparametric estimation of the FBSDE in this paper. Note that Z_t is usually unobservable and g can not be completely specified in the financial market. The problems of interest are therefore to give both proper estimations of the generator g and the process Z_t based on observed data (X_t, Y_t) and the terminal condition ξ. As an initial investigation, this paper only considers the model with generator being parametric structure; that is to say, g can be written in the form of $g = g(\theta, t, Y_t, Z_t)$, where θ is an unknown parameter vector. Even so, such a simplified form is widely used in financial markets, and, furthermore, the proposed methods can be extended to the other complicated forms.

It is worth mentioning that the key point of the method is the use of the integral equation rather than the differential equation. This change leads to a completely new work among the existing researches. Unlike the forward equation, because of the integral, the cumulative error appears not neglectable; nevertheless, the resultant estimation is still asymptotically unbiased for the condition of mixing dependency of X_t attached. Another difference from the ordinary model is that the generator contains the unobservable process Z_t, and then it is necessary to estimate Z_t first. After plugging the estimator of Z_t into the generator, I could infer generator g with the newly proposed methods.

The paper is organized as follows. In Section 2, the FBSDE is first rewritten as a special regression, and, by this representation, the estimation procedure for the FBSDE with linear generator is designed. Next I discuss the asymptotic properties in Section 3. A supplement for the inference of equation is suggested, and an extension for nonlinear model is briefly discussed in Section 4. Simulation study is proposed in Section 5 to illustrate the methods. The proofs of the theorems are presented in Section 6.

2. Terminal-Dependent Semiparametric Estimation for the FBSDE

2.1. Model and Its Statistical Version. I consider the integral form of the standard FBSDE:

$$\begin{aligned} Y_t &= \xi + \int_t^T g(s, X_s, Y_s, Z_s)\,ds - \int_t^T Z_s dB_s, \\ dX_t &= \mu(t, X_t)\,dt + \sigma(t, X_t)\,dB_t; \quad X_0 = x, \end{aligned} \tag{6}$$

where $\{B_t\}_{t\geq 0}$ is the Brownian motion and ξ is a smooth function. Here the generator g is a function of t, Y_t, and Z_t, with Z_t being usually unobservable. Furthermore, the adapted process Y_t, Z_t and terminal condition could be indicated as a function of X_t. As is known to everyone, the existence and uniqueness result of the FBSDE have been studied elaborately. This section is intended to represent the FBSDE as a statistical framework and then address the proper estimators of g and Z_t based on observed data $\{X_t, Y_t\}$ and the terminal condition ξ.

To recast the model (6) as a statistical model, I first examine the property of the last term of the first equation in (6). By the property of Itô integral and the relation between the two equations in (6), I have

$$E\left(\int_t^T Z_s dB_s\right) = 0, \qquad \mathrm{Var}\left(\int_t^T Z_s dB_s\right) = E\left(\int_t^T Z_s^2 ds\right). \tag{7}$$

Then I regard $-\int_t^T Z_s dB_s$ as error and consequently rewrite the first equation of model (6) as

$$Y_t = \xi + \int_t^T g(s, Y_s, Z_s)\,ds + \epsilon_t, \tag{8}$$

where ϵ_t is the error term with mean zero and bounded variance, and the adapted process Y_t, Z_t and terminal condition ξ depend on X_t via the second equation of (6).

Remark 1. It seems that formula (8) proposes a regression that is determined by both expectation and variance frameworks. However, such a regression is quite unlike the classical one. In the newly defined structure, although the expectation of the error is zero, the conditional expectation of the error is nonzero. Even so, the resultant estimation is asymptotically unbiased, and thus the consistency of the estimators

defined below still holds because of the condition of mixing dependency of X_t given below; for details see the following theorems and the proofs of the theorems.

Given the initial calendar time point t_1, I record the observed time series data $\{X(t_i), Y(t_i), i = 1, \ldots, n\}$ at the equally spaced time points $\{t_i = t_1 + (i-1)\Delta, i = 1, \ldots, n\} \subseteq [0, T]$. Denote $\Delta_i = t_{i+1} - t_i (= \Delta)$ for $1 \le i \le n-1$ and $\Delta_n = T - t_n$. Note that Δ_n is the distance between the last observation time t_n and the terminal time T; indeed it may be quite large and then makes the following formula (9) inaccurate. Therefore I first assume Δ_n small enough, that is, $\Delta_n = O(\Delta)$, and then propose an adjustment in Section 4 for the case with larger Δ_n. On the other hand, since the distribution of ξ is supposed known, I can get the samples $\{\xi_i, 1 \le i \le k\}$ for $k \ge 1/\Delta$.

In this section I assume g can be expressed as linear function $g(t, Y_t, Z_t) = a + bY_t + cZ_t$, where a, b, and c are unknown parameters. Then the model (8) can be approximately rewritten as

$$\begin{aligned} Y(t_i) &= \widehat{\xi} + \sum_{j=i}^{n} \left(a + bY\left(t_j\right) + cZ\left(t_j\right)\right)\Delta_j + O(\Delta) + \epsilon_i + \nu_s, \\ E(\epsilon_i) &= 0, \qquad \operatorname{Var}(\epsilon_i) = \sum_{j=i}^{n} \Delta_j Z^2\left(t_j\right) + O(\Delta), \\ & \qquad\qquad i = 1, \ldots, n, \end{aligned} \tag{9}$$

where $\widehat{\xi} = (1/k)\sum_{i=1}^{k} \xi_i$ and $\nu_s = \xi - \widehat{\xi}$, satisfying $E(\nu_s) = 0$ and $\operatorname{Var}(\nu_s) = \operatorname{Var}(\xi)(1 + (1/k))$.

This is the statistical version of (8), a new regression model. It is worth mentioning that the new model (9) is somewhat different from the classical regression; that is, in addition to the mean-variance structure, the new one has a complicated structure and contains a terminal information.

2.2. Semi-Parametric Estimation for the FBSDE. I now turn to estimating unknown parameter vector $\beta = (a, b, c)^\tau$ in model (9). While the generator contains unobservable interesting process Z_t, it is necessary to estimate Z for plugging the estimator into the generator firstly. After that, the common parametric estimation methods can be employed to estimate parameters.

Concerning inference of Z_t, despite the connection between Z_t and the variance of ϵ_i in (9), the second formula of (9) is related to the weighted sum of Z_t^2, which causes inconvenience for estimating Z_t by residual-based method. I now adopt a difference-based method instead.

To this end, consider the FBSDE model (6), motivated by Stanton [16], for the Markov process $\{X_s\}_{t \le s \le T}$ which follows the SDE,

$$dX_s = \mu\left(s, X_s\right) ds + \sigma\left(s, X_s\right) dB_s; \tag{10}$$

the infinitesimal generator $\mathscr{L} f(t, X_t)$ is defined as

$$\begin{aligned} &\mathscr{L} f\left(t, X_t\right) \\ &= \lim_{\Delta \to 0^+} \frac{1}{\Delta} \left\{E\left[f\left(t + \Delta, X_{t+\Delta}\right) \mid X_t = x\right] - f(t, x)\right\} \\ &= \frac{\partial f}{\partial t} + \mu(t, x) \frac{\partial f(t, x)}{\partial x} + \frac{1}{2}\sigma^2(t, x) \frac{\partial^2 f(t, x)}{\partial x^2}, \end{aligned} \tag{11}$$

where the bivariate function $f(\cdot, \cdot)$ satisfies the sufficient smoothing condition [17]. By Taylor's expansion, the condition expectation $E[f(t + \Delta, X_{t+\Delta}) \mid X_t = x]$ can be expressed as

$$\begin{aligned} &E\left[f\left(t + \Delta, X_{t+\Delta}\right) \mid X_t = x\right] \\ &= f(t, x) + \mathscr{L} f(t, x)\Delta + \frac{1}{2}\mathscr{L}^2 f(t, x)\Delta^2 \\ &\quad + \cdots + \frac{1}{n!}\mathscr{L}^n f(t, x)\Delta^n + O\left(\Delta^{n+1}\right), \end{aligned} \tag{12}$$

which implies that when the time increment $\Delta \to 0$, the first-order approximation formula for $\mathscr{L} f(t, x)$ can be given by

$$\begin{aligned} &\mathscr{L} f(t, x) \\ &= \frac{1}{\Delta} E\left[f\left(t + \Delta, X_{t+\Delta}\right) - f\left(t, X_t\right) \mid X_t = x\right] + O(\Delta). \end{aligned} \tag{13}$$

In addition, we need the following generalized Feynman-Kac formula. Let υ be a $\mathscr{C}^{1,2}$ function, and suppose there exists a constant C such that, for each (t, x),

$$|\upsilon(t, x)| + \left|\partial_x \upsilon(t, x)\sigma(t, x)\right| \le C(1 + |x|), \tag{14}$$

and υ is the solution of the following system of quasilinear parabolic partial differential equation

$$\begin{aligned} \mathscr{L}\upsilon(t, x) + f\left(t, x, \upsilon(t, x), \partial_x \upsilon(t, x)\sigma(t, x)\right) &= 0, \\ \upsilon(T, x) &= \phi(x). \end{aligned} \tag{15}$$

Then $Y_s^{t,x} = \upsilon(s, X_s^{t,x})$, $Z_s^{t,x} = \partial_x \upsilon(s, X_s^{t,x})\sigma(s, X_s^{t,x})$, a.s., where $(Y_s^{t,x}, Z_s^{t,x})$ is the unique solution of the FBSDE, based on the result in Pardoux and Peng [4].

Denote $(Y_s^{t,x}, Z_s^{t,x})$ by (Y_s, Z_s), respectively, for short. By using the Taylor's expansion of $f(s, x) = (\upsilon(s, x) - \upsilon(t, X_t))^2$,

$$\begin{aligned} \mathscr{L} f(s, x) &= 2\left(\upsilon(s, x) - \upsilon\left(t, X_t\right)\right)\mathscr{L}\upsilon(s, x) \\ &\quad + \upsilon_x^2(s, x)\sigma^2(s, x); \end{aligned} \tag{16}$$

then $\mathscr{L} f(t, X_t) = \upsilon_x^2(t, X_t)\sigma^2(t, X_t)$, and

$$\begin{aligned} &\mathscr{L} f\left(t, X_t\right) \\ &= \frac{1}{\Delta} E\left[\left(\upsilon\left(t + \Delta, X_{t+\Delta}\right) - \upsilon\left(t, X_t\right)\right)^2 \mid X_t = x\right] + O(\Delta). \end{aligned} \tag{17}$$

Finally an approximation of Z_t^2 could be expressed as

$$Z_t^2 = v_x^2(t, X_t)\,\sigma^2(t, X_t) = \mathscr{L} f(t, X_t) = \frac{1}{\Delta} E\left[\left(v(t+\Delta, X_{t+\Delta}) - v(t, X_t)\right)^2 \mid X_t = x\right] + O(\Delta); \tag{18}$$

that is,

$$Z_t^2 = \frac{1}{\Delta} E\left[\left(Y_{t+\Delta} - Y_t\right)^2 \mid X_t = x\right] + O(\Delta). \tag{19}$$

By (19), I regard $Z^2(x_0)$ as point-wise nonparametric regression function. For simplicity, here the N-W kernel estimator is taken as an example of nonparametric smooth estimators:

$$\widehat{Z}^2(x_0) = \frac{\sum_{i=1}^{n-1} \Delta^{-1}\left(Y(t_{i+1}) - Y(t_i)\right)^2 K_h\left(X(t_i) - x_0\right)}{\sum_{i=1}^{n-1} K_h\left(X(t_i) - x_0\right)}, \tag{20}$$

where $K_h(\cdot) = K(\cdot/h)/h$, $K(\cdot)$ is the kernel function satisfying the regularity condition given below and h is the bandwidth or smoothing parameter. Similarly, if Z_t also depends on t besides X_t, the corresponding estimator could be

$$\widehat{Z}^2(x_0, t_0) = \frac{\sum_{i=1}^{n-1} \Delta^{-1}\left(Y(t_{i+1}) - Y(t_i)\right)^2 K_{h_X}\left(X(t_i) - x_0\right) K_{h_t}(t_i - t_0)}{\sum_{i=1}^{n-1} K_{h_X}\left(X(t_i) - x_0\right) K_{h_t}(t_i - t_0)}. \tag{21}$$

Since having calculated $\widehat{Z}_t^2$, I plug it in the first formula of (9), obtaining

$$Y(t_i) \approx \widehat{\xi} + \sum_{j=i}^{n} \left(a + bY(t_j) + c\widehat{Z}(t_j)\right)\Delta_j + O(\Delta_i) + \epsilon_i + \nu_s, \quad i = 1, \ldots, n. \tag{22}$$

From the above, it is simple to deduce the estimator of $\beta = (a, b, c)^\tau$ with common parametric methods, the least square method for example, by minimizing

$$\sum_{i=1}^{n} \left(Y(t_i) - \widehat{\xi} - \sum_{j=i}^{n} \left(a + bY(t_j) + c\widehat{Z}(t_j)\right)\Delta t_j\right)^2. \tag{23}$$

For simplicity, denote

$$V = \frac{1}{T}\begin{pmatrix} Y(t_1) - \widehat{\xi} \\ \cdots \\ Y(t_n) - \widehat{\xi} \end{pmatrix},$$

$$U = \frac{1}{T}\begin{pmatrix} \sum_{j=1}^{n}\Delta_j & \sum_{j=1}^{n} Y(t_j)\Delta_j & \sum_{j=1}^{n} Z(t_j)\Delta_j \\ \cdots & \cdots & \cdots \\ \Delta_n & Y(t_n)\Delta_n & Z(t_n)\Delta_n \end{pmatrix}, \tag{24}$$

$$\widehat{U} = \frac{1}{T}\begin{pmatrix} \sum_{j=1}^{n}\Delta_j & \sum_{j=1}^{n} Y(t_j)\Delta_j & \sum_{j=1}^{n} \widehat{Z}(t_j)\Delta_j \\ \cdots & \cdots & \cdots \\ \Delta_n & Y(t_n)\Delta_n & \widehat{Z}(t_n)\Delta_n \end{pmatrix}.$$

Finally, I can write the estimator as

$$\widehat{\beta} = \left(\widehat{U}^\tau \widehat{U}\right)^{-1} \widehat{U}^\tau V. \tag{25}$$

3. Asymptotic Results

The following two theorems are concerned with asymptotic properties of the estimators deduced in the previous section.

First of all, I lead in several conditions.

(a) $X_1, \ldots, X_n$ are ρ-mixing dependent; namely, the ρ-mixing coefficients $\rho(l)$ satisfy $\rho(l) \to 0$ as $l \to \infty$, where

$$\rho(l) = \sup_{E(X_{i+l}X_i) - E(X_{i+l})E(X_i) \neq 0} \frac{\left|E(X_{i+l}X_i) - E(X_{i+l})E(X_i)\right|}{\sqrt{\mathrm{Var}(X_{i+l})\,\mathrm{Var}(X_i)}} \tag{26}$$

with $X_i = X(t_i)$.

(b) $|Z_i| \leq C$ (a.s.) uniformly for $i = 1, \ldots, n$, where C is a positive constant and $Z_i = Z(t_i)$.

(c) The continuous kernel function $K(\cdot)$ is symmetric about 0, with a support of interval $[-1, 1]$, and

$$\int_{-1}^{1} K(u)\,du = 1, \qquad \sigma_K^2 = \int_{-1}^{1} u^2 K(u)\,du \neq 0, \qquad \int_{-1}^{1} |u|^j K^k(u)\,du < \infty \quad \text{for } j \leq k = 1, 2. \tag{27}$$

(d) As $n \to \infty$,

$$\frac{1}{n} U^\tau U \xrightarrow{p} \Sigma, \qquad \frac{1}{nT^2} U^\tau U\,\mathrm{Var}(\epsilon) \xrightarrow{p} \Omega, \tag{28}$$

where the matrix Σ is nonsingular and satisfies

$$0 < C_1 < \lambda_{\min}(\Sigma) < \lambda_{\max}(\Sigma) < C_2 < \infty, \tag{29}$$

with $\lambda_{\min}(\Sigma)$ and $\lambda_{\max}(\Sigma)$ being the smallest and largest eigenvalues of Σ, respectively.

The condition (a) is commonly used for the weakly dependent process; see for example Rosenblatt [18, 19], Kolmogorov and Rozanov [20], Bradley and Bryc [21], Lin and Lu [22], and Su and Lin [14]. The condition (b) is also reasonable because, as is shown by (19), Z_t can be regarded as the deviation between the adjacent two observations. The condition (c) is standard for nonparametric kernel function, and the condition (d) is obviously common because it describes the property of average. Furthermore, as remarked in the previous section, to express the estimator related to X_t rather than model variables Y_t and Z_t, I apply conditions mainly on the latent variable X_t, including the stationary ρ-mixing Markov character used in the following theorems. Actually the process $\{Y_t\}$ may be unstationary.

Theorem 2. *Besides the conditions (a), (b), and (c), suppose that $X_i \in (x_0 - h, x_0 + h)$ is a stationary ρ-mixing Markov process with the ρ-mixing coefficients satisfying $\rho(l) = \rho^l$ for $0 < \rho < 1$ and has a common probability density $p(x)$ satisfying $p(x_0) > 0$, $Z^2(x_0) > 0$. Furthermore, functions $p(x)$ and $Z(x)$ have continuous two derivatives in a neighborhood of x_0. As $n \to \infty$, if $nh \to \infty$, $nh^5 \to 0$ and $nh\Delta^2 \to 0$, then*

$$\sqrt{(n-1)h}\left(\widehat{Z}^2(x_0) - Z^2(x_0)\right) \xrightarrow{\mathscr{D}} N\left(0, \frac{Z^4(x_0) J_K}{p(x_0)}\right). \tag{30}$$

The proof is presented in Section 6. The asymptotic result in the theorem is standard for nonparametric kernel estimator, and here undersmoothing is used to eliminate asymptotic bias.

Theorem 3. *In addition to the condition of Theorem 2, if the condition (d) holds, then as $n \to \infty$,*

$$\sqrt{n}\left(\widehat{\beta} - \beta\right) \xrightarrow{d} N\left(0, \sigma^2 \Sigma^{-1} + \Sigma^{-1} \Omega \Sigma^{-1}\right), \tag{31}$$

where $\sigma^2 = \mathrm{Var}(\xi/T)$.

The proof is also presented in Section 6. The result is eventually standard in the sense of asymptotic normality with the convergence rate of order $\sqrt{n}$. As was shown in the remark given in the previous section, even the conditional mean of error of the model is nonzero, the newly proposed estimation is consistency because of the mixing dependency; for details see the proof of Theorem 3. Furthermore, because of the terminal condition, the asymptotic variance is larger than that without use of the terminal condition.

4. Supplement and Extension

4.1. Supplement. As is mentioned in Section 2.1, when the last observation t_n is far away from the terminal T, the new model (9) appears inaccurate. In this case I need an adjustment to obtain a relatively accurate model. The main steps of adjustment are defined as follows: first I ignore the terminal condition to obtain both the accurate model and parameters estimations limited in $(0, t_n)$; next I estimate the unobservable variables in the interval (t_n, T) by the first step estimated model; finally, I substitute the estimators for the unobservable variables in (t_n, T) and build a relatively accurate model defined in the whole interval $[0, T]$ and related to the terminal condition.

For arbitrary $t \le t_n$,

$$Y_t = Y_n + \int_t^{t_n} g(s, Y_s, Z_s)\, ds - \int_t^{t_n} Z_s dB_s. \tag{32}$$

This equation is accurate and thus I can get the estimators $\widehat{g}$ and $\widehat{Z}_t$ of g and Z_t for $t \le t_n$ by the methods given in Section 2. When $t > t_n$, this method is however unsuitable for estimating Z_t because it cannot be extrapolated to the interval (t_n, T), so I attempt to complete the data within this interval.

Set $t_n < t_{n+1} < \cdots < t_{n+l} < T$. Discretize model (32) and write its forward linear version as

$$\begin{aligned} Y(t_{i+1}) = &-\left(\left(b - \frac{1}{\Delta_i}\right) Y(t_i) + cZ(t_i)\right)\Delta_i \\ &+ Z(t_i)\left(B_{i+1} - B_i\right). \end{aligned} \tag{33}$$

Similar to formula (9), the expectation-variance structure is shown as

$$\begin{aligned} &E\left(Y(t_{i+1}) \mid Y(t_i), Z(t_i)\right) \\ &\quad = -\left(\left(b - \frac{1}{\Delta_i}\right) Y(t_i) + cZ(t_i)\right)\Delta_i, \\ &\mathrm{Var}\left(Y(t_{i+1}) \mid Y(t_i), Z(t_i)\right) = \Delta_i Z^2(t_i). \end{aligned} \tag{34}$$

To estimate the unobservable data $(Y(t_i), Z(t_i))$ for $i = n+1, \ldots, n+l$, I treat Z_t as being parameterizable. It is known by, for example, Morris [23] that variance can be expressed as the quadratic function of mean for several common distributions, such as normal, gamma, binomial, negative binomial, and Poisson. For the mean-variance structure in (34), I might as well suppose the following parametric structure:

$$\begin{aligned} \Delta_i Z^2(t_i) = &\gamma_1 + \gamma_2\left(\left(b - \frac{1}{\Delta_i}\right) Y(t_i) + cZ(t_i)\right)\Delta_i \\ &+ \gamma_3\left(\left(b - \frac{1}{\Delta_i}\right) Y(t_i) + cZ(t_i)\right)^2 \Delta_i^2, \end{aligned} \tag{35}$$

for some parameters γ_k. By simply transforming and neglecting $O(\Delta^2)$ terms, I see

$$Z(t_i) = \omega_1 + \omega_2 \sqrt{\omega_3 + \omega_4 Y(t_i)}, \tag{36}$$

where $\omega_2 = 1$ or -1, and denote $\omega = (\omega_1, \omega_2, \omega_3, \omega_4)$.

Let $\overline{Z}(t_i) = \omega_1 + \omega_2\sqrt{\omega_3 + \omega_4 Y(t_i)}$ $(1 \le i \le n)$ and plug $\overline{Z}(t_i)$ into (32). I then could get the estimators through

the methods in Section 2; denote by $\widetilde{b}_S$, $\widetilde{c}_S$, and $\widetilde{\omega}$ the estimators of b, c and ω, respectively. Finally I could refine the original orbit and estimate $Z(t_{n+1})$ one by one, more precisely,

$$\widetilde{Y}(t_{n+1}) = -\left(\left(\widetilde{b}_S - \frac{1}{\Delta_i}\right) Y(t_n) + \widetilde{c}_S \widetilde{Z}(t_n)\right)\Delta_n,$$
$$\widetilde{Z}(t_{n+1}) = \widetilde{\omega}_1 + \widetilde{\omega}_2\sqrt{\widetilde{\omega}_3 + \widetilde{\gamma}_4 \widetilde{Y}(t_{n+1})}. \tag{37}$$

Iterating the above procedures, I obtain the complete data in $[0, T]$. Consequently, the same approaches as in Section 2 could be performed again, and a refined estimator of g could be constructed.

4.2. Extension. Consider that the semiparametric models in Section 2 are of linear structure in the sense that g is linearly related to parameters a, b, and c. However, some generators are nonlinear in parameters; thus the resulting model (9) will be nonlinear. For example Constantinides [24] presented the resulting model with the specification form:

$$dX_t = \left(\alpha_0 + \alpha_1 X_t + \alpha_2\sqrt{X_t - \alpha_3}\right)dt + \sigma_0(X_t - \alpha_3)\,dB_t. \tag{38}$$

See for other examples Fan [25], Fan and Zhang [26], Chan et al. [27], and Aït-Sahalia [28].

Then, for the flexibility of modeling the above case, a nonlinear semiparametric model can be defined as

$$Y_t = \xi + \int_t^T g(\theta, s, Y_s, Z_s)\,ds + \epsilon_t,$$
$$\mathrm{Var}(\epsilon_t) = E\left(\int_t^T Z_s^2 ds\right), \tag{39}$$

where $\epsilon_t = \int_t^T Z_s dB_s$ satisfying $E(\epsilon_t) = 0$, g is a given function, and θ is an unknown p-dimensional parameter vector.

Before estimating nonlinear model (39), Z_t can be estimated similarly by (19) or (20) because its estimator is free of the structure of g. Furthermore, the resulting estimator has the same asymptotic properties as in Theorem 2. Thus I only focus on the estimation of parameter vector θ here.

After plugging the estimator $\widehat{Z}_t$ of Z_t into the first formula of (39), I can adopt a common method to obtain an estimator of θ, for example, by minimizing

$$\widehat{Q}(\theta) = \sum_{i=1}^n \left(Y_i - \widehat{\xi} - \sum_{j=i}^n \widehat{g}_j(\theta)\,\Delta t_j\right)^2, \tag{40}$$

where $\widehat{g}_j(\theta) = g(\theta, t_j, Y_j, \widehat{Z}_j)$. Under regularity conditions, I can also get $\widehat{\theta}$ by solving the following equation:

$$\widehat{L}(\theta) = \widehat{Q}'(\theta)$$
$$= -2\sum_{i=1}^n \left[\left(Y_i - \widehat{\xi} - \sum_{j=i}^n \widehat{g}_j(\theta)\,\Delta t_j\right)\sum_{j=i}^n \widehat{g}_j'(\theta)\,\Delta t_j\right] = 0, \tag{41}$$

where $\widehat{Q}'(\theta)$ denotes the derivative of $\widehat{Q}(\theta)$. By the similar arguments used in the previous section, the resultant estimator is normally distributed; the details are omitted here.

5. Simulations

In this section I investigate the finite-sample behaviors by simulation. Despite Theorems 2 and 3 based on stationarity of X_t, I also extend this method to nonstationary process such as Geometric Brownian Motion. I use the mean, standard deviation (STD) or mean square error (MSE) to evaluate the estimations, based on 300 repetitions. Apparently, the model with stationary condition will work better.

Example 4. Consider Cox-Ingersoll-Ross (CIR) process:

$$dX_t = k(\theta - X_t)\,dt + \sigma X_t^{1/2} dB_t; \quad X_0 = x_0. \tag{42}$$

This model describes the interest rate dynamic system and is stationary when $2k\theta \geq \sigma^2$. On the other hand, the riskless asset with price per unit P_t is conducted as follows:

$$dP_t = rP_0 dt, \tag{43}$$

with r being the constant short rate. Let $n_0(t)$ and $n_1(t)$ denote the quantities invested in bond P_t and asset X_t, respectively. Naturally the total wealth process Y_t satisfies $Y_t = n_0(t)P_t + n_1(t)X_t$. Similar with the classic self-financing FBSDE model in El Karoui et al. [29], the resulting model is

$$dY_t = \left(n_1 k\theta + rY_t + \frac{k+r}{n_1\sigma^2}Z_t^2\right)dt + Z_t dB_t; \quad Y_T = \xi(X_T),$$
$$dX_t = k(\theta - X_t)\,dt + \sigma X_t^{1/2} dB_t; \quad X_0 = x_0. \tag{44}$$

Denote parameters $a = n_1 k\theta$, $b = r$, and $c = (k+r)/n_1\sigma^2$. I put the equal length $\Delta = 0.4$ of time period and choose sample size $n = 300$. So the time interval is $[0, 120]$. The terminal time is chosen as 122, which is quite near the former one. Let $k = 0.2$, $\theta = 0.06$, $\sigma = 0.08$, $r = 0.05$, and $n_0 = n_1 = 10$. In the estimation procedure, I use the Gaussian kernel defined by $K(t) = (1/\sqrt{2\pi})\exp(-t^2/2)$; meanwhile the optimal bandwidths would be $O(n^{-1/5})$ theoretically, and popular data-driven method can also be used, such as CV, GCV, or plug-in approach. In the simulation, I set $h = \mathrm{std}(x)n^{-1/5}$ for simplicity. The simulation results with other choices are similar.

I present the true curves and the N-W nonparametric estimation curves for Z_t and generator g and report the mean and MSE of estimator $\widehat{\beta}$ of $\beta \triangleq (a, b, c)$, respectively, in Table 1. These results show that the estimators of a and b work well. However, because of the plug-in estimator $\widehat{Z}_t$, the estimator of the coefficient c has fairly large bias and the MSE. On the other hand, Figure 1 shows that the estimation curves of drift and diffusion are closed to the true ones.

Example 5. In this part I consider the case that the terminal time is far away from the last observed time, as mentioned in

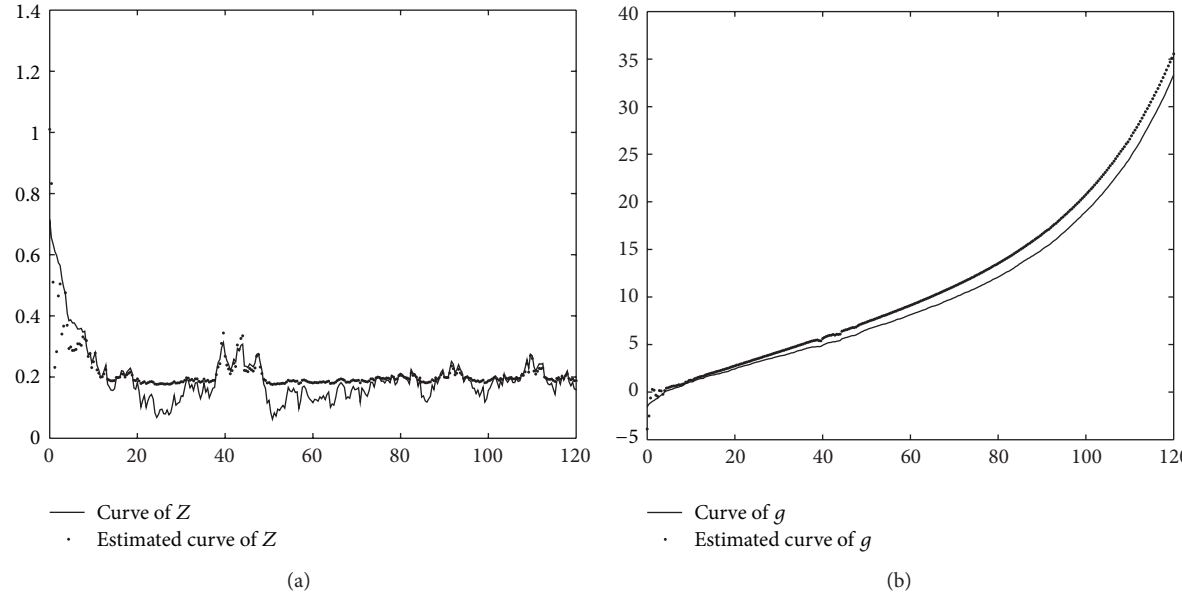

Figure 1: The real lines are the true curves of Z_t and function g respectively, and the dashed ones are estimated curves for them in Example 4.

Table 1

Parameter	True value	Mean	MSE
a	0.12	0.1404	0.0089
b	0.05	0.0503	$1.2694e-007$
c	−3.9062	−4.5826	4.6295

Table 2

Parameter	True value	Mean	MSE
a	0.12	0.1470	0.0319
b	0.05	0.0490	$1.6873e-006$
c	−3.9062	−3.8360	9.2929

the Supplement Section. The distance between $T = 124$ and $t_n = 120$ is larger than that in Example 4. I add 10 estimated points by the method given in Section 4 and employ the same model and parameters as before. Table 2 reports the simulation results, which tells us that the parameter estimators do not perform as well as before but still feasible. Besides, Figure 2 presents the estimated curves for Z_t and g, which also perform well although they are not better than the estimations in Example 4.

Example 6. I turn to the nonstationary case in this part. Obviously when forward process X_t does not satisfy the stationary condition, this cumulate effect induced by backward addition performs more significantly, which makes the statistical inference quite a challenge. Under this situation, I choose certain model and parameters to control the relative stationarity.

Table 3

Parameter	True value	Mean	STD
b	0.05	0.0473	0.0348
c	5	5.7788	7.3388

I consider a simple FBSDE as

$$\begin{aligned} dY_t &= \left(\frac{\mu - r}{\sigma} Z_t + rY_t\right) dt + Z_t dB_t \\ &\triangleq \left(bY_t + cZ_t\right) + Z_t dB_t; \quad Y_T = \xi\left(X_T\right), \end{aligned} \tag{45}$$

where X_t is Geometric Brownian Motion for modeling stock price satisfying

$$dX_t = \mu X_t dt + \sigma X_t dB_t; \quad X_0 = x, \tag{46}$$

while the riskless asset is the same as formula (43), $dP_t = rP_0 dt$.

Firstly, let $\mu = 0.1$, $\sigma = 0.01$, $\Delta = 0.12$, $n = 300$, $T = 36.6$, and $n_0 = n_1 = 10$. Obviously $Z_t = n_1 \sigma X_t$. I choose the same pattern kernel function and bandwidth $h = \text{std}(x) n^{-1/5}$. Table 3 reports the simulation results. The results show that the estimators of b work well, but c have larger bias and the STD because of the plug-in estimator $\widehat{Z}_t$. While the curves can still be fitted well, that is, the estimated curves of drift and diffusion are closed to the true ones, Figure 3 presents the estimated curves for diffusion Z_t and drift g by one simulation.

Finally, I choose σ relatively large as 0.05 and 0.12, which display different extension of volatilities. From Tables 4 and 5 and Figures 4 and 5, I can see that their performances are not so bad, which means that the approach could be applied more widely.

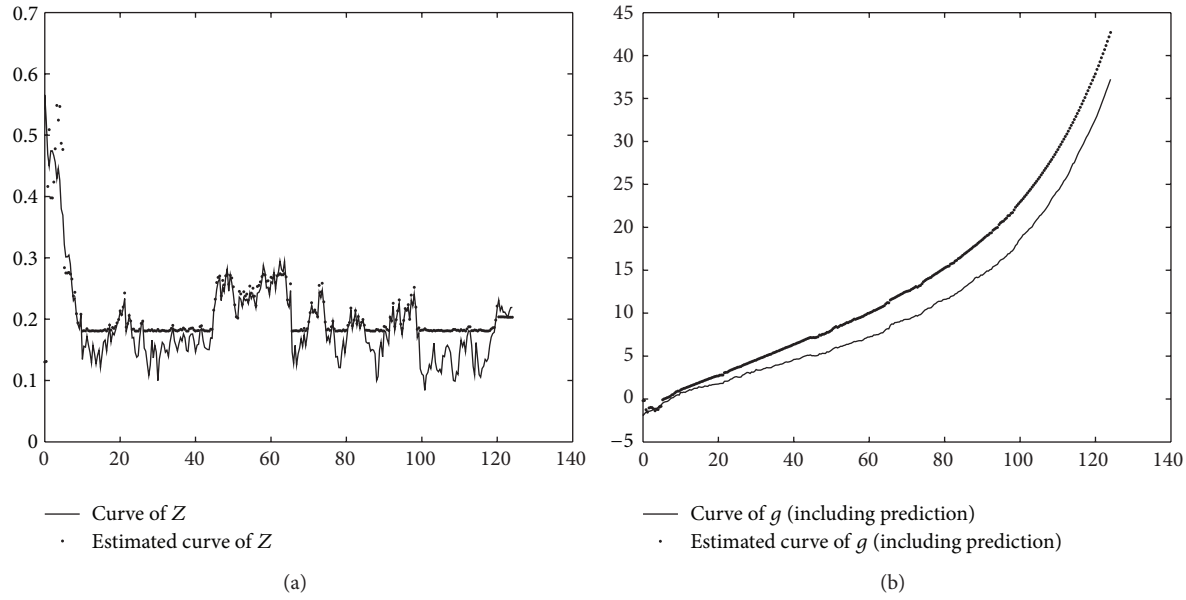

Figure 2: The real lines are the true curves of Z_t and function $g(t)$, respectively, and the dashed ones are estimated curves for them in Example 5.

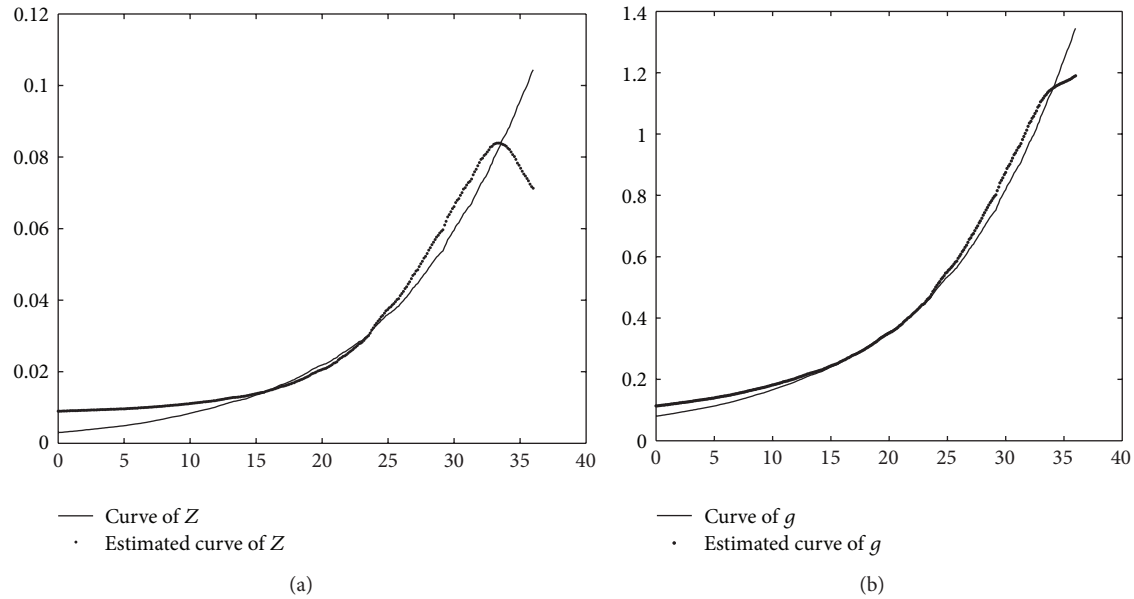

Figure 3: The real lines are the true curves of Z_t and function $g(t)$, respectively, and the dashed ones are estimated curves for them in Example 6.

6. Proofs

Proof of Theorem 2. Denote $\mathscr{C} = \{X_1, \ldots, X_n, \ldots\}$. By the Taylor expansion and formula (19), I have

$$E\left(\widehat{Z}^2(x_0) \mid \mathscr{C}\right) = \frac{\sum_{i=1}^{n-1} \Delta^{-1} K_h(X_i - x_0)\, E\left((Y_{i+1} - Y_i)^2 \mid \mathscr{C}\right)}{\sum_{i=1}^{n-1} K_h(X_i - x_0)}$$

$$= \frac{\sum_{i=1}^{n-1} K_h(X_i - x_0)\left(Z_i^2 + O(\Delta)\right)}{\sum_{i=1}^{n-1} K_h(X_i - x_0)}$$

$$= \left(\int K_h(X_i - x_0)\left(Z^2(x) + O(\Delta)\right) p(x)\, dx \times \left(1 + O_p(nh)^{-1/2}\right)\right)\left(\int K_h(X_i - x_0)\, p(x)\, dx \times \left(1 + O_p(nh)^{-1/2}\right)\right)^{-1}$$

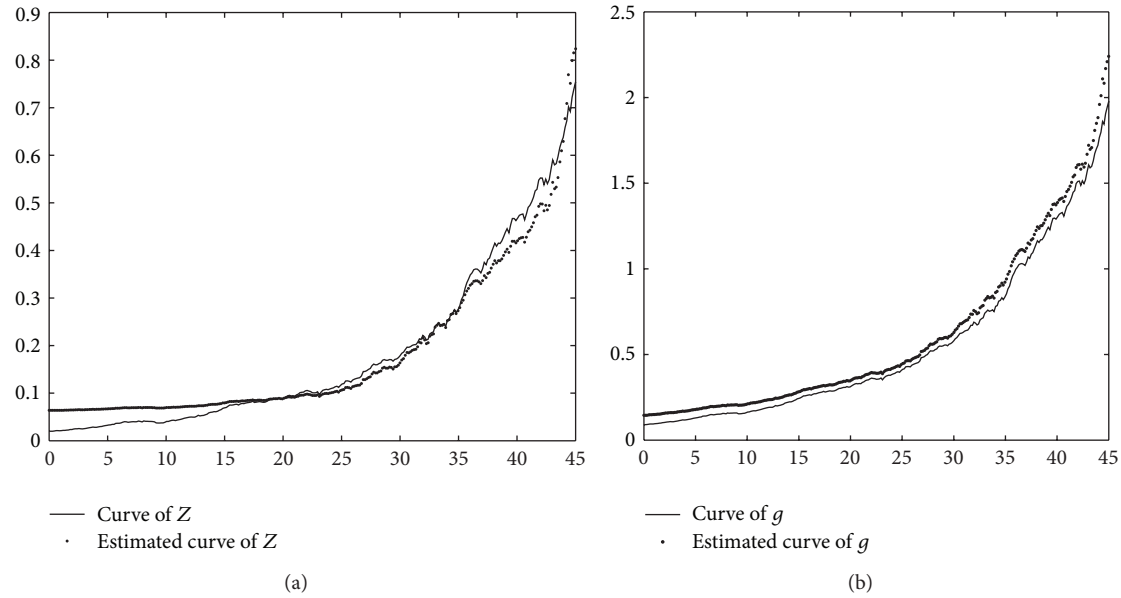

Figure 4: The real lines are the true curves of Z_t and function $g(t)$, respectively, and the dashed ones are estimated curves for them with $\sigma = 0.05$.

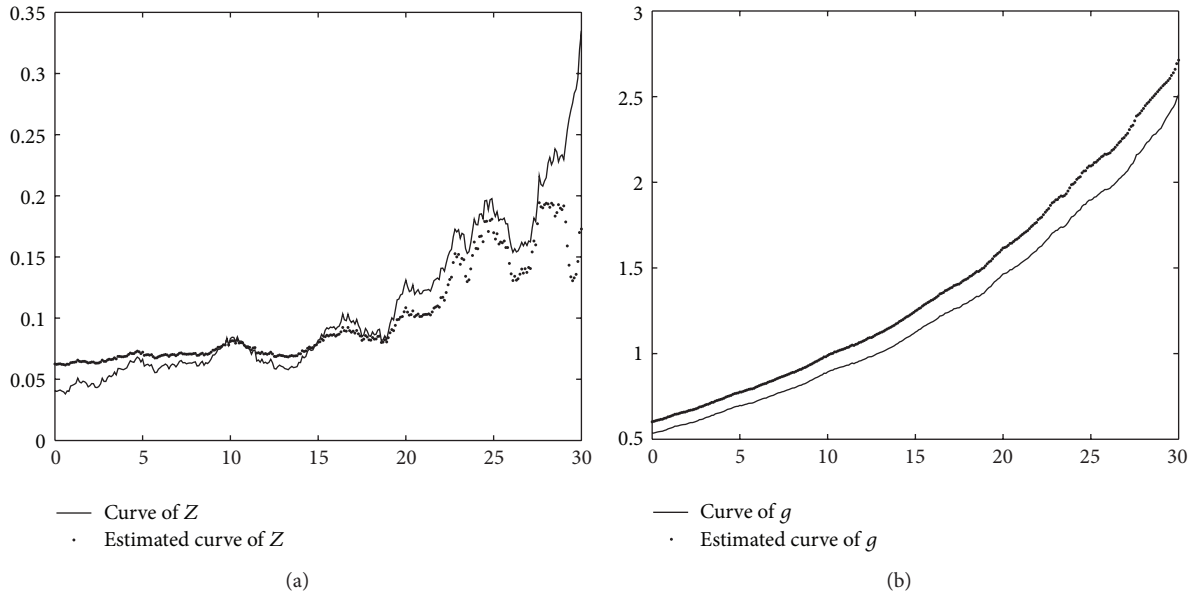

Figure 5: The real lines are the true curves of Z_t and function $g(t)$, respectively, and the dashed ones are estimated curves for them with $\sigma = 0.12$.

$$
\begin{aligned}
&= \left(\left(Z^2(x_0) + O(\Delta)\right)\left(p(x_0) + \frac{1}{2}h^2 p^{(2)}(x_0)\sigma_K^2 + o\left(h^2\right)\right)\right. \\
&\quad \left.\times \left(1 + O_p(nh)^{-1/2}\right)\right) \\
&\times \left(\left(p(x_0) + \frac{1}{2}h^2 p^{(2)}(x_0)\sigma_K^2 + o\left(h^2\right)\right)\right. \\
&\quad \left.\times \left(1 + O_p(nh)^{-1/2}\right)\right)^{-1} \\
&= Z^2(x_0) + \frac{p^{(2)}(x_0)}{2p(x_0)}h^2 Z^2(x_0)\sigma_K^2 + o\left(h^2\right) + O(\Delta).
\end{aligned} \tag{47}
$$

Furthermore,

$$
\begin{aligned}
&\operatorname{Var}\left(\widehat{Z}^2(x_0) \mid \mathscr{C}\right) \\
&= \frac{1}{\sum_{i=1}^{n-1} K_h^2(X_i - x_0)}
\end{aligned}
$$

$$\times \left\{ \sum_{i=1}^{n-1} \Delta^{-2} K_h^2 (X_i - x_0) \operatorname{Var}\left((Y_{i+1} - Y_i)^2 \mid \mathscr{C} \right) + \sum_{i=1}^{n-1} \sum_{k=1}^{n-i} \Delta^{-2} \operatorname{cov}\left(K_h (X_i - x_0)(Y_{i+1} - Y_i), K_h (X_{i+k} - x_0)(Y_{i+k+1} - Y_{i+k}) \mid \mathscr{C} \right) \right\}. \tag{48}$$

From the conditions of Markov process and ρ-mixing coefficient,

$$\begin{aligned} &\left| \sum_{i=1}^{n-1} \sum_{k=1}^{n-i} \Delta^{-2} \operatorname{cov}\left(K_h (X_i - x_0)(Y_{i+1} - Y_i), K_h (X_{i+k} - x_0)(Y_{i+k+1} - Y_{i+k}) \right) \right| \\ &= \frac{1}{(n-1)^2} \\ &\quad \times \sum_{i=1}^{n-1} \sum_{k=1}^{n-i} \Big| E\left((\Delta)^{-2} (Y_{i+1} - Y_i)^2 (Y_{i+k+1} - Y_{i+k})^2 \right. \\ &\qquad \times \left(K_h (X_i - x_0) - E\left(K_h (X_i - x_0) \right) \right) \\ &\qquad \left. \times \left(K_h (X_{i+k} - x_0) - E\left(K_h (X_{i+k} - x_0) \right) \right) \right) \Big| \\ &= \frac{1}{(n-1)^2} \Big| E\left(Z_i^2 Z_{i+l}^2 \left(K_h (X_i - x_0) - E\left(K_h (X_i - x_0) \right) \right) \right. \\ &\qquad \left. \times \left(K_h (X_{i+k} - x_0) - E\left(K_h (X_{i+k} - x_0) \right) \right) \right) \Big| + O(\Delta) \\ &\le \frac{C}{(n-1)^2 h} \sum_{i=1}^{n-1} \sum_{k=1}^{n-i} \rho^k = O\left(\frac{1}{nh} \right) = o(1). \end{aligned} \tag{49}$$

Note that $(Y_{i+1} - Y_i)/\sqrt{\Delta} = g(t_i, Y_i, Z_i)\sqrt{\Delta} + Z_i \eta_i$, where $E(\eta_i) = 0$, $\operatorname{Var}(\eta_i) = 1$. Thus $\operatorname{Var}((Y_{i+1} - Y_i)/\sqrt{\Delta}) = Z_i^4 + O(\Delta)$ and furthermore

$$\begin{aligned} &\operatorname{Var}\left(\widehat{Z}^2 (x_0) \mid \mathscr{C} \right) \\ &= \frac{\sum_{i=1}^{n-1} \Delta^{-2} K_h^2 (X_i - x_0) \operatorname{Var}\left((Y_{i+1} - Y_i)^2 \mid \mathscr{C} \right)}{\sum_{i=1}^{n-1} K_h^2 (X_i - x_0)} + O_p(1) \\ &= \frac{\sum_{i=1}^{n-1} K_h^2 (X_i - x_0) \left(Z^4 (x_0) + O\left(\sqrt{\Delta} \right) \right)}{\sum_{i=1}^{n-1} K_h^2 (X_i - x_0)} + O_p(1) \\ &= \frac{Z^4 (x_0) J_K + O\left(\sqrt{\Delta} \right)}{nhp(x_0)} \left(1 + O_p (nh)^{-1/2} \right). \end{aligned} \tag{50}$$

To my interest, both the conditional expectation and variance are independent of $\mathscr{C}$, so the condition could be erased.

Table 4

Parameter	True value	Mean	STD
b	0.05	0.0580	0.0217
c	1	0.9959	7.6034

Table 5

Parameter	True value	Mean	STD
b	0.05	0.0557	0.0421
c	0.4167	0.4227	6.5970

From Lemma 1 of Politis and Romano [30] and the relation between the α-mixing condition and the ρ-mixing condition (e.g., Theorem 1.1.1 of [22]), I can ensure that $\{(Y_{i+1} - Y_i)^2, i = 1, \ldots, n-1\}$ is a ρ-mixing-dependent process and the mixing coefficient, denoted by $\rho_Y(l)$, satisfies

$$\sum_{k=1}^{\infty} \rho_Y\left(2^k\right) \le C \sum_{k=1}^{\infty} \rho\left(2^k\right) = \sum_{k=1}^{\infty} \rho^{2^k} < \infty, \tag{51}$$

where C is a positive constant. Finally, I use the Central Limit Theorems for ρ-mixing-dependent process (e.g., Theorem 4.0.1 of [22]) to complete this proof. □

Proof of Theorem 3. I present the basic results for $(1/\sqrt{n})(\widehat{U} - U)^\tau U$, which leads to rate of convergence and asymptotic expansions. Similar to Cui et al. [31] or Su and Lin [14], I need the following decomposition:

$$\begin{aligned} &\left(\frac{1}{n} U^\tau U \right)^{-1} - \left(\frac{1}{n} \widehat{U}^\tau \widehat{U} \right)^{-1} \\ &= -\left(\frac{1}{n} U^\tau U \right)^{-1} \left\{ \frac{1}{n} \left(\widehat{U} - U \right)^\tau U \right\} \left(\frac{1}{n} U^\tau U \right)^{-1} \\ &\quad - \left(\frac{1}{n} U^\tau U \right)^{-1} \left\{ \frac{1}{n} U^\tau \left(\widehat{U} - U \right) \right\} \left(\frac{1}{n} U^\tau U \right)^{-1} \\ &\quad - \left(\frac{1}{n} U^\tau U \right)^{-1} \left\{ \frac{1}{n} \left(\widehat{U} - U \right)^\tau \left(\widehat{U} - U \right) \right\} \left(\frac{1}{n} U^\tau U \right)^{-1} \\ &\quad + \left\{ \left(\frac{1}{n} \widehat{U}^\tau \widehat{U} \right)^{-1} - \left(\frac{1}{n} U^\tau U \right)^{-1} \right\} \left\{ \frac{1}{n} \widehat{U}^\tau \widehat{U} - \frac{1}{n} U^\tau U \right\} \\ &\quad \times \left(\frac{1}{n} U^\tau U \right)^{-1} \\ &\triangleq I_1 + I_2 + I_3 + I_4. \end{aligned} \tag{52}$$

By the condition (d), $(1/n)U^\tau U \xrightarrow{p} \Sigma$ and all eigenvalues of Σ are bounded. Furthermore, by the uniform weak consistency kernel estimator of mixing-dependent variables, (see, e.g., [32, 33]), I have

$$\sup_x \left| \frac{1}{n-1} \sum_{i=1}^{n-1} K_{h,i} - p(x) \right| = O_p\left(h^2 + \left(\frac{\log(nh)}{nh} \right)^{1/2} \right). \tag{53}$$

By the proof of Theorem 2, I have

$$E\left(\frac{1}{n}\left(\widehat{U}-U\right)^{\tau}U\right)=O\left(h^{2}\right),$$
$$\operatorname{Var}\left(\frac{1}{n}\left(\widehat{U}-U\right)^{\tau}U\right)=O\left(\frac{1}{\left(n^{2}h\right)^{1/2}}\right). \tag{54}$$

It is easy to deduce that $I_1 = o_p(1/\sqrt{n})$, $I_2 = o_p(1/\sqrt{n})$, $I_3 = o_p(1/\sqrt{n})$, and $I_4 = o_p(1/\sqrt{n})$. Then I naturally get

$$\left(\frac{1}{n}\widehat{U}^{\tau}\widehat{U}\right)^{-1}=\left(\frac{1}{n}U^{\tau}U\right)^{-1}+o_p\left(\frac{1}{\sqrt{n}}\right). \tag{55}$$

Denote $I_5 = ((1/n)U^{\tau}U)^{-1}(1/\sqrt{n})(\widehat{U}-U)^{\tau}V$. Obviously $I_5 = o_p(1)$. Combining the results above, I can see that

$$\begin{aligned}
&\sqrt{n}\widehat{\beta}_I\\
&=\sqrt{n}\left(\widehat{U}^{\tau}\widehat{U}\right)^{-1}\widehat{U}^{\tau}V\\
&=\left[\left(\frac{1}{n}U^{\tau}U\right)^{-1}+o_p\left(\frac{1}{\sqrt{n}}\right)\right]\frac{1}{\sqrt{n}}\widehat{U}^{\tau}V\\
&=\left(\frac{1}{n}U^{\tau}U\right)^{-1}\frac{1}{\sqrt{n}}\widehat{U}^{\tau}V+o_p(1)\\
&=\left(\frac{1}{n}U^{\tau}U\right)^{-1}\frac{1}{\sqrt{n}}U^{\tau}V+I_5+o_p(1)\\
&=\left(\frac{1}{n}U^{\tau}U\right)^{-1}\frac{1}{\sqrt{n}}U^{\tau}V+o_p(1)\\
&=\sqrt{n}\beta+\left(\frac{1}{n}U^{\tau}U\right)^{-1}\frac{1}{T\sqrt{n}}\sum_{i=1}^{n}U_i'\left(\epsilon_j+\nu_s\right)+o_p(1)\\
&=\sqrt{n}\beta+\left(\frac{1}{n}U^{\tau}U\right)^{-1}\frac{1}{T\sqrt{n}}\sum_{i=1}^{n}U_i'\sum_{j=i}^{n}\Delta_j^{1/2}Z_j\varepsilon_j\\
&\quad+\left(\frac{1}{n}U^{\tau}U\right)^{-1}\frac{1}{T\sqrt{n}}\sum_{i=1}^{n}U_i'\nu_s+o_p(1),
\end{aligned} \tag{56}$$

where $\{\varepsilon_i\}$ is an unobservable sequence of independent identical distribution random variables with mean zero and variance one.

From $E(\nu_s) = 0$ and the central limit theorem it follows that

$$\frac{1}{T\sqrt{n}}\sum_{i=1}^{n}U_i'\nu_s\xrightarrow{\mathrm{d}}N\left(0,\sigma^{2}\Sigma\right). \tag{57}$$

On the other hand, the expectation of $1/(T\sqrt{n})\sum_{i=1}^{n}U_i'\sum_{j=i}^{n}\Delta t_j^{1/2}Z(t_j)\varepsilon_j$ does not converge to zero; that is to say, I have

$$\begin{aligned}
&\frac{1}{T\sqrt{n}}E\begin{pmatrix}\sum_{i=1}^{n}\left[\left(\sum_{j=i}^{n}\Delta t_j\right)\left(\sum_{k=i-1}^{n}\Delta t_k^{1/2}Z\left(t_k\right)\varepsilon_k\right)\right]\\ \sum_{i=1}^{n}\left[\left(\sum_{j=i}^{n}\Delta t_jY\left(t_j\right)\right)\left(\sum_{k=i-1}^{n}\Delta t_k^{1/2}Z\left(t_k\right)\varepsilon_k\right)\right]\\ \sum_{i=1}^{n}\left[\left(\sum_{j=i}^{n}\Delta t_jZ\left(t_j\right)\right)\left(\sum_{k=i-1}^{n}\Delta t_k^{1/2}Z\left(t_k\right)\varepsilon_k\right)\right]\end{pmatrix}\\
&=\sqrt{\frac{T}{n^4}}\begin{pmatrix}0\\ \sum_{i=1}^{n}\sum_{j=i-1}^{n}\sum_{k=1}^{n-j}E\left(Y\left(t_j\right)Z\left(t_{j+k}\right)\varepsilon_j\right)\\ \sum_{i=1}^{n}\sum_{j=i-1}^{n}\sum_{k=1}^{n-j}E\left(Z\left(t_j\right)Z\left(t_{j+k}\right)\varepsilon_j\right)\end{pmatrix}=\upsilon,
\end{aligned} \tag{58}$$

while $\upsilon \nrightarrow 0$. For simplicity, take the third competent as an example to estimate the value. From Lemma 1 of Politis and Romano [30], I can see that Y_t, Z_t are both ρ-mixing-dependent process and the mixing coefficient denoted by $\rho(l)$, too,

$$\begin{aligned}
&\frac{1}{T\sqrt{n}}E\\
&\quad\times\left(\sum_{i=1}^{n}\left[\left(\sum_{j=i}^{n}\Delta t_jZ\left(t_j\right)\right)\left(\sum_{k=i-1}^{n}\Delta t_k^{1/2}Z\left(t_k\right)\varepsilon_k\right)\right]\right)\\
&=\sqrt{\frac{T}{n^4}}E\left(\sum_{i=1}^{n}\sum_{j=i-1}^{n}\sum_{k=1}^{n-j}Z\left(t_{j+k}\right)Z\left(t_j\right)\varepsilon_j\right)\\
&=\sqrt{\frac{T}{n^4}}\sum_{i=1}^{n}\sum_{j=i-1}^{n}\sum_{k=1}^{n-j}E\left(Z\left(t_j\right)Z\left(t_{j+k}\right)\varepsilon_j\right)\\
&=O(1)\sqrt{\frac{T}{n^4}}\sum_{i=1}^{n}\sum_{j=i-1}^{n}\sum_{k=1}^{n-j}\rho^{k}\quad(*).
\end{aligned} \tag{59}$$

I can easily verify that, as $n\to\infty$, $0 < c_1\rho \le (*) \le c_2(\rho/(1-\rho))$.

By condition (d), the variance is bounded uniformly for $i = 1, \ldots, n$. Then

$$\begin{aligned}
&\left(\frac{1}{n}U^{\tau}U\right)^{-1}\left\{\frac{1}{T\sqrt{n}}\sum_{i=1}^{n}U_i'\sum_{j=i}^{n}\Delta t_j^{1/2}Z\left(t_j\right)\varepsilon\left(t_j\right)-\upsilon\right\}\\
&\quad\xrightarrow{\mathrm{d}}N\left(0,\Sigma^{-1}\Omega\Sigma^{-1}\right).
\end{aligned} \tag{60}$$

Summing up the above and the independency between ε_j and ν_s, I get

$$\sqrt{n}\left(\widehat{\beta}-\beta-\sqrt{n}(U^{\tau}U)^{-1}\upsilon\right)\xrightarrow{\mathrm{d}}N\left(0,\sigma^{2}\Sigma^{-1}+\Sigma^{-1}\Omega\Sigma^{-1}\right). \tag{61}$$

While the asymptotic bias $\sqrt{n}(U^{\tau}U)^{-1}\upsilon = o(\Sigma^{-1}\upsilon) \to 0$, therefore

$$\sqrt{n}\left(\widehat{\beta}-\beta\right)\xrightarrow{\mathrm{d}}N\left(0,\sigma^{2}\Sigma^{-1}+\Sigma^{-1}\Omega\Sigma^{-1}\right). \tag{62}$$

This completes the proof. □

Acknowledgments

This paper was supported by NBRP (973 Program 2007CB814901) of China, NNSF Project (10771123) of China, RFDP (20070422034) of China, and NSF Projects (Y2006A13 and Q2007A05) of Shandong Province of China.

References

[1] J. M. Bismut, "Conjugate convex functions in optimal stochastic control," *Journal of Mathematical Analysis and Applications*, vol. 44, pp. 384–404, 1973.

[2] É. Pardoux and S. G. Peng, "Adapted solution of a backward stochastic differential equation," *Systems & Control Letters*, vol. 14, no. 1, pp. 55–61, 1990.

[3] S. G. Peng, "Probabilistic interpretation for systems of quasilinear parabolic partial differential equations," *Stochastics and Stochastics Reports*, vol. 37, no. 1-2, pp. 61–74, 1991.

[4] É. Pardoux and S. Peng, "Backward stochastic differential equations and quasilinear parabolic partial differential equations," *Stochastic Partial Differential Equations and Their Applications*, Springer, vol. 176, pp. 200–217, 1992.

[5] É. Pardoux and S. Tang, "Forward-backward stochastic differential equations and quasilinear parabolic PDEs," *Probability Theory and Related Fields*, vol. 114, no. 2, pp. 123–150, 1999.

[6] S. Peng and Z. Wu, "Fully coupled forward-backward stochastic differential equations and applications to optimal control," *SIAM Journal on Control and Optimization*, vol. 37, no. 3, pp. 825–843, 1999.

[7] J. Ma and J. Yong, *Forward-Backward Stochastic Differential Equations and Their Applications*, vol. 1702 of *Lecture Notes in Mathematics*, Springer, Berlin, Germany, 1999.

[8] D. Nualart and W. Schoutens, "Backward stochastic differential equations and Feynman-Kac formula for Lévy processes, with applications in finance," *Bernoulli*, vol. 7, no. 5, pp. 761–776, 2001.

[9] D. Duffie and L. G. Epstein, "Stochastic differential utility," *Econometrica*, vol. 60, no. 2, pp. 353–394, 1992.

[10] N. El Karoui and M. C. Quenez, "Dynamic programming and pricing of contingent claims in an incomplete market," *SIAM Journal on Control and Optimization*, vol. 33, no. 1, pp. 29–66, 1995.

[11] L. Lin, F. Li, L. Zhu, and W. K. Härdle, "Mean volatility regressions," SFB 649 Economic Risk Berlin, Germany, 2010.

[12] M. C. Quenez, *Méthodes de contrôle stochastique en finance [Thèse de doctorat]*, Université Pierre et Marie Curie, 1993.

[13] Ł. Delong, *Backward Stochastic Differential Equations With Jumps and Their Actuarial and Financial Applications*, EAA, Springer, New York, NY, USA, 2013.

[14] Y. Su and L. Lin, "Semi-parametric estimation for forward-backward stochastic differential equations," *Communications in Statistics*, vol. 38, no. 11, pp. 1759–1775, 2009.

[15] X. Chen and L. Lin, "Nonparametric estimation for FBSDEs models with applications in finance," *Communications in Statistics*, vol. 39, no. 14, pp. 2492–2514, 2010.

[16] R. Stanton, "A nonparametric model of term structure dynamics and the market price of interest rate risk," *The Journal of Finance*, vol. 52, no. 5, pp. 1973–2002, 1997.

[17] B. Øksendal, *Stochastic Differential Equations*, Universitext, Springer, New York, NY, USA, 6th edition, 2003.

[18] M. Rosenblatt, "A central limit theorem and a strong mixing condition," *Proceedings of the National Academy of Sciences of the United States of America*, vol. 42, no. 1, pp. 43–47, 1956.

[19] M. Rosenblatt, "Density estimates and Markov sequencef," in *Selected Works of Murray Rosenblatt*, p. 240, Springer, New York, NY, USA, 2011.

[20] A. N. Kolmogorov and Y. A. Rozanov, "On strongmixing conditions for stationary gaussian processes," *Theory of Probability & Its Applications*, vol. 5, no. 2, pp. 204–208, 1960.

[21] R. C. Bradley and W. Bryc, "Multilinear forms and measures of dependence between random variables," *Journal of Multivariate Analysis*, vol. 16, no. 3, pp. 335–367, 1985.

[22] Z. Lin and C. Lu, *Limit Theory for Mixing Dependent Random Variables*, vol. 378 of *Mathematics and its Applications*, Springer, New York, NY, USA, 1996.

[23] C. N. Morris, "Natural exponential families with quadratic variance functions," *The Annals of Statistics*, vol. 10, no. 1, pp. 65–80, 1982.

[24] G. M. Constantinides, "A theory of the nominal term structure of interest rates," *The Review of Financial Studies*, vol. 5, no. 4, pp. 531–552, 1992.

[25] J. Fan, "A selective overview of nonparametric methods in financial econometrics," *Statistical Science*, vol. 20, no. 4, pp. 317–357, 2005.

[26] J. Fan and C. A. Zhang, "A reexamination of diffusion estimators with applications to financial model validation," *Journal of the American Statistical Association*, vol. 98, no. 461, pp. 118–134, 2003.

[27] K. C. Chan, G. A. Karolyi, F. A. Longstaff, and A. B. Sanders, "An empirical comparison of alternative models of the short-term interest rate," *The Journal of Finance*, vol. 47, no. 3, pp. 1209–1227, 1992.

[28] Y. Aït-Sahalia, "Testing continuous-time models of the spot interest rate," *The Review of Financial Studies*, vol. 9, no. 2, pp. 385–426, 1996.

[29] N. El Karoui, S. Peng, and M. C. Quenez, "Backward stochastic differential equations in finance," *Mathematical Finance*, vol. 7, no. 1, pp. 1–71, 1997.

[30] D. N. Politis and J. P. Romano, "A general resampling scheme for triangular arrays of α-mixing random variables with application to the problem of spectral density estimation," *The Annals of Statistics*, vol. 20, no. 4, pp. 1985–2007, 1992.

[31] X. Cui, W. Guo, L. Lin, and L. Zhu, "Covariate-adjusted nonlinear regression," *The Annals of Statistics*, vol. 37, no. 4, pp. 1839–1870, 2009.

[32] M. Peligrad, "Properties of uniform consistency of the kernel estimators of density and of regression functions under dependence assumptions," *Stochastics and Stochastics Reports*, vol. 40, no. 3-4, pp. 147–168, 1992.

[33] T. Y. Kim and D. D. Cox, "Uniform strong consistency of kernel density estimators under dependence," *Statistics & Probability Letters*, vol. 26, no. 2, pp. 179–185, 1996.

Hindawi Publishing Corporation
Discrete Dynamics in Nature and Society
Volume 2013, Article ID 980578, 16 pages
http://dx.doi.org/10.1155/2013/980578

Research Article

Hyperchaos Numerical Simulation and Control in a 4D Hyperchaotic System

Junhai Ma and Yujing Yang

College of Management and Economics, Tianjin University, Tianjin 300072, China

Correspondence should be addressed to Junhai Ma; lzqsly@126.com

Received 15 May 2013; Revised 29 July 2013; Accepted 19 August 2013

Academic Editor: Oswaldo Luiz do Valle Costa

Copyright © 2013 J. Ma and Y. Yang. This is an open access article distributed under the Creative Commons Attribution License, which permits unrestricted use, distribution, and reproduction in any medium, provided the original work is properly cited.

A hyperchaotic system is introduced, and the complex dynamical behaviors of such system are investigated by means of numerical simulations. The bifurcation diagrams, Lyapunov exponents, hyperchaotic attractors, the power spectrums, and time charts are mapped out through the theory analysis and dynamic simulations. The chaotic and hyper-chaotic attractors exist and alter over a wide range of parameters according to the variety of Lyapunov exponents and bifurcation diagrams. Furthermore, linear feedback controllers are designed for stabilizing the hyperchaos to the unstable equilibrium points; thus, we achieve the goal of a second control which is more useful in application.

1. Introduction

In recent years, hyperchaotic systems have been extensively studied because of exhibiting at least two positive Lyapunov exponents. That is to say, the dynamics of the system expand in more than one direction and generate a much more complex attractor compared with the chaotic system with only one positive Lyapunov exponent, which is studied by Rech et al. [1, 2]. It means that hyperchaotic systems generate much more dynamical behaviors compared with chaotic systems [3–5]. Historically, the noted four-dimensional hyperchaotic system was firstly reported by Lörenz [6]. Chen et al. [7, 8] have studied the dynamics of the fractional-order generalizations of the Lörenz hyperchaos equation and found a new chaotic attractor in a simple three-dimensional autonomous system, which resembles some familiar features from both the Lörenz and Rössler attractors. Nowadays, the application of the hyperchaos is becoming a hot topic in the field of chaos. Wang [9, 10] has presented a multiscroll chaotic system generated from a new quadratic autonomous system and introduced a new three-dimensional quadratic autonomous system, which can generate a pair of double-wing chaotic attractors. Moreover, he has also found that the system can generate three-wing and four-wing chaotic attractors with very complicated topological structures over a large range of parameters. On the basis of the analysis above, several useful issues are investigated either analytically or numerically. Ma et al. [11–13] have expressed many of the dynamical systems generating both hyperchaotic and chaotic behaviors, such as quadratic dynamic behaviors, and analyzed it furthermore in various fields. Yang [14] has analyzed an input control of exponential synchronization for a four-dimensional chaotic system and obtained some valuable conclusions. Wang et al. [15] have studied an asynchronous communication system based on the hyperchaotic system of 6th-order cellular neural network and drew some useful conclusions. Correia and Rech [16] have introduced a state feedback control to the first equation based on Wang and proposed a method that also considers the magnitude of the second largest Lyapunov exponent to numerically characterize points with hyperchaotic behavior, in which two parameters are simultaneously varied, and they obtained some practical and theoretical significance in the practice. Besides this, Choudhury and Van Gorder [17] have discovered hyperchaotic systems in the high-dimensional financial and economic systems and drew some useful conclusions. It has drawn much more attention to scholars because of its potential applications in synchronization, securer communications, and so on, and it

been studied by Yu et al. [18, 19]. Thus, there are important theoretical and practical meanings and wide foreground to further pursue this research.

Chaos and hyperchaos make a tremendous negative impact on the practice, so we can join disturbance or control in the system to delay the happening time of chaos. It is well known that there are many methods to control the chaotic and hyperchaotic systems, such as nonlinear feedback, speed feedback control, state feedback control [20], linear feedback control [21], and adaptive control. There are advantages and disadvantages in each control method. In this case, we should choose the correct method to achieve the goal of chaos and hyperchaos control based on the first control.

It is well known that when a state feedback control join into a three-dimension chaotic system, the original three-dimension chaotic systems achieve a steady state by changing the value of the control parameters at the same time the original system goes into a four-dimensional system. However, through the theory analysis and numerical simulation, we found that the new four-dimension system produces both chaos and hyperchaos under the condition of certain ranges of parameters. This paper makes further analysis on chaotic and hyperchaotic system based on the new four-dimension system which has been joined in the state feedback control.

Thus, the new system which generates both chaos and hyperchaos is presented, and the complex dynamic characters of the system are analyzed. We adopt the method for the control according to the following rules: firstly, it is well known that the sooner convergence of the chaotic or hyperchaotic system, the better convergence of the effect of the control; secondly, the chaos control of a system should have some practical meanings; last but not the least, the controllers adopted by us should be as simple as possible, because it will be easy for us to operate in the application. Motivated by the discussion above, the linear control is proposed to achieve a second control, and it can drive the new hyperchaos to chaos, the periodic orbit, or a steady state; similarly, it can also restore a chaotic state to the equilibrium point. We outline two innovations, and one of which is that we will analyze and compare both chaotic and hyperchaotic Lyapunov dimensions and give the corresponding chaotic attractors and hyperchaotic attractors; the other one is that we introduce a second controller to the chaotic or hyperchaotic system which has already controlled by introducing a state feedback controller to delay or control hyperchaos, realizing the goal of a second control.

The rest of the paper is organized as follows. In Section 2, a four-dimension system is introduced, and we know that the system can produce both chaos and hyperchaos through numerical simulations. In Section 3, the system is analyzed dynamically, including the chaotic and hyperchaotic attractors. In Section 4, the power spectrums and time charts are mapped via Lyapunov dimension, Lyapunov exponents, and bifurcation diagram. In Section 5, linear feedback controller is designed for driving the chaotic or hyperchaotic system to a steady state, and the purpose of a second control is achieved. In the last section, the results are summarized, and the future directs are indicated.

2. Construction of the Dynamic System

In this paper, the dynamic system which has already introduced a state feedback control to the first equation is proposed by Correia and Rech [16], and the system of four-dimensional autonomous differential equations can be described as follows:

$$\begin{aligned} \dot{x} &= a(x - y) - yz + w, \\ \dot{y} &= -by + xz, \\ \dot{z} &= -cz + dx + xy, \\ \dot{w} &= -e(x + y), \end{aligned} \tag{1}$$

where a, b, c, d, and e are the parameters of system (1). When parameters $a = 0.98$, $b = 9$, $c = 50$, $d = 0.06$, and $e = 0.9$ with the initial values $x = 11.28$, $y = -11.21$, $z = -9$, and $w = 20.49$, the four Lyapunov exponents of system (1) calculated by Wolf algorithm are

$$\begin{aligned} L1 &= 0.007332, \qquad L2 = 0.004414, \\ L3 &= -0.020359, \qquad L4 = -0.898567. \end{aligned} \tag{2}$$

As well as the detailed theoretical analysis, it has been confirmed that the new system (1) displays sophisticated and abundant hyperchaotic dynamical behaviors with parameters $a = 0.98$, $b = 9$, $c = 50$, $d = 0.06$, and $e = 0.9$. The chaotic and hyperchaotic attractors which describe the dynamical behaviors of the system are shown in Figures 1, 2, and 3.

3. Dynamics Analysis of the System

In this section, basic properties and complex dynamics of the new system (1) are investigated, such as Lyapunov exponents, fractal dimensions, and attractors. The new dynamic system has the following basic properties.

3.1. Symmetry. The dynamic system (1) which is invariant under the coordinate transformation $(x, y, z, w) \to (-x, -y, z, -w)$ under reflection about the z-axis; the symmetry persists for all values of the system parameters.

3.2. Dissipation and Attractor. For the dynamical system (1), we can obtain

$$\nabla V = \frac{\partial \dot{x}}{\partial x} + \frac{\partial \dot{y}}{\partial y} + \frac{\partial \dot{z}}{\partial z} + \frac{\partial \dot{w}}{\partial w} = a - b - c = m. \tag{3}$$

If we want the hyperchaotic system to become dissipative with $a - b - c = m$, then m which is a negative value will be required. Dynamical system which is described by system (1) is one dissipative system. It is worth noting that a volume element V_0 is apparently contracted by the flow into a volume element $V_0 e^{(a-b-c)t}$ in time t. From a mathematic point of view, it means that each volume containing the trajectory of this dynamical system shrinks to zero as t at an exponential rate $a - b - c = m$. Therefore, all the orbits are ultimately confined to a specific subset of zero volume, and trajectories of the system arrive to an attractor at last.

3.3. Equilibrium and Stability. The following equations are the equilibrium of the system satisfied:

$$\begin{aligned} a(x-y) - yz + w &= 0, \\ -by + xz &= 0, \\ -cz + dx + xy &= 0, \\ -e(x+y) &= 0. \end{aligned} \tag{4}$$

By calculation, there are three equilibrium points for the system, and the equilibrium points are as follows:

$E1\,(0,0,0,0)$, $E2\,(-(d/2 + \sqrt{d^2+4bc}/2)(2a-b), d/2 + \sqrt{d^2+4bc}/2, -d/2 - \sqrt{d^2+4bc}/2, -b)$, $E3\,(-(d/2 - \sqrt{d^2+4bc}/2)(2a-b), d/2 - \sqrt{d^2+4bc}/2, \sqrt{d^2+4bc}/2 - d/2, -b)$.

The Jacobian matrix evaluated at the three equilibrium points of the system can be expressed as follows:

$$J = \begin{pmatrix} a & -a-z & -y & 1 \\ z & -b & x & 0 \\ d+y & x & -c & 0 \\ -e & -e & 0 & 0 \end{pmatrix}. \tag{5}$$

It is easy to get the characteristic equation $|\lambda E - J| = 0$. Thus, we can obtain the eigenvalues at the equilibrium points by solving the characteristic equation. When

$$\begin{aligned} a &= 0.98, \quad b = 9, \quad c = 50, \\ d &= 0.06, \quad e = 0.9, \end{aligned} \tag{6}$$

the characteristic equation for equilibrium point $E2$ has four eigenvalues, and it is easy to show that the four eigenvalues are

$$\begin{aligned} \lambda_1 &= -51.5250, \quad \lambda_2 = -3.2647 + 10.8594i, \\ \lambda_3 &= -3.2647 - 10.8594i, \quad \lambda_4 = 0.0344. \end{aligned} \tag{7}$$

Obviously, λ_1 is a negative number, λ_2 and λ_3 are a pair of complex conjugate eigenvalues with negative real parts, and the forth number λ_4 is a positive real number. Hence, the equilibrium point $E2$ is an unstable saddle point in the system, and the hyperchaotic system is unstable at the point $E2$. At the same time, it is easy to prove that both the equilib-rium points $E1$ and $E3$ are also unstable saddle points.

3.4. Lyapunov Exponents and Lyapunov Dimensions. It is known that most of the dynamic systems can be charactered by the Lyapunov exponents. Figure 4 describes Lyapunov exponents with the variety of parameters a and b on the premise of other parameters fixed when the step length is 0.001. Figure 4(a) is the Lyapunov exponents with the variety of a when $a \in [1, 2.6]$, $b = 12$, $c = 5$, $d = 0.06$, and $e = 0.1$, and Figure 4(b) is the Lyapunov exponents with the varies of b when $a = 1$, $b \in [12, 22]$, $c = 5$, $d = 0.06$, and $e = 0.1$. As it can be seen in Figure 4(a), there is one positive value in certain ranges of parameter a, so it is chaotic at this time. In some ranges of parameter a, there are two positive Lyapunov exponents and two negative exponents; the system rushes into a hyperchaotic state. In some ranges of parameter a, there is one zero and three negative Lyapunov exponents, and the dynamic system appears periodic. In some special points, there are two zero and two negative Lyapunov exponents, and the dynamic system appears quasiperiodic. From Figure 4(b), it is easy to see that it is similar to Figure 4(a). In one word, the diversity for the combination of Lyapunov exponents results in the dynamic system appearing more complex behaviors. According to the theory of chaos, the Lyapunov exponents measure the exponential rates of divergence and convergence of nearby trajectories in phase space of dynamic system (1) [22–24]. As we know that for a chaotic attractor, one positive, one zero, and two negative Lyapunov exponents are needed in a dynamic system, while for the corresponding hyperchaotic attractors, the system should have two positive Lyapunov exponents at least.

3.4.1. Chaos. For the system when $a = 1$, $b = 12$, $c = 5$, $d = 0.06$, and $e = 0.1$, the four Lyapunov exponents are as follows:

$$L1 = 0.003202, \quad L2 = -0.000341, \tag{8}$$

$$L3 = -0.003468, \quad L4 = -0.173814. \tag{9}$$

It can be seen that the largest Lyapunov exponent is positive, indicating that the system has chaotic characteristics. The $L1$ is a positive Lyapunov exponent, and the rest three Lyapunov exponents are negative. Thus, the system is chaotic, not hyperchaotic. The fractal dimension is also a typical characteristic of chaos calculated Kaplan-Yorke dimension by Lyapunov exponents, and D_{ky} can be expressed as

$$D_{ky} = k + \sum_{i=1}^{k} \frac{L_i}{|L_{k+1}|}, \tag{10}$$

where k says the first k Lyapunov exponent is nonnegative, namely, k is the maximum value of i value which meets both $\sum_{i=1}^{k} L_i \gg 0$ and $\sum_{i=1}^{k} L_i < 0$ at the same time. L_i is in descending order of the sequence according to the sequence of Lyapunov exponents. D_{ky} is the upper bound of the dimension of the system information. For the system in this paper, by observing the values of four Lyapunov exponents in the above, we determine that the value of k is two, and then the Kaplan-Yorke dimension can be expressed from the above

$$D_{ky} = 2 + \frac{0.003202 - 0.000341}{|-0.003468|} = 2.824971 \approx 2.825. \tag{11}$$

So, chaos in this system is very obvious. Thus, the corresponding attractors are shown in Figure 5.

3.4.2. Hyperchaos. When $a = 1, b = 12, c = 50, d = 0.06$, and $e = 0.9$ and initial values are $x = 11.28$, $y = -11.21$, $z = -9$, and $w = 20.49$, the Lyapunov exponents are as follows:

$$\begin{aligned} L1 &= 0.007048, \quad L2 = 0.004036, \\ L3 &= -0.070032, \quad L4 = -0.855856. \end{aligned} \tag{12}$$

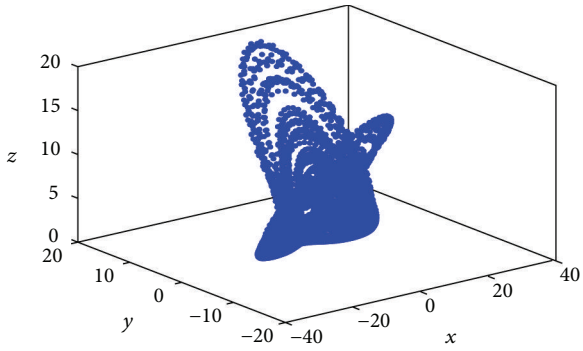

(a) 3D view in the x-y-z space

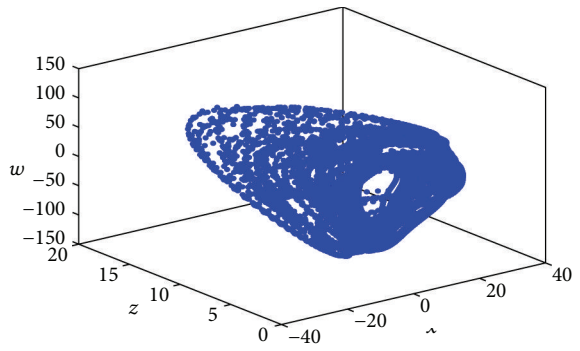

(b) 3D view in the x-z-w space

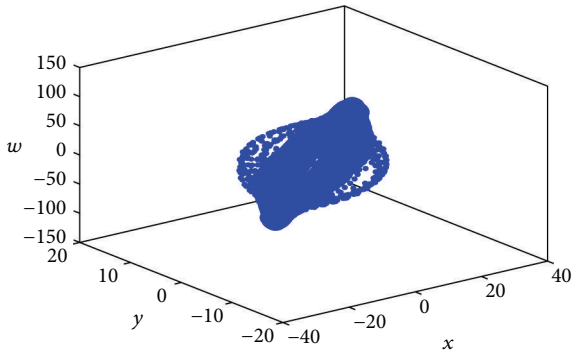

(c) 3D view in the x-y-w space

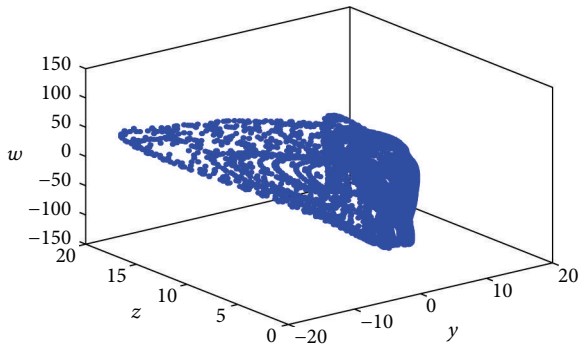

(d) 3D view in the y-z-w space

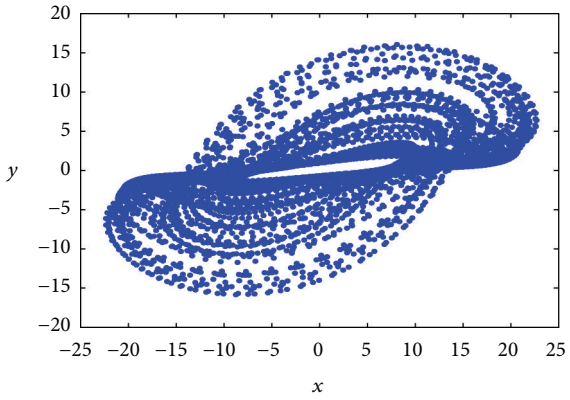

(e) Projection onto the x-y plane

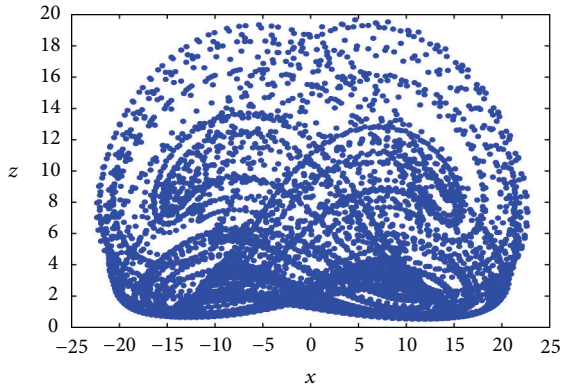

(f) Projection onto the x-z plane

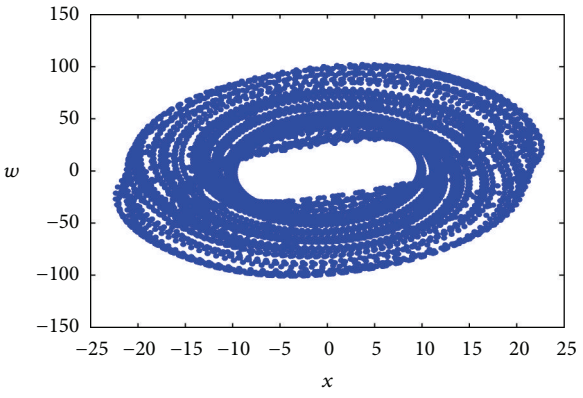

(g) Projection onto the x-w plane

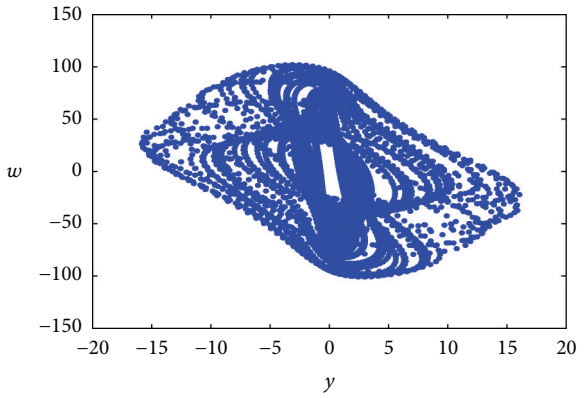

(h) Projection onto the y-w plane

Figure 1: Continued.

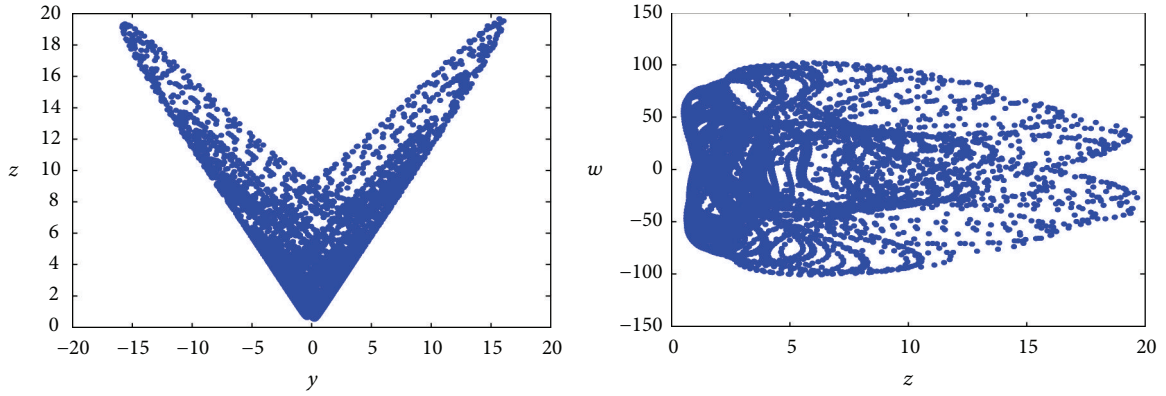

(i) Projection onto the y-z plane (j) Projection onto the z-w plane

Figure 1: Phase portraits of the dynamic system when $x = 11.28$, $y = -11.21$, $z = -9$, and $w = 20.49$ and $a = 0.9$, $b = 12$, $c = 6$, $d = 0.06$, and $e = 20$.

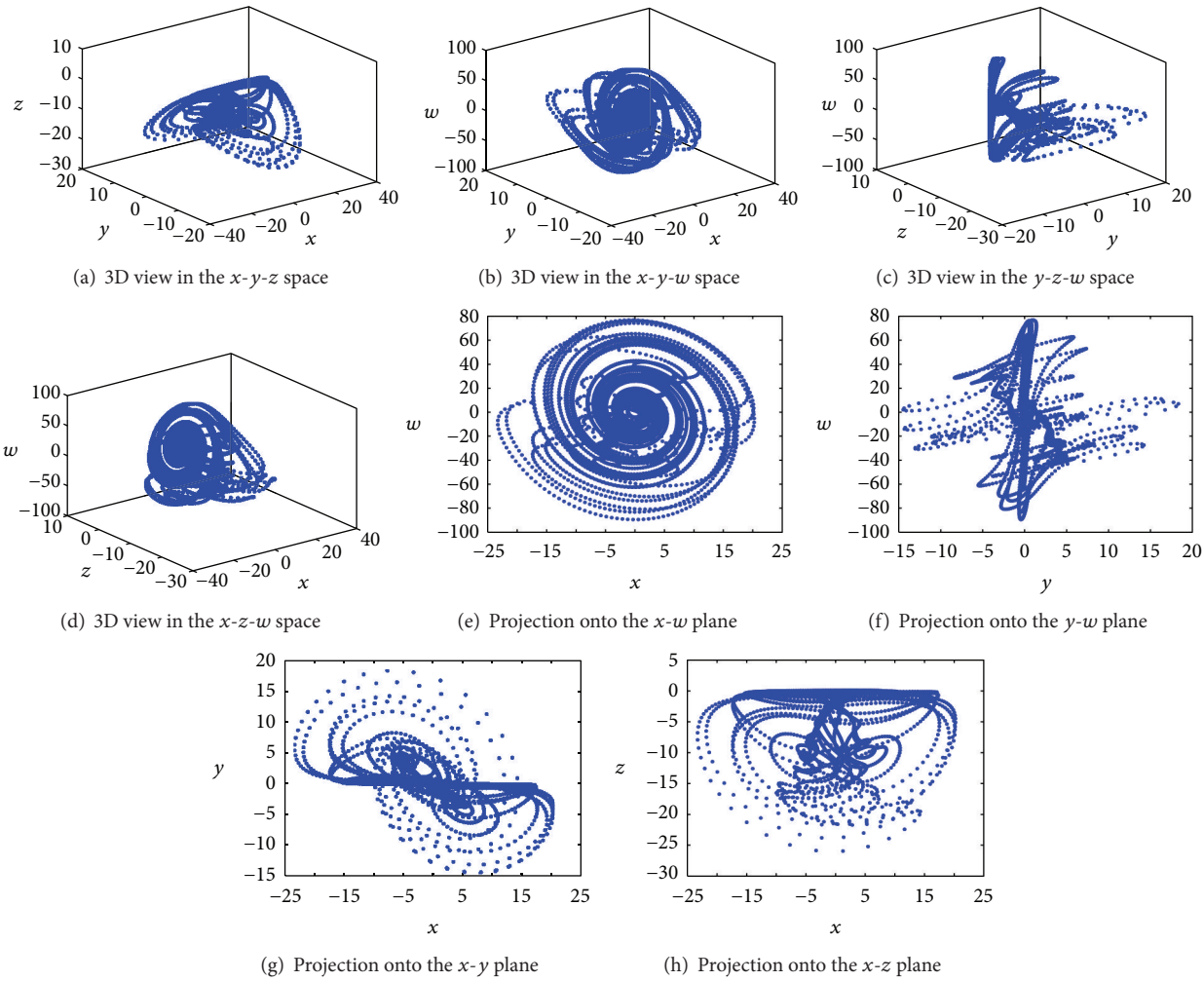

(a) 3D view in the x-y-z space (b) 3D view in the x-y-w space (c) 3D view in the y-z-w space

(d) 3D view in the x-z-w space (e) Projection onto the x-w plane (f) Projection onto the y-w plane

(g) Projection onto the x-y plane (h) Projection onto the x-z plane

Figure 2: Continued.

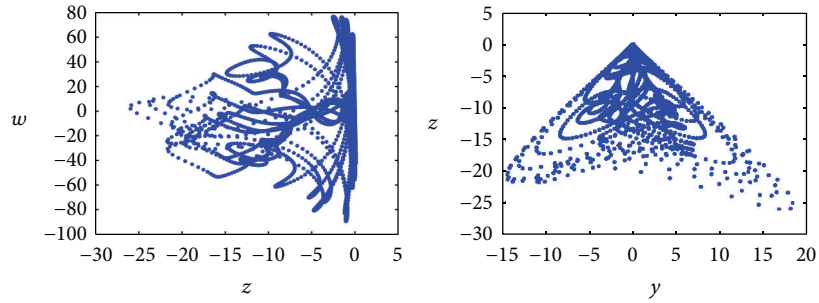

(i) Projection onto the z-w plane (j) Projection onto the y-z plane

FIGURE 2: Phase portraits of the dynamic system when $x = 11.28$, $y = -11.21$, $z = -9$, and $w = 20.49$ and $a = 0.9$, $b = 12$, $c = 2$, $d = 0.06$, and $e = 20$.

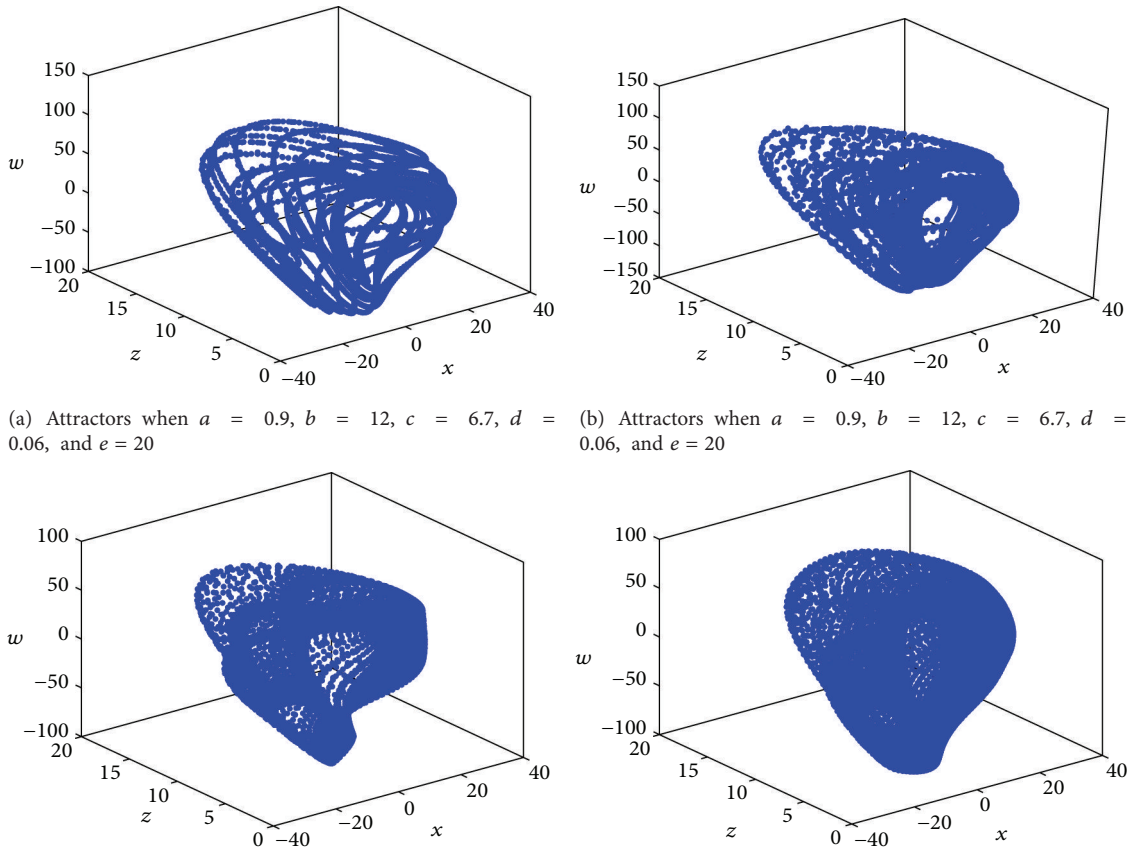

(a) Attractors when $a = 0.9$, $b = 12$, $c = 6.7$, $d = 0.06$, and $e = 20$

(b) Attractors when $a = 0.9$, $b = 12$, $c = 6.7$, $d = 0.06$, and $e = 20$

(c) Attractors when $a = 0.9$, $b = 12$, $c = 7.9$, $d = 0.06$, and $e = 20$

(d) Attractors when $a = 0.98$, $b = 12$, $c = 6$, $d = 0.06$, and $e = 24$

FIGURE 3: Attractors when $x = 11.28$, $y = -11.21$, $z = -9$, and $w = 20.49$ with different parameters.

The fractal dimension can be written as follows:

$$D_{ky} = 2 + \frac{0.007048 - 0.004036}{|-0.070032|} = 2.0430089 \approx 2.04. \quad (13)$$

As is well known, there is more than one positive exponent in the four-dimensional dynamic system. For the system which has been controlled by a state feedback controller, it is chaotic within certain ranges of parameters. However, the system will rush into a hyperchaotic state when there are two or more than two positive Lyapunov exponents. Thus, hyperchaotic attractors also exist in the system as it can be seen from Figure 6, and the behaviors of system will become much more complex. Therefore, both chaos and hyperchaos appear very obviously.

4. Bifurcation Diagrams

Generally speaking, the bifurcation diagram is the best method to describe all the possible behaviors as the parameter varies in one diagram. We take 500 as the total number of time

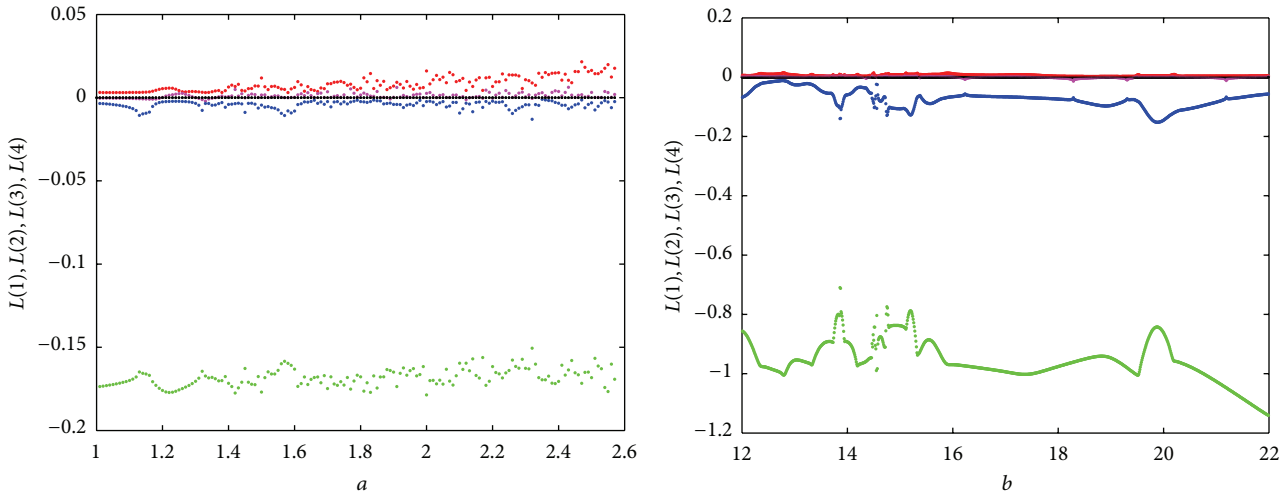

(a) The Lyapunov exponents with the variety of a, when $b = 12$, $c = 5$, $d = 0.06$, and $e = 0.1$

(b) The Lyapunov exponents with the variety of b, when $a = 1$, $c = 5$, $d = 0.06$, and $e = 0.1$

FIGURE 4: The Lyapunov exponents with the variety of parameters a ($a \in [1, 2.6]$) and b ($b \in [12, 22]$) when the step length is 0.001.

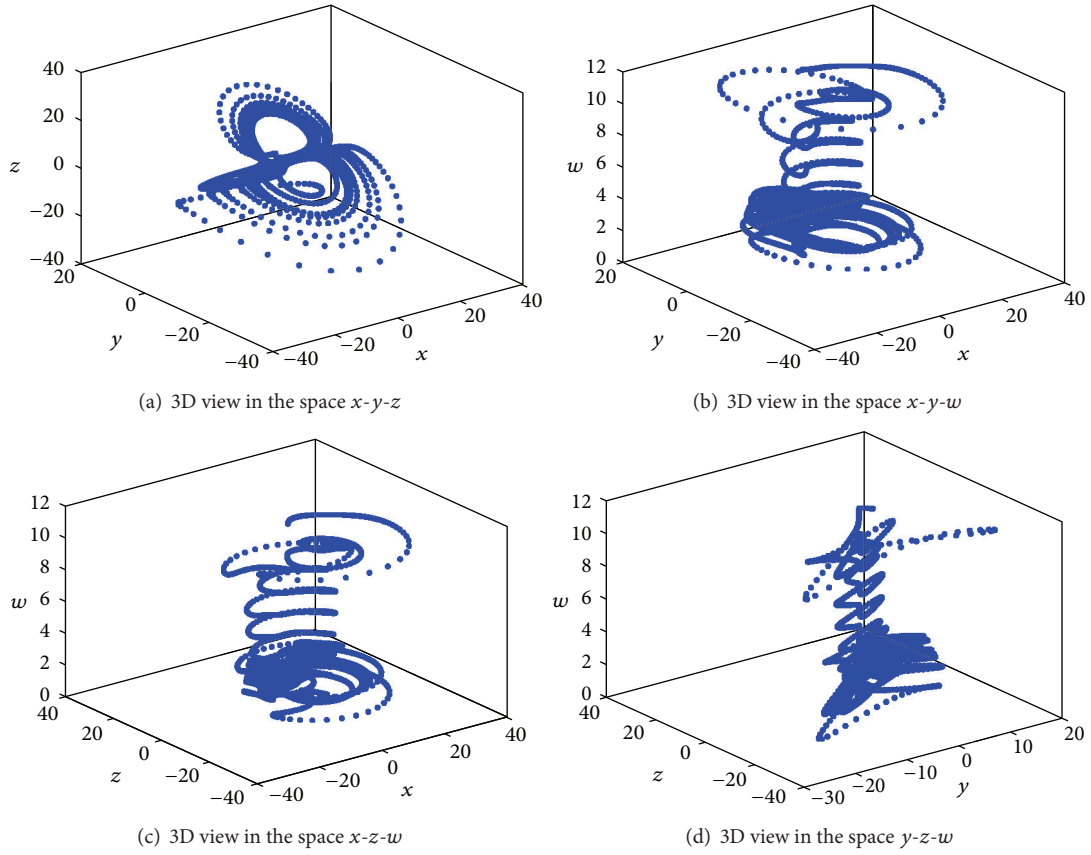

(a) 3D view in the space x-y-z

(b) 3D view in the space x-y-w

(c) 3D view in the space x-z-w

(d) 3D view in the space y-z-w

FIGURE 5: Chaotic attractors.

steps, 400 as the number of time steps discarded, and 0.001 as the step length, calculating and drawing the bifurcation diagram according to the definition of dynamical system. We map out the bifurcation diagrams with the variety of parameters a, b, c, d, and e, respectively, ($a \in [-3, 3]$, $b \in [0, 8]$, $c \in [-1, 6]$, $d \in [20, 30]$, and $e \in [33, 43]$) in Figures 7(a)–7(e). The bifurcation diagram of system (1) shows the complicated bifurcation phenomena. In order to make a detailed description of the behaviors of system, we map out the Lyapunov exponents with the variety of a, ($a \in [-3, 0.6]$) as an example in Figure 7(f). Thus, we can learn about the dynamic behaviors furthermore by comparing the

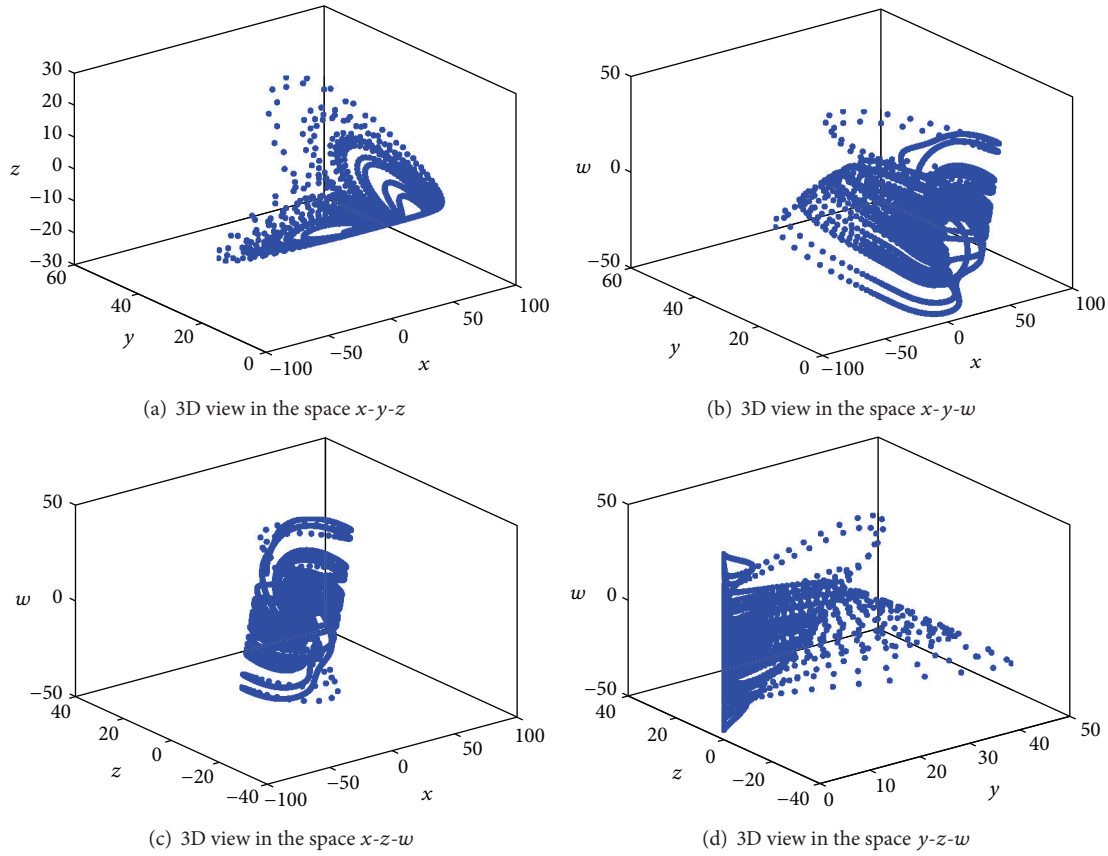

Figure 6: Hyperchaotic attractors.

bifurcation diagram and the Lyapunov exponents in different stages. Attractors are also mapped out in every stage as it can be seen in Figure 8.

Comparing Figure 7(a) with 7(f), it is easy to see that the two figures are consistent. When $b = 9$, $c = 5$, $d = 0.06$, and $e = 25$ and step length is 0.001, the values of $a = -1.59$ and $a = -0.56$ divide the system into several stages. We assume that four Lyapunov exponents of system (1) satisfying $L_1 > L_2 > L_3 > L_4$ and the dynamical behaviors can be described and classified as follows

(1) For $a < -1.59$, $L_1 < 0$, $L_2 < 0$, $L_3 < 0$, and $L_4 < 0$, the system (1) is in a steady state and stabilized to the equilibrium point.

(2) For $a = -1.59$, $L_1 = 0$, $L_2 < 0$, $L_3 < 0$, and $L_4 < 0$, the system (1) appears periodic, because there is one zero and three negative Lyapunov exponents; Figures 8(a)–8(d) show the corresponding attractors in this stage.

(3) For $-1.59 < a < -0.56$, $L_1 > 0$, $L_2 < 0$, $L_3 < 0$, and $L_4 < 0$, one positive Lyapunov exponent exists, and the system (1) is in a chaotic state at this time; Figures 8(e)–8(h) show the corresponding chaotic attractors in this stage.

(4) For $a = -0.56$, $L_1 > 0$, $L_2 = 0$, $L_3 < 0$, and $L_4 < 0$, the system (1) is still in a chaotic state, because there is one positive Lyapunov exponent, one zero Lyapunov exponent, and two negative Lyapunov exponents; Figures 8(i)–8(l) show the corresponding chaotic attractors in this stage.

(5) For $a > -0.56$, $L_1 > 0$, $L_2 > 0$, $L_3 < 0$, and $L_4 < 0$, two positive Lyapunov exponents exist, and the system (1) rushes into a hyperchaotic state, and hyperchaotic attractor appears. Figures 8(m)–8(p) show hyperchaotic attractors in this stage.

4.1. The Power Spectrum of the System. When $x = 11.28$, $y = -11.21$, $z = -9$, and $w = 20.49$, Figure 9 is the power spectrums of the system with different parameters. Figure 9(a) is the power spectrums of the dynamic system with $a = 0.98$, $b = 12$, $c = 6$, $d = 0.06$, and $e = 20$. Figure 9(b) is the power spectrums of the dynamic system with $a = 0.9$, $b = 12$, $c = 6$, $d = 0.06$, and $e = 20$. Figure 9(c) is the power spectrums of the dynamic system with $a = 0.9$, $b = 12$, $c = 6$, $d = 0.06$, and $e = 25$. Figure 9(d) is the power spectrums of the dynamic system when $x = 11.28$, $y = -11.21$, $z = -9$, and $w = 20.49$. According to numerical simulation of the system, take the cycle method to estimate the power spectrums of variables of the system, as it is shown in Figures 9(a)–9(d) with different parameters. According to the numerical calculation, the results show that with parameters changing, the values of the system have always been restricted in a certain range. This proves the

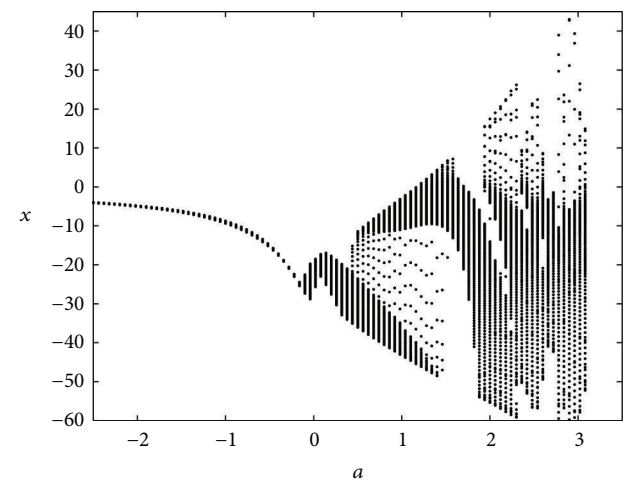

(a) Bifurcation diagram with the change of a, when $b = 9$, $c = 5$, $d = 0.06$, and $e = 25$

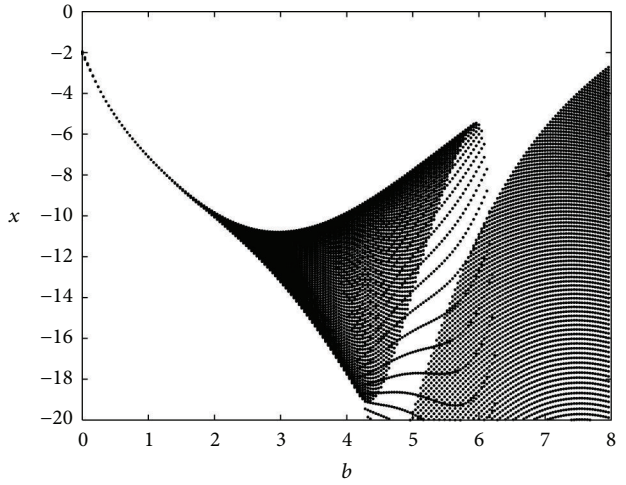

(b) Bifurcation diagram with the change of b with the rest fixed parameters

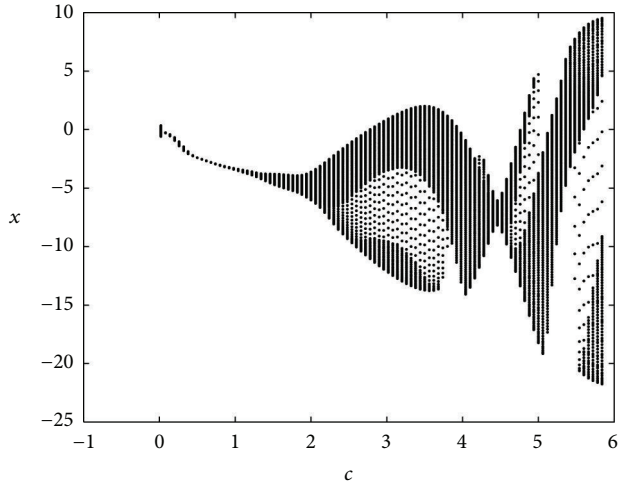

(c) Bifurcation diagram with the change of c with the rest fixed parameters

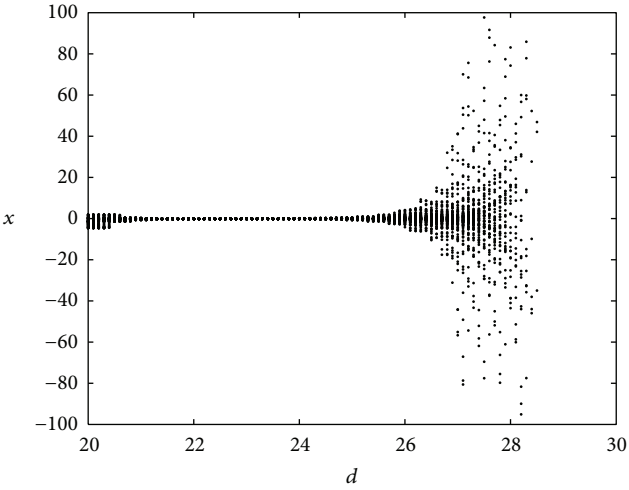

(d) Bifurcation diagram with the change of d with the rest fixed parameters

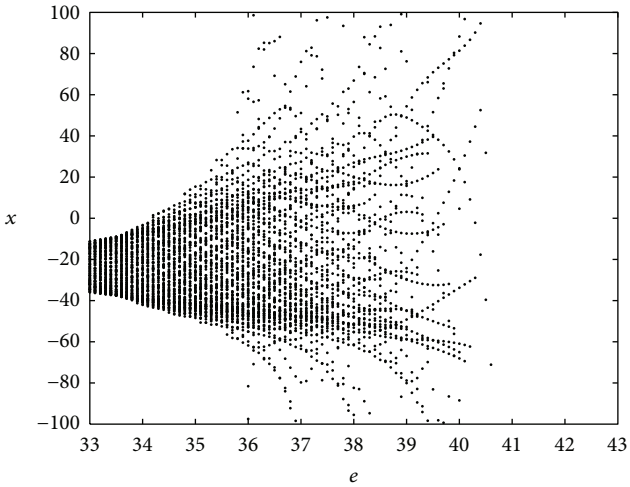

(e) Bifurcation diagram with the change of e with the rest fixed parameters

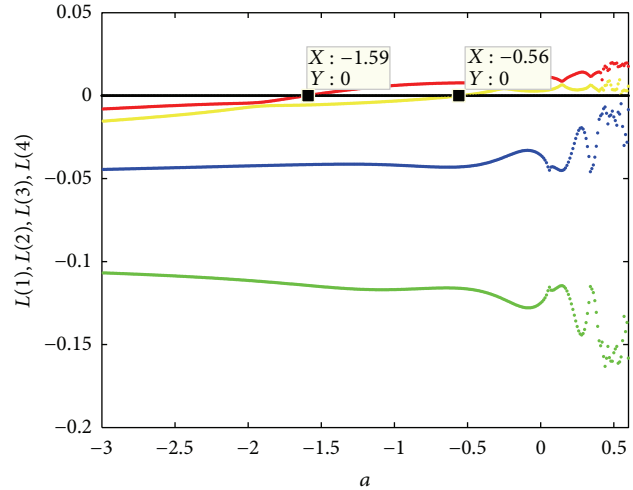

(f) Lyapunov exponent with the change of a, when $b = 9$, $c = 5$, $d = 0.06$, and $e = 25$

FIGURE 7: Bifurcation diagram and the Lyapunov exponent when $x = 11.28$, $y = -11.21$, $z = -9$, and $w = 20.49$ and the step length is 0.001.

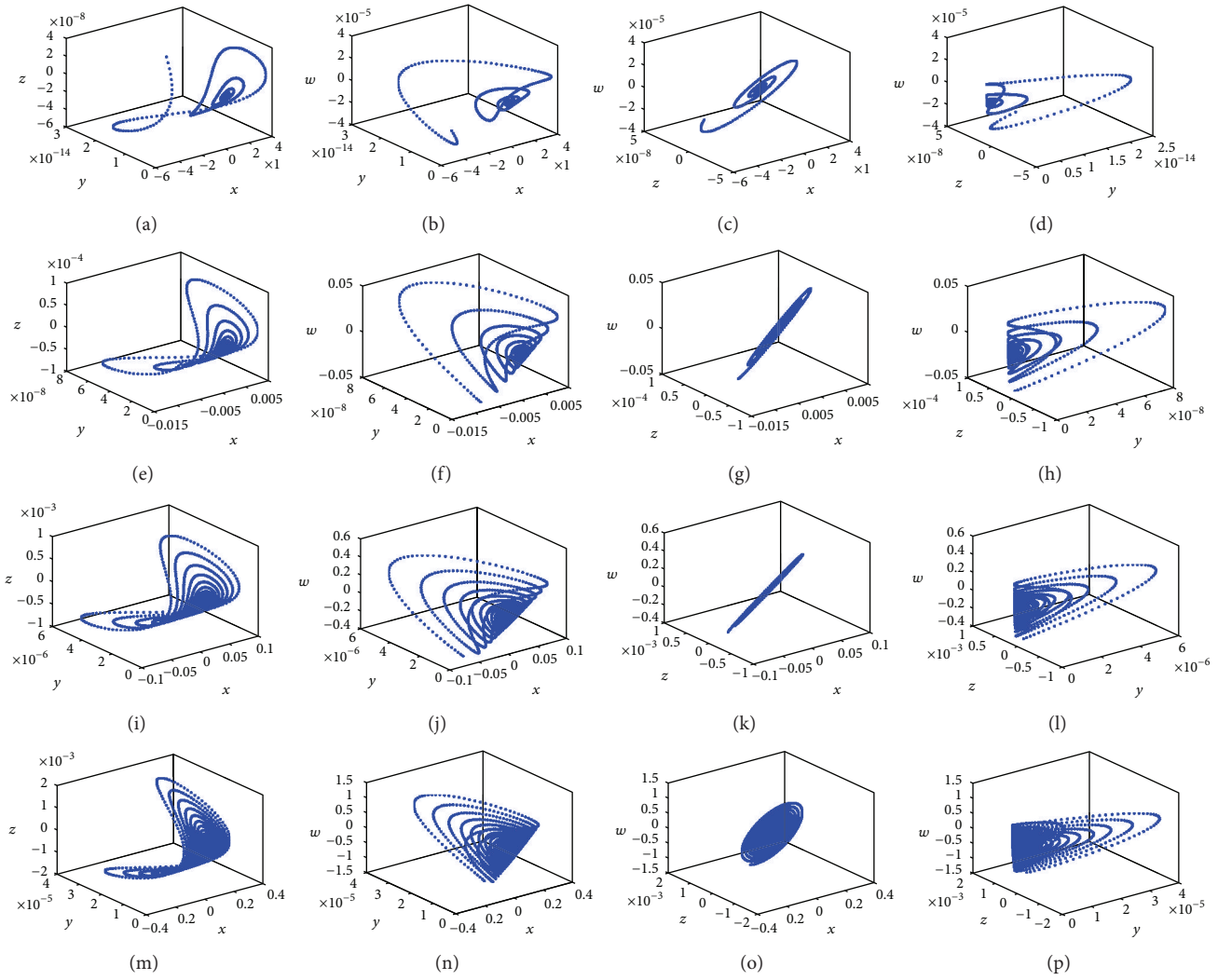

Figure 8: Typical dynamical behavior of system (1). (a)–(d): $a = -1.59$, (e)–(h): $a = -1.5$, (i)–(l): $a = -0.56$, and (m)–(p): $a = 0.2$.

characteristics of the chaotic system once again: boundedness and ergodicity. Therefore, there are some methods which can be taken to control the chaos and hyperchaos.

4.2. The Time Chart. The time chart is also a good method to display the behaviors as the parameter varies on the figure. It can be seen that the time charts of the system are shown in Figure 10 when $x = 11.28$, $y = -11.21$, $z = -9$, and $w = 20.49$ and $a = 0.98$, $b = 12$, $c = 6$, $d = 0.06$, and $e = 20$.

5. Chaos Control

Chaos and hyperchaos may cause irregular behaviors which are undesirable, so not all the partners in the system can make correct strategies or reasonable decisions in the market. However, in some special environment, chaos and hyperchaos are helpful to our economy. Thus, proper measures should be taken to control chaos in order to advance or delay the occurrence of the chaos or hyperchaos. In this chapter, we take the linear feedback control method. The method comes from the differences between the target signal and output chaotic signal or directly uses the chaotic output signal of the system itself, multiplied by the appropriate coefficient of linear feedback. Several characteristics of this method are described as follows: (1) the method can achieve control for any solution in the original system, such as the fixed point and unstable periodic orbits; (2) it is not affected by the changes of the small parameter, with the characteristic of anti-interference; and (3) there are certain difficulties for the actual system which exist in the interaction of many system variables. Therefore, we should make further improvement from the point of view of engineering application. Nonfeedback and the delay feedback are two methods for the chaos control. Thus, we can achieve the task of chaos control in this dynamic system. Firstly, we have a transformation of the system at the equilibrium point $E2$ as the following rules:

$$X = x + \left(\frac{d}{2} + \frac{\sqrt{d^2 + 4bc}}{2}\right)(2a - b),$$

$$Y = y - \left(\frac{d}{2} + \frac{\sqrt{d^2 + 4bc}}{2}\right),$$

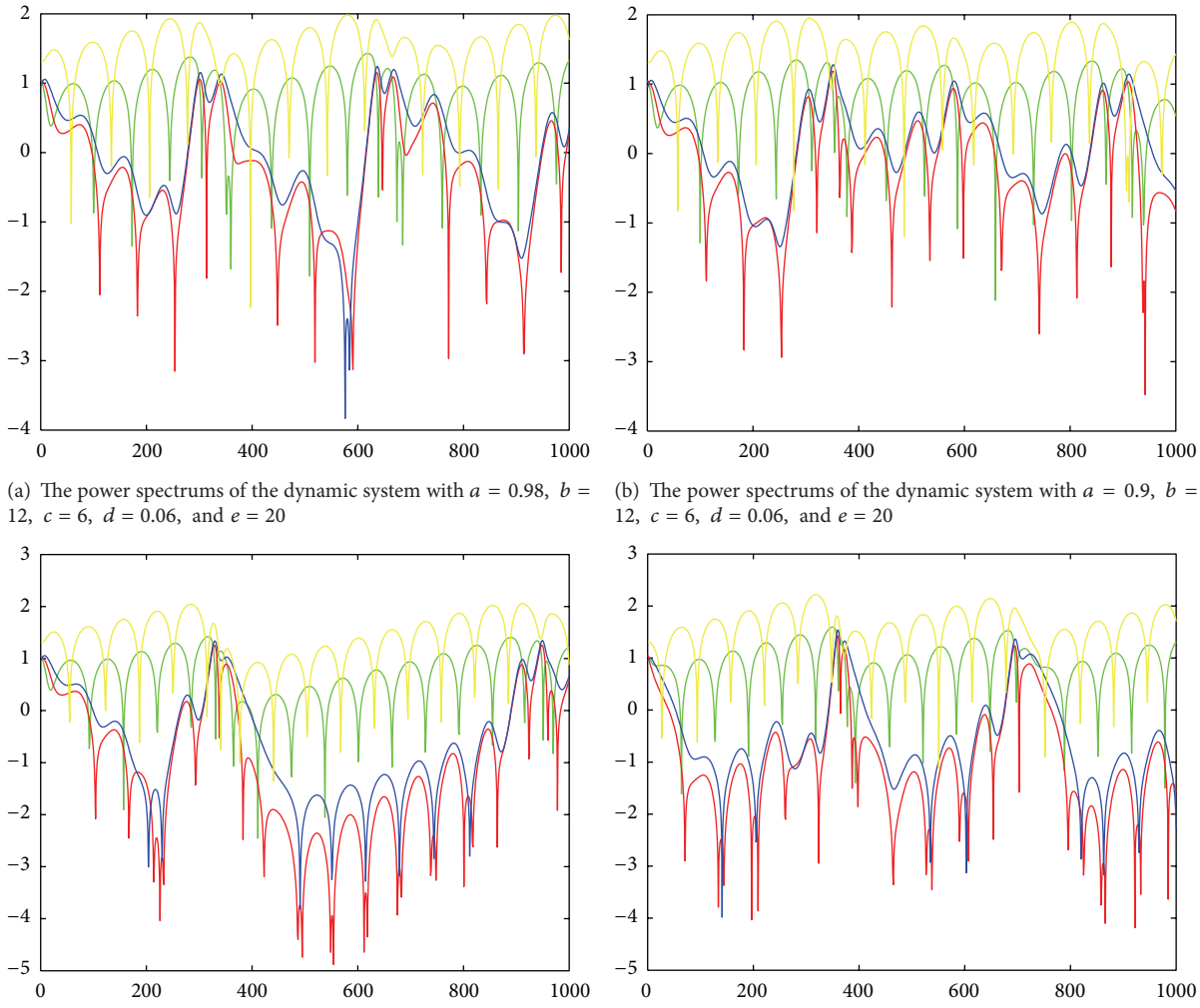

(a) The power spectrums of the dynamic system with $a = 0.98$, $b = 12$, $c = 6$, $d = 0.06$, and $e = 20$

(b) The power spectrums of the dynamic system with $a = 0.9$, $b = 12$, $c = 6$, $d = 0.06$, and $e = 20$

(c) The power spectrums of the dynamic system with $a = 0.9$, $b = 12$, $c = 6$, $d = 0.06$, and $e = 25$

(d) The power spectrums of the dynamic system with $a = 0.9$, $b = 20$, $c = 8$, $d = 0.06$, and $e = 25$

FIGURE 9: The power spectrums of the dynamic system when $x = 11.28$, $y = -11.21$, $z = -9$, and $w = 20.49$. (The red color stands for the power spectrum of x; the yellow color stands for the power spectrum of y; the blue color stands for the power spectrum of z; and the green color stands for the power spectrum of w.)

$$Z = z + \left(\frac{d}{2} + \frac{\sqrt{d^2 + 4bc}}{2}\right),$$
$$W = w + b. \tag{14}$$

Then, the dynamic system can be rewritten as follows:

$$\dot{X} = a\left[X - \left(\frac{d}{2} + \frac{\sqrt{d^2 + 4bc}}{2}\right)(2a - b) - Y - \left(\frac{d}{2} + \frac{\sqrt{d^2 + 4bc}}{2}\right)\right] - \left[Y + \left(\frac{d}{2} + \frac{\sqrt{d^2 + 4bc}}{2}\right)\right] \times \left[Z - \left(\frac{d}{2} + \frac{\sqrt{d^2 + 4bc}}{2}\right)\right] + (W - b),$$

$$\dot{Y} = -b\left[Y + \left(\frac{d}{2} + \frac{\sqrt{d^2 + 4bc}}{2}\right)\right] + \left[X - \left(\frac{d}{2} + \frac{\sqrt{d^2 + 4bc}}{2}\right)(2a - b)\right] \times \left[Z - \left(\frac{d}{2} + \frac{\sqrt{d^2 + 4bc}}{2}\right)\right],$$

$$\dot{Z} = -c\left[Z - \left(\frac{d}{2} + \frac{\sqrt{d^2 + 4bc}}{2}\right)\right] + d\left[X - \left(\frac{d}{2} + \frac{\sqrt{d^2 + 4bc}}{2}\right)(2a - b)\right] + \left[X - \left(\frac{d}{2} + \frac{\sqrt{d^2 + 4bc}}{2}\right)(2a - b)\right]$$

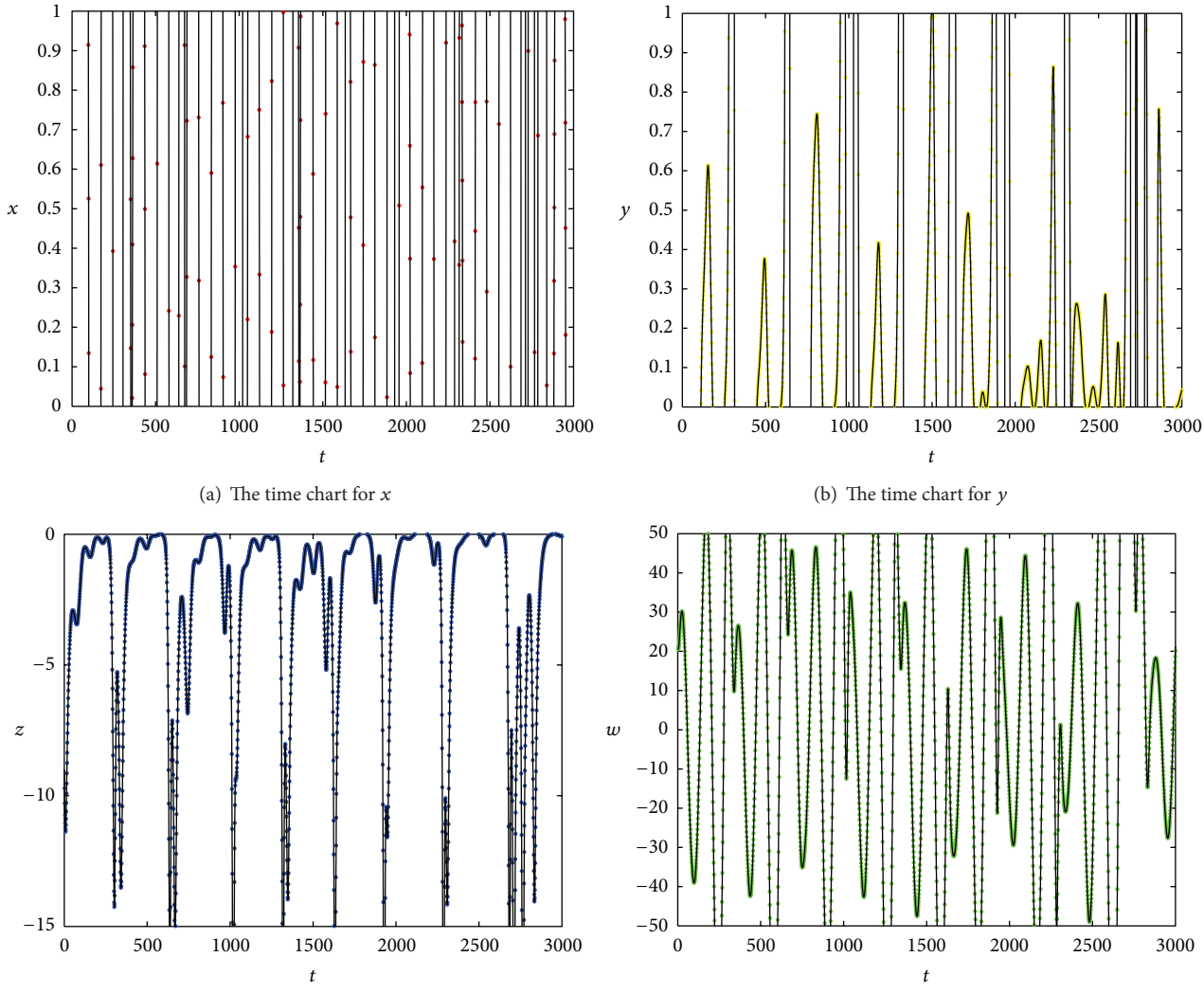

(a) The time chart for x

(b) The time chart for y

(c) The time chart for z

(d) The time chart for w

FIGURE 10: The time charts of the system with $x = 11.28$, $y = -11.21$, $z = -9$, and $w = 20.49$ and $a = 0.98$, $b = 12$, $c = 6$, $d = 0.06$, and $e = 20$.

$$\times \left[Y + \left(\frac{d}{2} + \frac{\sqrt{d^2 + 4bc}}{2} \right) \right],$$

$$\dot{W} = -e \left[X - \left(\frac{d}{2} + \frac{\sqrt{d^2 + 4bc}}{2} \right) (2a - b) \right] + Y + \left(\frac{d}{2} + \frac{\sqrt{d^2 + 4bc}}{2} \right). \tag{15}$$

We assume that the controlled dynamic system can be described as follows: assume that the controlled dynamic system can be described as follows:

$$\dot{X} = a \left[X - \left(\frac{d}{2} + \frac{\sqrt{d^2 + 4bc}}{2} \right) (2a - b) - Y - \left(\frac{d}{2} + \frac{\sqrt{d^2 + 4bc}}{2} \right) \right] - \left[Y + \left(\frac{d}{2} + \frac{\sqrt{d^2 + 4bc}}{2} \right) \right] \times \left[Z - \left(\frac{d}{2} + \frac{\sqrt{d^2 + 4bc}}{2} \right) \right] + (W - b) - kX,$$

$$\dot{Y} = -b \left[Y + \left(\frac{d}{2} + \frac{\sqrt{d^2 + 4bc}}{2} \right) \right] + \left[X - \left(\frac{d}{2} + \frac{\sqrt{d^2 + 4bc}}{2} \right) (2a - b) \right] \times \left[Z - \left(\frac{d}{2} + \frac{\sqrt{d^2 + 4bc}}{2} \right) \right] - kY,$$

$$\dot{Z} = -c \left[Z - \left(\frac{d}{2} + \frac{\sqrt{d^2 + 4bc}}{2} \right) \right]$$

$$+ d\left[X - \left(\frac{d}{2} + \frac{\sqrt{d^2+4bc}}{2}\right)(2a-b)\right] + \left[X - \left(\frac{d}{2} + \frac{\sqrt{d^2+4bc}}{2}\right)(2a-b)\right] \times \left[Y + \left(\frac{d}{2} + \frac{\sqrt{d^2+4bc}}{2}\right)\right] - kZ,$$

$$\dot{W} = -e\left[X - \left(\frac{d}{2} + \frac{\sqrt{d^2+4bc}}{2}\right)(2a-b)\right] + Y + \left(\frac{d}{2} + \frac{\sqrt{d^2+4bc}}{2}\right) - kW. \tag{16}$$

The Jacobian matrix of the controlled system is as follows:

$$J = \begin{pmatrix} a-k & -a + \left(\frac{d}{2} + \frac{\sqrt{d^2+4bc}}{2}\right) & -\left(\frac{\sqrt{d^2+4bc}}{2}\right) & 1 \\ -\left(\frac{\sqrt{d^2+4bc}}{2}\right) & -b-k & -\left(\frac{d}{2} + \frac{\sqrt{d^2+4bc}}{2}\right)(2a-b) & 0 \\ d + \left(\frac{d}{2} + \frac{\sqrt{d^2+4bc}}{2}\right) & -\left(\frac{d}{2} + \frac{\sqrt{d^2+4bc}}{2}\right)(2a-b) & -c-k & 0 \\ -e & -e & 0 & -k \end{pmatrix}, \tag{17}$$

and the characteristic polynomial is:

$$p(\lambda) = \lambda^4 + m_1\lambda^3 + m_2\lambda^2 + m_3\lambda + m_4, \tag{18}$$

where

$m_1 = b + c - 4k - 1$;

$m_2 = (\sqrt{d^2+4bc}/2) - b - c + e - 3k + 6k^2 - a^2(d^2+4bc) - (b^2(d^2+4bc)/4) + d\sqrt{d^2+4bc} - a^2d^2 - (b^2d^2/4) + bc + 3bk + 3ck + ab(d^2+4bc) + abd^2 - 2a^2d\sqrt{d^2+4bc} - (b^2d\sqrt{d^2+4bc}/2) + 2abd\sqrt{d^2+4bc}$;

$m_3 = -3k^2 + 4k^3 + a^2d^2 + (b^2d^2/4) + (b(d^2+4bc)/4) + (c(d^2+4bc)/4) + k(d^2+4bc) - bc + be + ce - 2bk - 2ck + 2ek + a^2(d^2+4bc) + (a\sqrt[3/2]{d^2+4bc}/2) + (b^2(d^2+4bc)/4) - (b\sqrt[3/2]{d^2+4bc}/4) - (e\sqrt{d^2+4bc}/2) + (3ad^3/4) - (3bd^3/8) + 3bk^2 + 3ck^2 + (3bd\sqrt{d^2+4bc}/4) + (cd\sqrt{d^2+4bc}/4) - 2a^2k(d^2+4bc) - (b^2k(d^2+4bc)/2) + 2dk\sqrt{d^2+4bc} - abd^2 + (7ad^2\sqrt{d^2+4bc}/4) + 2a^2d\sqrt{d^2+4bc} - (7bd^2\sqrt{d^2+4bc}/8) + (b^2d\sqrt{d^2+4bc}/2) - 2a^2d^2 - (b^2d^2k/2) - ab(d^2+4bc) + (3ad(d^2+4bc)/2) - (3bd(d^2+4bc)/4) + 2bck - 4a^2dk\sqrt{d^2+4bc} - b^2dk\sqrt{d^2+4bc} + 2abk(d^2+4bc) - 2abd\sqrt{d^2+4bc} + 2abd^2k + 4abdk\sqrt{d^2+4bc}$;

$m_4 = ((d^2+4bc)k^2/2) - bk^2 + bk^3 - ck^2 + ck^3 + ek^2 - k^3 + k^4 - a^2k^2(d^2+4bc) - (b^2k^2(d^2+4bc)/4) + dk^2\sqrt{d^2+4bc} - a^2d^2e - (b^2d^2e/4) + a^2d^2k + (b^2d^2k/4) - (ae(d^2+4bc)/2) + (be(d^2+4bc)/4) + (bk(d^2+4bc)/4) + (ck(d^2+4bc)/4) + bce - bck + bek + cek - a^2d^2k^2 - (b^2d^2k^2/4) - a^2e(d^2+4bc) - (b^2e(d^2+4bc)/4) - (ce\sqrt{d^2+4bc}/2) + a^2k(d^2+4bc) + (ak\sqrt[3/2]{d^2+4bc}/2) + (b^2k(d^2+4bc)/4) - (bk\sqrt[3/2]{d^2+4bc}/4) - (ek\sqrt{d^2+4bc}/2) - (3ad^2e/2) + (3bd^2e/4) + bck^4 + (3ad^3k/4) - (3bd^3k/8) - 2ade\sqrt{d^2+4bc} + bde\sqrt{d^2+4bc} + abk^2(d^2+4bc) + (3bdk\sqrt{d^2+4bc}/4) + (cdk\sqrt{d^2+4bc}/4) + abd^2e - abd^2k - 2a^2de\sqrt{d^2+4bc} - (b^2de\sqrt{d^2+4bc}/2)(7ad^2k\sqrt{d^2+4bc}/4) + 2a^2dk\sqrt{d^2+4bc} - (7bd^2k\sqrt{d^2+4bc}/8) + (b^2dk\sqrt{d^2+4bc}/2) + abd^2k^2 + abe(d^2+4bc) - abk(d^2+4bc) + (3adk(d^2+4bc)/2) - (3bdk(d^2+4bc)/4) - 2a^2dk^2\sqrt{d^2+4bc} - (b^2dk^2\sqrt{d^2+4bc}/2) + 2abde\sqrt{d^2+4bc} - 2abdk\sqrt{d^2+4bc} + 2abdk^2\sqrt{d^2+4bc}$.

When

$$a = 1, \quad b = 12, \quad c = 5, \quad d = 0.06, \quad e = 0.1, \tag{19}$$

the system is chaotic, and the conditions for the local stability of equilibrium are as follows:

$$H(1) = (m_1),$$

$$H(2) = \begin{pmatrix} m_1 & 1 \\ m_3 & m_2 \end{pmatrix},$$

$$H(3) = \begin{pmatrix} m_1 & 1 & 0 \\ m_3 & m_2 & m_1 \\ 0 & m_4 & m_3 \end{pmatrix}, \tag{20}$$

$$H(4) = \begin{pmatrix} m_1 & 1 & 0 & 0 \\ m_3 & m_2 & m_1 & 1 \\ 0 & m_4 & m_3 & m_2 \\ 0 & 0 & 0 & m_4 \end{pmatrix}.$$

For (20), they must satisfy $\det H_j > 0$ $(j = 1, 2, 3, 4)$, and then we get

$$\det H_1 = m_1 > 0,$$

$$\det H_2 = m_1m_2 - m_3 > 0,$$

$$\det H_3 = m_1m_2m_3 - m_3^2 - m_1^2m_4 > 0, \tag{21}$$

$$\det H_4 = m_4\left(m_1m_2m_3 - m_3^2 - m_1^2m_4\right) > 0.$$

And we can obtain the conditions for the local stability of equilibrium:

$$m_1 > 0,$$

$$m_1m_2 - m_3 > 0,$$

$$m_4 > 0, \tag{22}$$

$$m_1m_2m_3 > m_3^2 + m_1^2m_4,$$

where

$$\begin{aligned} m_1 &= 4k + 16 + 4k + 16; \\ m_2 &= 6k^2 + 48k + 104.032736; \\ m_3 &= 4k^3 + 48k^2 + 208.065472k + 1980.465427712; \\ m_4 &= k^4 + 16k^3 + 104.032736k^2 \\ &\quad + 1980.465427712k + 9.934656. \end{aligned} \tag{23}$$

Then, according to the condition of Routh-Hurwitz criteria, the local stability of equilibrium point $E2$ can be gained as follows:

$$\begin{aligned} &4k + 16 + 4k + 16 > 0, \\ &(4k16 + 4k + 16) \times \left(6k^2 + 48k + 104.032736\right) \\ &\quad - \left(4k^3 + 48k^2 + 208.065472k + 1980.465427712\right) > 0, \\ &k^4 + 16k^3 + 104.032736k^2 + 1980.465427712k \\ &\quad + 9.934656 > 0, \\ &(4k + 16 + 4k + 16) \times \left(6k^2 + 48k + 104.032736\right) \\ &\quad \times \left(4k^3 + 48k^2 + 208.065472k + 1980.465427712\right) \\ &\quad > \left(4k^3 + 48k^2 + 208.065472k + 1980.465427712\right)^2 \\ &\quad + (4k + 16 + 4k + 16)^2 \\ &\quad \times \left(k^4 + 16k^3 + 104.032736k^2 + 1980.465427712k \right. \\ &\quad \left. + 9.934656\right). \end{aligned} \tag{24}$$

When the control gain $k = 80$ is chosen in the system, the corresponding four characteristic values are

$$\begin{aligned} \lambda_1 &= -1.6493, \qquad \lambda_2 = -0.1066, \\ \lambda_3 &= -0.8021 + 0.0022i, \qquad \lambda_4 = -0.8021 - 0.0022i. \end{aligned} \tag{25}$$

Obviously, the equilibrium point $E2$ in chaotic state is driven into a steady state, and the goal of chaos control is realized.

Similarly, when

$$\begin{aligned} a &= 1, \qquad b = 12, \qquad c = 50, \\ d &= 0.06, \qquad e = 0.9, \end{aligned} \tag{26}$$

the system is in the hyperchaotic state. When $k = 120$ is in the hyperchaotic system, the eigenvalues are

$$\begin{aligned} \lambda_1 &= -392.5879, \qquad \lambda_2 = 94.9760, \\ \lambda_3 &= -123.1185, \qquad \lambda_4 = -120.2696. \end{aligned} \tag{27}$$

Obviously λ_2 is the positive real number, and the rest three are negative real numbers. Thus, we can get the result that the hyperchaotic system undergoes a Hopf bifurcation at the equilibrium $E2$.

When $k = 216$, we get the eigenvalues according to the equilibrium point $E2$:

$$\begin{aligned} \lambda_1 &= -488.5879, \qquad \lambda_2 = -1.0240, \\ \lambda_3 &= -219.1185, \qquad \lambda_4 = -216.2696. \end{aligned} \tag{28}$$

Here, λ_1, λ_2, λ_3, and λ_4 are negative real numbers, so the hyperchaotic system is restored into a steady state.

It is found that the controller gain k can suppress the chaotic behavior to a steady state. Furthermore, hyperchaotic behavior can also be driven to a steady state or chaos or a periodic orbit because of a linear feedback control.

It draws conclusions that it shows a positive correlation between the degree of stability of the system and the value of the linear controller gain k. The larger the value of the linear controller gain k, the lower the degree of complexity of the system. It means that the new four-dimensional system tends to undergo towards the direction of a steady state. When the value of controller gain k increases to a certain value, the hyperchaotic system reaches a steady state. The larger the value of controller gain k, the higher the performance of the stability of the system. Within certain parameters, $a = 1$, $b = 12$, $c = 5$, $d = 0.06$, and $e = 0.1$, the system is chaotic, and the controller gain $k = 80$ can drive the system to reach a steady state; when $a = 1$, $b = 12$, $c = 50$, $d = 0.06$, and $e = 0.9$, the system is hyperchaotic, and at this time the controller gain $k = 216$ can achieve the goal of making the original system to a steady state. The conclusion can be proved once again; the hyperchaos appears much more complex than chaos, and we need to increase the value of controller gain k to achieve the goal of making the system in a steady state. For the other systems which generate chaos or hyperchaos, the hyperchaotic controller designed in this paper indicates that this is a simple and feasible way to control and adjust parameters when hyperchaotic or chaotic phenomenon happens in the dynamic system.

There is also a problem that we should pay attention to regarding chaos control, because the chosen control gain k is difficult in the practice. Generally, we could analyze the equilibrium point and the stability of the chaotic or hyperchaotic system then map out the bifurcation diagram and calculate the Lyapunov exponents nearby the equilibrium point. At last, we get the coefficient control gain k. In this paper, we give Table 1 to express the values of control gain k to help us select a suitable controlled value as fast as possible in practice. Table 1 is control tag.

Besides this, there are other methods for chaos control, such as frequency master method, the dynamics state feedback control, period-doubling bifurcation control, and neural network control, so we can choose proper control method according to our needs.

6. Conclusion

A system designed via state feedback control is proposed, and the corresponding complex dynamic characteristics are analyzed by exhibiting bifurcation diagrams, Lyapunov

Table 1: Control tag.

Chaos: k	1	2	3	4
20	0.4934	−1.0493	$-0.2021 + 0.0022i$	$-0.2021 - 0.0022i$
40	0.2934	−1.2493	$-0.4021 + 0.0022i$	$-0.4021 - 0.0022i$
60	0.0934	−1.4493	$-0.6021 + 0.0022i$	$-0.6021 - 0.0022i$
80	−0.1066	−1.6493	$-0.8021 + 0.0022i$	$-0.8021 - 0.0022i$
100	−0.3066	−1.8493	$-1.0021 + 0.0022i$	$-1.0021 - 0.0022i$
120	−0.5066	−2.0493	$-1.2021 + 0.0022i$	$-1.2021 - 0.0022i$
140	−0.7066	−2.2493	$-1.4021 + 0.0022i$	$-1.4021 - 0.0022i$
160	−0.9066	−2.4493	$-1.6021 + 0.0022i$	$-1.6021 - 0.0022i$
180	−1.1066	−2.6493	$-1.8021 + 0.0022i$	$-1.8021 - 0.0022i$
200	−1.3066	−2.8493	$-2.0021 + 0.0022i$	$-2.0021 - 0.0022i$
Hyperchaos	1	2	3	4
0.000001	214.9760	−0.2696	−3.1185	−272.5879
0.05	214.9260	−0.3196	−3.1685	−272.6379
0.5	214.4760	−0.7696	−3.6185	−273.0879
1	213.9760	−1.2696	−4.1185	−273.5879
2	212.9760	−2.2696	−5.1185	−274.5879
5	209.9760	−5.2696	−8.1185	−277.5879
10	204.9760	−10.2696	−13.1185	−282.5879
20	194.9760	−20.2696	−23.1185	−292.5879
40	174.9760	−40.2696	−43.1185	−312.5879
60	154.9760	−60.2696	−63.1185	−332.5879
80	134.9760	−80.2696	−83.1185	−352.5879
100	114.9760	−100.2696	−103.1185	−372.5879
120	94.9760	−120.2696	−123.1185	−392.5879
140	74.9760	−140.2696	−143.1185	−412.5879
160	54.9760	−160.2696	−163.1185	−432.5879
180	34.9760	−180.2696	−183.1185	−452.5879
200	14.9760	−200.2696	−203.1185	−472.5879
216	−1.0240	−216.2696	−219.1185	−488.5879
220	−5.0240	−220.2696	−223.1185	−492.5879
240	−25.0240	−240.2696	−243.1185	−512.5879

exponents, Lyapunov dimensions, attractors, the power spectrums, the time chart, and so on. On the basis of the detailed numerical simulation as well as the theoretical analysis, it is observed that the system can generate both chaos and hyperchaos, and the behaviors of the hyperchaos are much more complex and abundant than the chaos.

A simple and effective controller which not only can drive the chaotic system to a steady state but also restore the hyperchaotic system to a periodic orbit or an equilibrium point is presented. A linear feedback controller is used to achieve a second control to the system based on the state feedback at the first time introduced and analyzed by Wang.

The next step of this paper is to further analyze and explore the effect of a second control, and there are several brave imaginations for the following analysis:

(1) what the difference between the first control and the second control is to the system in the aspects of effect of complexity and whether there is economic sense in practice;

(2) whether the goal will be realized for maximizing the benefits when the first control and the second control coordinate with and use the advantages of each other, complementary advantages. For example, whether the second controller can play a key role in the process of chaos control or hyperchaos control and realize the control for the second time.

Acknowledgments

The author extends this sincere thanks and appreciation to the institutions and people who have worked collaboratively to see that the aims and objectives to complete this research are attained. The author seizes this opportunity to thank the National Nature Science Foundation of China (Grant no. 61273231).

References

[1] P. C. Rech, "Chaos and hyperchao sina hopfield neural network," *I Neurocomputing*, vol. 74, pp. 3361–3364, 2011.

[2] S. Y. Li, S. C. Huang, C. H. Yang, and Z. M. Ge, "Generating trichaos attractors with three positive Lyapunov exponents in new four order system via linear coupling," *Nonlinear Dynamics*, vol. 69, no. 3, pp. 805–816, 2012.

[3] K. P. Harikrishnan, R. Misra, and G. Ambika, "Revisiting the box counting algorithm for the correlation dimension analysis of hyperchaotic time series," *Communications in Nonlinear Science and Numerical Simulation*, vol. 17, no. 1, pp. 263–276, 2012.

[4] J. L. Kaplan and J. A. Yorke, "Chaotic behavior of multidimensional difference equations," in *Functional Differential Equations and Approximation of Fixed Points*, vol. 730 of *Lecture Notes in Mathematics*, pp. 204–227, Springer, Berlin, Germany, 1979.

[5] L. Feng and J. Yinlai, "Hopf bifurcation analysis and numerical simulation in a 4D-hyoerchaotic system," *Nonlinear Dynamics*, vol. 67, no. 4, pp. 2857–2864, 2012.

[6] E. N. Lörenz, "Deterministic nonperiodic flow," *Journal of the Atmospheric Sciences*, vol. 20, pp. 130–141, 1963.

[7] G. Chen and T. Ueta, "Yet another chaotic attractor," *International Journal of Bifurcation and Chaos in Applied Sciences and Engineering*, vol. 9, no. 7, pp. 1465–1466, 1999.

[8] J. L. Lü and G. Chen, "A new chaotic attractor coined," *International Journal of Bifurcation and Chaos in Applied Sciences and Engineering*, vol. 12, no. 3, pp. 659–661, 2002.

[9] L. Wang, "3-scroll and 4-scroll chaotic attractors generated from a new 3-D quadratic autonomous system," *Nonlinear Dynamics*, vol. 56, no. 4, pp. 453–462, 2009.

[10] L. Wang, "Yet another 3D quadratic autonomous system generating three-wing and four-wing chaotic attractors," *Chaos*, vol. 19, no. 1, Article ID 013107, 6 pages, 2009.

[11] J. H. Ma and Q. Gao, "Stability and Hopf bifurcations in a business cycle model with delay," *Applied Mathematics and Computation*, vol. 215, no. 2, pp. 829–834, 2009.

[12] J. H. Ma and Q. Gao, "Analysis on the chaotic motion of a stochastic nonlinear dynamic system," *International Journal of Computer Mathematics*, vol. 87, no. 14, pp. 3266–3272, 2010.

[13] B. G. Xin, J. H. Ma, and Q. Gao, "Complex dynamics of an adnascent-type game model," *Discrete Dynamics in Nature and Society*, vol. 2008, Article ID 467972, 12 pages, 2008.

[14] C. C. Yang, "One input control of exponential synchronization for a four-dimensional chaotic system," *Applied Mathematics and Computation*, vol. 219, no. 10, pp. 5152–5161, 2013.

[15] X. Wang, B. Xu, and G. Luo, "Anasynchronous communication system based on the hyperchaotic system of 6th-order cellular neuralnetwork," *Optics Communications*, vol. 285, pp. 5401–5405, 2012.

[16] M. J. Correia and P. C. Rech, "Hyperchaotic states in the parameter-space," *Applied Mathematics and Computation*, vol. 218, no. 12, pp. 6711–6715, 2012.

[17] S. R. Choudhury and R. A. van Gorder, "Competitive modes as reliable predictors of chaos versus hyperchaos and as geometric mappings accurately delimiting attractors," *Nonlinear Dynamics*, vol. 69, no. 4, pp. 2255–2267, 2012.

[18] S. Yu and G. R. Chen, "Anti-control of continuous-time dynamical systems," *Communications in Nonlinear Science and Numerical Simulation*, vol. 17, no. 6, pp. 2617–2627, 2012.

[19] P. Yu and M. Han, "Bifurcation of limit cycles in 3rd-order Z2 Hamiltonian planar vector fields with 3rd-order perturbations," *Communications in Nonlinear Science and Numerical Simulation*, vol. 18, no. 4, pp. 978–988, 2013.

[20] K. Sun, X. Liu, C. Zhu, and J. C. Sprott, "Hyperchaos and hyperchaos control of the sinusoidally forced simplified Lorenz system," *Nonlinear Dynamics*, vol. 69, no. 3, pp. 1383–1391, 2012.

[21] H. Yu, G. Cai, and Y. Li, "Dynamic analysis and control of a new hyperchaotic finance system," *Nonlinear Dynamics*, vol. 67, no. 3, pp. 2171–2182, 2012.

[22] W. Wu, Z. Chen, and Z. Yuan, "The evolution of a novel four-dimensional autonomous system: among 3-torus, limit cycle, 2-torus, chaos and hyperchaos," *Chaos, Solitons and Fractals*, vol. 39, pp. 2340–2356, 2009.

[23] Z. Wang, S. Cang, E. O. Ochola, and Y. Sun, "A hyperchaotic system without equilibrium," *Nonlinear Dynamics*, vol. 69, no. 1-2, pp. 531–537, 2012.

[24] M. Sekikawa, N. Inaba, T. Tsubouchi, and K. Aihara, "Novel bifurcation structure generated in piecewise-linear three-LC resonant circuit and its Lyapunov analysis," *Physica D*, vol. 241, pp. 1169–1178, 2012.

Hindawi Publishing Corporation
Discrete Dynamics in Nature and Society
Volume 2013, Article ID 916978, 10 pages
http://dx.doi.org/10.1155/2013/916978

Research Article

Heuristic for Stochastic Online Flowshop Problem with Preemption Penalties

Mohammad Bayat, Mehdi Heydari, and Mohammad Mahdavi Mazdeh

Department of Industrial Engineering, Iran University of Science and Technology, Tehran 17347-93138, Iran

Correspondence should be addressed to Mohammad Bayat; mohammadbayat@iust.ac.ir

Received 20 May 2013; Accepted 26 August 2013

Academic Editor: Oswaldo Luiz do Valle Costa

Copyright © 2013 Mohammad Bayat et al. This is an open access article distributed under the Creative Commons Attribution License, which permits unrestricted use, distribution, and reproduction in any medium, provided the original work is properly cited.

The deterministic flowshop model is one of the most widely studied problems; whereas its stochastic equivalent has remained a challenge. Furthermore, the preemptive online stochastic flowshop problem has received much less attention, and most of the previous researches have considered a nonpreemptive version. Moreover, little attention has been devoted to the problems where a certain time penalty is incurred when preemption is allowed. This paper examines the preemptive stochastic online flowshop with the objective of minimizing the expected makespan. All the jobs arrive overtime, which means that the existence and the parameters of each job are unknown until its release date. The processing time of the jobs is stochastic and actual processing time is unknown until completion of the job. A heuristic procedure for this problem is presented, which is applicable whenever the job processing times are characterized by their means and standard deviation. The performance of the proposed heuristic method is explored using some numerical examples.

1. Introduction

The stochastic flowshop problems have not penetrated very far and remain challenging. The stochastic two-machine flowshop problem is inherently more complex than its deterministic counterpart. This complexity is much more when the preemptive online version of the problem is considered. In other words, the jobs are allowed to be preempted and restarted. We assume that preemption can occurr only on machine 1 in the flowshop problem. Moreover, all the jobs arrive overtime, which indicates that the existence and the parameters of each job are unknown until its release date. In the previous stochastic studies, preemptions are usually assumed to be "free" which means that each job can be preempted at any point of time and resumed later without incurring a penalty. However, this is not usually the case in practice. In many cases, such as melting furnaces, the time that has been spent before the preemption on a job is lost and considered as the preemption penalty.

Scheduling has become a well-studied problem and there are literally tremendous efforts on providing solution strategies for various kinds of modeling formulations such as job shop and flowshop. There are literally many applications for flowshop problem (e.g., Defersha and Chen [1]; Mahavi et al. [2]; Braglia et al. [3]). Two-machine flowshop problem with makespan objective function and deterministic processing time can be optimally solved by Johnson's rule [4]. This problem would be NP-hard if it consists of three or more machines [5]. Therefore, numerous heuristic algorithms have been presented for solving such problems in various studies. Framinan et al. have reviewed some of these articles [6]. Ruiz and Maroto referred to 53 articles on the heuristics presented for minimizing makespan in permutation flowshop problem [7].

In the stochastic flowshop problem, the processing time is a random variable. This simple difference leads to many complexities in stochastic problems. Makino developed a sequencing rule to find the schedule that minimizes the expected makespan in a flowshop problem with two jobs and exponentially distributed processing time [8]. Frostig and Adiri investigated three-machine flowshop stochastic scheduling with an objective of minimizing distribution of schedule length [9]. Sethi et al. offered feedback production planning in a stochastic two-machine flowshop based on asymptotic analysis and computational results [10]. Elmaghraby and Thoney

studied the two-machine stochastic flowshop problem with arbitrary processing time distributions [11]. In the stochastic flowshop problem with two machines and exponential processing times, the expected makespan value would be minimized in the case that the jobs are sorted nonincreasingly in terms of parameter $(1/\mu_{i1} - 1/\mu_{i2})$. This method was proposed by Talwar and is known as Talwar's Rule [12]. Later, Cunningham and Dutta proved its optimality [13]. Ku and Niu obtained a sufficient condition for stochastic dominance and showed that Talwar's Rule yields a stochastically minimal makespan [14]. Soroush and Allahverdi presented a stochastic two-machine flowshop scheduling problem with total completion time criterion [15]. Laha and Chakraborty presented an efficient stochastic hybrid heuristic for flowshop scheduling [16]. Portougal and Trietsch applied Johnson's Rule to stochastic problems [17]. They utilized, mean of the processing time of each job as its processing time in Johnson's Rule. Moreover, Kalczynski and Kamburowski applied Talwar's Rule for Weibull distribution [18]. Baker and Altheimer used three heuristic methods for the flowshop problem with m machines, supposing general distributions for processing times. They investigated the performance of these methods in a set of problems using simulation and noticed that these methods had near-optimal performance [19]. Baker and Trietsch also explored three heuristic methods for the two-machine stochastic model with a general distribution function. They compared Johnson's Heuristic method and Talwar's Heuristic method (applying mean of the processing time instead of job processing time in these two methods) and also the heuristic method of changing neighboring pairs (two neighboring jobs are separately considered and are displaced if their order can be optimized) and figured out that none of these methods dominate the other [20]. Heydari et al. proposed a heuristic method for minimization of expected value of the total weighted completion time in single machine problem with preemption penalties [21]. In this paper, the heuristic proposed by Baker and Trietsch has been applied for sequencing the jobs which are present in the shop.

In spite of the various studies in the last decades, a considerable research has not been performed on preemptive online flowshop problems with stochastic processing times. In this paper, a heuristic method to this problem is presented. The logic applied in this research is emphasizing on minimizing idling times in the second machine. In this method, decision about the preemption of one job at arrival of a new job is made based on the idling time produced in the second machine. In this research, we assume that the processing time is a random variable with normal distribution, and processing times of different jobs are independent from each other.

The remainder of this paper is organized as follows: research assumptions and definitions are presented in Section 2. In Sections 3 and 4, nonpreemptive and preemptive stochastic models are reviewed. Then, the proposed heuristic method is presented in Section 5. In Section 6, a numerical example has been solved with the proposed algorithm. The performance analysis of the proposed heuristic method is presented in Section 7. Finally, the conclusions are discussed in the last section.

2. Research Assumptions and Definitions

In the stochastic case, t_{ip} is used to denote (random) processing time of job i on machine p, but we retain $E(t_{ij})$ to represent its expected value. And, r_i is the release time of job i, which can only be known right on or after r_i. The processing time of each job is a random variable with normal distribution $t_{ip} \sim N(\mu_{ip}, \sigma_{ip}^2)$ and jobs are independent of each other. Our objective is to find a schedule to minimize the expected makespan. The applied symbols are as follows:

t_{ip}: processing time of job i on machine p.

μ_{ip}: mean of processing time of job i on machine p.

σ_{ip}^2: variance of processing time of job i on machine p.

I_i: idle time of the second machine from completing the job $i-1$ until starting the job i.

The considered assumptions in this article are as follows:

(i) Machines have constant speed that cannot be varied.

(ii) The order of processing the jobs is the same on the first and second machines.

(iii) Machines are ready to be utilized at zero time.

(iv) Every machine can operate at most one job at a time.

(v) Initiation of any job on the second machine would be after completion of the job on the first machine.

(vi) Preemption of the jobs can be occurred only on machine 1.

We consider the preemption-repeat model in which the job currently being processed may be preempted at any point of time. However, by preempting a job, all the ongoing progress is considered to be lost. Therefore, if the job is restarted at some later moment in time, then it has to be processed from the beginning.

3. Nonpreemptive Stochastic Flowshop Problem

For general distributions without any special conditions on processing times, only one thorough solution is known for the stochastic flowshop problem, proposed by Makino [8].

Theorem 1. *In the two-machine stochastic flowshop problem with two jobs, job i precedes job j in an optimal sequence if*

$$E\left(\min\left\{t_{i1}, t_{j2}\right\}\right) \leq E\left(\min\left\{t_{i2}, t_{j1}\right\}\right). \tag{1}$$

Based on Theorem 1, Baker and Trietsch proposed a method that uses the properties of an adjacent pair wise interchange (API) [20]. They assume that the processing times are random variables with normal distribution. In this method, the condition for job i to precede job j takes the following form:

$$\begin{aligned}\mu_{i1} - \sigma_{i1j2}\left[\phi\left(z_{i1j2}\right) + z_{i1j2}\cdot\Phi\left(z_{i1j2}\right)\right] \\ \leq \mu_{i2} - \sigma_{i2j1}\left[\phi\left(z_{i2j1}\right) + z_{i1j2}\cdot\Phi\left(z_{i2j1}\right)\right].\end{aligned} \tag{2}$$

This form of the API procedure uses the properties of normal distributions and is called the API Heuristic. In this method, the expected minimum of two variables with normal distribution is given by

$$E\left[\min\left\{X,Y\right\}\right] = \mu_X - \sigma_{XY}\left[\phi\left(z_{XY}\right) + z_{XY}\cdot\Phi\left(z_{XY}\right)\right], \quad (3)$$

where ϕ and Φ denote the density function and the cdf of the standard normal. In addition, $\mu_{XY} = \mu_X - \mu_Y$ and $\sigma_{XY}^2 = \sigma_X^2 + \sigma_Y^2$ and $z_{XY} = \mu_{XY}/\sigma_{XY}$ [22]. In this paper, for sequencing the jobs present at the shop, this heuristic method has been utilized.

4. Preemptive Stochastic Flowshop Problem

Since the objective function of this study is expected makespan minimization, and considering the fact that makespan increase is due to increase in idling time in the second machine, this paper focused on minimizing the sum of expected idling times of the second machine.

As shown in Figure 1 the value of makespan is as follows:

$$\begin{aligned} C_{\max} &= \sum_{i=1}^{n} I_i + \sum_{i=1}^{n} t_{i2} \\ &\Longrightarrow E\left[C_{\max}\right] = E\left[\sum_{i=1}^{n} I_i\right] + E\left[\sum_{i=1}^{n} t_{i2}\right], \end{aligned} \quad (4)$$

where I_i is the idling time of machine 2 before the starting of job i. Science the value of $E[\sum_{i=1}^{n} t_{i2}]$ is constant; minimizing $E[\sum_{i=1}^{n} I_i]$ leads to minimum value of makespan. Idling time of machine 2 is as follows:

$$\begin{aligned} &I_1 = t_{11}, \\ &I_2 = \max\left\{0, t_{11} + t_{21} - t_{12} - I_1\right\}, \\ &I_2 = \max\left\{0, t_{11} + t_{21} + t_{31} - t_{12} - t_{22} - I_1 - I_2\right\}, \\ &\quad\vdots \\ &I_k = \max\left\{0, \sum_{i=1}^{k} t_{i1} - \sum_{i=1}^{k-1} t_{i2} - \sum_{i=1}^{k-1} I_i\right\}. \end{aligned} \quad (5)$$

Thus, the total idle time of the second machine will be computed as follows:

$$\begin{aligned} &I_1 + I_2 = \max\left\{t_{11}, t_{11} + t_{21} - t_{12}\right\}, \\ &I_1 + I_2 + I_3 = \max\left\{t_{11}, t_{11} + t_{21} - t_{12}, \right. \\ &\qquad\qquad \left. t_{11} + t_{21} + t_{31} - t_{12} - t_{22}\right\}, \\ &\vdots \\ &\Longrightarrow \sum_{i=1}^{n} I_i = \max\left[t_{11}, \max_{2\le k\le n}\left\{\sum_{i=1}^{k} t_{i1} - \sum_{i=1}^{k-1} t_{i2}\right\}\right]. \end{aligned} \quad (6)$$

Assume that

$$U_k = \sum_{i=1}^{k} t_{i1} - \sum_{i=1}^{k-1} t_{i2}. \quad (7)$$

Therefore, the sum of idling times of machine 2 is given by

$$\sum_{i=1}^{n} I_i = \max_{1\le k\le n}\left(U_k\right). \quad (8)$$

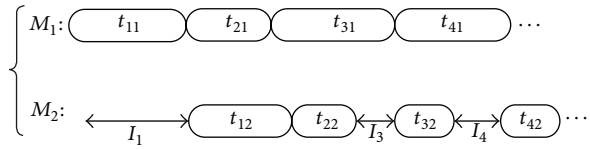

Figure 1: Two machine flowshop problem.

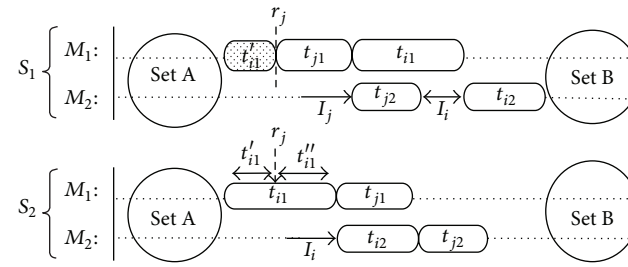

Figure 2: Schedules S_1 and S_2 at arrival of job j in preemption-repeat mode.

In the two-machine stochastic online flowshop problem, if in schedule 1 (S_1) job i precedes job j and in schedule 2 (S_2), these two jobs are replaced, then $E(C_{\max}^{S_1}) \le E(C_{\max}^{S_2})$ if

$$E\left[\max_{1\le k\le n}\left\{U_k\left(S_1\right)\right\}\right] \le E\left[\max_{1\le k\le n}\left\{U_k\left(S_2\right)\right\}\right], \quad (9)$$

where $E[\max_{1\le k\le n}\{U_k(S_1)\}]$ and $E[\max_{1\le k\le n}\{U_k(S_2)\}]$ are the expected values of the sum of idling time on machine 2 in schedule 1 and 2.

As mentioned before, minimizing the expected value of total idling time in machine 2 leads to expected makespan minimization. Since the expected value of makespan in S_1 is less than its value in S_2, the idle time of machine 2 in S_1 will be less than its value in S_2.

In preemptive online problem, assume that job i with processing time t_{i1} is being processed on machine 1. Let t''_{i1} be the remaining processing time of job i and the time spent for processing of job i is t'_{i1}. Therefore, we have

$$t_{i1} = t'_{i1} + t''_{i1}. \quad (10)$$

Suppose that the new job j with the processing time t_{jp} and the release time r_j arrives at the shop (Figure 2). The new job j becomes known at its release time.

Let A be the subset of completed jobs on machine 1 and B the subset of uncompleted jobs. First, the priority of job j is determined with the API heuristic method. If the priority of job j is more than the job i then one of the two S_1 and S_2 schedules would occur as shown in Figure 2; otherwise, it will be added to list of uncompleted jobs. In S_1 job i is preempted because of the higher priority for job j, but in S_2 job j will be processed after completion of job i. As mentioned before,

total idle time of machine 2 until start of job i and j in S_1 and S_2 schedules is as follows:

$$\begin{aligned} U_j(S_1) &= \sum_{h\in A} t_{h1} + t'_{i1} + t_{j1} - \sum_{h\in A} t_{h2}, \\ U_{i'}(S_1) &= \sum_{h\in A} t_{h1} + t'_{i1} - \sum_{h\in A} t_{h2}, \\ U_i(S_1) &= \sum_{h\in A} t_{h1} + t'_{i1} + t_{j1} + t_{i1} - t_{j2} - \sum_{h\in A} t_{h2}, \\ U_i(S_2) &= \sum_{h\in A} t_{h1} + t_{i1} - \sum_{h\in A} t_{h2}, \\ U_j(S_2) &= \sum_{h\in A} t_{h1} + t_{i1} + t_{j1} - t_{i2} - \sum_{h\in A} t_{h2}. \end{aligned} \tag{11}$$

Therefore, the expected value of makespan in S_1 is less than its value in S_2 and preemption will occur if

$$\begin{aligned} & E\left[\max\left\{U_{i'}(S_1), U_j(S_1), U_i(S_1)\right\}\right] \\ & < E\left[\max\left\{U_i(S_2), U_j(S_2)\right\}\right] \\ & \xrightarrow{U_j(S_1)>U_{i'}(S_1)} E\left[\max\left\{U_j(S_1), U_i(S_1)\right\}\right] \\ & < E\left[\max\left\{U_i(S_2), U_j(S_2)\right\}\right] \\ & \Longrightarrow E\left[\min\left\{-U_j(S_1), -U_i(S_1)\right\}\right] \\ & > E\left[\min\left\{-U_j(S_2), -U_i(S_2)\right\}\right]. \end{aligned} \tag{12}$$

The processing of the jobs in the subset A has been completed on machine 1, and their total processing time is a constant value. Thus, we assume that

$$\sum_{h\in A} t_{h1} = \lambda, \tag{13}$$

where λ is a constant value. Some of the jobs in the subset A have been completed and some of them have not been completed until time r_j. Let A' be the subset of completed jobs on machine 2, and let A'' be the subset of uncompleted jobs on this machine. Thus,

$$\begin{aligned} A' \cup A'' &= A, \\ \sum_{h\in A} t_{h2} &= \sum_{h\in A'} t_{h2} + \sum_{h\in A''} t_{h2}. \end{aligned} \tag{14}$$

Therefore, $\sum_{h\in A'} t_{h2}$ is constant value $\sum_{h\in A''} t_{h2}$ is a random variable with normal distribution

$$\begin{aligned} \sum_{h\in A'} t_{h2} &= \beta, \\ \sum_{h\in A''} t_{h2} &\sim N\left(\sum_{h\in A''} \mu_{h2}, \sum_{h\in A''} \sigma^2_{h2}\right), \end{aligned} \tag{15}$$

where β is a constant value. Hence, $U_j(S_1)$ and $U_i(S_1)$ are random variables with normal distribution and the following means and variances:

$$\begin{aligned} U_j(S_1) &\sim N\left(\lambda - \beta + t'_{i1} - \sum_{h\in A''} \mu_{h2} + \mu_{j1}, \sigma^2_{j1} + \sum_{h\in A''} \sigma^2_{h2}\right), \\ U_i(S_1) &= N\left(\lambda - \beta + t'_{i1} - \sum_{h\in A''} \mu_{h2} + \mu_{j1} + \mu_{i1} \right. \\ &\qquad \left. -\mu_{j2}, \sigma^2_{j1} + \sigma^2_{i1} + \sigma^2_{j2} + \sum_{h\in A''} \sigma^2_{h2}\right). \end{aligned} \tag{16}$$

In addition, for $U_j(S_2)$ and $U_i(S_2)$ we have

$$\begin{aligned} U_i(S_2) &= N\left(\lambda - \beta - \sum_{h\in A''} \mu_{h2} + \mu_{i1}, \sigma^2_{i1} + \sum_{h\in A''} \sigma^2_{h2}\right), \\ U_j(S_2) &= N\left(\lambda - \beta - \sum_{h\in A''} \mu_{h2} + \mu_{i1} + \mu_{j1} - \mu_{i2}, \right. \\ &\qquad \left. \sigma^2_{i1} + \sigma^2_{j1} + \sigma^2_{i2} + \sum_{h\in A''} \sigma^2_{h2}\right). \end{aligned} \tag{17}$$

In order for decision making about preemption, the following inequality should be explored:

$$\begin{aligned} & E\left[\min\left\{-U_j(S_1), -U_i(S_1)\right\}\right] \\ & > E\left[\min\left\{-U_j(S_2), -U_i(S_2)\right\}\right]. \end{aligned} \tag{18}$$

Assume that

$$\begin{aligned} X &= -U_j(S_1), \\ Y &= -U_i(S_1), \\ X' &= -U_i(S_2), \\ Y' &= -U_j(S_2). \end{aligned} \tag{19}$$

The expected minimum of two variables with normal distribution is calculated as discussed before. Thus, for computation of $E[\min\{X, Y\}]$ we have

$$\begin{aligned} \mu_X &= -\lambda + \beta - t'_{i1} + \sum_{h\in A''} \mu_{h2} - \mu_{j1}, \\ \mu_{XY} &= \mu_{i1} - \mu_{j2}, \\ \sigma^2_{XY} &= 2\sigma^2_{j1} + \sigma^2_{i1} + \sigma^2_{j2} + 2\sum_{h\in A''} \sigma^2_{h2}, \\ z_{XY} &= \frac{\mu_{XY}}{\sigma_{XY}} \\ &\Longrightarrow E[\min\{X, Y\}] \\ &= \mu_X - \sigma_{XY}\left[\phi(z_{XY}) + z_{XY}\cdot\Phi(z_{XY})\right], \end{aligned} \tag{20}$$

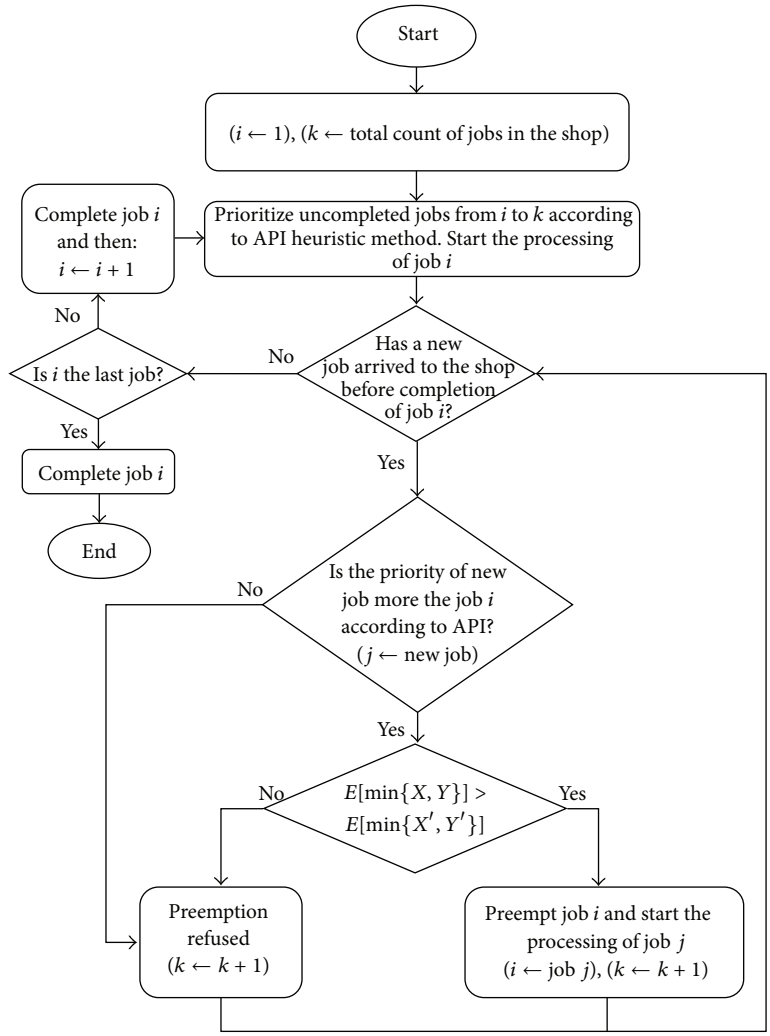

Figure 3: Proposed heuristic algorithm.

and $E[\min\{X', Y'\}]$ is as follows:

$$\begin{aligned}
\mu_{X'} &= -\lambda + \beta + \sum_{h \in A''} \mu_{h2} - \mu_{i1}, \\
\mu_{X'Y'} &= \mu_{j1} - \mu_{i2}, \\
\sigma^2_{X'Y'} &= 2\sigma^2_{i1} + \sigma^2_{j1} + \sigma^2_{i2} + 2 \sum_{h \in A''} \sigma^2_{h2}, \\
z_{X'Y'} &= \frac{\mu_{X'Y'}}{\sigma_{X'Y'}},
\end{aligned} \tag{21}$$

$$\begin{aligned}
&E\left[\min\left\{X', Y'\right\}\right] \\
&\quad = \mu_{X'} - \sigma_{X'Y'}\left[\phi\left(z_{X'Y'}\right) + z_{X'Y'} \cdot \Phi\left(z_{X'Y'}\right)\right].
\end{aligned}$$

Therefore, the preemption condition will be as presented in Lemma 2.

Lemma 2. *In the preemption-repeat stochastic online flowshop problem with two machines, job i will be preempted at arrival of job j (assuming that the job j priority is greater than the job i based on API) if and only if*

$$E\left[\min\left\{X, Y\right\}\right] > E\left[\min\left\{X', Y'\right\}\right]. \tag{22}$$

Proof. As mentioned before, by preemption of job i at arrival of job j the expected value of total idling time in machine 2 decreases if $E[\min\{X, Y\}] > E[\min\{X', Y'\}]$. □

5. Proposed Algorithm

In this section, a heuristic algorithm is proposed to minimize the expected value of makespan for the preemptive stochastic online flowshop problem with two machines. In addition, a schematic illustration of the algorithm is provided in Figure 3.

Step 0 (parameter definition). The parameter k denotes the total number of jobs in the shop and i is the job counter parameter whit the primary value of 1. Processing time of each job is a random variable with normal distribution.

Table 1: Specifications of jobs.

i	μ_{i1}	σ_{i1}	μ_{i2}	σ_{i2}	r_i
1	17	1.5	10	2.3	0
2	11	2	13	2.1	0
3	16	2	15	2.4	0
4	10	2.4	14	1.6	0
5	11	2.6	8	1.1	15
6	9	1.2	14	2	24

Arrival time of job i is denoted by r_i. Parameter j denotes the new job that arrives at the shop.

Step 1. Prioritize all uncompleted jobs with API heuristic method, from i to k.

Step 2. Process the job i until it is completed, or a new job arrives at the shop. If a new job arrives at the shop then assign index j to its characteristics and go to Step 4, otherwise go to next step.

Step 3. After completion of job i, if i is the last job then finish the algorithm; otherwise, increment the counter i by one and go to Step 1.

$$i \longleftarrow i + 1. \tag{23}$$

Step 4. If the priority of the new job according to API heuristic method is more than job i then follow the algorithm, otherwise go to Step 7.

Step 5. If $E[\min\{X, Y\}] > E[\min\{X', Y'\}]$ then go to next step, otherwise go to Step 7.

Step 6. The priority of job j is more than job i. Thus, job i will be preempted and job j will be preferred. And since then, the index i will be used for job j. Increment the counter k by one, and then go to Step 2.

$$\begin{aligned} k &\longleftarrow k + 1, \\ i &\longleftarrow \text{job } j. \end{aligned} \tag{24}$$

Step 7. Preemption is not allowed and the processing of job i will be continued. Increment the counter k by one, and then go to Step 2.

$$k \longleftarrow k + 1. \tag{25}$$

6. Numerical Example

In this section, the performance of the proposed algorithm is evaluated through a numerical example. Suppose a stochastic two-machine flowshop problem with 6 jobs and specifications given in Table 1.

In Table 1, r_i is arrival time of job i. Moreover, we assume that the actual processing time of a job on each machine is equal to its mean processing time on that machine. According the proposed algorithm, first, the jobs present at the shop at time zero should be scheduled with API heuristic method. We run the API algorithm by starting with the sequence 1-2-3-4. Table 2 shows the differences between $E[\min\{t_{i1}, t_{j2}\}]$ and $E[\min\{t_{i2}, t_{j1}\}]$ for these jobs, with job i corresponding to a row and j to a column. For instance, the calculation of $E[\min\{t_{11}, t_{22}\}]$ is as follows:

Table 2: Differences between $E[\min\{t_{i1}, t_{j2}\}]$ and $E[\min\{t_{i2}, t_{j1}\}]$.

i	j			
	1	2	3	4
1		3.7134	4.6283	5.2399
2	−3.7134		−1.9221	1.1447
3	−4.6283	1.9221		3.7873
4	−5.2399	−1.1447	−3.7873	

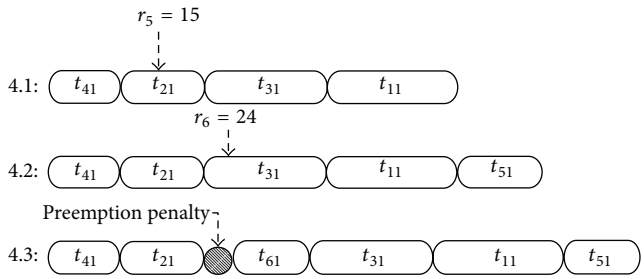

Figure 4: Scheduling a sample problem with proposed algorithm.

$$\begin{aligned} &E\left[\min\left\{t_{11}, t_{22}\right\}\right] \\ &\quad = \mu_{11} - \sigma_{(11)(22)}\left[\phi\left(z_{(11)(22)}\right) + z_{(11)(22)} \cdot \Phi\left(z_{(11)(22)}\right)\right], \\ &\qquad \mu_{11} = 17, \\ &\qquad \mu_{(11)(22)} = \mu_{11} - \mu_{12} = 17 - 13 = 4, \\ &\qquad \sigma^2_{(11)(22)} = \sigma^2_{11} + \sigma^2_{22} = 1.5^2 + 2.1^2 = 2.5807^2, \\ &\qquad z_{(11)(22)} = \frac{\mu_{(11)(22)}}{\sigma_{(11)(22)}} = 1.55, \\ &E\left[\min\left\{t_{11}, t_{22}\right\}\right] \\ &\quad = 17 - 2.5807\,[0.12 + 1.55 \times 0.9394] = 12.9326. \end{aligned} \tag{26}$$

Similarly, $E[\min\{t_{12}, t_{21}\}] = 9.2192$, and the first entry in Table 2 is the difference $12.9326 - 9.2192 = 3.7134$.

In Table 2, according to API method, negative values indicate stable sequences. For instance, 1-2 is not a stable sequence because the value of row 1 and column 2 is positive. Therefore, these two jobs should be substituted. Hence, API heuristic with altered order of the jobs yields the stable sequence 4-2-3-1 as shown in Figure 4 (4.1).

The machines will start to process the jobs according to the sequence 4-2-3-1. Job 5 with release time $r_5 = 15$ arrives at the shop as shown in Figure 4 (4.1). Job 2 is being processed at this time. According to API, The priority of job 5 is less than the priority of job 2 because if we schedule jobs 2, 5 with this

method, then the job 5 will has less priority. Thus, the preemption is not allowed. Processing of the jobs is continued and during the processing of job 3, job 6 with release time $r_6 = 24$ arrives to the shop as shown in Figure 4 (4.2). According to API, The priority of job 6 is more than the priority of job 3 at this time. Thus, the parameters at this time are as follows:

$$\begin{aligned} i &= 3, \\ i &\longleftarrow \text{job } 3, \\ j &\longleftarrow \text{job } 6, \\ t'_{31} &= 3. \end{aligned} \tag{27}$$

According to the proposed algorithm, satisfaction of the inequality $E[\min\{X, Y\}] > E[\min\{X', Y'\}]$ should be explored in order for decision making about the preemption:

$$\begin{aligned} \mu_X &= -\lambda + \beta - t'_{i1} + \sum_{h \in A''} \mu_{h2} - \mu_{j1} \\ &= -21 + 14 - 3 + 13 - 9 = -6, \\ \mu_{XY} &= \mu_{i1} - \mu_{j2} = 16 - 14 = 2, \\ \sigma^2_{XY} &= 2\sigma^2_{j1} + \sigma^2_{i1} + \sigma^2_{j2} + 2 \sum_{h \in A''} \sigma^2_{h2} \\ &= 2 \times 1.2^2 + 2^2 + 2^2 + 2 \times 2.1^2 = 4.4385^2, \\ z_{XY} &= \frac{\mu_{XY}}{\sigma_{XY}} = 0.4506 \\ &\Longrightarrow E[\min\{X, Y\}] \\ &= \mu_X - \sigma_{XY} [\phi(z_{XY}) + z_{XY} \cdot \Phi(z_{XY})] \\ &= -6 - 4.4385 (0.3604 + 0.4506 \times 0.6739) = -8.947. \end{aligned} \tag{28}$$

Similarly, $E[\min\{X', Y'\}] = -10.262$. Science $E[\min\{X, Y\}] > E[\min\{X', Y'\}]$, preemption is allowed. Job 3 will be preempted and job 6 will start. Consequently, the scheduling of jobs on machine 1 will be as shown in Figure 4 (4.3).

The computation of completion time of the jobs on machine 1 and 2 are provided in Table 3, where C_{ij} is the completion time of job i on machine.

As mentioned before, it is assumed that the actual processing time of the job is equal to the mean of processing time. Therefore, the expected value of makespan is equal to 85 for this example.

7. Performance Analysis

In order to evaluate the performance of the proposed algorithm, it was applied on a variety of problems with different sizes. Thus, 20,000 problems in 20 categories with different quantities for the number of jobs and the processing time specifications have been produced. The results are compared

Table 3: Completion time of jobs on machines 1 and 2.

i	R_{i1}	C_{i1}	R_{i2}	C_{i2}	r_i
4	10	10	14	24	0
2	11	21	13	37	0
6	9	33	14	51	25
3	16	49	15	66	0
1	17	66	10	76	0
5	11	77	8	85	15

to a lower bound of the optimum makespan that is defined as follows:

$$\begin{aligned} C^{\text{OPT}}_{\max} &\geq \max_{i \in \{1,2,3,\ldots,n\}} [r_i + E(t_{i1}) + E(t_{i2})], \\ C^{\text{OPT}}_{\max} &\geq \min_{i \in \{1,2,3,\ldots,n\}} [r_i + E(t_{i1})] + \sum_{i=1}^{n} E(t_{i2}), \\ C^{l}_{\max} &= \max \left\{ \max_{i \in \{1,2,3,\ldots,n\}} [r_i + E(t_{i1}) + E(t_{i2})], \right. \\ &\qquad \left. \min_{i \in \{1,2,3,\ldots,n\}} [r_i + E(t_{i1})] + \sum_{i=1}^{n} E(t_{i2}) \right\} \\ &\Longrightarrow C^{\text{OPT}}_{\max} \geq C^{l}_{\max}. \end{aligned} \tag{29}$$

Parameter ρ is the performance guarantee of the proposed method (MB) and called approximation factor if

$$C^{\text{MB}}_{\max} \leq \rho \times C^{l}_{\max} \Longrightarrow C^{\text{MB}}_{\max} \leq \rho \times C^{\text{OPT}}_{\max}, \tag{30}$$

where $C^{\text{MB}}_{\max}$ and $C^{\text{OPT}}_{\max}$ are the expected values of makespan that the MB method and an optimal method, respectively, achieve on each instance.

Other assumptions are as follows:

(1) Release dates are generated using uniform distribution within the interval [0, 1000].

(2) All jobs are preemption-restart.

(3) The actual processing time is assumed to be equal to the mean of processing time.

(4) We have produced 1000 problems for each category and based on the comparison between results of each method, the maximum value of factor ρ is calculated for these problems (worse case).

To compare the performance of the proposed method (MB) against OPT; first, the performance is analyzed with respect to the number of jobs which is varies from 10 to 100 and 10 categories are produced. The processing time follows a normal distribution. We assume that the mean of processing time and standard deviation of processing time are random values within the interval [10, 20] and [1, 3], respectively. Since the mean of processing time follows uniform distribution, the expected value of the processing time is $E(\mu_{ij}) = 15$. Table 4 and Figure 5 summarize the details of our implementations. Second and third columns of Table 4 are the mean of makespan for 1000 produced problems in each category. Whereas

Table 4: Makespan value of the proposed algorithm versus lower bound of optimum.

No. of jobs	$C_{max}^{MB} \times 10^{-3}$	$C_{max}^{OPT} \times 10^{-3}$	ρ_{max}
10	0.9316	0.9308	1.0225
20	0.9912	0.9874	1.0332
30	1.0039	0.9959	1.0476
40	1.0183	1.0046	1.0766
50	1.0361	1.0096	1.1394
60	1.0641	1.0129	1.1737
65	1.1054	1.0279	1.2209
70	1.1693	1.1016	1.1646
80	1.3257	1.2823	1.0901
90	1.496	1.4648	1.0718
100	1.6662	1.6367	1.0602

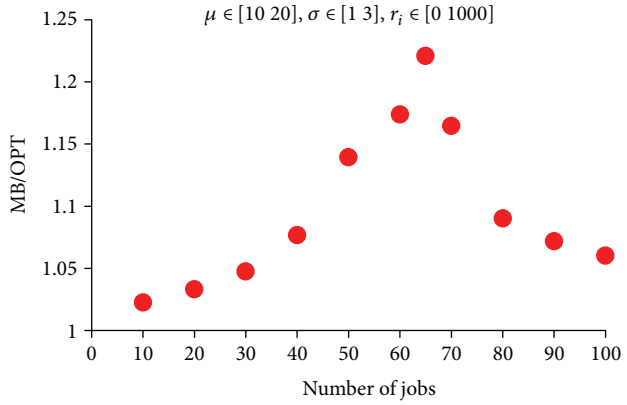

Figure 5: ρ versus the number of jobs.

Table 5: The performance of the proposed algorithm (MB) against OPT where the number of jobs is 25.

Mean of processing time	$C_{max}^{MB} \times 10^{-3}$	$C_{max}^{OPT} \times 10^{-3}$	ρ_{max}
[10 20]	0.9958	0.9907	1.0537
[10 30]	1.0156	1.0037	1.0874
[10 40]	1.0391	1.0151	1.1464
[10 50]	1.0783	1.0246	1.2579
[10 60]	1.1439	1.0365	1.3808
[10 70]	1.2466	1.0879	1.5433
[10 80]	1.3709	1.1847	1.5215
[10 90]	1.5226	1.3341	1.5087
[10 100]	1.6871	1.4994	1.4736
[10 110]	1.8537	1.6595	1.4653

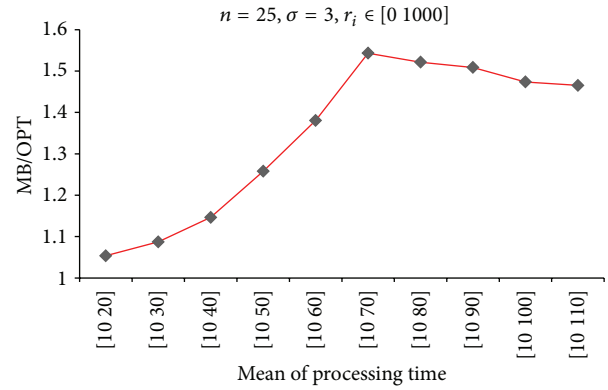

Figure 6: ρ versus mean of processing time.

the forth column is the maximum value of factor ρ among 1000 problems in each category. As can be observed, the proposed method (MB) performs up to 1.2209 times worse than the other one when number of jobs approaches 65. Note that when n extends beyond 65, the density of jobs will increase illogically and we have $n \times E(\mu_{ij}) > 1000$ while $r_i < 1000$. When the density of jobs increases illogically, the waiting time of jobs increases and the idle time of machine 2 decreases. Thus, the performance of proposed algorithm almost improves.

The performance of the proposed method has also been evaluated for different values of the mean of processing time. Ten categories have been produced and the number of jobs and the value of standard deviation have been fixed at constant values ($n = 25, \sigma = 3$). The results are shown in Table 5 and Figure 6. When the mean of processing time approaches to the interval [10, 70], the performance of the algorithm is in the worst condition because $n \times E(\mu_{ij})$ and $\max\{r_i\}$ are almost equal to 1000. For the next intervals, the density of jobs increase illogically and the idle time of machine 2 decrease. Hence, the performance of MB algorithm almost improves.

Moreover, the performance of the proposed method has been evaluated with respect to distribution of process times as the uniform distribution [1, 100] with the coefficient of variation being 0.05, 0.1, and 0.2. The number of jobs varies from 10 to 100, and ten categories have been produced. This mode of fixing the process-time distribution can yield better insight about the evaluation of computational performance of the algorithm. The processing times are generated using uniform distribution within the interval [1, 100]. It is assumed that the release dates are random values within the interval [0, 3000]. Taking into consideration the fact that the mean of processing time is uniformly distributed, the expected value of the processing time is $E(\mu_{ij}) = 50.5$. The details of implementations have been summarized in Table 6 and Figure 7. When n takes a value more than 60, an illogical increase will occur in the density of jobs and we have $n \times E(\mu_{ij}) > 3000$ while $r_i < 3000$. Hence, an increase is observed in the waiting time of jobs and the idle time of the second machine decreases. Therefore, the performance of the proposed algorithm improves.

8. Concluding Remarks

In this paper, preemptive stochastic online scheduling problem was investigated for two-machine flowshop. The objective function was minimizing the expected value of makespan. Inspired by Johnson's heuristic method for stochastic flowshop problem with an emphasis on minimal idle times of second machine, a heuristic method was presented.

Table 6: The performance of the proposed algorithm versus lower bound of optimum.

Coefficient of variation	0.05			0.1			0.2		
No. of jobs	$C_{\max}^{MB} \times 10^{-3}$	$C_{\max}^{OPT} \times 10^{-3}$	$\rho_{\max}$	$C_{\max}^{MB} \times 10^{-3}$	$C_{\max}^{OPT} \times 10^{-3}$	$\rho_{\max}$	$C_{\max}^{MB} \times 10^{-3}$	$C_{\max}^{OPT} \times 10^{-3}$	$\rho_{\max}$
10	2.7968	2.7897	1.0219	2.8459	2.8405	1.0254	2.8307	2.825	1.0227
20	2.964	2.9525	1.0326	2.9743	2.9622	1.0418	2.971	2.9589	1.0306
30	3.0341	3.007	1.0625	3.0188	2.989	1.0803	3.0386	3.0048	1.1078
40	3.0838	3.0329	1.0841	3.0749	3.0237	1.1027	3.0739	3.0203	1.1109
50	3.1526	3.0436	1.1444	3.1592	3.0535	1.1857	3.1721	3.046	1.1915
60	3.3512	3.1049	1.2379	3.3944	3.1656	1.2431	3.4213	3.1543	1.1947
70	3.7758	3.6411	1.1272	3.8438	3.7081	1.1174	3.8903	3.7421	1.1521
80	4.2539	4.1585	1.0656	4.3728	4.2702	1.079	4.4989	4.3706	1.0951
90	4.8665	4.6817	1.0641	4.8975	4.8162	1.0453	5.0656	4.9662	1.0567
100	5.2566	5.1918	1.0401	5.4189	5.3534	1.0376	5.6141	5.5313	1.0455

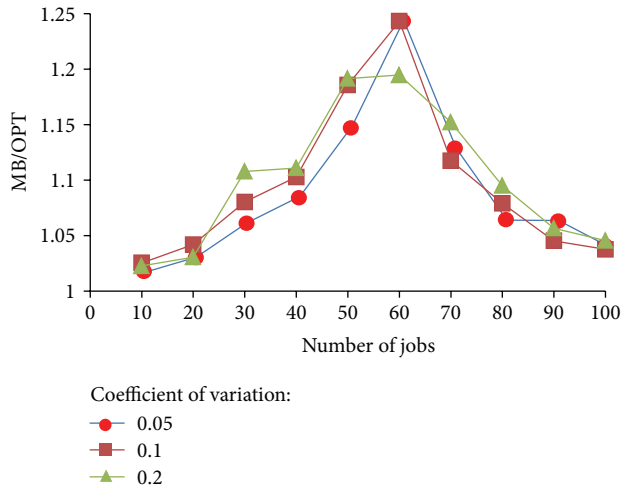

Figure 7: ρ versus the number of jobs and the coefficient of variation.

The implementation of the proposed method was demonstrated using a numerical example. The performance evaluation of the proposed method has been done with comparing to a lower bound of optimum. Primary results indicated that the proposed method had the approximation factor less than 2 for a wide range of problems. The proposed method utilized the properties of the normal distributions, and this method can be used as a heuristic method for other distributions, as long as their means and variances are available. Scheduling with preemption penalties is a novel research area in scheduling field especially for online stochastic problems and we strongly believe that this research could be well extended for problems with stochastic setup times, other distribution function for processing time, and flowshop problem with more than 2 machines.

References

[1] F. M. Defersha and M. Chen, "Mathematical model and parallel genetic algorithm for hybrid flexible flowshop lot streaming problem," *International Journal of Advanced Manufacturing Technology*, vol. 62, no. 1–4, pp. 249–265, 2012.

[2] M. Mahavi Mazdeh, F. Zaerpour, and F. Firouzi Jahantigh, "A fuzzy modeling for single machine scheduling problem with deteriorating jobs," *International Journal of Industrial Engineering Computations*, vol. 1, no. 2, pp. 147–156, 2010.

[3] M. Braglia, M. Frosolini, R. Gabbrielli, and F. Zammori, "CONWIP card setting in a flow-shop system with a batch production machine," *International Journal of Industrial Engineering Computations*, vol. 2, no. 1, pp. 1–18, 2011.

[4] S. M. Johnson, "Optimal two- and three-stage production schedules with setup times included," *Naval Research Logistics Quarterly*, vol. 1, no. 1, pp. 61–68, 1954.

[5] M. R. Garey, D. S. Johnson, and R. Sethi, "The complexity of flowshop and jobshop scheduling," *Mathematics of Operations Research*, vol. 1, no. 2, pp. 117–129, 1976.

[6] J. M. Framinan, J. N. D. Gupta, and R. Leisten, "A review and classification of heuristics for permutation flow-shop scheduling with makespan objective," *Journal of the Operational Research Society*, vol. 55, no. 12, pp. 1243–1255, 2004.

[7] R. Ruiz and C. Maroto, "A comprehensive review and evaluation of permutation flowshop heuristics," *European Journal of Operational Research*, vol. 165, no. 2, pp. 479–494, 2005.

[8] T. Makino, "On a scheduling problem," *Journal of the Operations Research Society Japan*, vol. 8, pp. 32–44, 1965.

[9] E. Frostig and I. Adiri, "Three-machine flowshop stochastic scheduling to minimize distribution of schedule length," *Naval Research Logistics Quarterly*, vol. 32, no. 1, pp. 179–183, 1985.

[10] S. Sethi, H. Yan, Q. Zhang, and X. Y. Zhou, "Feedback production planning in a stochastic two-machine flowshop: asymptotic analysis and computational results," *International Journal of Production Economics*, vol. 30-31, pp. 79–93, 1993.

[11] S. E. Elmaghraby and K. A. Thoney, "The two-machine stochastic flowshop problem with arbitrary processing time distributions," *IIE Transactions*, vol. 31, no. 5, pp. 467–477, 1999.

[12] P. P. Talwar, "A note on sequencing problems with uncertain job times," *Journal of the Operations Research Society of Japan*, vol. 9, pp. 93–97, 1967.

[13] A. A. Cunningham and S. K. Dutta, "Scheduling jobs, with exponentially distributed processing times, on two machines of a flow shop," *Naval Research Logistics Quarterly*, vol. 20, pp. 69–81, 1973.

[14] P. S. Ku and S. C. Niu, "On Johnson's two-machine flow shop with random processing times," *Operations Research*, vol. 34, no. 1, pp. 130–136, 1986.

[15] H. M. Soroush and A. Allahverdi, "Stochastic two-machine flowshop scheduling problem with total completion time criterion," *International Journal of Industrial Engineerin*, vol. 12, no. 2, pp. 159–171, 2005.

[16] D. Laha and U. K. Chakraborty, "An efficient stochastic hybrid heuristic for flowshop scheduling," *Engineering Applications of Artificial Intelligence*, vol. 20, no. 6, pp. 851–856, 2007.

[17] V. Portougal and D. Trietsch, "Johnson's problem with stochastic processing times and optimal service level," *European Journal of Operational Research*, vol. 169, no. 3, pp. 751–760, 2006.

[18] P. J. Kalczynski and J. Kamburowski, "A heuristic for minimizing the expected makespan in two-machine flow shops with consistent coefficients of variation," *European Journal of Operational Research*, vol. 169, no. 3, pp. 742–750, 2006.

[19] K. R. Baker and D. Altheimer, "Heuristic solution methods for the stochastic flow shop problem," *European Journal of Operational Research*, vol. 216, no. 1, pp. 172–177, 2012.

[20] K. R. Baker and D. Trietsch, "Three heuristic procedures for the stochastic two-machine flowshop problem," *Journal of Scheduling*, vol. 14, no. 5, pp. 445–454, 2011.

[21] M. Heydari, M. Mahavi Mazdeh, and M. Bayat, "Stochastic online scheduling with preemption penalties," *Journal of Mathematics and Computer Science*, vol. 6, pp. 238–250, 2013.

[22] K. R. Baker and D. Trietsch, *Principles of Sequencing and Scheduling*, John Wiley & Sons, Hoboken, NJ, USA, 2009.

Hindawi Publishing Corporation
Discrete Dynamics in Nature and Society
Volume 2013, Article ID 172648, 19 pages
http://dx.doi.org/10.1155/2013/172648

Research Article

Basel III Liquidity Risk Measures and Bank Failure

L. N. P. Hlatshwayo, M. A. Petersen, J. Mukuddem-Petersen, and C. Meniago

Faculty of Commerce & Administration, North-West University (Mafikeng), Private Bag x2046, Mmabatho 2735, South Africa

Correspondence should be addressed to M. A. Petersen; mark.petersen@nwu.ac.za

Received 18 April 2013; Accepted 30 May 2013

Academic Editor: Ivan Ivanov

Copyright © 2013 L. N. P. Hlatshwayo et al. This is an open access article distributed under the Creative Commons Attribution License, which permits unrestricted use, distribution, and reproduction in any medium, provided the original work is properly cited.

Basel III banking regulation emphasizes the use of liquidity coverage and nett stable funding ratios as measures of liquidity risk. In this paper, we approximate these measures by using global liquidity data for 391 hand-selected, LIBOR-based, Basel II compliant banks in 36 countries for the period 2002 to 2012. In particular, we compare the risk sensitivity of the aforementioned Basel III liquidity risk measures to those of traditional measures such as the nonperforming assets ratio, return-on-assets, LIBOR-OISS, Basel II Tier 1 capital ratio, government securities ratio, and brokered deposits ratio. Furthermore, we use a discrete-time hazard model to study bank failure. In this regard, we find that Basel III risk measures have limited ability to predict bank failure when compared with their traditional counterparts. An important result is that a higher liquidity coverage ratio is associated with a higher bank failure rate. We also find that market-wide liquidity risk (proxied by LIBOR-OISS) was the major predictor of bank failures in 2009 and 2010 while idiosyncratic liquidity risk (proxied by other liquidity risk measures) was less. In particular, our contribution is the first to achieve these results on a global scale over a relatively long period for a variety of banks.

1. Introduction

Liquidity describes a bank's ability to fund asset increases and meet financial obligations, without incurring damaging losses. The role of banks in the maturity transformation of short-term deposits into long-term loans makes them vulnerable to liquidity risk, both of an idiosyncratic and market-wide nature (see, for instance, [1, 2]). The financial crisis that began in mid-2007 re-emphasized the importance of liquidity to financial market and banking sector functioning. Prior to the turmoil, financial markets were buoyant and funding was readily available at low cost. The subsequent reversal in market conditions leads to the evaporation of liquidity with the accompanying illiquidity lasting for an extended period of time. The banking system came under severe stress, which necessitated central bank support for both the functioning of money markets and individual institutions (see [2] for more details).

In response to deficiencies in financial regulation exposed by the recent spate of crises such as the subprime mortgage, global financial and ongoing Eurozone sovereign debt crises, on Sunday, 12 September 2010, the Basel Committee on Banking Supervision (BCBS) announced a strengthening of existing banking rules (see, for instance, [3–5]). More specifically, Basel III was touted as a regulatory standard on bank capital adequacy, stress testing (see, for instance, [6]), and market liquidity risk devised by the BCBS and its subgroup Working Group on Liquidity (WGL) (see, for instance, [7]). In essence, Basel III builds on Basel I and Basel II and is intended to improve the banking sector's ability to absorb shocks arising from financial and economic stress. This is intended to reduce the risk of spill-over from the financial sector to the real economy (see, [2] for further discussion). Another objective of Basel III regulation is to increase the quantity as well as the quality of capital, with adequate capital charges needed in the trading book. Also, the regulation aims to enhance risk management and disclosure, introduce a leverage ratio to supplement risk weighted measures, and address counter-party risk posed by over-the-counter (OTC) derivatives (see, for instance, [8–11]).

In Basel III, as in this paper, the maintenance of the global liquidity as well as the standards, the liquidity coverage ratio (LCR) and nett stable funding ratio (NSFR), underlying liquidity management are important. The LCR imposes a requirement that banks maintain an adequate level of "unencumbered, high-quality liquid assets that can be

converted to cash to meet its liquidity needs for a 30 calendar day time horizon under severe liquidity stress conditions specified by supervisors." On the other hand, the NSFR standard is designed to "promote longer-term funding of the assets and activities of banking organizations by establishing a minimum acceptable amount of stable funding based on the liquidity of institution's assets and activities over a one-year horizon." This standard should facilitate a diversification of liquid assets—hence discouraging a situation where they could be accumulated and susceptible to exposures such as those relating to sovereign debts (see, for instance, [12]). It will, however, be highlighted in subsequent sections of the paper that the two new Basel liquidity standards will probably not achieve their desired objectives where such standards are not coupled with other risk measures and leverage ratios (see, for instance, [3, 13]). To the best of our knowledge, no prior studies have attempted to calculate the LCR and NSFR using global public banking data.

This contribution also considers traditional liquidity risk measures such as the nonperforming assets ratio (NPAR), return-on-assets (ROA), London Interbank Offered Rate-Overnight Indexed Swap Spread (LIBOR-OISS), Basel II Tier 1 capital ratio (BIIT1KR), government securities ratio (GSR), and brokered deposits ratio (BDR). Furthermore, we note that the traditional liquidity risk measures for asset liquidity include the GSR and LCR while funding stability is measured by the BDR and NSFR. NPAR (known as the Texas ratio under certain circumstances) exhibits robust bank failure predictive power (see [14, 15]). ROA relates to a bank's ability to generate a positive nett income from its investment in its assets. A positive correlation exists between ROA and bank liquidity (see, for instance, [16]). LIBOR is the rate at which banks indicate that they are willing to lend to other banks for a specified term of the loan. The OIS rate is the rate on a derivative contract on the overnight rate. In the US, the overnight rate is the effective federal funds rate. In such a contract, two parties agree that one will pay the other a rate of interest that is the difference between the term OIS rate and the geometric average the overnight federal funds rate over the term of the contract. The OIS rate is a measure of the market's expectation of the overnight funds rate over the term of the contract. There is very little default risk in the OIS market because there is no exchange of principal; funds are exchanged only at the maturity of the contract, when one party pays the nett interest obligation to the other. The LIBOR-OISS is assumed to be a measure of bank health because it reflects what banks believe is the risk of default associated with lending to other banks. It is a measure of market-wide liquidity risk. The capital adequacy ratio BIIT1KR is described in [17] (see, also, [3]) while GSR (proxy for asset liquidity) and BDR (proxy for fund stability) are discussed in [14].

1.1. Theoretical Perspectives on Basel III Liquidity Risk Measures. The difficulties experienced by some banks during the financial crisis—despite adequate capital levels—were due to lapses in basic principles of liquidity risk management (see, for instance, [2]). In response, as the foundation of its liquidity framework, the BCBS in 2008 published "Principles for Sound Liquidity Risk Management and Supervision" known as "Sound Principles" for short (see [1] for more details). These principles provide detailed guidance on the management and supervision of liquidity risk and is intended to promote improved liquidity risk management in the case of full implementation by banks and supervisors. As such, the BCBS coordinates follow-ups by supervisors to ensure that banks adhere to "Sound Principles" (see [1] for more details). To complement these principles, the BCBS has further strengthened its liquidity framework by developing two minimum standards for funding liquidity. They are described in the ensuing discussions (see, also, [2]).

1.1.1. Liquidity Coverage Ratio (LCR). The LCR aims at increasing the resilience of banks under severe stress over a 30-day period without special government or central bank support (see, for instance, [3, 17]). The LCR is a minimum requirement and, as such, pertains to large internationally active banks on a consolidated basis. The severe stress scenario referred to earlier combines market-wide and idiosyncratic stress including a three notch rating downgrade, the run-off of retail and wholesale deposits, the stagnation of primary and secondary markets (repo, securitization) for many assets, and large cash-outflows due to off-balance sheet items (OBS).

The LCR embellishes traditional liquidity "coverage" methodologies used internally by banks to assess exposure to stress events. This liquidity standard requires that a bank's stock of unencumbered high quality liquid assets (HQLAs) be larger than the projected nett cash outflow (NCOF) over a 30-day horizon under a stress scenario specified by supervisors such that

$$\text{LCR} = \frac{\text{Total Stock of High-Quality Liquid Assets (HQLAs)}}{\text{Total Nett Cash Outflows (NCOF) Over the Next 30 Calendar Days}} \geq 1. \quad (1)$$

Cash, excess central bank reserves (to the extent that these deposits can be withdrawn in times of stress; i.e., reserves exceeding the minimum reserve requirements), and government bonds with 0% risk weight under Basel II (including government guaranteed bonds, debt of central banks and public sector entities, etc.) are considered Level 1 assets (L1As). Level 2 assets (L2As) mainly consist of government bonds with a 20% risk weight under Basel II, covered and nonfinancial corporate bonds (rating at least AA−). L2As are further classified into Level 2A assets (L2AAs) and Level 2B assets (L2BAs). The latter are subject to higher haircuts and a limit. These include corporate debt securities rated A+ to

BBB− with a 50% haircut, certain unencumbered equities subject to a 50% haircut, and certain residential mortgage-backed securities rated AA or higher with a 25% haircut. However, additional conditions concerning the debt and breadth of the underlying markets, a haircut of at least 15%, and a maximum ratio of 40% of HQLAs (after haircuts) apply to L2As. Symbolically this means that

$$\begin{aligned}&\text{Market Value of L2As}\\&\quad\le 0.4\times\text{Market Value of Total Stock of HQLA}\\&0.15\le\text{Haircut Applied to L2A Current Market Value.}\end{aligned}\tag{2}$$

Total nett cash outflow is defined as the total expected cash outflow minus total expected cash inflow for the ensuing 30 calendar days. While calculating total nett cash outflow, total expected cash inflow is considered up to an aggregate cap of 75% of total expected cash outflow. Symbolically, we have

$$\begin{aligned}&\text{Total Nett Cash Outflows Over the Next 30 Calendar Days}\\&\quad=\text{Expected Outflows}\\&\qquad-\min\left[\text{Expected Inflows; 75\% of Expected Outflows}\right].\end{aligned}\tag{3}$$

Total expected cash inflows are calculated by multiplying the outstanding balances of various categories of contractual receivables by the rates at which they are expected to flow in under the stress scenario. In order to prevent banks' from relying solely on these inflows for its liquidity an upper cap of 75% of total expected cash outflows is set. This ensures that banks hold a minimum stock of HQLAs equal to 25% of cash outflows. Symbolically, we have

$$\begin{aligned}&\text{Total Expected Cash Inflows}\\&\quad\le 0.75\times\text{Total Expected Cash Outflows.}\end{aligned}\tag{4}$$

NCOF is calculated by applying binding run-off parameters to the contractual outflows of liabilities as well as OBS items and roll-over assumptions to the contractual inflows from assets. Repos in L1As (0% run-off), stable retail (including SMEs) deposits (3% run-off), and less stable retail deposits (10% run-off) are considered the most stable funding sources under severe stress. Repos with L2As and with central banks (also in non-LCR-eligible assets) are assigned run-off rates of 15% and 25%, respectively. The latter also applies to operational balances irrespective of the counterparty (but for the part of these balances covered by deposit insurance the CRD IV foresees a 5% run-off rate). Other unsecured wholesale funding from nonfinancial corporates, central banks, and public sector entities (PSEs) receives a 75% run-off rate.

Contractual outflows from most other balance sheet positions are assumed to run-off completely as are all OBS items except credit lines granted to nonfinancial corporates, central banks, and public sector entities (10%) and credit and liquidity lines granted to retail clients (5%). For some derivatives outflows, national discretion applies. Contractual cash inflows over the 30-day period are capped by 75% of total outflows. No inflows are recognized from operational balances at other banks, receivables from reverse repos in L1As, and undrawn liquidity lines and similar facilities. Reverse repos in L2As are treated symmetrically as well, so that 15% of the contractual inflows effectively count as inflows. Planned inflows from performing retail loans and loans to nonfinancial corporates are capped at 50%. Full recognition of contractual inflows is granted to reverse repos in noneligible assets and performing wholesale loans to financial institutions.

An example of computing the LCR is given below. As we have seen, two levels of assets can be applied towards the HQLA pool in the numerator of a bank's LCR. L1As include cash, central bank reserves, and debt securities issued or guaranteed by public authorities with a 0% capital risk weight under Basel III. L2As include debt securities issued by public authorities with a 20% risk weight plus highly rated nonfinancial corporate bonds and covered bonds. Moreover, L2As may comprise no more than 40% of a bank's total HQLA stock. In other words, the quantity of L2As included in the HQLA calculation can be at most 2/3 of the quantity of L1As. In addition, L2As are subject to a 15% haircut when added to HQLA. All assets included in the calculation must be unencumbered (e.g., not pledged as collateral) and operational (e.g., not used as a hedge on trading positions). A bank's stock of HQLAs, compared with (2), can then be written as

$$\text{HQLA}=\text{L1A}+\min\left(0.85\times\text{L2A},\frac{2}{3}\times\text{L1A}\right).\tag{5}$$

The stress scenario used for computation of nett cash outflows envisions a partial loss of retail deposits, significant loss of unsecured and secured wholesale funding, contractual outflows from derivative positions associated with a three-notch rating downgrade, and substantial calls on OBS exposures. The calibration of scenario run-off rates reflects a combination of the experience during the recent financial crisis, internal stress scenarios of banks and existing regulatory and supervisory standards. From these outflows, banks are permitted to subtract projected inflows for 30 calendar days into the future. However, the fraction of outflows that can be offset this way is capped at 75%. The expected nett cash outflows (compared with (3)) are, therefore, given by

$$\text{NCOF}=\text{Outflows}-\min\left[\text{Inflows},75\%\times\text{Outflows}\right].\tag{6}$$

As a first example, it is helpful to compute the LCR for Bank A. Bank A holds six types of assets, namely, cash, reserves, treasury securities, government and corporate bonds, and retail loans. In particular, reserves and treasuries are L1As, and we suppose that corporate bonds are L2As. Bank A funds itself using a combination of stable and less stable deposits, unsecured wholesale funding (nonfinancial corporate with no operational relationship), overnight interbank borrowing, borrowings from the central bank, and equity. Table 1 presents the balance sheet item values.

Table 1: Illustrative balance sheet for computing LCR.

Assets		Liabilities	
Cash (C)	50	Stable retail deposits (D^S)	150
Reserves (R)	25	Less stable retail deposits (D^L)	150
Treasuries ($\mathtt{T}$)	50	Unsecured wholesale funding (F^U)	210
Government bonds ($\mathtt{B}^G$)	100	Interbank borrowings (B^I)	80
Corporate bonds ($\mathtt{B}^C$)	50	Central bank borrowings (B^C)	50
Retail loans (Λ)	425	Equity (E)	60
Total	700	Total	700

The stock of HQLAs for LCR purposes is given by

$$\begin{aligned} A^{\mathrm{HQL}} &= C + R + \mathtt{T} + \mathtt{B}^G \\ &\quad + \min\left(0.85 \times \mathtt{B}^C, \frac{2}{3} \times \left(C + R + \mathtt{T} + \mathtt{B}^G\right)\right) = 267.5. \end{aligned} \tag{7}$$

The outflow of funds associated with the stress scenario depends on the run-off rates specified in the LCR rules for the different types of liabilities. Using Θ^j to denote the run-off rate for liabilities of type j and letting $O^c = 10$ denote contractual outflows, we have

$$\begin{aligned} O &= \Theta^{D^S} D^S + \Theta^{D^L} D^L + \Theta^{F^U} F^U + \Theta^{B^I} B^I + \Theta^{B^C} B^C + O^c \\ &= 0.075 \times 150 + 0.15 \times 150 + 0.75 \times 210 \\ &\quad + 1 \times 80 + 0.25 \times 50 + 10 = 306.25, \end{aligned} \tag{8}$$

where the run-off rate for stable retail deposits, less stable retail deposits, and unsecured wholesale funding are taken to be 7.5%, 15%, and 75%, respectively. Also, the run-off rate on overnight interbank borrowing is 100%, and the run-off for secured transactions with the central bank against non-HQLA is 25%. Assuming contractual inflows of 6, the expected nett cash outflow is given by

$$\begin{aligned} O^{\mathrm{NC}} &= 306.25 - \min(6, 0.75 \times 267.5) \\ &= 306.25 - \min(6, 200.625) = 300.25. \end{aligned} \tag{9}$$

Hence, the LCR, C^{Lr}, of the bank is given by

$$C^{\mathrm{Lr}} = \frac{267.5}{300.25} = 0.89 < 1. \tag{10}$$

As the LCR is below 100%, this bank would need to make changes to its balance sheet in order to comply with the new liquidity standards.

1.1.2. Nett Stable Funding Ratio (NSFR). The NSFR is the quotient of the amount of available stable funding (ASF) and required stable funding (RSF) over a 1-year stress period. Clearly, the objective of the NSFR is to reduce the maturity mismatch between assets and liabilities with remaining contractual maturities of one year or more (see, for instance, [12]). Stable funding is defined as the type of equity and liability financing expected from reliable sources during a stress scenario. It is important to note that in order to avoid reliance on central banks, funding from such banks is not considered in the evaluation of the NSFR liquidity standard. The ratio is defined as the available stable funding (ASF) over required stable funding (RSF). This standard is required to be greater than 100% by Basel III to ensure that the available funding meets the required funding over the evaluated period. Thus, we have

$$\mathrm{NSFR} = \frac{\text{Available Stable Funding (ASF)}}{\text{Required Stable Funding (RSF)}} \geq 1. \tag{11}$$

ASF is defined as the total amount of bank capital, preferred stock with maturity ≥1 year, liabilities with effective maturities ≥1 year, demand deposits and/or term deposits with maturities <1 year, and wholesale funding with maturities <1 year. In order to determine the actual ASF, the aforementioned capital and liability types have to be multiplied by a specific ASF factor assigned to each type. In the ASF calculation, capital and hybrids, and liabilities with a residual maturity of more than 1 year have a 100% weight, stable deposits and less stable deposits are weighted by 90% and 80%, respectively. Wholesale funding from nonfinancials is weighted by 50%; the rest is not recognized as stable funding.

Required stable funding (RSF) is defined as the weighted sum of the value of assets held and funded by the bank multiplied by a specific RSF factor assigned to each particular asset type. The weights are loosely linked to the run-off rates in the LCR: cash, commercial paper, bonds with a maturity of below 1 year, and nonrenewable interbank loans receive a weight of 0; government bonds (including public sector entities, multilateral development banks, European Commission (EC), Bank for International Settlements (BIS) and central banks, and government guaranteed debt) with a 0% risk weight under Basel II are assigned a weight of 5%; corporate bonds and covered bonds with a rating of AA− or better with a residual maturity of one year or more have a 20% weight; corporate bonds and covered bonds with a rating of below AA− but at least A− and a residual maturity of at least 1 year as well as loans to nonfinancial corporates with a residual maturity less than one year get a 50% weight; unencumbered mortgages with a risk weight of up to 35% under Basel I receive a 65% RSF weight; retail loans with a residual maturity of less than 1 year get a 85% weight; the rest are assigned a 100% weight (see, for instance, [12]).

Table 2: Illustrative balance sheet for computing NSFR.

Assets		Liabilities	
Cash (C)	50	Stable retail deposits (D^S)	150
Government bonds (B^G)	100	Less stable retail deposits (D^L)	150
Retail loans (Λ)	425	Unsecured wholesale funding (F^U)	210
		Equity (E)	65
Total	575	Total	575

As a second example, we compute the NSFR for Bank B. This bank holds three types of assets, namely, cash, government bonds, and retail loans. Bank B funds itself using a combination of stable and less stable deposits, unsecured wholesale funding (nonfinancial corporate with no operational relationship), and equity. Table 2 presents the balance sheet item values.

The ASF, F^{AS}, depends on the ASF factors specified in the NSFR rules for the different types of liabilities. Using Φ^j to denote the ASF factor for liabilities of type j, we have

$$\begin{aligned} F^{\mathrm{AS}} &= \Phi^{D^S} D^S + \Phi^{D^L} D^L + \Phi^{F^U} F^U + \Phi^E E \\ &= 0.85 \times 150 + 0.70 \times 150 + 0.50 \times 210 \\ &\quad + 1 \times 65 = 402.5, \end{aligned} \tag{12}$$

where the ASF factors for stable retail deposits, less stable retail deposits, unsecured wholesale funding, and equity are 85%, 70%, 50%, and 100%, respectively.

The RSF, F^{RS}, relies on the factors given in the NSFR specifications for the different asset types. Using Ψ^j to denote the RSF factor for liabilities of type j, we have

$$\begin{aligned} F^{\mathrm{RS}} &= \Psi^C C + \Psi^{B^G} B^G + \Psi^{\Lambda} \Lambda \\ &= 0.0 \times 50 + 0.05 \times 100 + 0.85 \times 425 = 366.25, \end{aligned} \tag{13}$$

where the RSF factors for cash, government bonds, and retail loans are 0%, 5%, and 85%, respectively.

Hence, the NSFR, F^{NSr}, of the bank is given by

$$F^{\mathrm{NSr}} = \frac{402.5}{366.25} = 1.1 > 1. \tag{14}$$

As the NSFR is above 100%, Bank B complies with the new liquidity standards.

1.2. Theoretical Perspectives on Bank Failure. In this subsection, we discuss issues related to the relationship between liquidity risk and bank failures. In this regard, we estimate a discrete-time hazard model, in which the conditional bank failure rate is linked to insolvency and liquidity risks. In this model, the log-hazard, h^i_{t+1}, is specified as

$$h^i_{t+1} = \alpha^0 + \mathscr{R}^{Ii}_{t+1} + \mathscr{R}^{Li}_{t+1}, \tag{15}$$

which consists of a constant α^0, a component associated with insolvency risk, $\mathscr{R}^{Ii}_{t+1}$, and a part attributed to liquidity risk, $\mathscr{R}^{Li}_{t+1}$.

1.2.1. Insolvency Risk Component. It is well-known that variables affecting bank insolvency risk include capital adequacy, asset quality, profitability, and local economic conditions. In this case, we specify the insolvency component as

$$\begin{aligned} \mathscr{R}^{Ii}_{t+1} &= \alpha^1 \frac{A^{bi}_t}{E^{ci}_t + R^i_t} \frac{\Pi^i_t}{r^{di}_t} + \alpha^2 \frac{K^{bi}_t - E^{ci}_t}{E^i_t + R^i_t} + \alpha^3 \frac{\Lambda^i_t r^{\Lambda i}_t}{E^{ci}_t + R^i_t} \\ &\quad + \alpha^4 \frac{S^i_t r^{Si}_t}{E^{ci}_t + R^i_t} + \alpha^5 \frac{X^{Ibi}_t}{E^{ci}_t + R^i_t} + \alpha^6 \frac{I^{nnbi}_t}{E^{ci}_t + R^i_t} \\ &\quad + \alpha^7 \frac{A^{ni}_t}{E^{ci}_t + R^i_t} + \alpha^8 \frac{A^{ni}_t}{E^{ci}_t + R^i_t} \Delta H^i_t + \alpha^9 \frac{A^{ni}_t}{E^{ci}_t + R^i_t} \Delta U^i_t. \end{aligned} \tag{16}$$

The first component in (16) is the market valuation component, $(A^{bi}_t/(E^{ci}_t + R^i_t))(\Pi^i_t/r^{di}_t)$, where $A^{bi}_t/(E^{ci}_t + R^i_t)$ is the ratio of the book value of a bank's total assets, A^{bi}_t, to the sum of its tangible common equity, E^{ci}_t, and loan and lease loss reserves, R^i_t. Since the aforementioned sum can be regarded as the effective capital of a bank, $A^{bi}_t/(E^{ci}_t + R^i_t)$ is a measure of leverage. Also, Π^i_t/r^{di}_t is the ratio of ROA, Π^i_t, to the market discount rate, r^{di}_t. We expect the coefficient on the market valuation component, α^1, to be negative, with increases in ROA reducing the hazard, while an increase in the market discount rate increases the hazard (see, for instance, [16]). The leverage term, $A^{bi}_t/(E^{ci}_t + R^i_t)$, serves as an amplifier for the effects of changes in Π^i_t and r^{di}_t.

The second component, $(K^{bi}_t - E^{ci}_t)/(E^{ci}_t + R^i_t)$, is the ratio of intangible capital, $K^{bi}_t - E^{ci}_t$, to effective capital, $E^{ci}_t + R^i_t$, with the book value of capital, K^{bi}_t, and tangible common equity, E^{ci}_t. Beforehand, we have no expectation about the sign of the coefficient α^2. On the one hand, $K^{bi}_t - E^{ci}_t$ increases the capital buffer, so one would expect it to reduce the hazard. On the other hand, intangible capital could overinflate the reported capital, which could lead to a positive sign on this coefficient.

The third component, $r^{\Lambda i}_t \Lambda^i_t/(E^{ci}_t + R^i_t)$, is the ratio of the interest income from loans, $r^{\Lambda i}_t \Lambda^i_t$, to effective capital, $E^{ci}_t + R^i_t$, where loan yields and total loans are denoted by $r^{\Lambda i}_t$ and Λ^i_t, respectively. We expect the loan interest income coefficient, α^3, to have a negative sign.

Similarly, the fourth component, $S^i_t r^{Si}_t/(E^{ci}_t + R^i_t)$, is the ratio of interest income from securities, $r^{Si}_t S^i_t$, to effective capital, $E^{ci}_t + R^i_t$. We expect their coefficient, α^4, to have a negative sign.

The fifth component, $X^{Ibi}_t/(E^{ci}_t + R^i_t)$, is the ratio of interest expense, X^{Ibi}_t, to effective capital, $E^{ci}_t + R^i_t$. We expect its coefficient, α^5, to have a positive sign.

The sixth component, $I^{nnbi}_t/(E^{ci}_t + R^i_t)$, is the ratio of nett noninterest income, I^{nnbi}, to effective capital, $E^{ci}_t + R^i_t$. Beforehand, we do not have any expectation about the sign of α^6. On the one hand, an income would reduce the hazard. On the other, if this income is associated with taking additional risk, it would increase the hazard.

The seventh component is the NPAR, $A_t^{ni}/(E_t^{ci} + R_t^i)$, that is the ratio of nonperforming assets, A^{ni}, to effective capital, $E_t^{ci} + R_t^i$. We expect its coefficient, α^7, to be positive.

The eighth component, $(A_t^{ni}/(E_t^{ci}+R_t^i))\Delta H_t^i$, is the interaction term between the NPAR, $A_t^{ni}/(E_t^{ci}+R_t^i)$, and the change in housing price indices, ΔH_t^i. We expect its coefficient, α^8, to be negative, as rising housing prices would reduce the loss severity.

We expect α^9 associated with $(A_t^{ni}/(E_t^{ci} + R_t^i))\Delta U_t^i$, the interaction term between the NPAR ratio and the change in unemployment rates, ΔU_t^i, to be positive because a high unemployment rate would increase the loss severity.

1.2.2. Liquidity Risk Component. The liquidity risk consists of two components. The first is the idiosyncratic component that differentiates between banks with strong and weak liquidity risk management practice. For example, a bank with more rigorous liquidity risk management is less exposed to idiosyncratic risk. The second component is the market-wide liquidity risk that affects every bank. For example, a severe liquidity disruption in the market could cause a shortage of funding for many banks. In this case, the component attributed to liquidity risk is specified as

$$\mathscr{R}_{t+1}^{Li} = \alpha^{10} O_t^s + \alpha^{11} C_t^{Ri} + \alpha^{12} F_t^{Ri}. \tag{17}$$

The LIBOR-OISS, O_t^s, measures the market-wide liquidity risk. We expect the coefficient on the LIBOR-OISS, α^{10}, to be positive, as a rise in the LIBOR-OISS would increase the market funding liquidity risk. The LCR and NSFR measure the idiosyncratic liquidity risk. We expect the coefficient of the LCR, α^{11}, to be negative, as banks with more liquid assets are less likely to encounter liquidity difficulties. Finally, the coefficient on the NSFR, α^{11}, is expected to be negative, as banks with more stable funding are less likely to run into funding problems.

Substituting (16) and (17) into (15), we obtain that

$$\begin{aligned} h_{t+1}^i = {} & \alpha^0 + \alpha^1 \frac{A_t^{bi}}{E_t^{ci} + R_t^i} \frac{\Pi_t^i}{r_t^{di}} + \alpha^2 \frac{K_t^{bi} - E_t^{ci}}{E_t^{ci} + R_t^i} + \alpha^3 \frac{\Lambda_t^i r_t^{\Lambda i}}{E_t^{ci} + R_t^i} \\ & + \alpha^4 \frac{S_t^i r_t^{Si}}{E_t^{ci} + R_t^i} + \alpha^5 \frac{X_t^{Ibi}}{E_t^{ci} + R_t^i} + \alpha^6 \frac{I_t^{nnbi}}{E_t^{ci} + R_t^i} \\ & + \alpha^7 \frac{A_t^{ni}}{E_t^{ci} + R_t^i} + \alpha^8 \frac{A_t^{ni}}{E_t^{ci} + R_t^i} \Delta H_t^i + \alpha^9 \frac{A_t^{ni}}{E_t^{ci} + R_t^i} \Delta U_t^i \\ & + \alpha^{10} O_t^s + \alpha^{11} C_t^{Ri} + \alpha^{12} F_t^{Ri}, \\ & \alpha^1, \alpha^3, \alpha^4, \alpha^8, \alpha^{11}, \alpha^{12} < 0; \quad \alpha^5, \alpha^7, \alpha^9, \alpha^{10} > 0. \end{aligned} \tag{18}$$

1.3. Main Questions and Outline. The main questions addressed in this chapter about liquidity and bank failure are listed below.

Question 1 (Basel III liquidity risk measure estimations). Can we calculate an approximate value for the Basel III liquidity risk measures (viz., LCR and NSFR)? How do their values compare with traditional risk measures (for instance, NPAR, ROA, LIBOR-OISS, BIIT1KR, GSR, and BDR)? (see Section 4).

Question 2 (liquidity risk measure information values). How sensitive are Basel III liquidity risk measures by comparison to traditional ones? (see Section 5).

Question 3 (bank failure and liquidity). Is there a link between bank failures and liquidity risk? If so, how can this link be quantified? (see Section 5).

Question 4 (liquidity contribution to bank failure). Was idiosyncratic or market-wide liquidity risk the major contributor to bank failures during the 2007 to 2009 financial crisis? (see Section 5).

This paper is arranged as follows. Section 2 provides a literature review while Section 3 provides data and methodology. Also, Section 4 describes the dynamics of liquidity risk measures from Basel III (viz., LCR and NSFR) and traditional risk measures (for instance, NPAR, ROA, LIBOR-OISS, BIIT1KR, GSR, and BDR) while Section 5 examines the sensitivity of these risk measures. Also, Section 5 presents the results and discussion of liquidity risk measures and its connection with Class I and II bank failure. Finally, Section 6 provides some concluding remarks and possible topics for future research.

2. Literature Review

In this section, we review the literature about traditional liquidity risk measures, Basel III liquidity standards, and liquidity and bank failure.

2.1. Literature Review of Traditional Liquidity Risk Measures. As we have seen before, NPAR, ROA, LIBOR-OISS, BIIT1KR, GSR, and BDR are measures of an individual bank's liquidity risk. It was shown in [14] that the NPAR exhibits robust bank failure predictive power. The idea is that when a bank's ratio goes above 100%, it is at risk of failure. In fact, [14] proves that once a bank breaches the 100% mark, the chances of rehabilitation are a mere 5.06% (see, also, [15]). The connection between profitability in the form of ROA and liquidity is discussed in [23]. In particular, ROA as a liquidity measure is explained (see [16] for more discussions). The LIBOR-OISS is a measure of market-wide liquidity risk. The capital adequacy ratio BIIT1KR is described in [17] (see, also, [3]) while GSR (proxy for asset liquidity) and BDR (proxy for fund stability) are discussed in [14].

2.2. Literature Review of Basel III Liquidity Risk Measures. Although the "sound principles" in [1] focuses on liquidity risk management at medium and large complex banks, it has broad applicability to all types of banks. The implementation of these principles by both banks and supervisors was tailored to the size, nature of business, and complexity of banking

Table 3: Liquidity studies [18–22] for Group 1 and 2 banks.

Organization	BCBS			EBA	
Contribution	[18]	[19]	[20]	[21]	[22]
Report date	Sep-12	Apr-12	Dec-10	Sep-12	Apr-12
Bank data date	12/31/2011	06/30/2011	12/31/2009	12/31/2011	06/30/2011
Bank count	(102, 107)	(103, 102)	(NA, NA)	(44, 112)	(NA, NA)
Total assets (Euro Trillions)	61.40	58.50	NA	31.00	31.00
Weighted average LCR	(0.91, 0.98)	(0.90, 0.83)	(0.83, 0.98)	(0.72, 0.91)	(0.71, 0.70)
LCR shortfall ($ Trillions)	2.33	2.28	2.24	1.52	1.55
Weighted average NSFR	(0.98, 0.95)	(0.94, 0.93)	(0.93, 1.03)	(0.93, 0.94)	(0.89, 0.90)
NSFR shortfall ($ Trillions)	3.24	3.60	3.74	1.81	2.46

activities. Since the "sound principles," guidance for supervisors has been augmented substantially. In particular, proposed Basel III liquidity regulation explained in [24, 25] has added a great deal. These prescripts emphasize the importance of supervisors assessing the adequacy of a bank's liquidity and the associated risk management framework. Also, it suggests steps that supervisors should take if these are deemed inadequate. The BCBS expects banks and supervisors to implement the revised principles promptly and thoroughly and that the BCBS will actively review progress in implementation (see, for instance, [24, 25]).

Some of the first results involving Basel III liquidity standards is to be found in [18–22]. A summary table of these contributions is presented later.

We have that the BCBS's [18–20] as well as [21, 22] from the European Banking Authority (EBA) represent five quantitative impact studies or monitoring exercises using nonpublic bank data reported in December 2009, June 2011, and December 2011. Table 3 summarizes the results of these studies. The most recent BCBS monitoring exercise was based on bank data reported on Thursday, 31 December 2011. This study covers a total of 209 banks across the world, including 102 Group 1 banks 6 and 107 Group 2 banks. This study finds that the weighted average LCR is 91% for Group 1 banks and 98% for Group 2 banks. It also reports an aggregate LCR shortfall of $2.33 trillion. The weighted average NSFR is 95% for Group 1 banks and 94% for Group 2 banks. The aggregate NSFR shortfall is $3.24 trillion.

The contents of this paper is strongly related to [12] where Basel III liquidity measures are discussed. In particular, this paper computes the NSFR in accordance with Basel III prescripts. The study [12] finds that the funding ratio appears to have satisfied Basel III minimum liquidity standards for certain developing countries during this period. Our contribution also has connections with [26–28]. In the former, we use actuarial methods to discuss liquidity risk management focusing on cash inflows and securities allocation. The main objective in [26] is to minimize liquidity risk in the form of funding and credit crunch risk in an incomplete market (see, also, [2, 27, 28]). In order to accomplish this, we construct a stochastic model that incorporates reference processes. However, the current paper is an improvement on [26] in that it complies with Basel III liquidity regulation related to NSFRs (see Section 3).

2.3. Literature Review of Liquidity and Bank Failure. While recent research studies how liquidity risk causes or exacerbates the financial crisis (see, for instance, [29–32]), few empirical investigations have probed the relationships between bank failures and liquidity risk. One obvious reason for this is that there had been few bank failures globally between 1995 and 2007. The massive number of bank failures subsequently provides us with a costly opportunity to improve our understanding of bank failures and liquidity risk (see, for instance, [29, 32]).

While the new liquidity standards aim at strengthening individual banks' liquidity risk management, it remains to be seen whether idiosyncratic liquidity risk was the major contributor to bank failures during the 2007–2009 financial crisis. Furthermore, [33] shows that tight risk management of individual financial firms could lead to market illiquidity at the aggregate level. While an individual firm appears to benefit from tightening its risk management, it becomes more reluctant to provide liquidity to other firms. As a consequence, the aggregate market liquidity declines. Therefore, further investigations are needed to assess the effectiveness of Basel III liquidity standards on reducing bank failures (see, for instance, [29–32]).

3. Liquidity Risk Data and Methodology

In this section, we consider the public data and methodology used to probe the liquidity risk measures on asset liquidity (LCR and GSR) and capital stability (NSFR and BDR) in both the traditional and proposed Basel III paradigm. Also, we consider 4 other liquidity risk measures, namely, NPAR, LIBOR-OISS, BIT1KR, and ROA.

3.1. Data for Liquidity Risk Measures. We use EMERG global liquidity data that consist of observations for LIBOR-based banks for the period 2002 to 2012 (see [34]). In particular, we use databases consisting of individual banks' income statements as well as on- and off-balance sheet items. We study liquidity for Class I banks that have Tier 1 capital (T1 K) in excess of US $4 billion and are internationally active and Class II banks that do not satisfy these conditions. Of course, there are Class II banks that could have been classified as Class I if they were internationally active. These banks contributed greatly to the total assets of the Class II banks.

A total of 391 LIBOR-based Basel II compliant banks from 36 countries were included in the study, including 157 Class I and 234 Class II banks. These banks (with the number of Class I and Class II banks in parenthesis for each jurisdiction) are located in Australia (5,2), Austria (2,6), Belgium (1,2), Brazil (3,1), Canada (7,3), China (7,1), Czech Republic (4,3), Denmark (1,3), Finland (0,14), France (5,5), Germany (8,25), Hong Kong (1,8), Hungary (1,2), India (6,6), Indonesia (1,3), Ireland (3,1), Italy (2,11), Japan (14,5), Korea (6,4), Luxembourg (0,1), Malta (0,3), Mexico (1,8), Netherlands (3,13), Norway (1,6), Poland (0,5), Portugal (3,3), Russia (0,3), Saudi Arabia (4,1), Singapore (5,0), South Africa (4,5), Spain (2,4), Sweden (4,0), Switzerland (3,5), Turkey (7,1), United Kingdom (8,5), and United States (35,66).

In particular, we neither considered subsidiaries, central banks, banks with incomplete records (e.g., with inconsistent noncontinuous information) nor bank-year observations with negative HQLA, NCO, ASF, RSF, or other values. Furthermore, we mostly use nonpermanent samples for regression analysis and investigation of cross-sectional patterns. By contrast to permanent samples, the nonpermanent ones do not suffer from survivorship bias. Bank failure data for the period 2002 to 2012 were obtained from deposit insurance schemes in the aforementioned countries. For instance, for the US, bank failure data was obtained from the Federal Insurance Corporation (FDIC) and matched with call report data. We choose the period 2002–2012 because EMERG global liquidity data does not allow us to accurately calculate the LCR and NSFR prior to 2002 (see [34]).

It must be emphasized that there are difficulties in calculating the LCR and NSFR using the available public data. Firstly, the prescripts related to Basel III liquidity risk standards are ambiguous and constantly changing. Therefore, we have to use our discretion in applying the aforementioned guidelines. Secondly, the data available is limited and incomplete in terms of format and granularity between EMERG global banking data and the information required for determining Basel III LCR and NSFR (see [34]). When data is unavailable, this necessitates a reliance on specific interpolation and extrapolation techniques.

3.2. Methodology for Liquidity Risk Measures. In this subsection, we describe the methodologies related to calculating the approximate and information values of liquidity risk measures.

3.2.1. Approximate Value of Liquidity Risk Measures. We use extrapolation (and interpolation) techniques to approximate LCR and NSFR with an acceptable degree of accuracy.

In the first instance, calculating the LCR requires information about liabilities with a remaining maturity of less than one month. However, the quarterly data we use only reports information about liabilities with a remaining maturity of less than three months. So we have to extrapolate the liabilities with a remaining maturity of one month. There are two approaches to doing this. Firstly, we can assume that the maturity schedule is evenly distributed, such that the amount of liabilities with a remaining maturity of less than one month equals one-third of the amount of liabilities with a remaining maturity within three months. This is the approach adopted in this paper. Second, as a robustness check, one can assume an extreme case such that all liabilities with a remaining matur ity within three months mature within the first month.

Secondly, the guidelines require dividing liabilities into subcategories of retail deposits, unsecured wholesale funding, and secured funding with different run-off rates. However, the information available from the call report data lacks such granularity. In this case, we have to make assumptions on the distribution of subcategories within their parent category. Without additional information, we generally assume equal distribution of subcategories within the parent category.

Finally, except for unused commitments, letters of credit, and the nett fair value of derivatives, we do not have the information required for calculating the liquidity needs of all OBS items, such as the increased liquidity needs related to downgrade triggers embedded in financing transactions, derivatives, and other contracts. Our calculations of the LCR and NSFR are partial measures that capture a bank's liquidity risk as reflected by both its on- and off-balance sheet items.

3.2.2. Information Value of Liquidity Risk Measures. Each of the aforementioned liquidity risk measures (NPAR, ROA, LIBOR-OISS, BIIT1KR, GSR, BDR, LCR, and NSFR) contains information on bank liquidity. It is to be expected that some measures are less informative than others for the purpose of assessing such liquidity. In our case, we would like to know how we can assess the rationality and effectiveness of the measures' use in the process of determining liquidity. For that purpose, we use the information value (IV) criterion. We calculate the information value, V^I, of the aforementioned risk measures for predicting bank failures in one year via the formula

$$V^I = \sum_{k=1}^{m} \left(p^k - q^k\right) \log\left(\frac{p^k}{q^k}\right), \tag{19}$$

where p^k and q^k are probability distributions associated with liquid and illiquid banks, respectively. In general, our investigations will show that the information value of the two approximate Basel III risk measures, LCR and NSFR, are very low.

4. Liquidity Risk Measure Dynamics

In this section, we provide liquidity risk measure plots and descriptive statistics as well as LCR and NSFR shortfalls for Class I and II banks.

4.1. Liquidity Risk Measure Plots. Figure 1 plots the LCR, NSFR, GSR, and BDR for Class I and II banks.

It shows that LCR and NSFR had been in downward trends from 2002 through 2007. The average LCR had risen sharply from 2007 to 2009 and peaked in 2009. On the other hand, the average NSFR had risen sharply from 2007 to 2010 and peaked in 2010. The same figure presents the average GSR and BDR. The GSR declined until 2008, when this trend reversed. On the other hand, the average BDR had been in

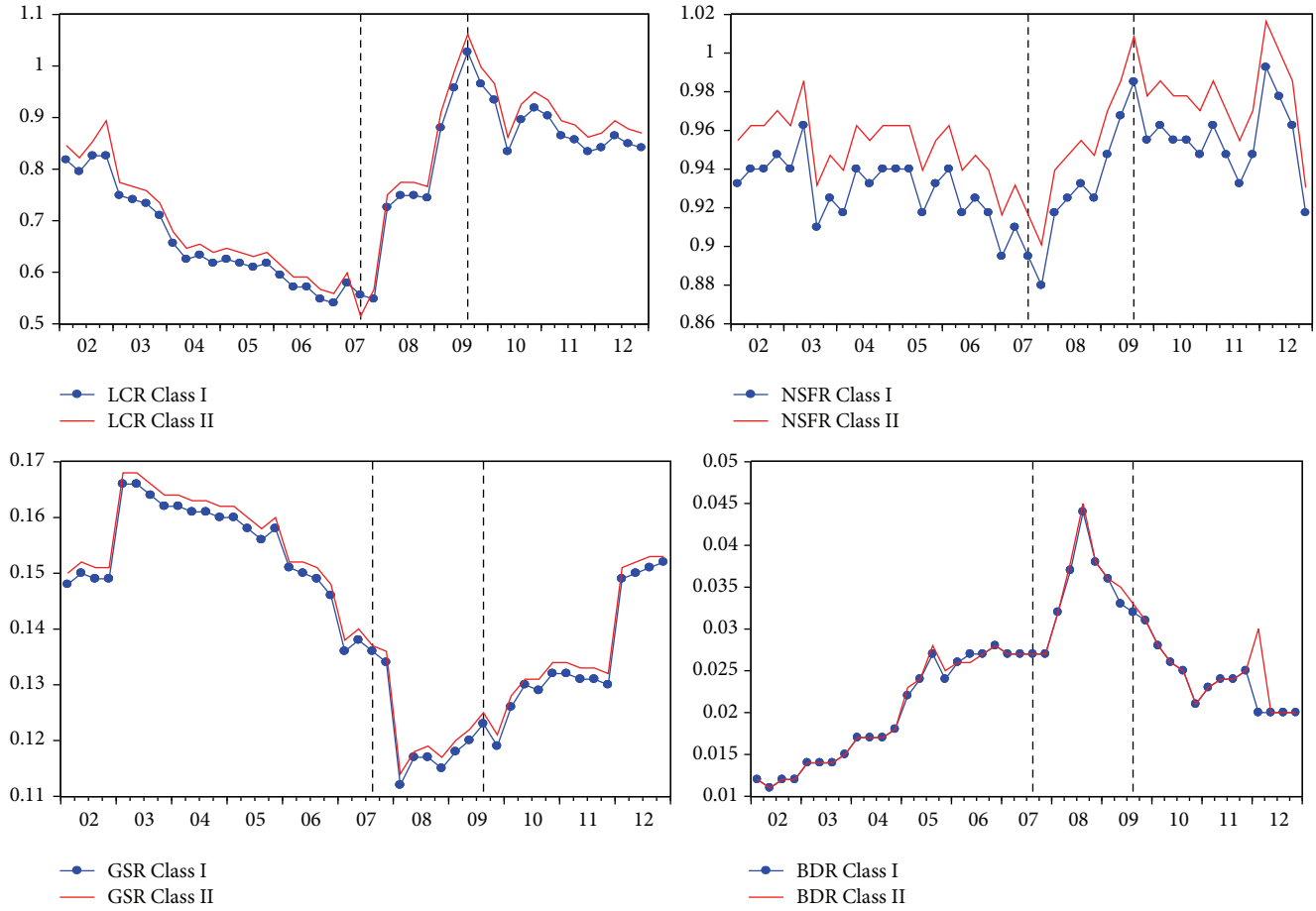

Figure 1: LCR, NSFR, GSR, and BDR for Class I and II banks.

an upward trend from 2001 through 2008, followed by a trend reversal. The general impression from Figure 1 is that the time series is nonstationary.

Analogous to Figure 1, we can represent NPAR, ROA, LIBOR-OISS, and BIIT1KR for Class I and II banks as follows.

Figure 2 shows that the NPAR, ROA, LIBOR-OISS, and BIIT1KR for Class I and II banks had exhibited varying behavior in the period from 2002 to 2007. The NPAR had risen sharply from 2007 to 2009 and peaked in 2009. On the other hand, the average NSFR had risen sharply from 2007 to 2010 and peaked in 2010. The same figure presents the average GSR and BDR. The GSR declined until 2008, when this trend reversed. On the other hand, the average BDR had been in an upward trend from 2001 through 2008, followed by a trend reversal.

4.2. Descriptive Statistics of Liquidity Risk Measures. The descriptive statistics of the LCR, NSFR, GSR, and BDR as well as NPAR, ROA, LIBOR-OISS, and BIIT1KR are presented later.

4.2.1. Descriptive Statistics of LCR, NSFR, GSR, and BDR. In Table 4, the mean, median, standard deviation, skewness, kurtosis, and Jarque-Bera statistics for LCR, NSFR, GSR, and BDR are described.

In Table 4, three out of four variables show positive skewness, namely, LCR, NSFR, and BDR while GSR is negatively skewed. This table also reports the summary statistics of the approximate measures of the LCR, NSFR, GSR, and BDR for Class I banks. It is clear that the mean for the LCR and NSFR is 74.96% and 93.76%, respectively. The value of the kurtosis for all the variables in Table 4 is equal to or less than 3, which means that the distribution is flat. All risk measures show forms of normality because the probability values in the said table have a P value greater than 5%. Nevertheless, the normality test is very sensitive to the number of observations and may only produce desirable and efficient results if observations are large. From Table 4, it is clear that the NSFR for most banks seem to have satisfied the Basel III minimum liquidity standard of 100% (compare with [2]). On the other hand, in the absence of empirical evidence, it is hard to conclude that the Basel III LCR standard had complied with these standards.

4.2.2. Descriptive Statistics of NPAR, ROA, LIBOR-OISS, and BIIT1KR. In Table 5, the mean, median, standard deviation,

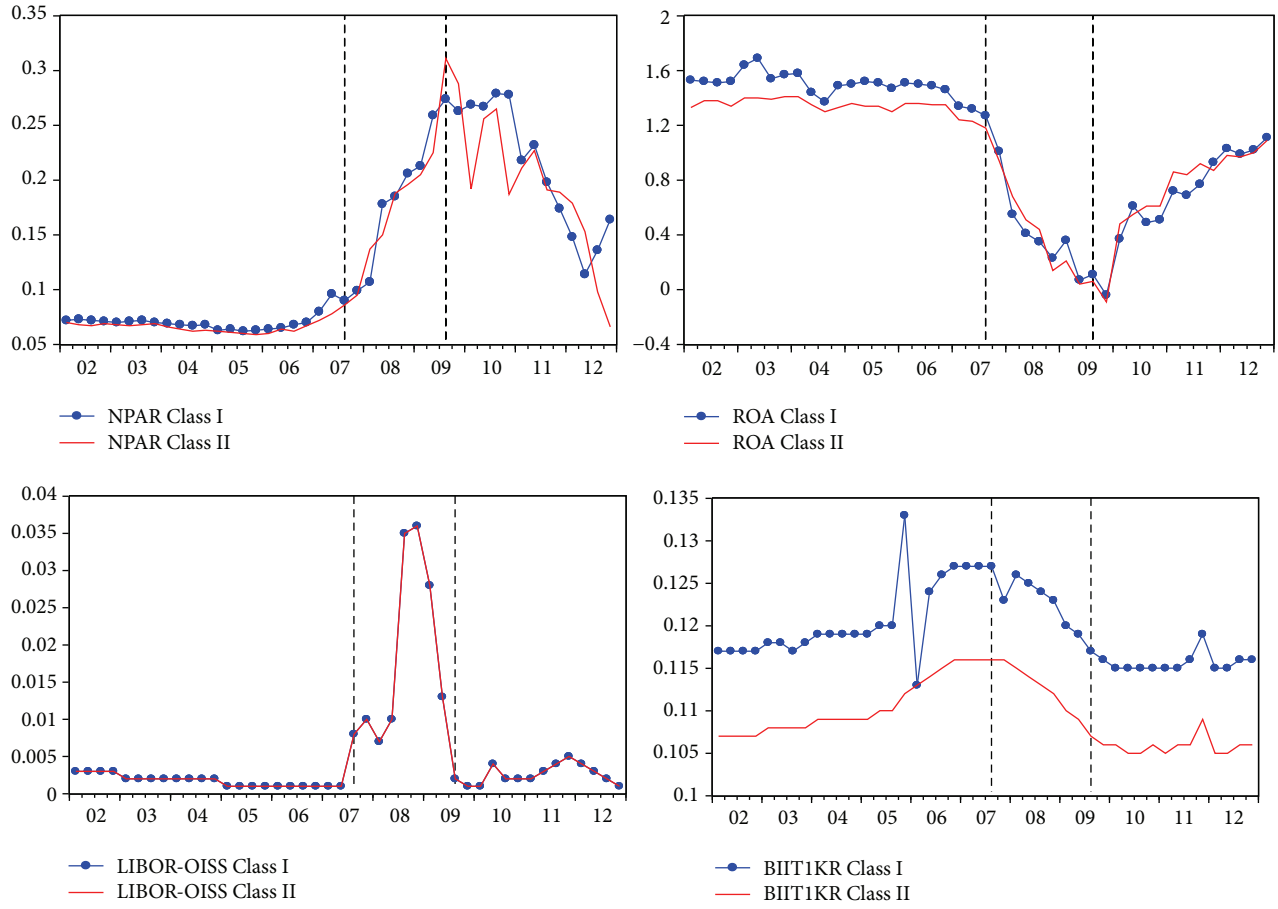

Figure 2: NPAR, ROA, LIBOR-OISS, and BIIT1KR for Class I and II banks.

Table 4: Descriptive statistics of LCR, NSFR, GSR, and BDR for Class I and II banks.

Parameter	Basel III liquidity standards		Traditional liquidity risk measures	
	LCR	NSFR	GSR	BDR
Mean	(0.748720, 0.773430)	(0.937550, 0.959670)	(0.142136, 0.144023)	(0.023750, 0.024136)
Median	(0.748840, 0.774060)	(0.940000, 0.962500)	(0.148500, 0.150500)	(0.024000, 0.025000)
Maximum	(1.026760, 1.061340)	(0.992690, 1.016400)	(0.166000, 0.168000)	(0.044000, 0.045000)
Minimum	(0.540400, 0.514560)	(0.879840, 0.900900)	(0.112000, 0.114000)	(0.011000, 0.011000)
Std. Dev.	(0.027670, 0.143466)	(0.023357, 0.023991)	(0.016247, 0.016286)	(0.007644, 0.007864)
Skewness	(0.027670, −0.029454)	(0.005426, −0.004725)	(−0.248100, −0.241821)	(0.333869, 0.304656)
Kurtosis	(1.825270, 1.855696)	(3.167401, 3.133101)	(1.782049, 1.782182)	(2.846654, 2.832527)
Jarque-Bera	(2.535599, 2.406985)	(0.051591, 0.032643)	(3.170968, 3.147815)	(0.860545, 0.732065)
Probability	(0.281450, 0.300144)	(0.974534, 0.983811)	(0.204849, 0.207234)	(0.650332, 0.693480)
Sum	(32.94368, 34.03091)	(41.25221, 42.22550)	(6.254000, 6.337000)	(1.045000, 1.062000)
Sum Sq. Dev.	(0.794993, 0.885043)	(0.023458, 0.024750)	(0.011351, 0.011405)	(0.002512, 0.002659)
Observations	(44, 44)	(44, 44)	(44, 44)	(44, 44)

skewness, kurtosis, and Jarque-Bera statistics for NPAR, ROA, LIBOR-OISS, and BIIT1KR are described.

Similar comments as those for the liquidity measures in Table 4 can be made about Table 5 involving NPAR, ROA, LIBOR-OISS, and BIIT1KR.

4.3. LCR and NSFR Shortfalls. In this subsection, we report the LCR and NSFR shortfalls for Class I and II banks (Figure 3).

The BCBS issued the full text of the revised LCR in [35] following endorsement by its governing body, the Group of

Table 5: Descriptive statistics of NPAR, ROA, LIBOR-OISS, and BIIT1KR for Class I and II banks.

Parameter	Basel III liquidity standards		Traditional liquidity risk measures	
	NPAR	ROA	LIBOR-OISS	BIIT1KR
Mean	(0.133841, 0.125932)	(1.058636, 0.989545)	(0.005023, 0.005023)	(0.119500, 0.109432)
Median	(0.093000, 0.075000)	(1.295000, 1.205000)	(0.002000, 0.002000)	(0.118500, 0.109000)
Maximum	(0.279000, 0.311000)	(1.690000, 1.410000)	(0.036000, 0.036000)	(0.133000, 0.116000)
Minimum	(0.062000, 0.059000)	(−0.040000, −0.090000)	(0.001000, 0.001000)	(0.113000, 0.105000)
Std. Dev.	(0.078458, 0.075746)	(0.519461, 0.447416)	(0.008168, 0.008168)	(0.004542, 0.003669)
Skewness	(0.713759, 0.822853)	(−0.601728, −0.939206)	(2.949292, 2.949292)	(0.967224, 0.607675)
Kurtosis	(1.927948, 2.345809)	(1.944343, 2.676113)	(10.78247, 10.78247)	(3.209685, 2.049259)
Jarque-Bera	(5.843023, 5.749916)	(4.698321, 6.661111)	(174.8269, 174.8269)	(6.941108, 4.365138)
Probability	(0.053852, 0.056419)	(0.095449, 0.035773)	(0.000000, 0.000000)	(0.031100, 0.112751)
Sum	(5.889000, 5.541000)	(46.58000, 43.54000)	(0.221000, 0.221000)	(5.258000, 4.815000)
Sum Sq. Dev.	(0.264696, 0.246713)	(11.60312, 8.607791)	(0.002869, 0.002869)	(0.000887, 0.000579)
Observations	(44, 44)	(44, 44)	(44, 44)	(44, 44)

Table 6: Minimum LCR requirements (2015–2019).

Years	2015	2016	2017	2018	2019
Minimum LCR requirement	60%	70%	80%	90%	100%

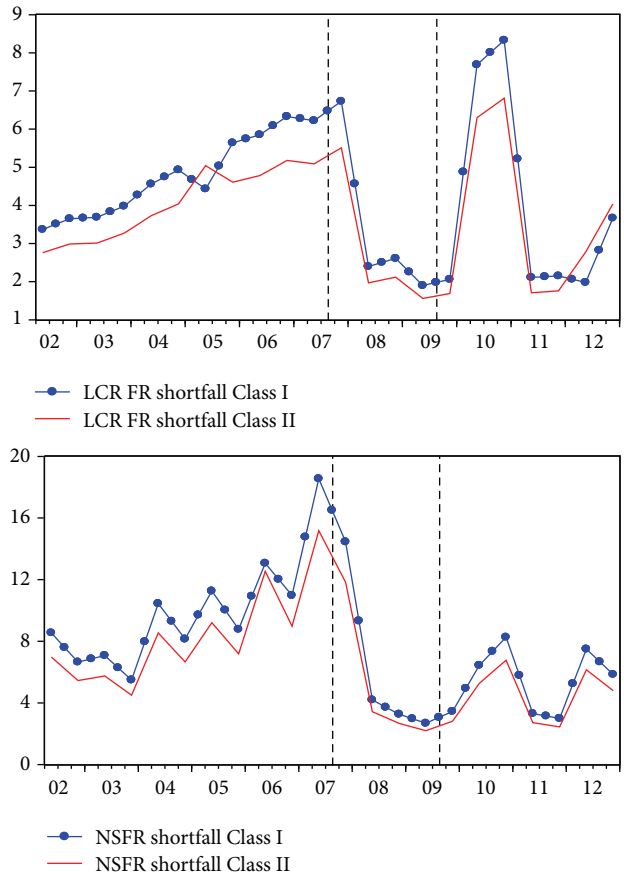

Figure 3: LCR and NSFR shortfalls for Class I and II banks.

Central Bank Governors and Heads of Supervision (GHOS). Specifically, the LCR will be introduced as planned on 1 January 2015, but the minimum requirement will begin at 60%, rising in equal annual steps of 10% to reach 100% on 1 January 2019 (Table 6). This graduated approach is designed to ensure that the LCR can be introduced without disruption to the orderly strengthening of banking systems or the ongoing financing of economic activity.

To meet the standards, banks can scale back business activities which are most vulnerable to a significant short-term liquidity shock or by lengthening the term of their funding beyond 30 days. Banks may also increase their holdings of HQLAs. The GHOS agreed that during periods of stress it would be entirely appropriate for banks to use their stock of HQLA, thereby falling below the minimum. Moreover, it is the responsibility of bank supervisors to give guidance on usability according to circumstances.

5. Liquidity Risk Measures and Bank Failure

In this section, we present the results and discussion of liquidity risk measures and bank failure for both Class I and II banks.

5.1. Liquidity Risk Measure Sensitivity for Class I and II Banks. In this subsection, we examine the sensitivity of the approximate liquidity risk measures from Basel III. A risk measure is more risk sensitive if it has higher predicting power of bank failures than other variables. Therefore, we compare the predictive power of different risk measures for predicting bank failures within one year. To do this, we divide each variable into 10 deciles and calculate its information value for predicting bank failures in one year. Table 7 reports the information value of 8 liquidity risk measures.

As Table 7 has shown, the LCR and NSFR rank very low in terms of risk sensitivity. In this regard, their information values—0.83371, 0.69743 and 0.38681, 0.49621, respectively—are much lower than those of the six traditional liquidity risk

Table 7: Information values of liquidity risk measures for Class I and II banks.

Rank	Liquidity risk measure	V^I
1	NPAR	(6.40507, 6.15319)
2	ROA	(5.35271, 5.68749)
3	LIBOR-OISS	(5.03623, 4.76481)
4	BIIT1KR	(3.06038, 3.25412)
5	GSR	(1.66051, 1.49787)
6	BDR	(1.28143, 1.12909)
7	LCR	(0.83371, 0.69743)
8	NSFR	(0.38681, 0.49621)

measures. The Class I bank liquidity risk measures, NPAR, LIBOR-OISS, GSR, BDR and LCR have information values that are greater than their Class II counterparts.

5.2. Class I and II Bank Failure. From Section 1.2, we recall that the discrete-time hazard model—hereafter known as Model A—that we will use to investigate bank failure can be represented by

$$\begin{aligned} h_{t+1}^{Ai} &= \alpha^0 + \alpha^1 \frac{A_t^{bi}}{E_t^{ci}+R_t^i}\frac{\Pi_t^i}{r_t^{di}} + \alpha^2 \frac{K_t^{bi}-E_t^{ci}}{E_t^{ci}+R_t^i} + \alpha^3 \frac{\Lambda_t^i r_t^{\Lambda i}}{E_t^{ci}+R_t^i} \\ &\quad + \alpha^4 \frac{S_t^i r_t^{Si}}{E_t^{ci}+R_t^i} + \alpha^5 \frac{X_t^{Ibi}}{E_t^{ci}+R_t^i} + \alpha^6 \frac{I_t^{nnbi}}{E_t^{ci}+R_t^i} \\ &\quad + \alpha^7 \frac{A_t^{ni}}{E_t^{ci}+R_t^i} + \alpha^8 \frac{A_t^{ni}}{E_t^{ci}+R_t^i}\Delta H_t^i + \alpha^9 \frac{A_t^{ni}}{E_t^{ci}+R_t^i}\Delta U_t^i \\ &\quad + \alpha^{10} O_t^s + \alpha^{11} C_t^{Ri} + \alpha^{12} F_t^{Ri}, \\ &\quad \alpha^1, \alpha^3, \alpha^4, \alpha^8, \alpha^{11}, \alpha^{12} < 0; \quad \alpha^5, \alpha^7, \alpha^9, \alpha^{10} > 0. \end{aligned} \tag{20}$$

From this model we can derive Model B, Model C, and Model D where LCR and NSFR are excluded, the LIBOR-OISS and liquidity risk is excluded; respectively. In essence, this means that Models B to D can be represented by

$$\begin{aligned} h_{t+1}^{Bi} &= \alpha^0 + \alpha^1 \frac{A_t^{bi}}{E_t^{ci}+R_t^i}\frac{\Pi_t^i}{r_t^{di}} + \alpha^2 \frac{K_t^{bi}-E_t^{ci}}{E_t^{ci}+R_t^i} + \alpha^3 \frac{\Lambda_t^i r_t^{\Lambda i}}{E_t^{ci}+R_t^i} \\ &\quad + \alpha^4 \frac{S_t^i r_t^{Si}}{E_t^{ci}+R_t^i} + \alpha^5 \frac{X_t^{Ibi}}{E_t^{ci}+R_t^i} \\ &\quad + \alpha^6 \frac{I_t^{nnbi}}{E_t^{ci}+R_t^i} + \alpha^7 \frac{A_t^{ni}}{E_t^{ci}+R_t^i} + \alpha^8 \frac{A_t^{ni}}{E_t^{ci}+R_t^i}\Delta H_t^i \\ &\quad + \alpha^9 \frac{A_t^{ni}}{E_t^{ci}+R_t^i}\Delta U_t^i + \alpha^{10} O_t^s, \\ &\quad \alpha^1, \alpha^3, \alpha^4, \alpha^8 < 0; \quad \alpha^5, \alpha^7, \alpha^9, \alpha^{10} > 0, \end{aligned} \tag{21}$$

$$\begin{aligned} h_{t+1}^{Ci} &= \alpha^0 + \alpha^1 \frac{A_t^{bi}}{E_t^{ci}+R_t^i}\frac{\Pi_t^i}{r_t^{di}} + \alpha^2 \frac{K_t^{bi}-E_t^{ci}}{E_t^{ci}+R_t^i} + \alpha^3 \frac{\Lambda_t^i r_t^{\Lambda i}}{E_t^{ci}+R_t^i} \\ &\quad + \alpha^4 \frac{S_t^i r_t^{Si}}{E_t^{ci}+R_t^i} + \alpha^5 \frac{X_t^{Ibi}}{E_t^{ci}+R_t^i} + \alpha^6 \frac{I_t^{\text{nnbi}}}{E_t^{ci}+R_t^i} \\ &\quad + \alpha^7 \frac{A_t^{ni}}{E_t^{ci}+R_t^i} + \alpha^8 \frac{A_t^{ni}}{E_t^{ci}+R_t^i}\Delta H_t^i + \alpha^9 \frac{A_t^{ni}}{E_t^{ci}+R_t^i}\Delta U_t^i \\ &\quad + \alpha^{11} C_t^{Ri} + \alpha^{12} F_t^{Ri}, \end{aligned} \tag{22}$$

$$\begin{aligned} h_{t+1}^{Di} &= \alpha^0 + \alpha^1 \frac{A_t^{bi}}{E_t^{ci}+R_t^i}\frac{\Pi_t^i}{r_t^{di}} + \alpha^2 \frac{K_t^{bi}-E_t^{ci}}{E_t^{ci}+R_t^i} + \alpha^3 \frac{\Lambda_t^i r_t^{\Lambda i}}{E_t^{ci}+R_t^i} \\ &\quad + \alpha^4 \frac{S_t^i r_t^{Si}}{E_t^{ci}+R_t^i} + \alpha^5 \frac{X_t^{Ibi}}{E_t^{ci}+R_t^i} + \alpha^6 \frac{I_t^{\text{nnbi}}}{E_t^{ci}+R_t^i} \\ &\quad + \alpha^7 \frac{A_t^{ni}}{E_t^{ci}+R_t^i} + \alpha^8 \frac{A_t^{ni}}{E_t^{ci}+R_t^i}\Delta H_t^i + \alpha^9 \frac{A_t^{ni}}{E_t^{ci}+R_t^i}\Delta U_t^i, \end{aligned} \tag{23}$$

respectively.

The bank failure rates for the 391 LIBOR-based, Basel II compliant banks from 36 countries for 2002 to 2012 included in our study are given in Table 8.

From Table 8, we note that 6 Class I and 17 Class II banks failed in the period 2002 to 2012.

Table 9 provides the bank failure rate by decile for Class I and II banks in the case of the LCR, NSFR, and 6 other liquidity risk measures.

Both the LCR and NSFR have very low discriminatory power. It is interesting to note that, contrary to popular belief, the higher LCR is associated with the higher bank failure rate. This result is not surprising because of the following facts. Firstly, as we have seen in Figures 1 and 2, the average LCR has risen sharply since 2007. Secondly, Table 8 shows that there have been a large number of bank failures since 2007. As a result, a higher LCR is associated with a higher bank failure rate.

5.3. Estimating Discrete-Time Hazard Models for Class I and II Banks. In this subsection, we estimate four discrete-time hazard models. The first model is based on (18), which is the benchmark model. We call it Model A. In Model B, we exclude the LCR and NSFR from Model A but keep the LIBOR-OISS. Therefore, we can estimate the contribution of the LCR and NSFR for predicting bank failures by comparing Models B and A. For Model C, we exclude the LIBOR-OISS from Model A but keep the LCR and NSFR. Comparison of Models A and C allows us to measure the contribution of market-wide liquidity risk. Finally, Model D excludes idiosyncratic and market-wide liquidity risk measures (i.e., the LCR, NSFR, and LIBOR-OISS). The model statistics include the number of observations, N, Pseudo R^2, AIC, BIC, Log Likelihood, AUC Statistic, HL Statistic, and HL P Value. The estimation results are reported in Table 10.

As can be seen from Table 10, there is small differences in model statistics between Models A and B. On the other

Table 8: Class I and Class II bank failures (2002–2012).

Quarter	Total bank count	Total bank failures	Bank failure rate	Class I and II bank count	Class I and II failures	Class I and II bank failure rate
02Q1	391	0	0.000	(157, 234)	(0, 0)	(0.000, 0.000)
02Q2	391	1	0.003	(157, 234)	(0, 1)	(0.000, 0.004)
02Q3	390	0	0.000	(157, 233)	(0, 0)	(0.000, 0.000)
02Q4	390	0	0.000	(157, 233)	(0, 0)	(0.000, 0.000)
03Q1	390	0	0.000	(157, 233)	(0, 0)	(0.000, 0.000)
03Q2	390	0	0.000	(157, 233)	(0, 0)	(0.000, 0.000)
03Q3	390	0	0.000	(157, 233)	(0, 0)	(0.000, 0.000)
03Q4	390	0	0.000	(157, 233)	(0, 0)	(0.000, 0.000)
04Q1	390	0	0.000	(157, 233)	(0, 0)	(0.000, 0.000)
04Q2	390	0	0.000	(157, 233)	(0, 0)	(0.000, 0.000)
04Q3	390	0	0.000	(157, 233)	(0, 0)	(0.000, 0.000)
04Q4	390	0	0.000	(157, 233)	(0, 0)	(0.000, 0.000)
05Q1	390	0	0.000	(157, 233)	(0, 0)	(0.000, 0.000)
05Q2	390	0	0.000	(157, 233)	(0, 0)	(0.000, 0.000)
05Q3	390	0	0.000	(157, 233)	(0, 0)	(0.000, 0.000)
05Q4	390	0	0.000	(157, 233)	(0, 0)	(0.000, 0.000)
06Q1	390	0	0.000	(157, 233)	(0, 0)	(0.000, 0.000)
06Q2	390	0	0.000	(157, 233)	(0, 0)	(0.000, 0.000)
06Q3	390	0	0.000	(157, 233)	(0, 0)	(0.000, 0.000)
06Q4	390	0	0.000	(157, 233)	(0, 0)	(0.000, 0.000)
07Q1	390	0	0.000	(157, 233)	(0, 0)	(0.000, 0.000)
07Q2	390	0	0.000	(157, 233)	(0, 0)	(0.000, 0.000)
07Q3	390	0	0.000	(157, 233)	(0, 0)	(0.000, 0.000)
07Q4	390	0	0.000	(157, 233)	(0, 0)	(0.000, 0.000)
08Q1	390	0	0.000	(157, 233)	(0, 0)	(0.000, 0.000)
08Q2	390	0	0.000	(157, 233)	(0, 0)	(0.000, 0.000)
08Q3	390	1	0.003	(157, 233)	(0, 1)	(0.000, 0.004)
08Q4	389	2	0.005	(157, 232)	(1, 1)	(0.006, 0.004)
09Q1	387	1	0.003	(156, 231)	(0, 1)	(0.000, 0.004)
09Q2	386	2	0.005	(156, 230)	(1, 1)	(0.006, 0.004)
09Q3	384	4	0.010	(155, 229)	(1, 3)	(0.006, 0.013)
09Q4	380	4	0.010	(154, 226)	(2, 2)	(0.013, 0.009)
10Q1	376	3	0.008	(152, 224)	(1, 2)	(0.007, 0.009)
10Q2	373	2	0.005	(151, 222)	(0, 2)	(0.000, 0.009)
10Q3	371	0	0.000	(151, 220)	(0, 0)	(0.000, 0.000)
10Q4	371	0	0.000	(151, 220)	(0, 0)	(0.000, 0.000)
11Q1	371	0	0.000	(151, 220)	(0, 0)	(0.000, 0.000)
11Q2	371	1	0.003	(151, 220)	(0, 1)	(0.000, 0.005)
11Q3	370	0	0.000	(151, 219)	(0, 0)	(0.000, 0.000)
11Q4	370	0	0.000	(151, 219)	(0, 0)	(0.000, 0.000)
12Q1	370	0	0.000	(151, 219)	(0, 0)	(0.000, 0.000)
12Q2	370	1	0.003	(151, 219)	(0, 1)	(0.000, 0.005)
12Q3	369	1	0.003	(151, 218)	(0, 1)	(0.000, 0.005)
12Q4	368	0	0.000	(151, 217)	(0, 0)	(0.000, 0.000)

Table 9: Bank failure rate by decile for Class I and II banks.

Decile	LCR	NSFR	GSR	BDR	BIIT1KR	NPAR	ROA
0	(0.0030, 0.0030)	(0.0070, 0.0070)	(0.0210, 0.0210)	(–, –)	(0.0435, 0.0435)	(0.0000, 0.0000)	(0.0470, 0.0470)
1	(0.0020, 0.0020)	(0.0070, 0.0070)	(0.0120, 0.0120)	(–, –)	(0.0025, 0.0025)	(0.0000, 0.0000)	(0.0015, 0.0015)
2	(0.0010, 0.0010)	(0.0070, 0.0070)	(0.0070, 0.0070)	(–, –)	(0.0015, 0.0015)	(0.0007, 0.0007)	(0.0005, 0.0005)
3	(0.0030, 0.0030)	(0.0090, 0.0090)	(0.0050, 0.0050)	(0.0015, 0.0015)	(0.0015, 0.0015)	(0.0005, 0.0005)	(0.0000, 0.0000)
4	(0.0020, 0.0020)	(0.0060, 0.0060)	(0.0040, 0.0040)	(–, –)	(0.0010, 0.0010)	(0.0000, 0.0000)	(0.0000, 0.0000)
5	(0.0030, 0.0030)	(0.0040, 0.0040)	(0.0030, 0.0030)	(–, –)	(0.0005, 0.0005)	(0.0007, 0.0007)	(0.0003, 0.0003)
6	(0.0040, 0.0040)	(0.0040, 0.0040)	(0.0020, 0.0020)	(0.0040, 0.0040)	(0.0010, 0.0010)	(0.0015, 0.0015)	(0.0001, 0.0001)
7	(0.0060, 0.0060)	(0.0030, 0.0030)	(0.0010, 0.0010)	(0.0060, 0.0060)	(0.0000, 0.0000)	(0.0010, 0.0010)	(0.0005, 0.0005)
8	(0.0080, 0.0080)	(0.0020, 0.0020)	(0.0010, 0.0010)	(0.0115, 0.0115)	(0.0000, 0.0000)	(0.0015, 0.0015)	(0.0003, 0.0003)
9	(0.0200, 0.0200)	(0.0010, 0.0010)	(0.0000, 0.0000)	(0.0240, 0.0240)	(0.0000, 0.0000)	(0.0465, 0.0465)	(0.0010, 0.0010)

hand, there are substantial differences between Model A and C that excludes the market-wide liquidity risk measures. Furthermore, the coefficient of LCR in Model A is positive and insignificant, suggesting that the LCR has little predictive power of bank failures. On the other hand, the coefficient of the LIBOR-OISS is statistically significant and positive, which implies that market-wide liquidity risk is a significant predictor of bank failures. Table 10 provides ROC curves that measure rank-ordering power for Models A to D. These ROC curves are similar with Model D having the highest AUC statistic. This statistic is represented by the area under the ROC curves.

5.4. Observed and Predicted Bank Failure Rates for Class I and II Banks. Models A to D observed and predicted bank failure rates are displayed in Table 11.

Table 11 provides information about the observed conditional failure rate and predicted values from Models A to D as well as the marginal contribution of the LCR and NSFR approximate measures for Class I and II banks. Also, Table 11 displays the observed one-year conditional bank failure rates against the predicted values from Models A to D. Columns 2, 3, and 4 display the observed one-year conditional bank failure rates against the predicted values from Models A and B, which excludes the LCR and NSFR. The differences between the predictions of Models A and B are negligible. Since Model B excludes the approximate measures of the LCR and NSFR, the differences between the predicted values of Models A and B measure the marginal contribution of these approximate measures. As can be seen, the predicted failure rates of Models A and B are very similar, and both closely match the observed failure rate.

On the other hand, Table 11 also displays the marginal contribution of the LIBOR-OISS in predicting bank failures. Columns 2, 3, and 5 show the observed one-year conditional bank failure rates against the predicted values from Model A and Model C, which excludes the LIBOR-OISS. The differences between the predictions of these two models are substantial for 2009 and 2010. As can be seen from the aforementioned columns, there are significant differences between the predicted failure rates of Models A and C in 2009 and 2010. The predicted failure rate of Model C is lower than that of Model A in 2009, while it is higher than that of Model A in 2010. We offer the following explanation. First, by looking at Table 11 again, we can see that the LIBOR-OISS was extremely high in 2008 and was extremely low in 2009. The former caused more banks to fail in 2009. On the other hand, the extremely low LIBOR-OISS (perhaps because of central banks interventions) in 2009 helped reduce the number of bank failures in 2010.

Columns 2, 3, and 6 in Table 11 display the observed one-year conditional bank failure rates against the predicted values from Model A and Model D that excludes liquidity risk. The differences between the predictions of these two models are substantial for 2009 and 2010. Because Model C excludes the LIBOR-OISS, the differences between the predicted values of Models A and C measure the marginal contribution of the LIBOR-OISS. Furthermore, as can be seen from Table 11, the predicted values of Models C and D are very close to each other, suggesting that the LIBOR-OISS accounts for a majority of the marginal contribution of liquidity risk.

In summary, the results of Table 11 suggest that the LIBOR-OISS was a major predictor of bank failures in 2009 and 2010. On the other hand, the approximate LCR and NSFR measures had very little information value in predicting bank failures.

6. Conclusions and Future Directions

In this section, we draw the most important conclusions arrived at our analysis and suggest possible topics for future research.

6.1. Conclusions about Liquidity Risk Sensitivity and Bank Failure. New Basel III banking regulation emphasizes the liquidity risk measures LCR and NSFR. In this paper, we approximated these measures by using global banking data for 391 LIBOR-based banks in 36 countries for the period 2002 to 2012 (see [34]). To the best of our knowledge, no prior studies have attempted to approximate the LCR and NSFR using global public data (see Question 1). In addition, we compare the information values of LCR and NSFR to traditional measures in terms of their power to predict bank failures. We find that the new liquidity measures have relatively low information values when compared with traditional liquidity risk measures, such as the NPAR, ROA, LIBOR-OISS, BIIT1KR, GSR, and BDR (compared with Question 2).

Table 10: Models A to D estimation results for Class I and II banks.

(a) Model statistics

	Model A	Model B LCR and NSFR excluded	Model C LIBOR-OISS excluded	Model D Liquidity risk excluded
N	(2 978, 4 413)	(2 978, 4 413)	(2 978, 4 413)	(2 978, 4 413)
Psuedo R^2	(0.642, 0.645)	(0.639, 0.635)	(0.618, 0.620)	(0.610, 0.609)
AIC	(172.967, 173.5180)	(175.113, 176.073)	(183.980, 184.036)	(188.973, 189.256)
BIC	(184.877, 185.496)	(186.347, 186.096)	(197.674, 196.0993)	(198.086, 199.773)
Log likelihood	(−85.379, −85.557)	(−87.657, −86.956)	(−91.816, −91.433)	(−93.886, −94.004)
AUC statistic	(0.9823, 0.9821)	(0.9832, 0.9829)	(0.9807, 0.9809)	(0.9842, 0.9839)
HL statistic	(19.841, 19.983)	(6.464, 6.089)	(21.747, 20.947)	(24.963, 25.072)
HL P value	(0.011, 0.011)	(0.063, 0.062)	(0.007, 0.007)	(0.002, 0.002)

(b) Parameter estimates

	Model A	Model B LCR and NSFR excluded	Model C LIBOR-OISS excluded	Model D Liquidity risk excluded
α^0	(-0.0138^{***}, -0.0242^{***})	(0.0023^{***}, 0.0019^{***})	(-0.0230^{***}, -0.0290^{***})	(0.0002, 0.0010)
	([0.003], [0.003])	([0.0011], [0.0013])	([0.0024], [0.0026])	([0.0013], [0.0011])
α^1	(-0.0918^{***}, -0.0369^{***})	(-0.0888^{***}, -0.0354^{***})	(-0.0900^{***}, -0.0356^{***})	(-0.0834^{***}, -0.0322^{***})
	([0.010], [0.011])	([0.009], [0.010])	([0.008], [0.009])	([0.0007], [0.0007])
α^2	(0.0140, 0.0157)	(0.0143^{***}, 0.0165^{***})	(0.0131, 0.0127)	(0.0134^{***}, 0.0144^{***})
	([0.0112], [0.0111])	([0.0087], [0.0086])	([0.0117], [0.0116])	([0.0097], [0.0096])
α^{3*}	(−0.0173, −0.0055)	(-0.0218^{***}, -0.0109^{***})	(−0.0121, −0.0026)	(−0.0205, −0.0116)
	([0.0218], [0.0221])	([0.0203], [0.0205])	([0.0216], [0.0219])	([0.0197], [0.0200])
α^4	(−0.0067, −0.0073)	(−0.0043, 0.0029)	(0.0003, −0.0011)	(0.0072, 0.0124)
	([0.0039], [0.0034])	([0.0037], [0.0041])	([0.0053], [0.0056])	([0.0055], [0.0066])
α^5	(0.0993^{***}, 0.5733^{***})	(0.0884, 0.8119)	(0.1199^{***}, 0.6088^{***})	(0.1069^{***}, 0.9680^{***})
	([0.0297], [0.0297])	([0.0285], [0.0286])	([0.0274], [0.0273])	([0.0246], [0.0247])
α^6	(-0.1326^{***}, -0.7184^{***})	(-0.1095^{***}, -0.9477^{***})	(-0.1539^{***}, -0.7255^{***})	(-0.1054^{***}, -1.0600^{***})
	([0.0490], [0.0490])	([0.0648], [0.0649])	([0.0250], [0.0251])	([0.0526], [0.0529])
α^7	(0.0116^{***}, 0.0185^{***})	(0.0139^{***}, 0.0233^{***})	(0.0103^{***}, 0.0144^{***})	(0.0164^{***}, 0.0210^{***})
	([0.0010], [0.0010])	([0.0009], [0.0010])	([0.0009], [0.0009])	([0.0008], [0.0009])
α^8	(0.0013^{***}, 0.0006^{***})	(0.0010^{***}, 0.0002^{***})	(0.0014, 0.0000)	(0.0009, −0.0007)
	([0.1362], [0.1698])	([0.1354], [0.1688])	([0.1535], [0.1914])	([0.1566], [0.1952])
α^9	(0.0001, 0.0005)	(0.0002, 0.0006)	(−0.0002, 0.0001)	(−0.0002, 0.0001)
	([0.0006], [0.0004])	([0.0008], [0.0008])	([0.0005], [0.0007])	([0.0007], [0.0006])
α^{10*}	(0.0963^{***}, 0.1036^{***})	(-0.1226^{***}, -0.1243^{***})	(−, −)	(−, −)
	([0.0091], [0.0092])	([0.0095], [0.0094])	([−], [−])	([−], [−])
α^{11}	(0.0024, 0.0015)	(−, −)	(0.0062, 0.0046)	(−, −)
	([0.0286], [0.0293])	([−], [−])	([0.0250], [0.0266])	([−], [−])
α^{12*}	(0.0155^{***}, 0.0260^{***})	(−, −)	(0.0211^{***}, 0.0282^{***})	(−, −)
	([0.0007], [0.0007])	([−], [−])	([0.0008], [0.0008])	([−], [−])

* and *** indicate statistical significance at the 10% and 1% level, respectively.

An important result is that the higher LCR is associated with the higher bank failure rate. If this result is not caused by the inaccuracy of our approximate LCR measure, it would imply that the LCR is poor in predicting bank failures (see Question 3). Also, we estimate a bank failure model that differentiates between idiosyncratic and market-wide liquidity risks. We find that market-wide liquidity risk as encapsulated by LIBOR-OISS was the major predictor of bank failures in 2009 and 2010, while idiosyncratic liquidity risk played only a minimal role. This finding implies that an effective liquidity risk management framework needs to target banks at both individual and market-wide levels. This explanation provides an answer to Question 4.

Because our study is based on EMERG global liquidity data (see [34]), we cannot directly compare our results with those of the BCBS (see, in particular, [18–20]) and EBA

Table 11: Observed and predicted bank failure rates for Class I and II banks (2002–2012).

Model A to D bank failures (2002–2012)					
Parameter	Observed bank failure rates	Predicted bank failure rates			
		Model A	Model B	Model C	Model D
02Q1	(0.000, 0.000)	(0.000, 0.000)	(0.000, 0.000)	(0.000, 0.000)	(0.000, 0.000)
02Q2	(0.000, 0.004)	(0.000, 0.004)	(0.000, 0.004)	(0.000, 0.004)	(0.000, 0.004)
02Q3	(0.000, 0.000)	(0.000, 0.000)	(0.000, 0.000)	(0.000, 0.000)	(0.000, 0.000)
02Q4	(0.000, 0.000)	(0.000, 0.000)	(0.000, 0.000)	(0.000, 0.000)	(0.000, 0.000)
03Q1	(0.000, 0.000)	(0.000, 0.000)	(0.000, 0.000)	(0.000, 0.000)	(0.000, 0.000)
03Q2	(0.000, 0.000)	(0.000, 0.000)	(0.000, 0.000)	(0.000, 0.000)	(0.000, 0.000)
03Q3	(0.000, 0.000)	(0.000, 0.000)	(0.000, 0.000)	(0.000, 0.000)	(0.000, 0.000)
03Q4	(0.000, 0.000)	(0.000, 0.000)	(0.000, 0.000)	(0.000, 0.000)	(0.000, 0.000)
04Q1	(0.000, 0.000)	(0.000, 0.000)	(0.000, 0.000)	(0.000, 0.000)	(0.000, 0.000)
04Q2	(0.000, 0.000)	(0.000, 0.000)	(0.000, 0.000)	(0.000, 0.000)	(0.000, 0.000)
04Q3	(0.000, 0.000)	(0.000, 0.000)	(0.000, 0.000)	(0.000, 0.000)	(0.000, 0.000)
04Q4	(0.000, 0.000)	(0.000, 0.000)	(0.000, 0.000)	(0.000, 0.000)	(0.000, 0.000)
05Q1	(0.000, 0.000)	(0.000, 0.000)	(0.000, 0.000)	(0.000, 0.000)	(0.000, 0.000)
05Q2	(0.000, 0.000)	(0.000, 0.000)	(0.000, 0.000)	(0.000, 0.000)	(0.000, 0.000)
05Q3	(0.000, 0.000)	(0.000, 0.000)	(0.000, 0.000)	(0.000, 0.000)	(0.000, 0.000)
05Q4	(0.000, 0.000)	(0.000, 0.000)	(0.000, 0.000)	(0.000, 0.000)	(0.000, 0.000)
06Q1	(0.000, 0.000)	(0.000, 0.000)	(0.000, 0.000)	(0.000, 0.000)	(0.000, 0.000)
06Q2	(0.000, 0.000)	(0.000, 0.000)	(0.000, 0.000)	(0.000, 0.000)	(0.000, 0.000)
06Q3	(0.000, 0.000)	(0.000, 0.000)	(0.000, 0.000)	(0.000, 0.000)	(0.000, 0.000)
06Q4	(0.000, 0.000)	(0.000, 0.000)	(0.000, 0.000)	(0.000, 0.000)	(0.000, 0.000)
07Q1	(0.000, 0.000)	(0.000, 0.000)	(0.000, 0.000)	(0.000, 0.000)	(0.000, 0.000)
07Q2	(0.000, 0.000)	(0.000, 0.000)	(0.000, 0.000)	(0.000, 0.000)	(0.000, 0.000)
07Q3	(0.000, 0.000)	(0.000, 0.000)	(0.000, 0.000)	(0.000, 0.000)	(0.000, 0.000)
07Q4	(0.000, 0.000)	(0.000, 0.000)	(0.000, 0.000)	(0.000, 0.000)	(0.000, 0.000)
08Q1	(0.000, 0.000)	(0.000, 0.000)	(0.000, 0.000)	(0.000, 0.000)	(0.000, 0.000)
08Q2	(0.000, 0.000)	(0.000, 0.000)	(0.000, 0.000)	(0.000, 0.000)	(0.000, 0.000)
08Q3	(0.000, 0.004)	(0.000, 0.004)	(0.000, 0.004)	(0.000, 0.004)	(0.000, 0.004)
08Q4	(0.006, 0.004)	(0.006, 0.004)	(0.006, 0.004)	(0.003, 0.002)	(0.003, 0.002)
09Q1	(0.000, 0.004)	(0.000, 0.004)	(0.000, 0.004)	(0.000, 0.003)	(0.000, 0.003)
09Q2	(0.006, 0.004)	(0.006, 0.004)	(0.006, 0.004)	(0.005, 0.003)	(0.004, 0.003)
09Q3	(0.006, 0.013)	(0.006, 0.013)	(0.006, 0.013)	(0.006, 0.013)	(0.006, 0.013)
09Q4	(0.013, 0.009)	(0.013, 0.009)	(0.013, 0.009)	(0.014, 0.010)	(0.014, 0.011)
10Q1	(0.007, 0.009)	(0.007, 0.009)	(0.007, 0.009)	(0.008, 0.011)	(0.006, 0.010)
10Q2	(0.000, 0.009)	(0.000, 0.009)	(0.000, 0.009)	(0.000, 0.010)	(0.000, 0.010)
10Q3	(0.000, 0.000)	(0.000, 0.000)	(0.000, 0.000)	(0.003, 0.004)	(0.002, 0.003)
10Q4	(0.000, 0.000)	(0.000, 0.000)	(0.000, 0.000)	(0.002, 0.003)	(0.003, 0.004)
11Q1	(0.000, 0.000)	(0.000, 0.000)	(0.000, 0.000)	(0.000, 0.000)	(0.000, 0.000)
11Q2	(0.000, 0.005)	(0.000, 0.005)	(0.000, 0.005)	(0.000, 0.007)	(0.000, 0.006)
11Q3	(0.000, 0.000)	(0.000, 0.000)	(0.000, 0.000)	(0.000, 0.000)	(0.000, 0.000)
11Q4	(0.000, 0.000)	(0.000, 0.000)	(0.000, 0.000)	(0.000, 0.000)	(0.000, 0.000)
12Q1	(0.000, 0.000)	(0.000, 0.000)	(0.000, 0.000)	(0.000, 0.000)	(0.000, 0.000)
12Q2	(0.000, 0.005)	(0.000, 0.005)	(0.000, 0.005)	(0.000, 0.007)	(0.000, 0.006)
12Q3	(0.000, 0.005)	(0.000, 0.005)	(0.000, 0.005)	(0.000, 0.005)	(0.000, 0.006)
12Q4	(0.000, 0.000)	(0.000, 0.000)	(0.000, 0.000)	(0.000, 0.000)	(0.000, 0.000)

Table 12: Summary table of the nett stable funding ratio.

Available stable funding (sources)		Required stable funding (uses)	
Item	ASF factor	Item	RSF factor
(i) T1K and T2K instruments (ii) Other preferred shares and capital instruments in excess of T2K allowable amount having an effective maturity of 1 yr or >1 yr (iii) Other liabilities with an effective maturity of 1 yr or >1 yr	100%	(i) Cash (ii) Short-term unsecured actively-traded instruments (<1 yr) (iii) Securities with exactly offsetting reverse repo (iv) Securities with remaining maturity <1 yr (v) Nonrenewable loans to financials with remaining maturity <1 yr	0%
Stable deposits of retail and small business customers (nonmaturity or residual maturity <1 yr)	90%	Debt issued or guaranteed by sovereigns, central banks, BIS, IMF, EC, noncentral government, multilateral development banks with a 0% risk weight under Basel II standardized approach	5%
Less stable deposits of retail and small business customers (nonmaturity or residual maturity <1 yr)	80%	Unencumbered non-financial senior unsecured corporate bonds and covered bonds rated at least AA−, and debt that is issued by sovereigns, central banks, and PSEs with a risk-weighting of 20%; maturity ≥1 yr	20%
Wholesale funding provided by non-financial corporate customers, sovereign central banks, multilateral development banks, and PSEs (non-maturity or residual maturity <1 yr)	50%	(i) Unencumbered listed equity securities or non-financial senior unsecured corporate bonds (or covered bonds) rated from A+ to A−, maturity ≥1 yr (ii) Gold (iii) Loans to non-financial corporate clients, sovereigns, central banks, and PSEs with a maturity <1 yr	50%
All other liabilities and equity not included above	0%	Unencumbered residential mortgages of any maturity and other unencumbered loans, excluding loans to financial institutions with a remaining maturity of 1 yr or >1 yr that would qualify for the 35% or lower risk weight under Basel II standardized approach for credit risk	65%
		Other loans to retail clients and small businesses having a maturity <1 yr	85%
		All other assets	100%
		Off balance sheet exposures	
		Undrawn amount of committed credit and liquidity facilities	5%
		Other contingent funding obligations	National supervisory discretion

(see, more specifically, [21, 22]). As was mentioned before, there are gaps between the call report data and the data required for calculating the new liquidity risk ratios. It is likely that our results are less accurate. Nevertheless, our study covers a relatively long period between 2002 and 2012, while the BCBS and EBA studies cover only three reporting dates. Because the banks participating in the BCBS studies are large international banks, they tend to be more similar to each other. On the other hand, there is more variation in our sample, which includes more than 300 banks over a 10-year period. The large sample size and the long sample period allow us to perform additional analyses that cannot be performed in the BCBS and EBA studies.

6.2. Future Directions. As recent financial crises showed, the BCBS needs to recognize the inherent limitations and weaknesses of liquidity provisioning. The proposals at an international level to supplement Basel III liquidity risk measures with other internationally harmonized and appropriately calibrated liquidity standards have been welcomed and could lead to its adoption by a wide range of countries in the future. The LCR and NSFR cannot do the job alone; it needs to be complemented by other prudential tools or measures to ensure a comprehensive picture of the dissipation of liquidity in banks as well as the financial system. Additional measures to provide a comprehensive view of aggregate liquidity, including embedded liquidity, and to trigger enhanced surveillance by supervisors need to be developed.

There appears to be consensus that no single tool or measure would have prevented the financial crisis and that an adequate policy response requires a mix of macro- and microprudential policy tools. The LCR and NSFR can be

useful prudential tools and can be relatively easy to implement, for jurisdictions that do not want to rely solely on risk-sensitive capital requirements. Combining the LCR and NSFR with Basel-type capital rules can reduce the risk of depleted liquidity in banks. As the findings in this paper showed, however, policy makers need to be cognizant of the inherent limitations and weaknesses of the LCR and NSFR.

Appendix

ASF and RSF Summaries

In Table 12, we represent a summary of the ASF and RSF components of the NSFR together with their multiplication factors.

References

[1] Basel Committee on Banking Supervision, "Principles for sound liquidity risk management and supervision," Bank for International Settlements (BIS) Publications, 2008, http://www.bis.org/publ/bcbs144.htm.

[2] F. Gideon, J. Mukuddem-Petersen, and M. A. Petersen, "Minimizing banking risk in a Lévy process setting," *Journal of Applied Mathematics*, vol. 2007, Article ID 32824, 25 pages, 2007.

[3] Basel Committee on Banking Supervision (BCBS), "Basel III: a global regulatory framework for more resilient banks and banking systems," Bank for International Settlements (BIS), 2010, http://www.bis.org/publ/bcbs189.htm.

[4] Bank for International Settlements (BIS), "Macroprudential policy tools and frameworks: update to G20 finance ministers and central bank governors," BIS Publications, 2011, http://www.bis.org/publ/othp13.htm.

[5] A. Locarno, "The macroeconomic impact of Basel III on the Italian economy. Questioni di Economia e Finanza," Occasional Paper 88, 2011, http://ssrn.com/abstract=1849870.

[6] C. Schmieder, H. Hesse, B. Neudorfer, C. Puhr, and S. W. Schmitz, "Next generation system-wide liquidity stress testing," IMF Working Paper WP/12/3, Monetary and Capital Markets Department, 2012.

[7] S. Amediku, "Was Basel III necessary and will it bring about prudent risk management in banking?" 2011, http://papers.ssrn.com/sol3/papers.cfm?abstract_id=1769822.

[8] K. Kamada and K. Nasu, "How can leverage regulations work for the stabilization of financial systems?" Bank of Japan Working Paper 19-E-2., 2010.

[9] S. Brandauer, "Sovereign debt and economic policies in global markets: a political economy approach," 2006, http://edoc.ub.uni-muenchen.de/5082/.

[10] G. Calice, J. Chen, and J. Williams, "Liquidity interactions in credit markets: an analysis of the Eurozone sovereign debt crisis," *Electronic Journal of Economics*, 2011, http://papers.ssrn.com/sol3/papers.cfm?abstract_id=1776425.

[11] N. Isaac, "bailouts fail to keep European sovereign debt markets afloat," 2011, http://www.elliottwave.com/.

[12] M. A. Petersen, B. de Waal, L. N. P. Hlatshwayo, and J. Mukuddem-Petersen, "A note on Basel III and liquidity," *Applied Economic Letters*, vol. 20, no. 8, pp. 777–780, 2013.

[13] Basel Committee on Banking Supervision, "Consultative document: strengthening the resilience of the banking system," Bank for International Settlements (BIS) Publications, 2009, http://www.bis.org/publ/bcbs164.htm.

[14] A. J. Cullen, "Why do banks fail?" 2011, http://ssrn.com/abstract=1957843.

[15] K. R. Jesswein, "Bank failure models: a preliminary examination of the Texas ratio," Proceedings of the Allied Academies International Conference, 2009, http://www.sbaer.uca.edu/research/allied/2009-neworleans/ABS/02.pdf.

[16] J. Mukuddem-Petersen, M. A. Petersen, I. M. Schoeman, and B. A. Tau, "Maximizing banking profit on a random time interval," *Journal of Applied Mathematics*, vol. 2007, Article ID 29343, 22 pages, 2007.

[17] Basel Committee on Banking Supervision (BCBS), "Basel III: a global regulatory framework for more resilient banks and banking systems—a revised version June 2011," Bank for International Settlements (BIS) Publications, 2011, http://www.bis.org/publ/bcbs189.htm.

[18] Basel Committee on Banking Supervision, "Results of the Basel III monitoring exercise as of 31 December 2011," Bank for International Settlements (BIS) Publications, 2012, http://www.bis.org/publ/bcbs231.htm.

[19] Basel Committee on Banking Supervision, "Results of the Basel III monitoring exercise as of 30 June 2011," Bank for International Settlements (BIS) Publications, 2012, http://www.bis.org/publ/bcbs217.htm.

[20] Basel Committee on Banking Supervision, "Results of the comprehensive quantitative impact study," Bank for International Settlements (BIS) Publications, 2010, http://www.bis.org/publ/bcbs186.htm.

[21] European Banking Authority (EBA), "Results of the Basel III monitoring exercise based on data as of 30 June 2011," EBA Working Paper, 2012.

[22] European Banking Authority (EBA), "Results of the Basel III monitoring exercise based on data as of 31 December 2011," EBA Working Paper, 2012.

[23] R. Y. Goyenko, C. W. Holden, and C. A. Trzcinka, "Do liquidity measures measure liquidity?" *Journal of Financial Economics*, vol. 92, no. 2, pp. 153–181, 2009.

[24] Basel Committee on Banking Supervision (BCBS), "Basel III: international framework for liquidity risk measurement, standards and monitoring," Bank for International Settlements (BIS) Publications, 2010, http://www.bis.org/publ/bcbs188.htm.

[25] Basel Committee on Banking Supervision, "Consultative document: international framework for liquidity risk measurement, standards and monitoring," Bank for International Settlements (BIS) Publications, 2009, http://www.bis.org/publ/bcbs165.htm.

[26] M. A. Petersen, B. de Waal, J. Mukuddem-Petersen, and M. P. Mulaudzi, "Subprime mortgage funding and liquidity risk," *Quantitative Finance*, 2012.

[27] M. A. Petersen, L. N. P. Hlatshwayo, J. Mukuddem-Petersen, and F. Gideon, "Economics of debt," in *Basel III and Liquidity*, Economics, chapter 10, Nova Science, New York, NY, USA, 2013.

[28] M. A. Petersen, M. C. Senosi, and J. Mukuddem-Petersen, *Subprime Mortgage Models*, Banking and Banking Developments, Nova Science, New York, NY, USA, 2012.

[29] V. V. Acharya, D. Gale, and T. Yorulmazer, "Rollover risk and market freezes," *Journal of Finance*, vol. 66, no. 4, pp. 1177–1209, 2011.

[30] M. A. Petersen, L. N. P. Hlatshwayo, J. Mukuddem-Petersen, and F. Gideon, "Basel III and liquidity," in *Economics of Debt*,

M. A. Petersen, Ed., Economics Issues, Problems and Perspectives: Global Economic Studies, chapter 10, pp. 237–316, Nova Science, New York, NY, USA, 2013.

[31] D. W. Diamond and R. G. Rajan, "Liquidity shortages and banking crises," *Journal of Finance*, vol. 60, no. 2, pp. 615–647, 2005.

[32] Z. He and W. Xiong, "Rollover risk and credit risk," *Journal of Finance*, vol. 67, no. 2, pp. 391–430, 2012.

[33] N. Gârleanu and L. H. Pedersen, "Liquidity and risk management," *American Economic Review*, vol. 97, no. 2, pp. 193–197, 2007.

[34] M. A. Petersen, L. N. P. Hlatshwayo, and J. Mukuddem-Petersen, "EMERG global liquidity data (2002–2012)," 2013, http://emerg.com/global/liquidity/data.

[35] Basel Committee on Banking Supervision, "Basel III: the liquidity coverage ratio and liquidity risk monitoring tools," Bank for International Settlements (BIS), 2013, http://www.bis.org/publ/bcbs238.htm.

Hindawi Publishing Corporation
Discrete Dynamics in Nature and Society
Volume 2013, Article ID 398750, 10 pages
http://dx.doi.org/10.1155/2013/398750

Research Article

Sublinear Expectation Nonlinear Regression for the Financial Risk Measurement and Management

Yunquan Song[1,2] and Lu Lin[1]

[1] *School of Mathematics, Shandong University, Jinan 250100, China*
[2] *College of Science, China University of Petroleum, Qingdao 266580, China*

Correspondence should be addressed to Lu Lin; linlu@sdu.edu.cn

Received 24 March 2013; Accepted 30 May 2013

Academic Editor: Ivan Ivanov

Copyright © 2013 Y. Song and L. Lin. This is an open access article distributed under the Creative Commons Attribution License, which permits unrestricted use, distribution, and reproduction in any medium, provided the original work is properly cited.

Financial risk is objective in modern financial activity. Management and measurement of the financial risks have become key abilities for financial institutions in competition and also make the major content in finance engineering and modern financial theories. It is important and necessary to model and forecast financial risk. We know that nonlinear expectation, including sublinear expectation as its special case, is a new and original framework of probability theory and has potential applications in some scientific fields, specially in finance risk measure and management. Under the nonlinear expectation framework, however, the related statistical models and statistical inferences have not yet been well established. In this paper, a sublinear expectation nonlinear regression is defined, and its identifiability is obtained. Several parameter estimations and model predictions are suggested, and the asymptotic normality of the estimation and the mini-max property of the prediction are obtained. Finally, simulation study and real data analysis are carried out to illustrate the new model and methods. In this paper, the notions and methodological developments are nonclassical and original, and the proposed modeling and inference methods establish the foundations for nonlinear expectation statistics.

1. Introduction

Finance is the core of economy, and financial safety is directly related to economic safety. Financial risk management is a huge field with diverse and evolving components, as evidenced by both its historical development and current best practice. One such component—probably the key component—is risk measurement. The 2007-2008 financial crisis and its long-lasting aftermath make people more aware that it is a very urgent and necessary thing to model and forecast financial risk.

It is well known that among all the assumption conditions imposed to the classical statistical models, the most vital one is of course that the models under study have a certain probability distribution that may or may not be known. The classical linear expectation and determinant statistics are built on such a distribution certainty or model certainty. The distribution certainty, however, is not always the case in practice, such as in risk measure and superhedging in finance (see, e.g., El Karoui et al. [1], Artzner et al. [2] Chen and Epstein [3], Follmer and Schied [4]). Without the distribution certainty, the resulting expectation is of nonlinearity, usually. The earlier work on nonlinear expectation may ascend to Huber [5] in the sense of robust statistics or ascent to Walley [6] in the sense of imprecise probabilities. In recent decades, the theory and methodology of nonlinear expectation have been well developed and received much attention in some application fields such as finance risk measure and control. A typical example of the nonlinear expectation, called g-expectation (small g), was introduced in Peng [7] in the framework of backward stochastic differential equations. As a further development, G-expectation (big g) and its related versions are proposed by Peng [8]. Under the nonlinear expectation framework, the most common distribution is the so-called G-normal distribution, which was first introduced in Peng [8]. Furthermore, as the theoretical basis of the nonlinear expectation, the law of large numbers as well as the central limit theorem is also established by Peng [9, 10]. Also, from different points of view, many authors studied the nonlinear expectation, its application, and the related issues; see, for

example, Briand et al. [11], Coquet et al. [12], Denis and Martini [13], Denis et al. [14], Gao [15], Li and Peng [16], Rosazza [17], Soner et al. [18], and Xu and Zhang [19]. Other references include Chen and Peng [20], Peng [21–24], Soner et al. [25–27], and Song [28], among many others.

Contrary to the fast development of the nonlinear expectation in probability theory, little attention has been paid to the related statistical models and statistical inferences to the best of our knowledge. Although the earlier work of Huber [5] refers initially to the upper and the lower expectations, a special nonlinear expectation, the main aspects focus on robust statistics, and the underlying true model is supposed implicitly to have a certain distribution. Gross error model, for example, contains a certain true distribution in the contaminated distribution set, and on such a distribution set, the supper and the lower expectations can be defined; see, for example, Strassen [29] and Huber [5]. In classical statistical frameworks, heteroscedastic model may be the closest one to the model uncertainty aforementioned, but it only has the variance uncertainty, and the corresponding inference methods do not involve any notion of the nonlinear expectation. In the nonparametric framework, the model structure is not given, and in Bayesian framework, the model parameter is random. But the two statistical frameworks are essentially different from the model uncertainty aforementioned, and the corresponding methods are completely unrelated to any nonlinear expectation. In time series models, although the data depend on observation time, the strict stationarity or the weak stationarity is required to guarantee the certainty of statistical inferences. In one word, under the classical statistics frameworks, including parameter models, nonparametric models, Bayes models, and time series models, the defined expectations are of linearity. Without this linearity, it is essentially difficult or impossible by the classical methods to achieve the classical certain conclusions, such as estimation consistency, asymptotic normality of the estimation.

Under the model-uncertainty frameworks, the classical statistics methods are no longer available, usually. The classical maximum likelihood, for example, is nonexistent or can not be uniquely determined due to without a certain likelihood function. Also the classical least squares is invalid because it is required that the data are derived from a certain distribution, such as normal distribution. Moreover, the classical statistical models such as linear regression model, may not be well-defined as their identifiability depends on the mean-certainty; without the mean-certainty, the regression notion has to be redefined so that the new one is of identifiability. Thus, to achieve the target of statistics inference, it is necessary to develop new statistical frameworks and new statistical methods.

Lin et al. [30] establish a framework of sublinear expectation regression for the model with distribution uncertainty. Based on a sublinear expectation space, a sublinear expectation linear regression is defined, and its identifiability is achieved. We often meet nonlinear model in the study of finance risk measure and management. It is a kind of simple and approximate methods that we deal with nonlinear model with the theory of linear model. The approximate often brings many problems. Moreover, it is not consistent with the fact of the conclusion. As a result, since the actual model is nonlinear model, we should use the method of nonlinear science to deal with the actual model. Motivated by Lin et al. [30], we propose a sublinear expectation nonlinear regression in this paper. And we achieve its identifiability. Our model is always available for both cases of the variance uncertainty and the mean-variance uncertainty. Unlike the classical regression, the new model tends to use a large value to predict response variable and obtains the mini-max prediction risk. It implies that our method is a robust strategy and therefore has potential applications in finance risk measure and management. New parameter estimation methods are suggested, and the resulting estimators are asymptotically normal distributed for the case of high-frequency data. It is worth mentioning that under the model-uncertainty framework, the certainty-statistical inferences are established in this paper, including the parameter certainty, the prediction certainty, and the distribution certainty of the parameter estimation. The notions and methodologies developed here are nonclassical and original, and the theoretical framework establishes the foundations for nonlinear expectation statistics.

The remainder of the paper is organized in the following way. In Section 2, a sublinear expectation nonlinear regression model is built, and its identifiability is obtained. The estimation and prediction methods are suggested in Section 3, and the asymptotic normality of the estimators and the minimax property of the predictions are established as well in this section. Simulation study and real data analysis are carried out in Section 4 to illustrate the new model and methodology. The proofs of the theorems and the definition of the sublinear expectation space are postponed to appendices.

2. Sublinear Expectation Nonlinear Regression

In this section we establish a framework of sublinear expectation nonlinear regression, including modeling, estimation, prediction, and the asymptotic properties.

2.1. Model. We consider the following nonlinear regression model:

$$Y = f(\mathbf{x}, \beta) + \varepsilon, \tag{1}$$

where Y is a scalar response variable, $\mathbf{x} = (X_1, \ldots, X_p)'$ is the associated p-dimensional covariate having a certain distribution $F_{\mathbf{x}}(x)$, and $\beta = (\beta_1, \ldots, \beta_p)'$ is a p-dimensional vector of unknown parameters. We assume that the function $f(\cdot)$ is a known function, and it is twice continuously differentiable. Furthermore, it is supposed that the error ε is independent of $\mathbf{x}$. We need the independency condition only for simplicity. The idea and methodology developed in the following can be extended to the dependent case, but the notations and algorithm are relatively complex. It is worth pointing out that the essential difference from the classical nonlinear regression model is that here the error ε has distribution uncertainty, which is defined in the following way.

Let Ω be a given set, and let $\mathscr{H}$ be a linear space of real valued functions defined on Ω. Furthermore, let $\mathbb{E}$ denote

a sublinear expectation: $\mathscr{H} \to \mathscr{R}$, satisfying monotonicity, constant preserving, subadditivity, and positive homogeneity; for the details of the definitions; see appendices. The triple $(\Omega, \mathscr{H}, \mathbb{E})$ is then called a sublinear expectation space. In this paper, we assume that ε is defined on a sublinear expectation space $(\Omega, \mathscr{H}, \mathbb{E})$. It can be seen from the definition that the probability distribution of ε is uncertain. For regression analysis, we suppose that $\mathscr{H}$ contains linear and quadratic functions, and although the sublinear expectation $\mathbb{E}$ is supposed to be existent, its exact form may be unknown. Thus, a remarkable point of view is that since regression analysis depends mainly on expectation, we here only define a sublinear expectation space, instead of the well-accepted probability space.

As was known by Peng [10, 31], the sublinear expectation of a function $g(\varepsilon) \in \mathscr{H}$ can be expressed as a supremum of linear expectations.

Lemma 1. *There exists a family of linear expectations* $\{E_f : f \in \mathscr{F}\}$ *defined on* $\mathscr{H}$ *such that*

$$\mathbb{E}\left[g(\varepsilon)\right] = \sup_{f \in \mathscr{F}} E_f\left[g(\varepsilon)\right] \quad \text{for } g \in \mathscr{H}, \tag{2}$$

and there exists a $f_g \in \mathscr{F}$ *such that*

$$\mathbb{E}\left[g(\varepsilon)\right] = E_{f_g}\left[g(\varepsilon)\right]. \tag{3}$$

Write $\overline{u} = \mathbb{E}[\varepsilon]$, $\underline{u} = -\mathbb{E}[-\varepsilon]$, $\overline{\sigma}^2 = \mathbb{E}[\varepsilon]^2$, $\underline{\sigma}^2 = -\mathbb{E}[-\varepsilon^2]$. Then, the intervals $[\underline{u}, \overline{u}]$ and $[\underline{\sigma}^2, \overline{\sigma}^2]$ characterize the mean-uncertainty and the variance uncertainty of ε, respectively.

When $\mathbf{x}$ is a random variable, for regression modeling, it is required to define the sublinear conditional expectation $\mathbb{E}[Y \mid \mathbf{x}]$. Lin et al. [30] gave the definition of the sublinear conditional expectation $\mathbb{E}[Y \mid \mathbf{x}]$. For example, by the representation theorem given previuosly, the previuos $\mathbb{E}[Y \mid \mathbf{x}]$ can be defined as

$$\mathbb{E}\left[Y \mid \mathbf{x}\right] = \sup_{f_{Y|\mathbf{x}} \in \mathscr{F}_{Y|\mathbf{x}}} E_{f_{Y|\mathbf{x}}}\left[Y \mid \mathbf{x}\right], \tag{4}$$

where $\{E_{f_{Y|\mathbf{x}}} : f_{Y|\mathbf{x}} \in \mathscr{F}_{Y|\mathbf{x}}\}$ is a family of linear conditional expectations. With this definition, the properties of monotonicity, constant preserving, subadditivity, and positive homogeneity given in appendices still hold.

2.2. G-Normal Regression. We first consider the case when the error ε is supposed to be G-normally distributed; namely,

$$\varepsilon \sim \mathscr{N} = N\left(\{0\} \times \left[\underline{\sigma}^2, \overline{\sigma}^2\right]\right). \tag{5}$$

Under this situation, ε has a certain zero mean, but its variance is uncertain, a special distribution uncertainty. As was defined by Peng [8], ε is called G-normally distributed if it is defined on a sublinear expectation space $(\Omega, \mathscr{H}, \mathbb{E})$ and satisfies that for each $a, b \geq 0$, $a\varepsilon + b\overline{\varepsilon} \overset{\mathrm{d}}{=} \sqrt{a^2 + b^2}\varepsilon$, where $\overline{\varepsilon}$ is an independent copy of ε and "$\overset{\mathrm{d}}{=}$" stands for equal in distribution. For the definition and the representation of G-normal distribution, see Peng [8]. It follows from the cash translatability of the sublinear conditional expectation that for regression model (1), if ε is G-normally distributed as in (5), then

$$\mathbb{E}\left[Y \mid \mathbf{x}\right] = f\left(\mathbf{x}, \beta\right). \tag{6}$$

The above relationship (6) could be thought of as a G-normal expectation nonlinear regression because $\mathbb{E}$ is the G-normal expectation, a special sublinear expectation.

Remark 2. (1) Note that $\mathbf{x}$ has an identical distribution. Then, if ε is G-normally distributed as in (5), the G-expectation of Y is identifiable in the sense that $\mathbb{E}(Y \mid \mathbf{x})$ can be uniquely determined by $f(\mathbf{x}, \beta)$ as in (6). (2) Here we emphasize the use of G-normal regression because a quadratic loss function will be employed in the following to construct a quasi-maximum likelihood estimation; for the details, see the next section. In fact the notion proposed here can be directly extended to general mean-certainty sublinear expectation regressions. Specifically, we only assume that ε has the mean certainty, instead of G-normal distribution. Under this situation, model (6) could be regarded as a mean-certainty sublinear expectation regression.

2.3. Sublinear Expectation Regression. Now we investigate the model in which the error ε has both the mean uncertainty and the variance uncertainty. By the cash translatability of the sublinear conditional expectation, we have

$$\mathbb{E}\left[Y \mid \mathbf{x}\right] = f\left(\mathbf{x}, \beta\right) + \overline{u}. \tag{7}$$

This model could be thought of as a sublinear expectation nonlinear regression because $\mathbb{E}$ is a sublinear expectation.

Remark 3. (1) If $\underline{u} < \overline{u}$, then, given $\mathbf{x}$, the sublinear expectation of Y has a shift $\overline{u}$, and more precisely, the sublinear expectation of Y has the framework of (7). (2) In the face of the mean uncertainty, we still can uniquely determine the parameter vector β and then use the mean-shift framework $f(\mathbf{x}, \beta) + \overline{u}$ instead of $f(\mathbf{x}, \beta)$ to predict the response variable Y. Such a framework reflects the robust feature of sublinear expectation nonlinear regression. If Y is a measure of the risk of a financial product, then the sublinear expectation regression tends to use a relatively large value to predict the risk and moreover, and the increment of the risk measure is just the sublinear expectation $\overline{u}$ of the error ε.

3. Estimation and Prediction

It is supposed in this section that the dimension p of β is fixed. Let $\{(Y_i, \mathbf{x}_i) : i = 1, \ldots, N\}$ be a sample from model (1), satisfying

$$Y_i = f\left(\mathbf{x}_i, \beta\right) + \varepsilon_i, \quad i = 1, \ldots, N. \tag{8}$$

Unlike the classical ones, here $Y_1, \ldots, Y_N$ may have distribution uncertainty because of the distribution uncertainty of $\varepsilon_1, \ldots, \varepsilon_N$. Then the corresponding estimation method should be different from the classical ones that apply only to linear expectation regression models.

We now introduce a mini-max method to construct the estimator of β.

3.1. The Case of the Mean Certainty. We first consider the case of ε having the mean certainty. Because Y has the sublinear expectation $f(\mathbf{x}, \beta)$ given $\mathbf{x}$, theoretically, we should choose β, so that it can minimize the sublinear expectation square loss:

$$\mathbb{E}\left[\left(Y - f\left(\mathbf{x}, \beta\right)\right)^2\right]. \tag{9}$$

We can easily verify that the previous sublinear expectation square loss is a convex function of β. Thus the optimization problem has a unique global optimal solution. The previous is in fact a sublinear expectation least squares.

Remark 4. It is worth mentioning that under G-normal distribution, we have that if φ is a convex function, then

$$\mathbb{E}\left[\varphi\left(\varepsilon\right)\right] = \frac{1}{\sqrt{2\pi}} \int_{-\infty}^{\infty} \varphi\left(\overline{\sigma} u\right) \exp\left\{-\frac{u^2}{2}\right\} du, \tag{10}$$

and if φ is a concave function, then

$$\varphi\left(\varepsilon\right) = \frac{1}{2\pi} \int_{-\infty}^{\infty} \varphi\left(\underline{\sigma} u\right) \exp\left\{-\frac{u^2}{2}\right\} du. \tag{11}$$

For the details see Peng [8]. These imply that under the convex function and concave function spaces, the G-normal has density functions $(1/\sqrt{2\pi\overline{\sigma}}) \exp\{-u^2/2\overline{\sigma}^2\}$ and $(1/\sqrt{2\pi\underline{\sigma}}) \exp\{-u^2/2\underline{\sigma}^2\}$, respectively. Therefore, the previous sublinear expectation least squares could be thought of as a quasi maximum likelihood.

To implement the estimation procedure, we need the following assumption.

(C1) There exists an index decomposition: I_i, $i = 1, \ldots, m$, such that when $(ij) \in I_i$, $\varepsilon_{i1}, \ldots, \varepsilon_{im}$ are independent and have an identical distribution.

We suppose from now on that the numbers of elements in I_i, $i = 1, \ldots, m$, are equal; that is, $n_1 = n_2 = \cdots = n_m = n$, without loss of generality. Because it is assumed that $\varepsilon_{i1}, \ldots, \varepsilon_{in}$ are identically distributed, the independence of $\varepsilon_{i1}, \ldots, \varepsilon_{in}$ in the condition *(C1)* is the same as in the linear expectation framework, instead of the independence in the nonlinear expectation. Here we need the independence only for simplicity. Without the independence, for example, $\varepsilon_{i1}, \ldots, \varepsilon_{in}$ are weakly dependent, and the conclusions given in the following still hold; for weakly dependent processes and the properties of the estimation, see, for example, Rosenblatt [32, 33], Kolmogorov and Rozanov [34], Bradley and Bryc [35], and Lu and Lin [36]. Furthermore, a common decomposition is built according to the observation time order; more precisely, $\varepsilon_1, \ldots, \varepsilon_N$ are reindexed as $\varepsilon_{ij} = \varepsilon_{(i-1)n+j}$, $i = 1, \ldots, m$, $j = 1, \ldots, n$, and then the index sets I_i's are defined as $I_i = \{(ij) : j = 1, \ldots, n\}$. It is known that in a small time interval, the characteristic of the data could be regarded as to be changeless exactly or approximately. With this point of view, the condition *(C1)* is relatively mild. Also we can decompose the index sets according to the values of Y in a descending order, for example. Moreover, we will further weaken *(C1)* and suggest a data-driven decomposition after Theorem 5 given in the following.

Denote by F_i the common distribution function of $\varepsilon_{ij}, (ij) \in I_i$. By the representation theorem of sublinear expectation given in (2), the sublinear expectation loss (9) can be written as $\max_{1 \le i \le m} E_{F_i}[(Y - f(\mathbf{x}, \beta))^2]$, and therefore its empirical version is

$$\max_{1 \le i \le m} \frac{1}{n} \sum_{j=1}^{n} \left[Y_{ij} - f\left(\mathbf{x}_{ij}, \beta\right)\right]^2. \tag{12}$$

By minimizing the previous empirical square loss, we obtain the mini-max estimator of β as

$$\widehat{\beta}_G = \arg\min_{\beta \in \mathscr{B}} \max_{1 \le i \le m} \frac{1}{n} \sum_{j=1}^{n} \left[Y_{ij} - f\left(\mathbf{x}_{ij}, \beta\right)\right]^2. \tag{13}$$

It can be easily verified that $\max_{1 \le i \le m} (1/n) \sum_{j=1}^{n} [Y_{ij} - f(\mathbf{x}_{ij}, \beta)]^2$ is a convex function of β. Thus the resulting estimator $\widehat{\beta}_G$ is a unique global optimal solution in the previous optimization problem. Since there is in general no explicit formula for the sublinear expectation nonlinear estimator $\widehat{\beta}$, the minimization of (13) must usually be carried out by some iterative method. There are two general types of iteration methods: the Newton-Raphson iteration and the Gauss-Newton iteration. Denote $\sigma_i^2 = E(\varepsilon_{ij}^2)$ for $(ij) \in \mathrm{I}_i$ and $\sigma_{i_*}^2 = \max_{1 \le i \le m} \sigma_i^2$, and for simplicity, assume that

$$\sigma_{i_*}^2 > \sigma_i^2 \quad \text{for all } i \ne i_*. \tag{14}$$

The previous mini-max estimator is asymptotic normally distributed.

In order to give the following theorem, we need the following conditions:

(I) the parameter space $\mathscr{B}$ is compact (closed and bounded), and β_0 is its interior point;

(II) the following inequality holds: $(1/n) \sum_{j=1}^{n} f(\mathbf{x}_{ij}, \beta_1) f(\mathbf{x}_{ij}, \beta_2)$ converges uniformly in $\beta_1, \beta_2 \in \mathscr{B}$;

(III) $\lim_{n \to \infty} (1/n) \sum_{j=1}^{n} [f(\mathbf{x}_{ij}, \beta_0) - f(\mathbf{x}_{ij}, \beta)]^2 \ne 0$ if $\beta \ne \beta_0$;

(IV) $\lim_{n \to \infty} (1/n) \sum_{j=1}^{n} (\partial f/\partial \beta)|_{\beta_0} (\partial f/\partial \beta')|_{\beta_0} (\equiv C)$ exist and is nonsingular;

(V) $(1/n) \sum_{j=1}^{n} (\partial f/\partial \beta)(\partial f/\partial \beta')$ converges uniformly in β in an open neighborhood of β_0;

(VI) $(1/n) \sum_{j=1}^{n} [\partial^2 f/\partial \beta_i \partial \beta_j]^2$ converges uniformly in β in an open neighborhood of β_0.

Theorem 5. *For the mean-certainty model, if the condition (C1) holds, and conditions (I), (II), and (III) hold, as $n \to \infty$ and with probability tending to 1, the estimator defined in* (13) *satisfies (a)*

$$\widehat{\beta}_G \longrightarrow \beta_0. \tag{15}$$

(b) In addition to the previous condition, if conditions (IV), (V), and (VI) hold, as $n \to \infty$,

$$\sqrt{n}\left(\widehat{\beta}_G - \beta\right) \xrightarrow{d} N\left(0, \sigma_{i_*}^2 C^{-1}\right), \tag{16}$$

where $\xrightarrow{d}$ *stands for convergence in distribution, and* $N(0, \sigma_{i_*}^2 C^{-1})$ *is a classical normal distribution.*

This theorem establishes the theoretical foundation for further statistical inferences such as constructing confidence interval and test statistic. We can see that the condition *(C1)* can be replaced by the following relatively weak condition:

(C1′) $\varepsilon_{i_*1}, \ldots, \varepsilon_{i_*n}$ are independent and have an identical distribution.

This condition only involves the errors with indexes in I_{i_*}. However, recognizing the fact that the number n of data in each small time slice I_i should be relative large, the conditions *(C1)* and *(C1′)* only apply to high-frequency data. Moreover, by the two conditions, it is implicitly assumed that the index compositions I_i, $i = 1, \ldots, m$, or I_{i_*} are known completely. Under some situations, however, it is difficult or impossible to get such exact compositions in advance. Thus, the data-driven decompositions are desired in practice. Now we briefly discuss this issue. By the condition *(C1′)*, the proof of Theorem 5 and (3), the mini-max estimator in (13) can be approximately recasted as

$$\widehat{\beta}_G = \arg\min_{\beta \in \mathscr{B}} \frac{1}{n} \sum_{j=1}^{n} \left[Y_{i_* j} - f\left(\mathbf{x}_{i_* j}, \beta\right) \right]^2. \tag{17}$$

Thus, a simple approach is to identify I_{i_*} or its subset. Let $I_i^0 = \{(ij) : j = 1, \ldots, n^0\}$, $i = 1, \ldots, m^0$ be the initial compositions according to the observation time order, for example, where $n^0 > p$. Note that under the model with the mean certainty, the common LS estimator $\widehat{\beta}_{\mathrm{LS}}$ of β is consistent. We then arrange $\sum_{j=1}^{n^0} [Y_{ij} - f(\mathbf{x}_{ij}, \widehat{\beta}_{\mathrm{LS}})]^2$, $i = 1, \ldots, m^0$, in the descending order as

$$\begin{aligned} \sum_{j=1}^{n^0} \left[Y_{i_1 j} - f\left(\mathbf{x}_{i_1 j}, \widehat{\beta}_{\mathrm{LS}}\right) \right]^2 &\geq \sum_{j=1}^{n^0} \left[Y_{i_2 j} - f\left(\mathbf{x}_{i_2 j}, \widehat{\beta}_{\mathrm{LS}}\right) \right]^2 \\ &\geq \cdots \geq \sum_{j=1}^{n^0} \left[Y_{i_m j} - f\left(\mathbf{x}_{i_m j}, \widehat{\beta}_{\mathrm{LS}}\right) \right]^2. \end{aligned} \tag{18}$$

When p is relatively small, the index set $I_{i_1}^0 = \{(i_1 j) : j = 1, \ldots, n^0\}$ can be chosen as an initial choice of I_{i_*} or a subset of I_{i_*}. We can use the data in $I_{i_1}^0$, together with approximate formula (17) to build the estimator. Since the data size in $I_{i_1}^0$ may be small, it is necessary to enlarge the initial choice $I_{i_1}^0$. To this end, we consider the following hypothesis testing:

$$H_0 : \sigma_2^2 = v_1^2 \Longleftrightarrow H_1 : \sigma_2^2 < v_1^2, \tag{19}$$

where σ_2^2 is the supposed variance of $\varepsilon_{i_2 j}$ for $(i_2 j) \in I_{i_2}^0 = \{(i_2 j) : j = 1, \ldots, n^0\}$ and $v_1^2 = (1/(n^0 - p)) \sum_{j=1}^{n^0} [Y_{i_1 j} - f(\mathbf{x}_{i_1 j}, \widehat{\beta}_{\mathrm{LS}})]^2$. The classical methods can be used to test the hypothesis H_0. If H_0 is not rejected, then $I_{i_1}^0 \bigcup I_{i_2}^0$ could be chosen as an enlarged choice of I_{i_*}. The procedure is repeated until the remainder variances are significantly smaller than v_1^2.

After the estimator $\widehat{\beta}_G$ being obtained, a natural prediction of Y is

$$\widehat{Y} = f\left(\mathbf{x}, \widehat{\beta}_G\right). \tag{20}$$

If the model uncertainty is ignored and the common least squares (LS) method is used to construct the estimator $\widehat{\beta}_{\mathrm{LS}}$ of β, then the LS based prediction is

$$\widehat{Y} = f\left(\mathbf{x}, \widehat{\beta}_{\mathrm{LS}}\right). \tag{21}$$

Comparing the two estimators by maximum prediction risk and average prediction risk, we have the following conclusion.

Theorem 6. *Under the condition of the mean certainty, whether the variance uncertainty exists or not, the following relationships always hold:*

$$\begin{aligned} \max_{1 \leq i \leq m} \frac{1}{n} \sum_{j=1}^{n} \left[Y_{ij} - f\left(\mathbf{x}, \widehat{\beta}_G\right) \right]^2 &\leq \max_{1 \leq i \leq m} \frac{1}{n} \sum_{j=1}^{n} \left[Y_{ij} - f\left(\mathbf{x}, \widehat{\beta}_{LS}\right) \right]^2, \\ \frac{1}{m} \sum_{i=1}^{m} \frac{1}{n} \sum_{j=1}^{n} \left[Y_{ij} - f\left(\mathbf{x}, \widehat{\beta}_G\right) \right]^2 &\geq \frac{1}{m} \sum_{i=1}^{m} \frac{1}{n} \sum_{j=1}^{n} \left[Y_{ij} - f\left(\mathbf{x}, \widehat{\beta}_{LS}\right) \right]^2. \end{aligned} \tag{22}$$

Remark 7. The theorem indicates that the sublinear expectation nonlinear regression is a robust strategy that can reduce the maximum prediction risk. Thus, it can be expected that such a regression could be useful for measuring and controlling financial risk.

3.2. The Case of the Mean-Variance Uncertainty. We now consider the case of ε having both the mean-uncertainty and the variance uncertainty. In this case Y has the sublinear expectation $f(\mathbf{x}, \beta) + \overline{u}$ given $\mathbf{x}$. Theoretically, we should choose β, so that it can minimize the sublinear expectation square loss:

$$\mathbb{E}\left[\left(Y - f\left(\mathbf{x}, \beta\right) - \overline{u} \right)^2 \right]. \tag{23}$$

However, we cannot directly complete the estimation procedure as $\overline{u}$ is unknown usually. We then design a profile estimation procedure as follows. Let $\widehat{\beta}$ be an initial estimator of β, which may be the estimator obtained in case of the mean certainty or by common least squares. We then estimate $\overline{u}$ by

$$\widehat{\overline{u}} = \max_{1 \leq i \leq m} \frac{1}{n} \sum_{j=1}^{n} \left[Y_{ij} - f\left(\mathbf{x}_{ij}, \widehat{\beta}\right) \right] \tag{24}$$

and finally estimate β by

$$\widetilde{\beta}_G = \arg\min_{\beta \in \mathscr{B}} \max_{1 \leq i \leq m} \frac{1}{n} \sum_{j=1}^{n} \left[Y_{ij} - f\left(\mathbf{x}_{ij}, \widehat{\beta}\right) - \widehat{\overline{u}} \right]^2. \tag{25}$$

Denote $u_i = E[\varepsilon_{ij}]$, $\sigma_i^2 = E(\varepsilon_{ij} - u_i)^2$, $v_i^2 = \sigma_i^2 + (\overline{u} - u_i)^2$, and $\sigma_{k_*}^2 = \max\{v_i^2 : i = 1, \ldots, m\}$, and for simplicity, assume

$\sigma^2_{k_*} > v_i^2$ for all $i \neq k_*$. By the same argument as in Theorem 5, we can prove that the estimator $\widetilde{\beta}_G$ is asymptotically normal distributed. The following theorem presents the details.

Theorem 8. *For mean-variance uncertainty, if the condition C1 holds, and conditions (I), (II), and (III) hold, as $n \to \infty$ and with probability tending to 1, the estimator defined in* (25) *satisfies (a)*

$$\widetilde{\beta}_G \longrightarrow \beta_0. \tag{26}$$

(b) In addition to the previous condition, if conditions (IV), (V), and (VI) hold, as $n \to \infty$,

$$\sqrt{n}\left(\widetilde{\beta}_G - \beta\right) \xrightarrow{d} N\left(0, \sigma^2_{k_*} C^{-1}\right), \tag{27}$$

where $\xrightarrow{d}$ stands for convergence in distribution and $N(0, \sigma^2_{k_*} C^{-1})$ is a classical normal distribution.

For proof of the theorem, see appendices. This theorem establishes a foundation for further statistical inference and data analysis. Here we also need to check the condition C1. From the estimation procedure given previously, we see that it is asymptotically equivalent to determine two index sets, with which the mean of the error and $(1/n)\sum_{j=1}^{n}[Y_{k_* j} - f(\mathbf{x}_{k_* j}, \beta) - \widehat{\overline{u}}]^2$ achieve the maximum values $\overline{u}$ and $v^2_{k_*}$, respectively. The approaches are similar to that used in case of the mean-certainty and thus the details are omitted here.

With the estimator, a natural prediction of Y is

$$\widetilde{Y} = f\left(\mathbf{x}, \widetilde{\beta}_G\right) + \overline{u}. \tag{28}$$

Similar to the properties in Theorem 6, the prediction $\widetilde{Y}$ can obtain mini-max prediction risk.

Theorem 9. *Whether the mean uncertainty and the variance uncertainty exist or not, the following relationship always holds:*

$$\begin{aligned} &\max_{1\le i\le m} \frac{1}{n}\sum_{j=1}^{n}\left[Y_{ij} - f\left(\mathbf{x}, \widetilde{\beta}_G\right) - \widehat{\overline{u}}\right]^2 \\ &\quad \le \max_{1\le i\le m} \frac{1}{n}\sum_{j=1}^{n}\left[Y_{ij} - f\left(\mathbf{x}, \widehat{\beta}_{LS}\right) - \widehat{\overline{u}}\right]^2. \end{aligned} \tag{29}$$

It shows that our proposal is a robust strategy and is therefore useful for measuring and controlling financial risk. Meanwhile, the simulation study given in Section 4 will verify that when model has the mean-variance uncertainty, the average prediction error of the new method is usually smaller than that of the LS method; namely,

$$\begin{aligned} &\frac{1}{m}\sum_{i=1}^{m}\frac{1}{n}\sum_{j=1}^{n}\left[Y_{ij} - f\left(\mathbf{x}, \widetilde{\beta}_G\right) - \overline{u}\right]^2 \\ &\quad < \frac{1}{m}\sum_{i=1}^{m}\frac{1}{n}\sum_{j=1}^{n}\left[Y_{ij} - f\left(\mathbf{x}, \widehat{\beta}_{\mathrm{LS}}\right) - \overline{u}\right]^2. \end{aligned} \tag{30}$$

It is because the prediction bias of $f(\mathbf{x}, \widehat{\beta}_{\mathrm{LS}})$ is between $\underline{u}$ and $\overline{u}$, which is not ignorable special for the case of $\underline{u}\,\overline{u} > 0$.

Table 1: Simulation results of estimation and prediction for Experiment 1 with $m = 10$ and $n = 10$.

MSE	β_1	β_2	β_3	MPE	APE
$\widehat{\beta}_G$	0.0089	0.0327	0.0385	7.0248	4.6245
$\widehat{\beta}_{\mathrm{LS}}$	0.0043	0.0068	0.0052	8.3124	3.6279

4. Simulation Study and Real Data Analysis

4.1. Simulation Study. In this section we present several simulation examples to compare the finite-sample performances of the sublinear expectation nonlinear regression proposed in this paper. To get comprehensive comparisons, we use mean square error (MSE), maximum prediction error (MPE), and average prediction error (APE) to assess the different methods. From the simulations given, we will get the following findings: (1) the new methods can significantly reduce the MPE under all the situations; (2) when the model has the mean certainty, the advantages of the new methods over the LS methods are not very obvious; (3) for the model with the mean uncertainty, the prediction of the LS methods does not work and even breaks down, but the new methods can get valid prediction because the impact of the mean uncertainty on the new methods can be successfully eliminated by the use of the sublinear expectation of the error.

Experiment 1. We first consider the following simple nonlinear model:

$$Y = f\left(\mathbf{x}, \beta\right) + \varepsilon, \tag{31}$$

where $f(\mathbf{x}, \beta) = (\beta_3/(\beta_1 + \beta_2))(\exp\{-\beta_1 X_1\} - \exp\{\beta_2 X_2\} + \exp\{\beta_3 X_3\})$. In the simulation procedure, the regression coefficients are chosen as $\beta_k = 1, k = 1, 2, 3$, and the observation values of X_k are independent and identically distributed from $N(10, 2)$, $k = 1, 2, 3$. We choose $\varepsilon \sim N(\{0\} \times [0, 3])$, a G-normal distribution with certain zero mean. In this case, the model has the mean certainty. The following way is used to generate the data of G-normal distribution, approximately. Generate variance values σ_i^2, $i = 1, \ldots, m$, from the uniform distribution $U[0, 3]$, and then generate the values ε_{ij}, $j = 1, \ldots, n$, of ε from the common normal distribution $N(0, \sigma_i^2)$.

For $m = 10$ and $n = 10$, the simulation results are reported in Table 1, in which MSE, MPE, and APE denote the mean squared error, maximum prediction error, and average prediction, respectively; for the definitions of MPE and APE see Theorem 6. It is clear that the MSE and APE of common LS estimation $\widehat{\beta}_{\mathrm{LS}}$ are significantly smaller than those of the G-normal estimation $\widehat{\beta}_G$. Such a result is not surprising because, under the mean-certainty model, the common LS estimation $\widehat{\beta}_{\mathrm{LS}}$ is consistent, but the construction of the new estimation $\widehat{\beta}_G$ only uses the data in a small time interval (the number of the data used to construct the estimator is only 10). On the other hand, the MPE by the new one $\widehat{\beta}_G$ is significantly small than that by the LS estimator $\widehat{\beta}_{\mathrm{LS}}$, which implies than the new method can reduce the maximum prediction risk and therefore is a robust strategy.

Table 2: Simulation results of estimation and prediction for Experiment 2 with $m = 10$ and $n = 10$.

MSE	β_1	β_2	β_3	MPE	APE
$\widehat{\beta}_G$	0.2485	0.3697	0.3289	16.0952	7.3548
$\widehat{\beta}_{\mathrm{LS}}$	0.1324	0.2819	0.2305	39.4257	22.6957

Table 3: Simulation results of estimation and prediction for Experiment 3.

MSE	β_1	β_2	β_3	MPE	APE
$\widehat{\beta}_G$	0.2374	0.4738	0.4326	13.2590	7.8835
$\widehat{\beta}_{\mathrm{LS}}$	0.1962	0.2653	0.2739	39.0364	22.4357

The simulation results in Table 1 indicate that when model has the mean certainty, the advantages of the new methods over the common LS are not rather obvious. Moreover, the new methods even have the disadvantage of instability. In the following, we will see that when model has the mean-uncertainty, our new methods have rather clear advantages over the LS based methods.

Experiment 2. We reconsider the nonlinear model

$$Y = f\left(\mathbf{x}, \beta\right) + \varepsilon, \tag{32}$$

where $f(\mathbf{x}, \beta) = (\beta_3/(\beta_1 + \beta_2))(\exp\{-\beta_1 X_1\} - \exp\{\beta_2 X_2\} + \exp\{\beta_3 X_3\})$. which is the same in form as in Experiment 1. However, here the model has the mean-variance uncertainty as $\varepsilon \sim N([3,5] \times [0,3])$. The other experiment conditions are designed as $X_k \sim N(0,1)$, $k = 1,2,3$, $m = 10$, and $n = 20$. The values of ε are generated by the following way. First, the values u_i of the mean and the values σ_i^2 of the variance are generated from the uniform distributions $U[3,5]$ and $U[0,4]$, respectively, and then the values ε_{ij}, $j = 1, \ldots, n$ of ε are generated from the common normal distribution $N(u_i, \sigma_i^2)$ for $i = 1, \ldots, m$. The simulation results are listed in Table 2. For the MSE of the parameter estimation, the results are similar to those in Experiment 1; that is, the MES of the LS estimation is smaller than that of the new estimation because the new method only uses the data in a small subinterval. However, when the mean uncertainty and variance uncertainty appear in the model, both the MPE and the APE of the new one are significantly smaller than those of the LS estimator. Particularly, the prediction by the LS seems to be totally invalid. It indicates that ignoring the model uncertainty will lead to a serious prediction risk.

4.2. Real Data Analysis

Experiment 3. In economics, the Cobb-Douglas functional form of production functions is widely used to represent the relationship of an output to inputs. It was proposed by Knut Wicksell (1851–1926) and tested against statistical evidence by Charles Cobb and Paul Douglas in 1900–1928. We consider the Cobb-Douglas production function with an additive error

$$Y = \beta_1 L^{\beta_2} K^{\beta_3} + \varepsilon_t, \tag{33}$$

where Y is total production (the monetary value of all goods produced in a year), L is labor input, K is capital input, β_1 is total factor productivity, β_2 and β_3 are the output elasticities of labor and capital, respectively. These values are constants determined by available technology. We assume that the model has the mean-variance uncertainty as $\varepsilon \sim N([0,1] \times [0,1])$.

Here, the statistical data comes from China Statistical Yearbook (2003), total production Y is the gross domestic product (GDP), labor input L is employment, and capital input K is fixed asset investment. The simulation results are listed in Table 3. When the mean uncertainty and variance-uncertainty appear in the model, both the MPE and the APE of the new one are significantly smaller than those of the LS estimator. Particularly, the prediction by the LS seems to be totally invalid. It indicates that ignoring the model-uncertainty will lead to a serious prediction risk.

The simulation results in Table 3 indicate that when model has the mean certainty, the advantages of the new methods over the common LS are not rather obvious. Moreover, the new methods even have the disadvantage of instability. In the following, we will see that when model has the mean-uncertainty, our new methods have rather clear advantages over the LS based methods.

Appendices

A. Definition of Sublinear Expectation

Let Ω be a given set, and let $\mathscr{H}$ be a linear space of real valued functions defined on Ω. Suppose that $\mathbb{E} : \mathscr{H} \to \mathbb{R}$ satisfies the following properties: for all $U, V \in \mathscr{H}$,

(i) monotonicity: if $U \geq V$, then $\mathbb{E}[U] \geq \mathbb{E}[V]$;

(ii) constant preservation: $\mathbb{E}[c] = c$ for any constant c;

(iii) subadditivity: $\mathbb{E}[U + V] \leq \mathbb{E}[U] + \mathbb{E}[V]$;

(iv) positive homogeneity: $\mathbb{E}[\lambda U] = \lambda \mathbb{E}[U]$ for each $\lambda \geq 0$.

Then $(\Omega, \mathscr{H}, \mathbb{E})$ is called a sublinear expectation space.

It can verified that (iii) and (iv) together imply

(v) convexity: $\mathbb{E}[\alpha U + (1-\alpha)V] \leq \alpha \mathbb{E}[U] + (1-\alpha)\mathbb{E}[V]$ for $\alpha \in [0,1]$.

Furthermore, (ii) and (iii) together lead to

(vi) cash translatability: $\mathbb{E}[U + c] = \mathbb{E}[U] + c$ for any constant c.

B. Proofs

Proof of Theorem 5. It follows from *(C1)* that

$$\frac{1}{n}\sum_{j=1}^{n}\left[Y_{ij} - f\left(\mathbf{x}_{ij}, \beta\right)\right]^2 = \sigma_i^2 + o_p\left(\frac{1}{n}\right). \tag{B.1}$$

Consequently,

$$\max_{1 \leq i \leq m} \frac{1}{n}\sum_{j=1}^{n}\left[Y_{ij} - f\left(\mathbf{x}_{ij}, \beta\right)\right]^2 = \sigma_{i_*}^2 + o_p\left(\frac{1}{n}\right). \tag{B.2}$$

Then, when n is large enough,

$$\max_{1\le i\le m}\frac{1}{n}\sum_{j=1}^{n}\left[Y_{ij}-f\left(\mathbf{x}_{ij},\beta\right)\right]^2 = \frac{1}{n}\sum_{j=1}^{n}\left[Y_{i_*j}-f\left(\mathbf{x}_{i_*j},\beta\right)\right]^2+o_p\left(\frac{1}{n}\right). \tag{B.3}$$

It implies that when n is large enough, $\widehat{\beta}_G$ is actually the common LS estimator of β obtained by the data with index in the small time interval I_{i_*}. By the asymptotic normality of the LS estimation under linear expectation framework, we can get the asymptotic normality of $\widehat{\beta}_G$. That is, first, let us consider the part (a) of the Theorem 5 as follows:

$$\begin{aligned}&\frac{1}{n}\sum_{j=1}^{n}\left[Y_{i_*j}-f\left(\mathbf{x}_{i_*j},\beta\right)\right]^2\\&=\frac{1}{n}\sum_{j=1}^{n}\varepsilon_t^2+\frac{2}{n}\sum_{j=1}^{n}\left[f\left(\mathbf{x}_{i_*j},\beta_0\right)-f\left(\mathbf{x}_{i_*j},\beta\right)\right]\varepsilon_t\\&\quad+\frac{1}{n}\sum_{j=1}^{n}\left[f\left(\mathbf{x}_{i_*j},\beta_0\right)-f\left(\mathbf{x}_{i_*j},\beta\right)\right]^2\\&=A_1+A_2+A_3.\end{aligned} \tag{B.4}$$

First, $P\lim A_1=\sigma_{i_*}^2$ by a law of large numbers. Secondly, for fixed β_0 and β, $P\lim A_1=0$ follows from the convergence of $(1/n)\sum_{j=1}^{n}[f(\mathbf{x}_{i_*j},\beta_0)-f(\mathbf{x}_{i_*j},\beta)]^2$ by Chebyshevs inequality

$$P\left[\left\{n^{-1}\sum_{j=1}^{n}\left[f\left(\mathbf{x}_{i_*j},\beta_0\right)-f\left(\mathbf{x}_{i_*j},\beta\right)\right]\varepsilon_i\right\}^2>\epsilon^2\right]<\frac{\sigma_{i_*}^2}{\epsilon^2n^2}\sum_{j=1}^{n}\left[f\left(\mathbf{x}_{i_*j},\beta_0\right)-f\left(\mathbf{x}_{i_*j},\beta\right)\right]^2. \tag{B.5}$$

By the condition (II), we know that the uniform convergence of A_2 follows from the uniform convergence of the right-hand side of (B.5). Having thus disposed of A_1 and A_2, we need only to prove that $P\lim A_3$ is uniquely minimized at β_0. By the condition (II), we know that $\lim_{n\to\infty}(1/n)\sum_{j=1}^{n}[f(\mathbf{x}_{ij},\beta_0)-f(\mathbf{x}_{ij},\beta)]^2\neq 0$ if $\beta\neq\beta_0$. Thus, we get the result that as $n\to\infty$ and with probability tending to 1, $\widehat{\beta}_G\to\beta_0$.

(b) With ease of presentation, we denote $S_n(\beta)=\sum_{j=1}^{n}[Y_{i_*j}-f(\mathbf{x}_{i_*j},\beta)]^2$. Because $f(\cdot)$ is twice continuously differentiable with respect to β, the asymptotic normality of the estimator $\widehat{\beta}_G$ can be derived from the following Taylor expansion:

$$\left.\frac{\partial S_n(\beta)}{\partial\beta}\right|_{\widehat{\beta}_G}=\left.\frac{\partial S_n(\beta)}{\partial\beta}\right|_{\beta_0}+\left.\frac{\partial^2S_n(\beta)}{\partial\beta\partial\beta'}\right|_{\beta^*}\left(\widehat{\beta}_G-\beta_0\right), \tag{B.6}$$

where $\partial^2S_n(\beta)/\partial\beta\partial\beta'$ is a $p\times p$ matrix of second-order derivatives and β^* lies between $\widehat{\beta}_G$ and β_0. Since the left-hand side of (B.6) is zero (because $\widehat{\beta}_G$ minimizes $S_n(\beta)$), from (B.6) we obtain

$$\sqrt{n}\left(\widehat{\beta}_G-\beta_0\right)=-\left[\frac{1}{n}\left.\frac{\partial^2S_n(\beta)}{\partial\beta\partial\beta'}\right|_{\beta^*}\right]^{-1}\frac{1}{\sqrt{n}}\left.\frac{\partial S_n(\beta)}{\partial\beta}\right|_{\beta_0}. \tag{B.7}$$

Thus, we are done if we can show that (i) the limit distribution of $(1/\sqrt{n})(\partial S_n(\beta)/\partial\beta)|_{\beta_0}$ is normal and (ii) $(1/n)(\partial^2S_n(\beta)/\partial\beta\partial\beta')|_{\beta^*}$ converges in probability to a nonsingular matrix. We will consider these two statements in turn.

The proof of statement (i) is straightforward. Differentiating $S_n(\beta)=\sum_{j=1}^{n}[Y_{i_*j}-f(\mathbf{x}_{i_*j},\beta)]^2$ with respect β, we obtain

$$\frac{\partial S_n(\beta)}{\partial\beta}=-2\sum_{j=1}^{n}\left[Y_{i_*j}-f\left(\mathbf{x}_{i_*j},\beta\right)\right]\frac{\partial f}{\partial\beta}. \tag{B.8}$$

Evaluating (B.8) at β_0 and dividing it by $\sqrt{n}$, we have

$$\left.\frac{1}{\sqrt{n}}\frac{\partial S_n(\beta)}{\partial\beta}\right|_{\beta_0}=-\frac{2}{\sqrt{n}}\sum_{j=1}^{n}\varepsilon_i\left.\frac{\partial f}{\partial\beta}\right|_{\beta_0}. \tag{B.9}$$

By the condition (IV) and the Lindberg-Feller central limit theorem, we can get

$$\left.\frac{1}{\sqrt{n}}\frac{\partial S_n(\beta)}{\partial\beta}\right|_{\beta_0}\longrightarrow N\left(0,4\sigma_{i_*}^2C\right). \tag{B.10}$$

Proving (ii) poses a more difficult problem. Differentiating (B.8) again with respect to β and dividing by n yields

$$\begin{aligned}\frac{1}{n}\frac{\partial^2S_n(\beta)}{\partial\beta\partial\beta'}&=\frac{2}{n}\sum_{j=1}^{n}\frac{\partial f}{\partial\beta}\frac{\partial f}{\partial\beta'}\\&\quad-\frac{2}{n}\sum_{j=1}^{n}\left[f\left(\mathbf{x},\beta_0\right)-f\left(\mathbf{x},\beta\right)\right]\frac{\partial^2S_n(\beta)}{\partial\beta\partial\beta'}\\&\quad-\frac{2}{n}\sum_{j=1}^{n}\varepsilon_i\frac{\partial^2S_n(\beta)}{\partial\beta\partial\beta'}.\end{aligned} \tag{B.11}$$

We must show that each of the three terms in the right-hand side of (B.11) converges almost surely to a nonstochastic function uniformly in β. By the conditions (V) and (VI), we can get

$$P\lim\frac{1}{n}\left.\frac{\partial^2S_n(\beta)}{\partial\beta\partial\beta'}\right|_{\beta^*}=2C. \tag{B.12}$$

Finally, from (B.7), (B.10), and (B.12), we obtain

$$\sqrt{n}\left(\widehat{\beta}_G-\beta\right)\xrightarrow{\mathrm{d}}N\left(0,\sigma_{i_*}^2C^{-1}\right). \tag{B.13}$$

Thus we prove the conclusion of theorem. □

Proof of Theorem 6. The definitions of the two estimations lead directly to the conclusions of the theorem. □

Proof of Theorem 8. From the proof of Theorem 5, we see that $\widehat{\beta}_G$ is actually the common LS estimator of β obtained by data

$(Y_{i_* j}, \mathbf{x}_{i_* j})$, $j = 1, \ldots, n$. Thus $\widehat{\beta}_G = \beta + o_p(1/n)$, where β is the true regression coefficient given by (7) in the mean-certainty model. Moreover, by the same argument as used in the proof of Theorem 5, we have

$$\max_{1\le i\le m} \frac{1}{n}\sum_{j=1}^{n} \left[Y_{ij} - f\left(\mathbf{x}_{ij}, \beta\right)\right] = \max_{1\le i\le m} E_{F_i}\left[\varepsilon\right] + o_p\left(\frac{1}{n}\right). \quad \text{(B.14)}$$

The previous discussion ensures that

$$\begin{aligned} \widehat{\overline{u}} &= \max_{1\le i\le m} \frac{1}{n}\sum_{j=1}^{n} \left[Y_{ij} - f\left(\mathbf{x}_{ij}, \beta\right)\right] + o_p\left(\frac{1}{n}\right) \\ &= \max_{1\le i\le m} E_{F_i}\left[\varepsilon\right] + o_p\left(\frac{1}{n}\right) = \overline{u} + o_p\left(\frac{1}{n}\right), \end{aligned} \quad \text{(B.15)}$$

where F_i is the distribution of data in I_i. Consequently,

$$\begin{aligned} &\max_{1\le i\le m} \frac{1}{n}\sum_{j=1}^{n} \left[Y_{ij} - f\left(\mathbf{x}_{ij}, \beta\right) - \widehat{\overline{u}}\right]^2 \\ &= \max_{1\le i\le m} \frac{1}{n}\sum_{j=1}^{n} \left[Y_{ij} - f\left(\mathbf{x}_{ij}, \beta\right) - \overline{u}\right]^2 + o_p\left(\frac{1}{n}\right). \end{aligned} \quad \text{(B.16)}$$

On the other hand,

$$\begin{aligned} &\frac{1}{n}\sum_{j=1}^{n} \left[Y_{ij} - f\left(\mathbf{x}_{ij}, \beta\right) - \overline{u}\right]^2 \\ &= \frac{1}{n}\sum_{j=1}^{n} \left[\varepsilon_{ij} - u_i - \left(\overline{u} - u_i\right)\right]^2 \\ &= \sigma_i^2 + \left(\overline{u} - u_i\right)^2 + o_p\left(\frac{1}{n}\right). \end{aligned} \quad \text{(B.17)}$$

Then,

$$\begin{aligned} &\frac{1}{n}\sum_{j=1}^{n} \left[Y_{ij} - f\left(\mathbf{x}_{ij}, \beta\right) - \overline{u}\right]^2 \\ &= \frac{1}{n}\sum_{j=1}^{n} \left[Y_{k_* j} - f\left(\mathbf{x}_{k_* j}, \beta\right) - \overline{u}\right]^2 + o_p\left(\frac{1}{n}\right), \end{aligned} \quad \text{(B.18)}$$

where $\mathbf{x}_{k_* j}$ is the covariate matrix with index in I_{k_*}. By the similar steps of of Theorem 5, we can prove the conclusion of theorem. □

Proof of Theorem 9. The proof of the theorem follows directly from the definitions of the two estimators. □

Acknowledgments

This research was supported by NNSF Project (11171188, 11221061, and 11231005) of China, NSF and SRRF Projects (ZR2010AZ001 and BS2011SF006) of Shandong Province of China, and K C Wong-HKBU Fellowship Programme for Mainland China Scholars 2010-11.

References

[1] N. E. Karoui, S. Peng, and M. C. Quenez, "Backward stochastic differential equations in finance," *Mathematical Finance*, vol. 7, no. 1, pp. 1–71, 1997.

[2] Ph. Artzner, F. Delbaen, J. M. Eber, and D. Heath, "Thinking coherently," *RISK*, vol. 10, pp. 86–71, 1997.

[3] Z. Chen and L. Epstein, "Ambiguity, risk, and asset returns, in continuous time," *Econometrica*, vol. 70, no. 4, pp. 1403–1443, 2002.

[4] H. Follmer and A. Schied, *Statistic Finance, An Introduction in Discrete Time*, Walter de Gruyter, Berlin, Germany, 2nd edition, 2004.

[5] P. J. Huber, *Robust Statistics*, John Wiley & Sons, New York, NY, USA, 1981.

[6] P. Walley, *Statistical Reasoning with Imprecise Probabilities*, Chapman & Hall/CRC, New York, NY, USA, 1991.

[7] S. Peng, "Backward SDE and related g-expectations," in *Backward Stochastic Differential Equations*, N. El Karoui and L. Mazliak, Eds., vol. 364 of *Pitman Research Notes in Mathematics Series*, pp. 141–159, 1997.

[8] S. Peng, "G-expectation, G-brownian motion and related stochastic calculus of itô's type," in *The Abel Symposium 2005, Abel Symposia 2*, Benth et al., Ed., pp. 541–567, Springer, New York, NY, USA, 2006.

[9] S. Peng, "Law of large numbers and central limit theorem under nonlinear expectations," In press.

[10] S. Peng, "Multi-dimensional G-Brownian motion and related stochastic calculus under G-expectation," *Stochastic Processes and their Applications*, vol. 118, no. 12, pp. 2223–2253, 2008.

[11] Ph. Briand, F. Coquet, Y. Hu, J. Mémin, and S. Peng, "A converse comparison theorem for BSDEs and related properties of g-expectation," *Electronic Communications in Probability*, vol. 5, pp. 101–117, 2000.

[12] F. Coquet, Y. Hu, J. Mémin, and S. Peng, "Filtration-consistent nonlinear expectations and related g-expectations," *Probability Theory and Related Fields*, vol. 123, no. 1, pp. 1–27, 2002.

[13] L. Denis and C. Martini, "A theoretical framework for the pricing of contingent claims in the presence of model uncertainty," *The Annals of Applied Probability*, vol. 16, no. 2, pp. 827–852, 2006.

[14] L. Denis, M. Hu, and S. Peng, "Function spaces and capacity related to a sublinear expectation: application to G-brownian motion paths," *Potential Analysis*, vol. 34, no. 2, pp. 139–161, 2011.

[15] F. Gao, "Pathwise properties and homeomorphic flows for stochastic differential equations driven by G-Brownian motion," *Stochastic Processes and their Applications*, vol. 119, no. 10, pp. 3356–3382, 2009.

[16] X. Li and S. Peng, "Stopping times and related Itô's calculus with G-Brownian motion," *Stochastic Processes and their Applications*, vol. 121, no. 7, pp. 1492–1508, 2011.

[17] G. E. Rosazza, "Risk measures via g-expectations," *Insurance*, vol. 39, no. 1, pp. 19–34, 2006.

[18] H. M. Soner, N. Touzi, and J. Zhang, "Martingale representation theorem for the G-expectation," *Stochastic Processes and their Applications*, vol. 121, no. 2, pp. 265–287, 2011.

[19] J. Xu and B. Zhang, "Martingale characterization of G-Brownian motion," *Stochastic Processes and their Applications*, vol. 119, no. 1, pp. 232–248, 2009.

[20] Z. Chen and S. Peng, "A general downcrossing inequality for g-martingales," *Statistics and Probability Letters*, vol. 46, no. 2, pp. 169–175, 2000.

[21] S. Peng, "Monotonic limit theorem of BSDE and nonlinear decomposition theorem of Doob-Meyer's type," *Probability Theory and Related Fields*, vol. 113, no. 4, pp. 473–499, 1999.

[22] S. Peng, "Filtration consistent nonlinear expectations and evaluations of contingent claims," *Acta Mathematicae Applicatae Sinica English Series*, vol. 20, no. 2, pp. 191–214, 2004.

[23] S. Peng, "Nonlinear expectations and nonlinear Markov chains," *Chinese Annals of Mathematics B*, vol. 26, no. 2, pp. 159–184, 2005.

[24] S. Peng, "Survey on normal distributions, central limit theorem, Brownian motion and the related stochastic calculus under sublinear expectations," *Science in China A*, vol. 52, no. 7, pp. 1391–1411, 2009.

[25] H. M. Soner, N. Touzi, and J. Zhang, "Quasi-sure stochastic analysis through aggregation," *Electronic Journal of Probability*, vol. 16, pp. 1844–1879, 2011.

[26] H. M. Soner, N. Touzi, and J. Zhang, "Wellposedness of second order backward SDEs," *Probability Theory and Related Fields*, vol. 153, pp. 149–190, 2012.

[27] M. Soner, N. Touzi, and J. Zhang, "Dual formulation of second order target problems," *Annals of Applied Probability*, vol. 23, pp. 308–347, 2013.

[28] Y. Song, "Uniqueness of the representation for G-martingales with finite variation," *Electronic Journal of Probability*, vol. 17, article 24, 2012.

[29] V. Strassen, "Messfehler und information," *Zeitschrift für Wahrscheinlichkeitstheorie und Verwandte Gebiete*, vol. 2, pp. 267–284, 1964.

[30] L. Lin, Y. Shi, X. Wang, and S. Yang, "Sublinear expectation regression," *Annals of Statistics*. In press.

[31] S. Peng, "Nonlinear expectations and stochastic calculus under uncertainty," In press.

[32] M. Rosenblatt, "A central limit theorem and a strong mixing condition," *Proceedings of the National Academy of Sciences*, vol. 42, pp. 43–47, 1956.

[33] M. Rosenblatt, "Density estimates and Markov sequences," in *Nonparametric Techniques in Statistical Inference*, M. Puri, Ed., pp. 199–210, Cambridge University Press, London, UK, 1970.

[34] A. N. Kolmogorov and U. A. Rozanov, "On the strong mixing conditions of a stationary Gaussian process," *Theory of Probability and Its Applications*, vol. 5, no. 2, pp. 204–208, 1960.

[35] R. C. Bradley and W. Bryc, "Multilinear forms and measures of dependence between random variables," *Journal of Multivariate Analysis*, vol. 16, no. 3, pp. 335–367, 1985.

[36] C. R. Lu and Z. Y. Lin, *Limit Theories for Mixing Dependent Variables*, Science Press, Beijing, China, 1997.